DESIGN FOR RECLAMATION OF UNITIZED FAÇADE SYSTEMS

Research into connections in contemporary unitized façade systems for improving reclamation potential of components

Master thesis Djurre Barten

TU Delft Delft University of Technology

SCHELDEBOUW

Djurre Barten
4839757

Building Technology Graduation Report

Author
Djurre Barten 4839757

Master Architecture, Urbanism and Building Sciences
Track of Building Technology

First Mentor
Rebecca Hartwell | Structural Design & Mechanics

Second Mentor
Marcel Bilow | Façade & Products Innovation

Delegate of the Board of Examiners
Jorge Mejia Hernandez

Company supervisors
Hans Jansen | Scheldebouw
Samanwita Ghosh | Scheldebouw

Date
11-06-2025

ABSTRACT

The transition to a circular economy is essential in the building sector, where façades account for a significant portion of material use. Current unitized façade systems are optimized for performance but not designed for future disassembly or reuse. This research explores how façade systems can be redesigned to increase their reclamation potential, using a practical, design-based approach in collaboration with Scheldebouw, a Dutch façade manufacturer.

A literature review outlines circular design principles, with a focus on Design for Disassembly, connection techniques, and methods to evaluate disassembly potential. A case study of an existing façade element is used to identify key barriers through system analysis, factory observations, and disassembly experiments.

Multiple redesigns are developed: a modular “carrier frame” that simplifies the removal of insulating glass units (IGUs), and a screw-based thermal break connection that enables partial disassembly of aluminum profiles. These innovations aim to improve adaptability and support future reuse. The proposed designs are evaluated against existing systems in terms of thermal and disassembly potential using MOST and eDim. Results showed a significant improvement in both disassembly potential and thermal performance of the new system.

KEYWORDS: Circular Economy, Design for Disassembly, MOST, façade, thermal break, reclamation

ACKNOWLEDGEMENTS

This master's thesis marks the end of my Master's degree in Building Technology at the TU Delft. It has been a long, yet above all, highly educational journey. This path would not have been possible without the help and support of many people.

First and foremost, I would like to thank my first mentor, Rebecca, for her knowledge and expertise in the subject, as well as her continuous support in guiding me to take the next step throughout my research. Her insights into both the content of the field and the structure and planning of the research process have been invaluable. I am also grateful for her role in facilitating contact with Scheldebouw.

I would also like to thank Marcel, my second mentor, for his outstanding input on the technical and practical aspects of the project. The depth of information he provided was crucial to the development of the final designs produced during this research.

In addition to my mentors, I want to express my gratitude to Hans Jansen and Samanwita Ghosh. As supervisors during my graduation internship at Scheldebouw, they steered my project in a direction that resulted in outcomes I could not have hoped for. The opportunity to travel to London and observe several building façades — including the Citibank Tower during renovation — was of immense value. Moreover, being granted access to a former panel from the ABN AMRO building, and the ability to dismantle it for research purposes, played a key role in shaping the conclusions and final outcomes of this thesis. The incredible opportunities and knowledge I gained at Scheldebouw, thanks to the entire team — with special thanks to Hans de Ridder — will stay with me forever. The willingness to teach me during my time at the office was truly exceptional.

Lastly, I want to thank my dear parents and my girlfriend for their support and trust during moments of doubt.

Thank you all,

Djurre Barten

SUMMARY

The building sector currently consumes vast amounts of materials, significantly contributing to the industry's carbon footprint. To reduce this impact, the entire sector must transition towards a circular economy that enables the effective reuse of materials. High-rise buildings, due to their substantial material demands, are an important focus in this shift. One of the key components of such buildings is the façade, which incorporates a wide variety of materials. At present, unitized façade systems, commonly used in high-rise construction, play a particularly prominent role in this context. These systems are most often designed for optimal performance, typically under the assumption of an indefinite service life. In reality, most facades are estimated to have a maximum service life of 60 years. Designing with focus on disassembly principles and high-value reuse in mind, is found to be essential to reduce the overall environmental impact of facades. Therefore, this research focusses on the possibilities to design systems in which reclamation of components becomes more feasible.

This research is conducted in collaboration with Scheldebouw which is a manufacturer of unitized facades and based in the Netherlands. The study begins by outlining the research framework, including the background, motivation, problem statement, and research objectives. The main research question and sub-questions are then presented. The literature review explores the principles of the circular economy and identifies key strategies relevant to this study. Particular focus is placed on the concept of Design for Disassembly, connection and fastening methods, and disassembly techniques. The different ways of connecting and fastening are outlined, and different disassembly methods are described. Frameworks, guidelines and examples of applications in other industries are explained. After that different measurement methods are described to validate the ease of disassembly. Lastly, the used components in systems and their impact are analyzed.

After the literature research the practical research is described in which a case study is introduced. The façade of the ABN AMRO headquarters is used for this research to redesign a new system while reusing the old. This design process aims to find barriers for designing for reclamation and uses a disassembly experiment to find out what the basic tasks during disassembly processes of facades are. With the analyses of this system and observing assembly processes of new panels in the factory hall of Scheldebouw, all connection types can be listed and ranked for their ease of disassembly. Finally, the connections that are found to be barriers are listed.

In the following step these a redesign for these connections is proposed and worked out in detail. The main outcomes are a new so-called ‘carrier frame principle’ which holds the complete IGU and can be easily connected and disconnected to the main frame of a unit. The second main outcome is a redesign for the thermal break in aluminum profiles. This redesign makes disassembly possible and allows the changing of the front of mullion and transoms. Making the total frame of a unit more adaptable.

The new systems and connections are then validated for their ease of disassembly and compared with the old ABN AMRO design. Also, thermal performance and application potential is reviewed. Results showed a significant improvement in both disassembly potential and thermal performance of the new system.

The research concludes by answering all research questions and offering recommendations for future study and practical implementation.

CONTENT

ABSTRACT 3

ACKNOWLEDGEMENTS *4*

SUMMARY *5*

A. INTRODUCTION 8

1. RESEARCH FRAMEWORK 8

1.1 Background and motivation 9
1.2 Problem statement 10
1.3 Research objectives 10
1.4 Research questions 11
1.5 Research scope 11
1.6 Approach and methodology 12
1.6.1 Methodology 12
1.6.2 Planning and organization 14
1.7 Scheldebouw 15
1.8 Relevance 15

B. LITERATURE RESEARCH 17

2. CIRCULAR ECONOMY 17

2.1 General principles of Circular Economy 18
2.2 Circular Economy in building sector 22
2.3 Circular Economy in Façades 23
2.4 Materials and impact in façade systems 24
2.5 Challenges in façade circularity 27
2.6 Conclusion 29

3. DESIGN FOR DISASSEMBLY 31

3.1 Design for Disassembly, principles 32
3.2 Types of connections 33
3.3 DfD techniques 36
3.4 Guidelines for DfD 38
3.5 Applications of DfD techniques in other industries 41
3.6 Measurement methods 44
3.6.1 DGBC method 44
3.6.2 eDim method 47
3.7 Conclusion 50

C. PRACTICAL RESEARCH 52

4. CASE STUDY: ABN AMRO FAÇADE PANEL 52

4.1 Introduction ABN AMRO facade 53
4.2 Service life components 57
4.3 Disassembly potential 59
4.4 Reclamation potential 61
4.5 Disassembly experiment 64
4.5.1 Objectives 64
4.5.2 Setup 65
4.5.3 Findings derived from experiment 69
4.6 Conclusion 70

5. CONNECTION TYPES IN UNITIZED FAÇADE SYSTEMS 71

5.1 Current connections and fastening methods 72
5.2 Validating ease of disassembly of connections 79

6. TARGETING CONNECTIONS *82*
6.1 Identification of key connections for redesign 83
6.1.1 Façade frame 83
6.1.2 IGU connection 83
6.1.3 Thermal break 84
6.2 Conclusion 85

D. DESIGNING AND VALIDATION 87

7. REDESIGNING OF CONNECTIONS *87*
7.1 Improvements frame connection 88
7.2 New carrier frame principle for old frame units 89
7.3 New thermal break design 101
7.3.1 Design considerations 101
7.3.2 Final redesign 102
7.4 Conclusion 107

8. VALIDATION OF REDESIGN *108*
8.1 Validation of designed products 109
8.2 Calculating disassembly potential 109
8.3 Calculating thermal performance 112
8.3.1 Horizontal detail 01 112
8.3.2 Horizontal detail 02 113
8.3.3 Vertical detail 01 114
8.3.4 Vertical detail 02 115
8.3.5 Total U-value façade element 115
8.4 Calculation avoided carbon 117
8.5 Structural verification carrier frame 118
8.5.1 Maximum bending deformation glass 118
8.5.2 Number of screws 118
8.6 Thermal break application 120
8.7 Conclusion 122

E. CONCLUSION AND RECOMMENDATIONS 124

9. CONCLUSIONS & RECOMMENDATIONS *124*
9.1 Conclusions 125
9.2 Recommendations 127

REFERENCES *128*

APPENDICES *131*
Appendix 1.1 132
Appendix 1.2 135
Appendix 1.3 142
Appendix 2.1 144
Appendix 2.2 145
Appendix 2.3 146
Appendix 2.4 150
Appendix 3 151
Appendix 4 152
Appendix 5.1 154
Appendix 5.2 156

A. INTRODUCTION

1. RESEARCH FRAMEWORK

Chapter 1 describes the research framework which explains how the study was conducted. A brief description of the background and motivation is provided, followed by an explanation of the specific problem to be addressed. Next, the objectives of the study are outlined, along with the research questions formulated to achieve them. A timeline and methodology are presented, followed by an introduction to Scheldebouw.

1.1 Background and motivation

The building sector is a significant contributor to the global increase in carbon emissions. Carbon is released at various stages of a building's life cycle, from the production of components and materials to the energy consumption during its operational life span. At the end-of-life, the recovery and processing old components play a vital role in the total emissions of the cycle. These different stages make that the complete building sector is responsible for approximately 35% of all carbon emissions on global level (European Commision, 2011). Next to that the building sector uses 30% to 50% of the raw materials and produces about 40% of waste to landfill (Walker et al., 2007).

The 'green buildings' movement, where the focus laid on reducing the emissions during the operational stage, was found to be insufficient to lower emissions of the building sector (Pomponi & Moncaster, 2017). However, it did result in the design and production of new highly advanced systems, to reduce cooling and heating demand for buildings and the aim to improve indoor climate. This resulted in better insulated systems for facades and laid foundation for research to advanced systems.

The embedment of circular economy (CE) principles in the design of buildings offers the opportunity to further reduce the environmental impact of facade systems. Circular design aims to transition toward regenerative systems by minimizing resource input, waste, emissions, and energy loss. This is achieved by slowing, closing, and narrowing material and energy loops (Stahel, 1982). When a building consistently achieves high levels of comfort with nearly zero energy consumption, the choice of building materials becomes a key determinant of its ecological quality (Hilbrand, 2012). At the same time building components and systems nowadays use a larger variety of materials and more complex connections are introduced in designs. This resulted in highly complex multi-material systems which affects the possibilities in the circular economy. This can be found mainly in façade systems of a building.

Building skins are a critical component of architecture, influencing and being influenced by various disciplines and numerous segments of the value chain. The building envelope is estimated to represent the largest single contribution to the total embodied carbon in buildings (Kragh & Jakica, 2021). Additionally, facades typically have a shorter service life compared to the building's primary structure. As a result, the building skin has a substantial short-term impact while also contributing to long-term considerations such as maintenance and potential replacement throughout the building's lifecycle (Kragh & Jakica, 2021). For this reason, it is necessary to find new ways to reduce the environmental impact of façade systems at the end-of-life.

In the context of building material circularity, the reclamation of individual components from larger systems is a crucial step. Reclamation refers to a broad category of actions taken at the end of a product's service life. The reclamation potential refers to the extent to which building systems can be disassembled and reused at the end of their service life. It is primarily influenced by the individual components and the nature of the interfaces between them (Hartwell, 2019).

The circularity of a reversible façade design relies on transformability at both the technical and material levels. This flexibility creates opportunities for new value propositions throughout the façade's life cycle. According to Kragh & Jakica (2021) the technical design of connections plays a critical role in enabling design for disassembly. As such, the way connections are designed significantly impacts the reclamation potential and overall circularity of façade systems.

1.2 Problem statement

The motive for this is research is the problem that façade systems currently have a large part in the total carbon footprint of buildings.
Current performance requirement in buildings and facades have over the years led to very sophisticated systems. These systems are often designed to maximize performance in terms of insulation, weather tightness, acoustics and durability. This resulted into highly complex systems with a large number of different materials. Therefore, a lot of different connections are currently being applied in order to join different components together. These connections are designed to enable practical assembly of facade systems while maximizing the overall strength and durability of the system. The connections are often not designed to be disassembled in the future. At the same time the building sector aims to move into the strategy of a circular economy (CE), in order to lower the total carbon footprint. In the facade systems however some components last much longer than others, but due to difficult or permanent connections, short-life components are not easy to take apart from long-life components. This complicates the possibilities for circularity in buildings and facades. That opens up questions if it may be possible to find new ways for connections to make disassembly after the life span possible. Can demountable but durable connection types be implemented in facade systems? And can future façade systems and future designs be equipped with certain techniques?

1.3 Research objectives

General objective
The general objective of this research is to reduce the environmental impact of future façade systems. This will be done by focusing on increasing the reclamation of façade components. To make this possible a comprehensive review to existing connection types in contemporary façade systems will be conducted. This can be followed by the potential redesign of connections which should aim to improve disassembly potential.

Sub-objectives
Gaining general knowledge of existing challenges in the reclamation of façade systems and their constituent components is necessary. What are the primary barriers to reuse and remanufacturing as perceived by manufacturers and clients?

In addition, it is important to identify which materials are suitable for disassembly and can offer significant benefits through their potential for reuse. This includes exploring existing frameworks for the reclamation of building components and examining current research on component reusability.

A more challenging aspect involves testing and validating a newly designed connection. It is essential to establish methods for assessing improvements in disassembly potential. To achieve this, existing or newly developed frameworks that evaluate and rank the ease of disassembly of connections should be applied.

Final product
The final product of this research will be a redesign of one or multiple redesigns of connections currently used in façade systems. These redesigns will be provided in drawings and in physical model(s). These are tested using existing measurement methods for disassembly potential, which compares the existing connections with the new. In addition, validation will be carried out for the thermal and structural performance of the system.

1.4 Research questions

Main question:
"In what ways can connections in unitized façade systems be improved to make disassembly of components possible and thereby make a contribution to the circular economy in the built environment?"

Sub-questions:

1. What is the current status/view on circularity in built environment and facades?
   - What are the challenges in reclamation of facades?
   - What does the concept of Design for Disassembly entail?
   - How can the existing methods for assessing disassembly potential be applied to facade systems?

2. Which components and/or materials exhibit high potential for reclamation?

3. Which types of connections are currently used in unitized façade systems, and how can they be ranked based on specific disassembly criteria?

4. Which connection types currently limit the reusability or prevent the reclamation of long-life components?

5. How can connections be redesigned and tested to make disassembly possible and therefore increases the possibilities of the Circular Economy?

1.5 Research scope

This research focuses on façade systems for high- and mid-rise buildings. These buildings nowadays are usually built, not by using solid (non-)loadbearing but by using a so-called curtain-wall façade. This system hangs from the floor slabs and is practically independent from the main structure of the building. Curtain walls can have different type of facades systems where two main types are distinguished: *stick systems* and *unitized systems*. This research purely focusses on unitized façade systems for buildings. In this research a large variety of different unitized designs is reviewed, however the connection types and strategies in a lot of cases are similar. At the same time some connection types may be applied in stick systems. This will be entirely based on coincidence and will not be further investigated in this study. The findings of this research might potentially apply to certain stick systems, but this falls outside the scope of the study.

This study is set up to investigate and improve the ease of disassembly of connection types in facade systems. Some connections might exist of chemically or adhesively bonded connections. This research won't focus on exploring new chemical connections or finding new adhesives.

1.6 Approach and methodology

1.6.1 Methodology

Phase 1

The first phase of this research will focus on existing research which will clarify what the reason is that the built environment should aim for a circular economy. The target is to find out what current challenges and reasons are why the built environment not yet has accomplished these goals. Existing frameworks and guidelines need to be lined up as well as the knowledge already available about demands and barriers for manufacturers or clients of facades for designing for disassembly. Although the first face will consist of a lot of literature research, also in the other phases literature will be used to clarify and help providing information when needed.

Phase 2

The second phase focuses mainly on a practical study and gaining information from the existing physical systems. This study will consist of a review of existing systems and observation of (dis)assembly processes and connections methods. To do so a case study is used to find out what the barriers and challenges in connections are during a design process. A case study allows the use of a real-life design process to identify practical barriers in designing for reclamation and to determine which connections present challenges during disassembly. This process is a way of Design Based Research (DBR) which focusses on the use of prototypes that can immediately form an intervention in practice and reflects on theory. In this phase preliminary designs can be created and considered.

Phase 3

In the third phase, a selection of connections will be made, followed by the development and detailed elaboration of alternative redesigns. The selection of connections will be based on the research into reference studies and existing connections, as well as the literature review, which will reveal what components are preferred to be separated. Preliminary prototypes can then be assembled. These potential improved connections can then be tested and validated using existing guidelines and existing legislation or requirements.

Phase 4

In the fourth phase a prototype of certain connections is finalized. This phase will further provide an overview of the research process and will state final conclusions and recommendations.

Research methodology scheme

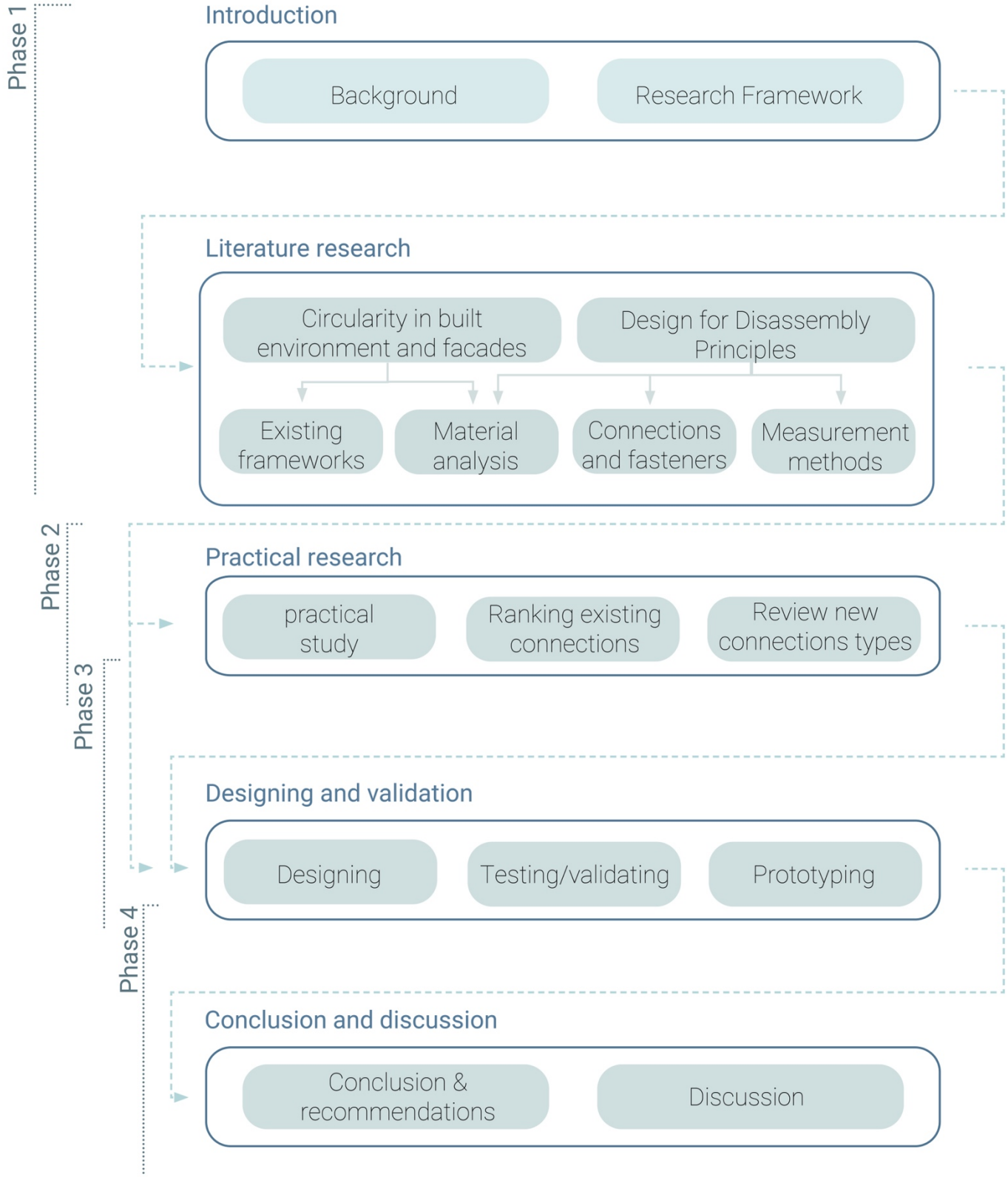

1.6.2 Planning and organization

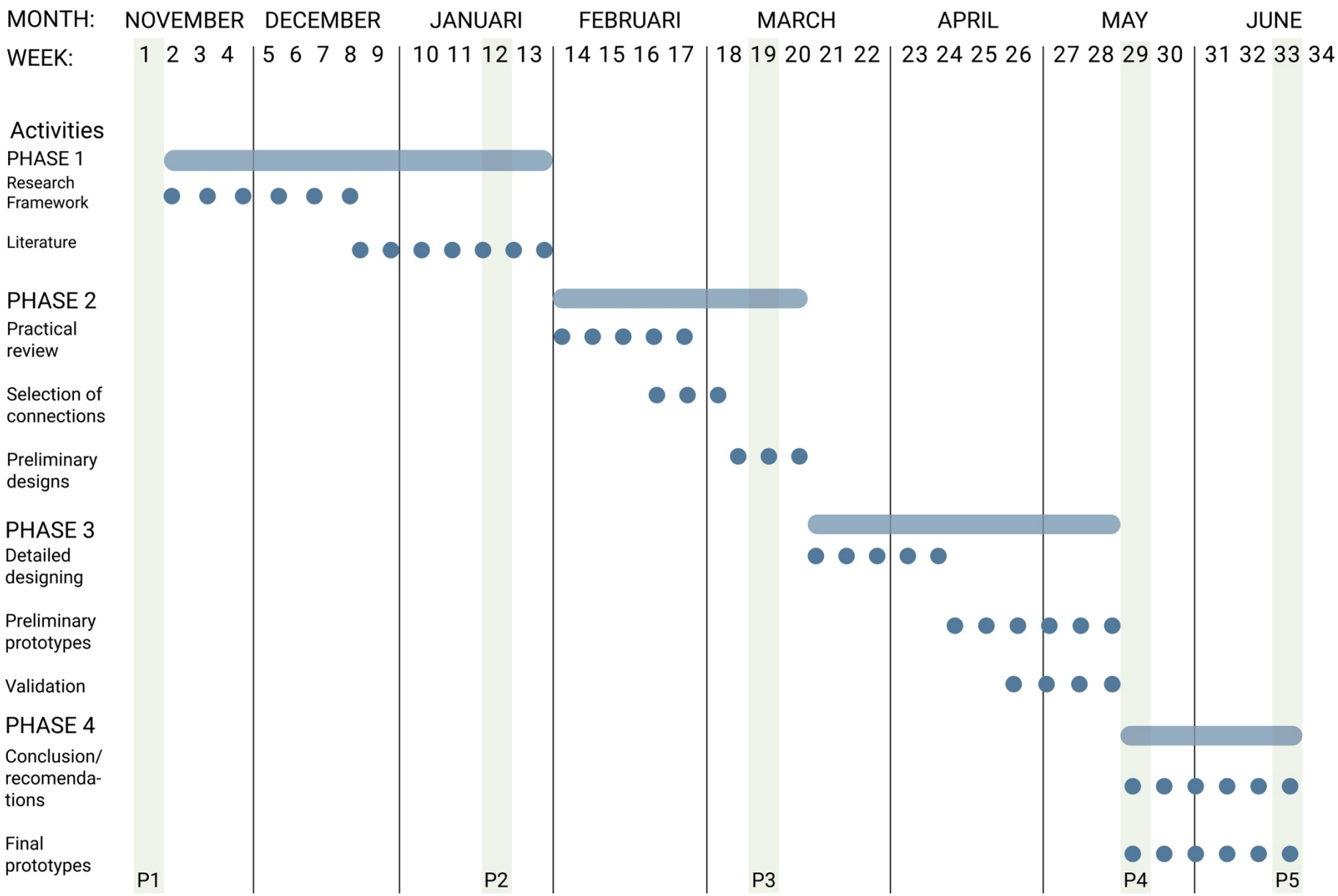

1.7 Scheldebouw

This research was conducted in collaboration with Scheldebouw, a façade systems manufacturer based in the Netherlands. Scheldebouw was founded in 1933 to produce lightweight aluminum components for shipbuilding and lightweight aircraft. In 1958, Scheldebouw began producing façade components for curtain wall façades and has since grown into one of the larger façade manufacturers in Europe. In 1995, it joined the Permasteelisa Group and became part of a global leader in the curtain wall industry. Well-known projects include 'The Shard' in London (UK) and 'De Rotterdam' in Rotterdam (The Netherlands).

In their production hall in Middelburg, located next to their office spaces, unitized façade systems are built. Equipped with a mock-up area and a clean room, they can test their system designs against various requirements. In addition to system production, the Permasteelisa Group also offers services for other phases of the building process. They assist in architectural design, project management, and the installation of façades. This allows the company to have a comprehensive view of the entire façade engineering process, from start to finish.

At present, more and more buildings are reaching the end-of-life stage, a phase in which several options are available. Scheldebouw can play a crucial role in this stage and could incorporate it into their business model. The end-of-life phase is currently not a primary focus, however, it is of great importance to achieve the full circular potential. This requires specific attention to practical aspects, such as technical details. This research can assist Scheldebouw in gaining insights and exploring design possibilities. This way it helps achieving their objective of using materials more circular and enhance circularity within the company.

At the same time, Scheldebouw can provide this research with highly valuable information, as it is involved not only in the design and construction phases but also in the dismantling phase. Moreover, the company provides physical insight into a wide range of different systems and their associated design considerations. This will be of crucial value throughout the course of this research.

1.8 Relevance

This research aims to find the important barriers inside façade system that holdback the reclamation of materials and components. Connections between these components currently are not designed to be reversible. Although durability and performance are very important factors for manufacturers and clients/users, façade systems do not have infinite life spans. It is important for manufacturers to design systems with the end-of-life scenario in mind. Looking at the fact that a lot of systems containing materials and components which have a longer life span than other components, reclamation should be a possibility. Since potential of disassembly of components starts at the connections, a redesign of the ones that hold back this potential is vital. By finding ways to use reversible connections the circularity potential of components and materials can be increased. Leading to a smaller carbon and environmental impact of façade systems of future buildings.

A company like Scheldebouw can therefore have a large impact in the complete industry and the circularity potential. By increasing the disassembly potential of new facade systems, they can profit from it themselves by staying involved in the life cycle of the façade. Not only during the production and maintenance phase of but also during the end-of-life phase where the company can be consulted for dismantling of the system and have personal benefit of reclaiming materials and components.

B. LITERATURE RESEARCH

2. CIRCULAR ECONOMY

This chapter explores the fundamentals of the Circular Economy and discusses why integrating these principles is essential. It provides an overview of the objectives of Circular Economy and then delves deeper into the application of circular economy principles in the built environment, followed by a focus on circularity in façade systems. The aim is to gain an understanding of the Circular Economy and identify ways to contribute to its advancement.

2.1 General principles of Circular Economy

"A Circular Economy (CE) can be said to be one that is restorative and regenerative by design and aims to keep products, components, and materials at their highest utility and value at all times" (Hart et al., 2019).

The industrial economy of today has hardly changed from its linear consumption pattern what it was from the beginning. This linear 'take-make-dispose' pattern as the Ellen MacArthur foundation (2013) calls it, can be seen as a line in which a company harvest material, a manufacturer makes the product and sells to the consumer, who discards it when it no longer serves. This process makes that in 2017 for the first time the mark of 100 billion tons material entering the economy per year had been reached. As a result of this process, the annual flow of materials entering the economy surpassed 100 billion tons for the first time in 2017 (Circle Economy, 2020). A circular economy aims to replace the 'end-of-life' concept with restoration, promotes the transition to renewable energy, eliminates toxic chemicals that hinder reuse, and strives to eliminate waste through the advanced design of materials, products, systems, and associated business models (Ellen MacArthur Foundation, 2013).
This economy is based on some simple principles. At first it focusses on eliminating waste as an option in the process. Products should be designed and optimized for a cycle of disassembly and reuse. These small cycles of materials and components define CE and set it apart from disposal. The second principle defines a difference between consumable components and durable components. Consumable components should be made largely out of biological and non-toxic materials. Durable components, which most of the time consist of non-biological materials like plastics and metals, should be designed for reuse from the beginning. Lastly the energy to produce and maybe fuel the products should be renewable (Ellen MacArthur Foundation, 2013).

The research of Stahel (1982) can be seen as a vision from where the CE had his starting point. In this research Stahel emphasizes the importance of extending the lifespan of products to achieve sustainable development. He underlines the need for a systemic change in how products are designed, used, and disposed of, promoting a circular economy where the value of products and materials is maintained for as long as possible. It describes three approaches to product life:

A: *fast-replacement,* which is basically the before mentioned 'take-make-dispose' pattern.
B: *slow-replacement*, which mainly focusses on using less production energy and making lifespans longer.
C. *the self-replenishing systems*, systems that are designed to regenerate themselves, minimizing resource input and waste output.

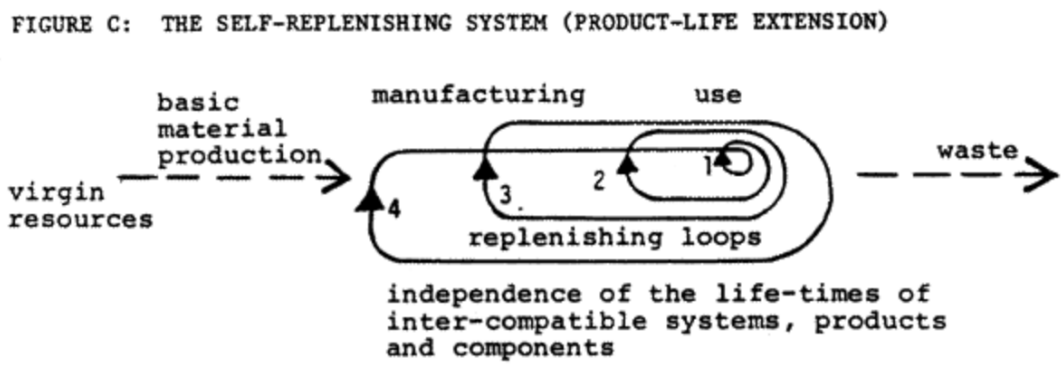

Figure 1: The self-replenishing system principle (Stahel, 1982).

This principle of making lifespans of products longer, can later been seen in the principles of CE from the MacArthur foundation.

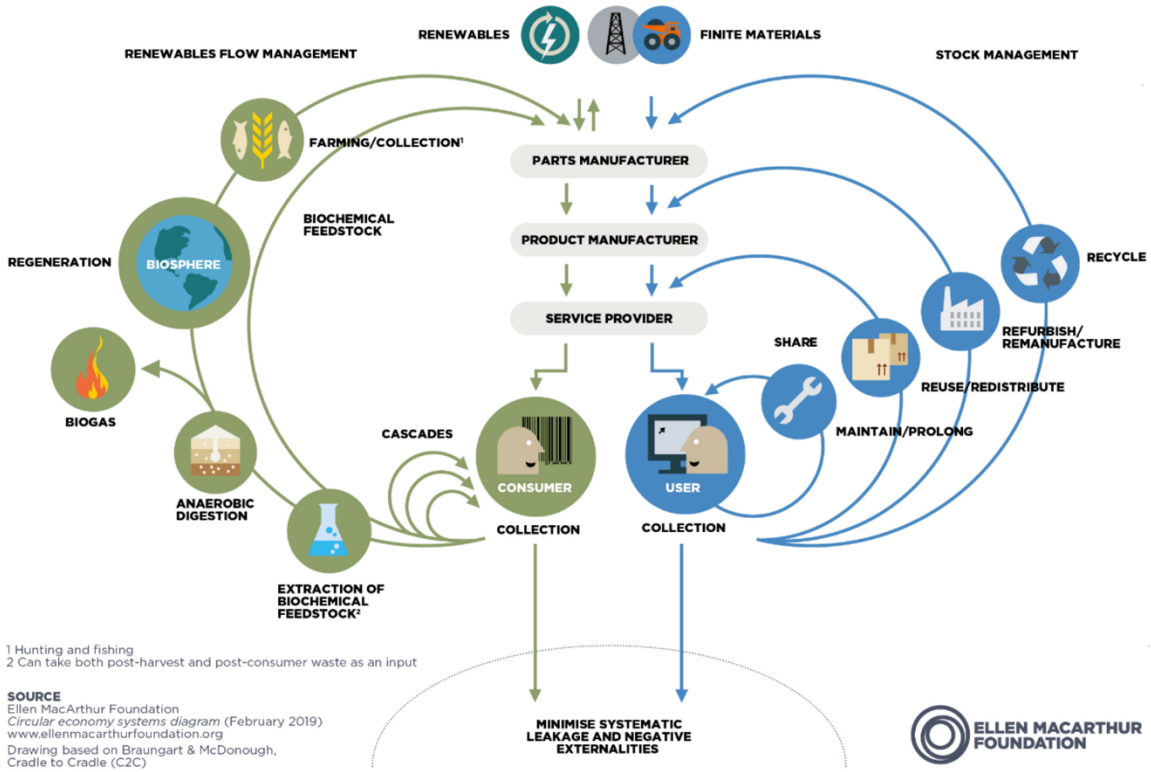

Figure 2: The circular economy: an industrial system that is restorative by design (Ellen MacArthur Foundation, 2013).

In the report the target to move from a focus on a consumer to a user is explained. Visible is the large number of possibilities for a product on the user side (right), unlike the consumer (left). Figure 2 shows the so called 'power of inner circle', which means that how tighter the circle the less a product must be changed before it can be used again. Another value is the 'power of cascaded use' which the research describes with the example of cotton clothing, which first can be reused second hand, then cross the furniture industry as fiber-fill, and later can be used as material in insulation materials. This way it keeps functioning as a virgin material inflow in different production processes.

Further building on these findings and approaches, Metabolic et al. (2018) later introduced their seven performance characteristics. This framework showed the optimal use of materials, energy and water resources, accounting positive support for biodiversity, human culture, health and maximizing value generation.

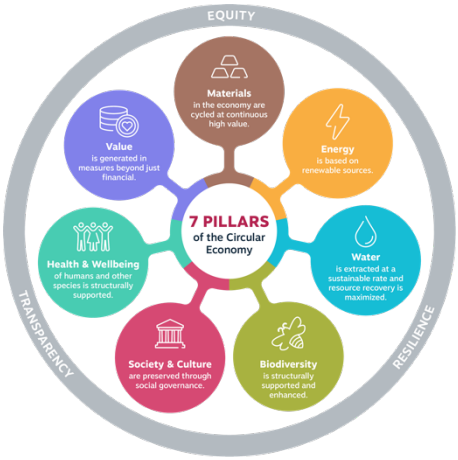

Figure 3: performance characteristics CE (Metabolic et al., 2018).

These seven performance characteristics later lead to seven strategies:

1. Prioritize regenerative resources
2. Preserve & extend what's already made
3. Use waste as a resource
4. Rethink the business model
5. Design for the future
6. Incorporate digital technology
7. Collaborate to create joint value

(Metabolic et al., 2018)

The principle of Circular Economy visualized by Ellen MacArthur Foundation (2013) leads to what in literature is described as so-called R-Strategies. The number of these different strategies can vary from 3 to 10 different 'steps'. The steps together present the circularity ladder or 'R-ladder'. The circularity ladder focuses on the function of products, rather than the products themselves. This way it also becomes possible to deliver functions using completely different products. The ladder organizes circularity strategies in a hierarchical order. Generally, the higher a strategy is on the ladder, the greater its potential for resource efficiency and savings, resulting in more significant environmental benefits. This concept is closely linked to the idea of "value retention" (Kishna & Prins, 2024).

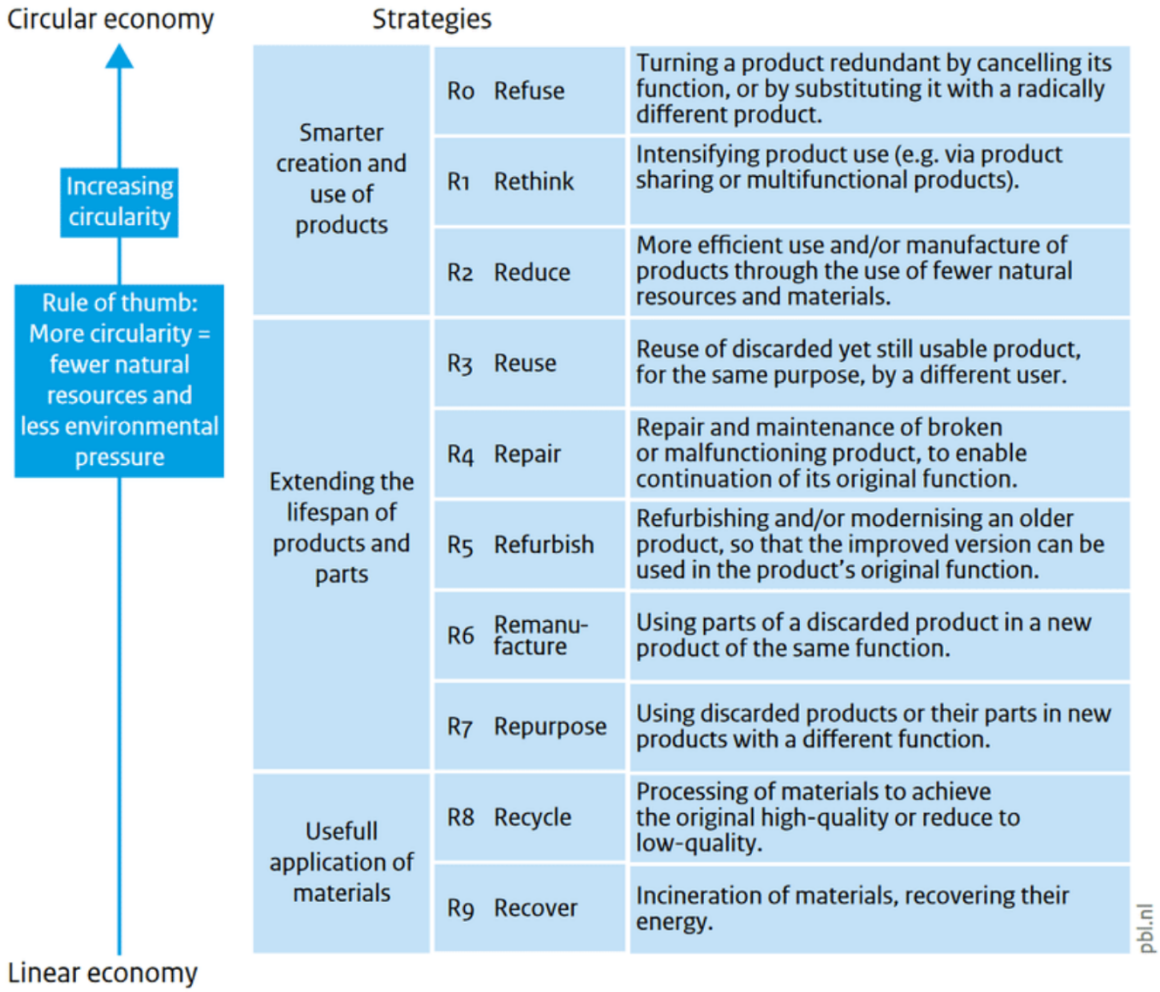

Figure 4: Ladder with R-strategies (Kishna & Prins, 2024).

This ladder does not show every possible change that is necessary to move to a Circular Economy. Important needs, for example education about CE, creating targets and adjusting legislation, are not visible on this ladder. The ladder provides an overview of circularity strategies that directly impact resource usage for product functions and can be ranked based on the expected resource savings (Kishna & Prins, 2024).
The ladder can be organized in three larger parts. In which first the way of creating a product should be considered. The second part is about finding ways to extend the lifespan of an existing product. The third part focusses on the ways a separate material can be extracted from a product in the most circular way.

The R-strategies hang close together with three different subjects which are relevant for manufacturers of products which want to move to CE. *Innovation* is an important aspect and essential part of the circularity strategies. There are three types of innovation that are related to the strategies: *designing*, *business model* and *technology*.
For designing there are different terms used to describe circular design, examples are: redesign, design for reuse, design for repair, design for recycling, design for disassembly, modular design, and design for dismantling. These show similarities with the nine R-strategies. By designing a product in a way it can be repaired or reused, less products need to be produced. The impact of an innovative product design is therefore linked to the circularity strategy enabled by the design.

In the business model these strategies can also be applied by for example offering a product as a service or offering pay-per-use. This intensifies the use of a product. Also extending lifetime by creating a repair or maintenance service as model is contributing to CE.
Lastly the technology is an important term in all parts of CE since it can improve many different strategies. It can provide new options for circular designing but also for example improving recycling processes or create better systems for the new business models (Kishna & Prins, 2024).

2.2 Circular Economy in building sector

Circular building: *"A building that is developed, used and reused without unnecessary resource depletion, environmental pollution and ecosystem degradation. It is constructed in an economically responsible way and contributes"* (Metabolic et al., 2018).

As stated in many studies, the construction sector has a significant share in global carbon emissions. To summarize the key points once again:

- The construction sector currently uses 30-50% of the available raw materials.
- It produces 40% of all waste sent to landfills.
- It generates an average of 40% of all greenhouse gases worldwide.

(Kragh & Jakica, 2021)

The building sector is currently a perfect example of the linear economy of the 'take-make-dispose' principle. It utilizes construction materials for building purposes and discards them at the end of the building's life. These materials are designed and assembled for single use, without incorporating mechanisms to reintegrate them into the system. This model prioritizes the finite lifespan of resources, neglecting considerations for the end-of-life phase of components (Oluleye et al., 2022).
The amount of research for implementing CE as a solution in the built environment is slowly growing over the past years (Metabolic et al., 2018). Many of these claim that this linear approach can be overcome by the implementation of CE. Still, it is stated that the current state of implementation of CE in the building sector is not satisfactory. At the moment from the seven performance and strategy dimensions shown before, the best performing is the energy dimension. The waste dimension turns out to be the worst performing (Bilal et al., 2020).

To create a clear overview of all these different CE studies in built environment of the last years, Benachio et al. (2020) identified six areas of CE within the construction sector: development of CE, reuse of materials, material stocks, CE in the built environment, life cycle assessment (LCA) analysis and material passport. This research shows that there is enough awareness in the building sector to change from the linear economy to CE. At the same time, it shows that there are currently not enough standardized methods and practices for practitioners to implement in their construction projects. It also shows another very important factor for positive impact on circularity: the necessity to

implement CE concepts from the project design phase. Considering these concepts in the early stages of a project can help evaluate the reuse potential of materials and guide decision-makers in selecting the most suitable materials aligned with circular principles. This approach also enables more effective management of resources throughout the building's entire life cycle (Benachio et al., 2020). Since the early stages of a process mainly consist out of designing, the focus turns to designing in a way that components can be disassembled after its life span. Design-for-Disassembly (DfD) principles are recognized as a crucial enabler for product recovery and the implementation of circular economy practices in construction materials like concrete, steel, and timber. DfD will be addressed in a later chapter in this research.

2.3 Circular Economy in Façades

Research claims that facades (or building envelopes) have the largest impact on the total carbon emission of buildings (Kragh & Jakica, 2021). Other research shows that this is not the case but still has a large part in it (Teeuwen, 2023) (Hilbrand, 2012). This includes the production phase with used materials in the façade, and the installation and maintenance phase. In Figure 5 the total life span of different building components is shown.

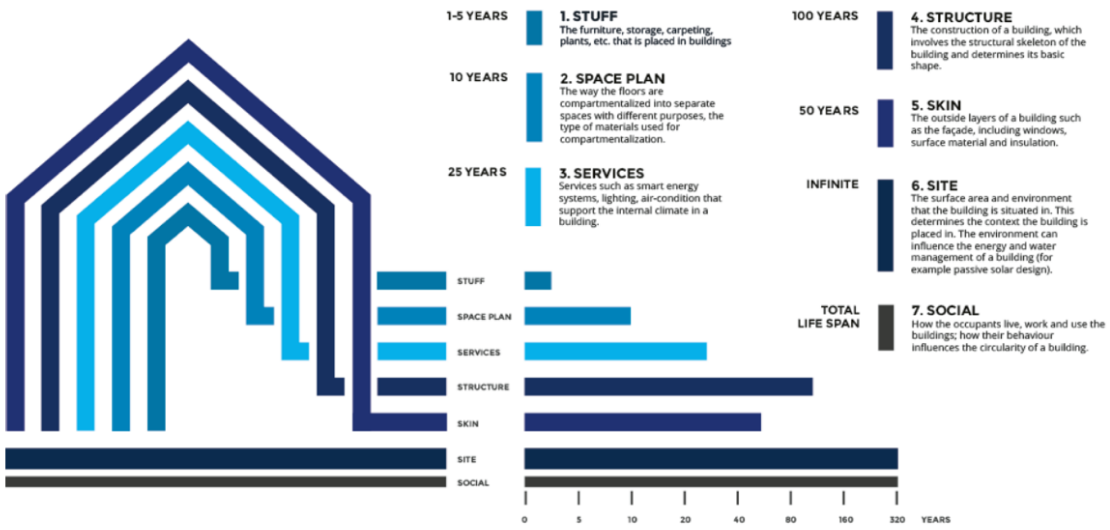

Figure 5: Building components and life span (Teeuwen, 2023).

The building envelope is shown to have a life expectancy of 50 years. This may be longer or shorter due to the high number of different façade types and range of materials used in building industries. At the same time a building structure can have a life span twice as long. The same thing happens if zoom in more on a certain component of a building. In Figure 6 is the total service life of components of a glass façade system visualized. The service life of a component is the period in which a component remains productive before being replaced or removed. This service life can come to an end for different reasons like environmental or functional impact (Hartwell, 2019).

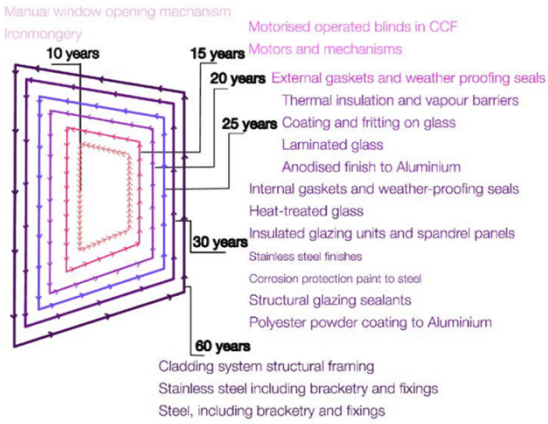

Figure 6: Service life figures for curtain wall unit (Hartwell, 2019).

Currently, the technical service lifetime of a facade is limited by that of its shorter service lifetime element (Hartwell & Overend, 2019). A permanent connection to a short-lifespan component can affect the overall service life of a façade. If long-lifespan components cannot be reclaimed due to such permanent links, this can indirectly have a significant impact on the building's total emissions, especially considering the substantial contribution of façades to overall building-related emissions. According to (Hartwell, 2019), there is no evidence of a focus on designing façade systems for disassembly in a way that materials can be reclaimed for reuse and re-cycling at the end-of-life. This is due to the high number of different materials and the use of durable but permanent connections which is counterproductive for adaptation of DfD principles. Therefore, recovery of façade components for secondary use is not possible. Because of that the only way will be to demount the complete façade and install a new one, which will be the only option to reuse the long-life building structure. Another option will be complete demolition of the building. Since both of these options will increase the total carbon footprint of the building, the possibility for disassembling and reclaiming the façade will be an attractive alternative.

Several studies already focus on simple ways to move to the circular economy in façade designs. For example, materials with a high carbon footprint—such as metal—should be designed for future reuse by avoiding welding and instead using screw connections (Kragh & Jakica, 2021). Although this may sound like a simple and smart solution, the question arises whether this is truly what needs to be achieved in the field of circular façades, given that metal components are typically the longest-lasting elements in a façade system according to (Hartwell, 2019).

2.4 Materials and impact in façade systems

In façade systems a lot of different components are combined with each other. The general objective of this research, and of implementing Design for Disassembly in these systems, is to reduce the carbon impact of high-rise building façades. When using DfD principles the disassembly potential of components can be increased. This however does not mean that it also reduces the environmental impact because different materials

will have a different amount of impact. It is necessary to identify which materials are used within a unit, and which could positively affect the environmental impact if they were possible to disassemble.

Teeuwen (2023) has made an overview of the materials that are used within the design of a unitized façade system. This specifically focusses on systems from Scheldebouw. The structure of façade systems can be made of three different materials: steel, aluminum or wood. Since most contemporary systems use aluminum and most systems from Scheldebouw use this, this research mainly focusses on systems with this material.

A standard unitized façade element normally consists of four categories

1. *Infill*: a transparent part, which could exist of glass, sealant and a spacer. Or opaque part which can consist of a metal sheet, insulation or opaque glass.
2. *Framing*: the framing carries the infill and can consist of aluminum extrusions with composites (for thermal break), used in combination with gaskets, sealants and fasteners.
3. *Connections with building structure*: these connections make assembly to the primary structure of the building possible.
4. *External elements*: elements that are added to the unit for aesthetic or functional reasons like decorations or sun shading.

Teeuwen (2023) investigated six different system design from which the weight of different materials could be derived.

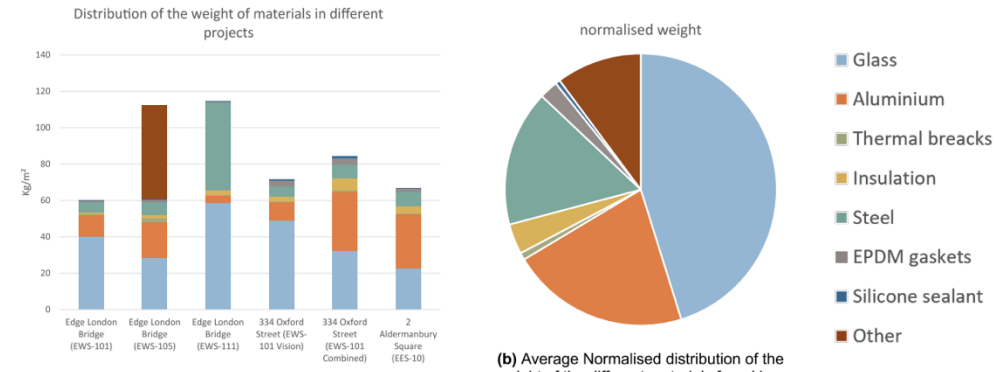

(a) Normalised distribution of the weight of the different materials found in a facade

(b) Average Normalised distribution of the weight of the different materials found in a facade

Figure 7: Normalized weight unitized facade systems (Teeuwen, 2023).

The research uses these values to then determine the environmental impact of different materials using their embodied carbon, showed in Figure 8. From these values the conclusion can be derived that aluminum has the largest impact in the complete system. Aluminum can be subdivided into extrusions, used for framing, and sheets, used for infill, and fixations. On the right these subsets are shown.

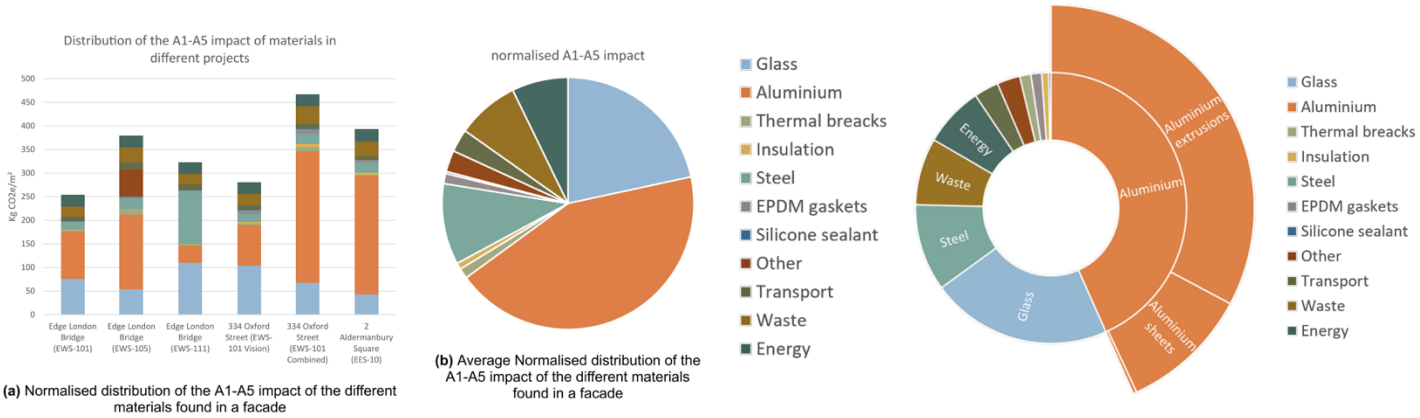

Figure 8: environmental impact per material in unitized facade systems (Teeuwen, 2023).

Next to aluminum also glass has a large impact of approximately 22% of the total impact environmental impact between stages A1-A5 of the life cycle.
Another important aspect of the materials used in façade systems is the life expectancy of the materials. there are different types of life spans that could be considered. To start, there is the guaranteed life span, which is the period in which a manufacturer will provide service and maintenance to the system when it is not performing to its requirements. The service life of a component is the time of a component in the system in which it is still productive before being replaced or abandoned. The end of service life may be reached due to different reasons like environmental influences or economic, social or technical changes. The guaranteed period set by the manufacturer is 10 years. According to the manufacturer, the estimated service life of the full envelope system is 60 years. In this

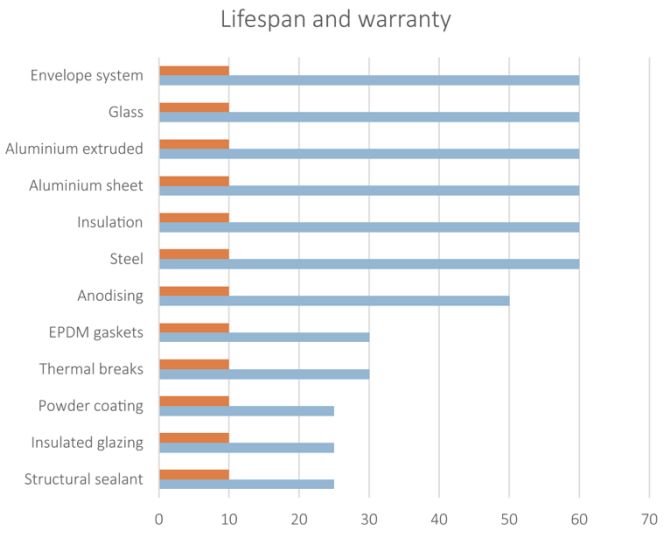

Figure 9: Guaranteed and estimated lifespan of materials in unitized facade systems according to (Teeuwen, 2023).

total system, the materials with the lowest life span are currently the insulated glass units (IGU's), the structural sealant and the EPDM gaskets (Teeuwen, 2023).

2.5 Challenges in façade circularity

Several studies were conducted to identify the reasons why the current façade industry is struggling to implement circularity and Design for Disassembly (DfD) principles in its processes. Hartwell (2021) did comprehensive research into the challenges of the CE in façade industry. The research describes the outcome of several online surveys and interviews in which all stakeholders were questioned to give their insight in the difficulties of applying circularity. For this research clients, architects, main contractors, façade contractors, material processors and demolition contractors were involved.
The survey stated that in the process the façade contractor and demolition contractor showed the most willingness to consider reusability of components of façade systems. The main contractor showed the least willingness. Next to that the reuse potential of different façade components was identified by the survey correspondents. According to the survey the framework came out to have the largest reuse potential. The insulation, connections and insulated glass units were considered to have the lowest potential.

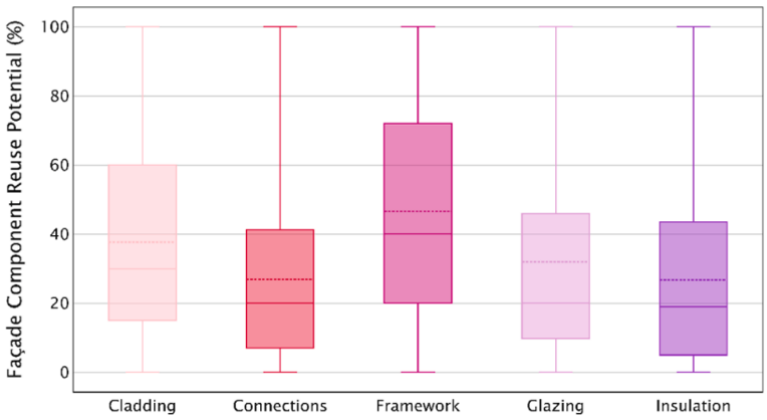

Figure 10: Reuse potential of different facade components as identified by different stakeholders (Hartwell, 2021).

Next to that, the correspondents were asked to what they considered to be the most important reason for façade replacement. According to the stakeholders, performance related reasons (due to component degradation) and aesthetical reasons were the most important reasons for replacements. The interviews with various stakeholders revealed both the barriers and challenges they face in implementing circular principles. In behavioral terms, stakeholders are afraid that they need to compromise in terms of performance and freedom of design. It seemed there is a stigma which says that everyone wants 'new' and façade manufacturers state that it is already hard to meet the aesthetic demands of architects, especially in glass facades. Stakeholders state that there is not enough knowledge about the possibilities of circular materials and say that since the clients are not motivated to specify End-of-Life criteria, the façade manufacturers and architects also won't focus on it. This is then emphasized by demolition contractors which state that façade manufacturers only focus on "design for build ability and maintenance but not for disassembly"(Hartwell et al., 2021). The stakeholders mentioned that the existing levels of recycling where dependent on the type of materials

and manufacturing operations. The overall supply chain was investigated, and it was questioned by stakeholders who would want to receive reclaimed materials. It was stated that current circularity processes are just very labor intensive and hard because original drawings are not always available. This makes that in the current supply chain the demolition contractor is mainly responsible for the reusability potential of components. In terms of technological constraints, it was mentioned that there is lack of standardization and the problem of design focus on longevity and not disassembly which makes rapid removal of components difficult and described that the more 'high-tech', the less reusable (Hartwell et al., 2021).

Droste (2023) describes several challenges for disassembly of components. It first calls the sequence of disassembly, which is usually a reverse process, and an important factor which is not always clear in the disassembly process. The variety of connection methods and the accessibility of connections, together with needed safety measures can lead to an increase of time and labor. Next to that the materials currently in a system are not easy to track or identify. Also, a market on which these materials can be advertised is not yet implemented in the industry.

Insulated glass units (IGU's) reclaimed from building sites are currently not always possible to use in one of the higher R-strategies. The current design of an IGU exists of two glass panes glued on a spacer in between and sealed of along all sides using butyl sealant. This design does not allow easy disassembly and reuse of components. The result is that most of outdated IGU's will be crushed and downgraded at EoL stage and for example will be used in the underlayers of asphalt road building. Current technological developments in the glass industry mainly focus on increasing energy performance which most of the time has a bad influence on the ability to recover the materials (Hartwell & Overend, 2019). Since there was no aim for reaching higher R-strategies like recycling or refurbishment of these components, there was low motivation for disassembling IGU's in a non-destructive way. However recent technologies have made it easier to disassemble the different materials within an IGU and therefore created the possibility for reuse these materials. An example is created by the company HEGLA which build their so-called IG2Pieces program in which they automated the separation of glass panes from a spacer by cutting through the sealant. This way the two panes can be used in a new IGU in combination with a new pane which contains the modern coating for reaching high thermal performance (HEGLA, 2023).

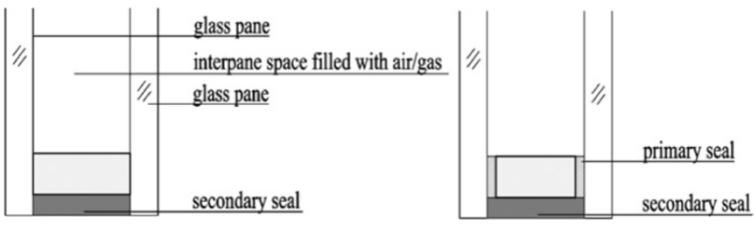

Figure 11: Schematic section of IGU with different components (Kouvela, 2022).

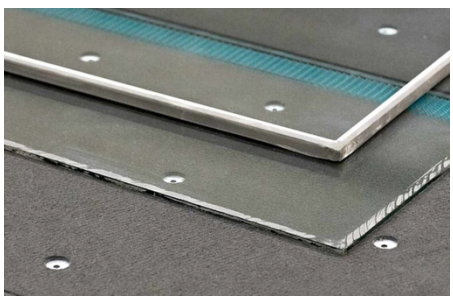

Figure 12: Separation of glass panes and spacer by HEGLA (HEGLA, 2023).

The implementation of these new techniques shows that the reuse of IGU components is possible and therefore it is necessary that non-destructive disassembly of IGU's from a facade can be possible.
Patterson & Vaglio (2011) describes the challenges of retrofitting aluminum glazed facades. It states that the glazing joints which glue the glass to the framing units can be difficult to access and the separation of these components therefore can be hard. Unitized systems present challenges because of the way components interlock, making ad hoc removal difficult. Next to that an important barrier for retrofitting of façade elements is the need to move ongoing operations to another location. This increases costs and therefore makes it less interesting for clients. Designing in a way components can be removed or replaced on-site can be a solution to this problem.

2.6 Conclusion

The literature reviewed in this chapter gives insight in the current status and view of the circular economy. The CE aims to move from the fast replacement economy, which is referred to as 'take-make-dispose', to an economy in which systems are designed to regenerate themselves. Within this economy it is important for designers to focus on design for users instead of consumers. From the circular economy the ladder of R-strategies can be derived. In which the higher the strategy, the larger potential savings and reduction of environmental impact. In the building sector CE helps to focus on the life after the operational stage of a building. It turns out that circular principles are not yet embedded enough in the building industry. The reduction of waste in the industry requires more focus. Zoomed in to the façade as a system, the problem becomes clear where several materials with a different life span are combined and mixed with each other without taking this into account during the design phase. Since a complete system only lasts as long as its weakest permanent bonded connection, a single connection type can have a large impact on the total carbon footprint of a building. Design for Disassembly principles are named to be an important factor for moving to CE.
The research of Teeuwen (2023) shows that from all the materials currently used in Scheldebouw's façade systems, some stand out in terms of carbon impact. Mainly glass and aluminum are materials which have a large part in the total footprint of the façade systems. At the same time these materials differ 35 years in life expectancy, which means that permanent bonding of the two components will have large impact on the total carbon footprint of the building when glass needs replacement. Also, structural sealants and gaskets show a lower life expectancy. This chapter also describes research conducted by Hartwell et al. (2021) in which a variety in different stakeholders in the total life cycle of a façade system is interviewed. This research gives important insights on which part the focus should be when aiming for a circular system. It shows that the frame is likely to have the highest reuse potential. At this moment the demolition contractor has the largest influence on the circularity of a system which most of the time is not build for reclamation of components but for longevity and durability. Stakeholders mention lack of standardization as one of the challenges. Also, recent techniques in the reuse of glass from old IGU's shows the need for non-destructive ways to reclaim glass from old systems. The possibility to disassemble and replace components on site could make future retrofitting projects more feasible. In summary, a key finding of paragraphs 2.4 and 2.5 is the identification of the materials with a high carbon impact, which provides a

clearer focus for design strategies aimed at reclamation. Next to that the statements from steak holders help to identify barriers for achieving the high R-strategies during the complete process, naming the standardization as one of the most important.

3. DESIGN FOR DISASSEMBLY

This chapter describes the principles of Design for Disassembly (DfD). The goal is to provide insight into the objectives of DfD and the resources available to achieve them. The chapter offers an overview of the types of connections and the methods for disassembling them. It highlights the various techniques within DfD and discusses a framework that can assist in adhering to DfD principles. Finally, it examines other industries where DfD is applied and explores new technologies that can be derived from these applications.

3.1 Design for Disassembly, principles

As been shown in the previous chapter, Design for Disassembly principles play a vital role in the switch to CE in built environment and therefore also in façade systems.
DfD is a practice aimed at simplifying deconstruction processes through thoughtful planning and design. Deconstruction involves dismantling a building while preserving the usability of its materials. This approach fundamentally transforms the traditional waste management process. DfD serves as a key strategy for conserving raw materials and promoting sustainable practices (Rios et al., 2015). In many cases the different components in a product can last longer than the system as a whole. DfD focusses on connecting components in a reversable way, which should allow dismantling without reducing their remaining lifetime and their value. Dismantling requires also good accessibility. Also, a component should be dismantlable without the need to remove or damage other components. To make this process feasible it should be simple and little time consuming, in order to make it also financially worthy (cambier et al., 2019).

In summary DfD involves three targets:

1. Simplifying the de-manufacturing process,
2. Reducing needed time and cost for disassembly,
3. Allowing recovery of components and materials.

(Abuzied et al., 2020)

By applying DfD principles in early stages, it is possible to reclaim components with high embodied energy after the lifespan of a complete product. These products typically end up as waste; however, if components were designed for disassembly, only certain parts, or potentially nothing at all, would need to be discarded. As stated in the previous chapter, the Circular Economy emphasizes the elimination of waste as a key strategy for reducing emissions in the building sector. Enabling deconstruction and material recovery, alongside promoting the concept of Design for Disassembly (DfD), is essential for closing the loop on construction materials (Campos Soto, 2023).
Past studies have showed that the current obstacle for simple deconstruction lays in the design phase of a project (Rios et al., 2015) (Güngör, 2006). At this moment, buildings, and therefore also facades are designed without considering the end of life and the reclamation of building products and materials. Designers do often think their creation will be permanent and do not implement solutions for the end of its life span. In addition, the joints between these different components are becoming increasingly complex, which reduces the potential for reclamation and makes it more difficult to implement circular economy (CE) principles in building and façade structures (Rios et al., 2015).
Design for disassembly does not have a specific target at the circularity ladder which was showed in the previous chapter. There are different R-strategies that can be achieved using DfD. In fact, all strategies between R3 and R9 can be easier managed by using DfD principles. Like has been mentioned before, the higher the aimed R-strategy, the better its potential for efficiency of resources.

Various aspects and methods are shown to be important when considering Design for Disassembly. Güngör (2006) identifies two key principles:

1. **Minimizing the number of components in a product**: This approach can facilitate repairs and maintenance by making parts more accessible and allowing for quicker installation of new components. The same principle applies to the recovery of components, where the process can proceed faster with fewer fasteners and a reduced need for diverse tools.

2. **Using connectors that are easy to disconnect**: Not only the quantity but also the ease of disconnection plays a significant role. This requires the comparison and testing of different types of connection options to determine the most effective solutions.

Like stated before, contemporary façade systems contain a large number of different materials. These materials are needed to achieve the different performance requirements in terms of insulation, weather tightness, acoustics and durability. To change these materials or to find ways in which less material is needed for the same performance is hard but will in practice also be already in favor of a designer, who is designing for aesthetics but also minimum weight and costs of the system. For this reason, this research looks to the disassembly potential of these materials and components by focusing directly on the connections. Therefore, in the complete field of Design for Disassembly it is necessary to look deeper into the different connection types that can be identified. Next to that, guidelines and possible frameworks about disassembly processes of different connection types need to be reviewed.
Lastly, it is also important to look to other industries which are dealing with similar problems. Since industries tend to only focus on their own innovations and creating their own techniques, some might be a solution in the façade industry as well.

3.2 Types of connections

During product disassembly, a key activity is the unfastening of connectors. Unfastening involves disengaging a fastener's role within the product. This process removes the fastener, either with or without the use of tools, allowing the parts it held together to be separated. The way in which a connection is designed or used decides whether a product can be taken apart in a destructive or non-destructive way. Although, destructive ways of disassembly like cutting, breaking, or tearing are chosen more often, a non-destructive way should be chosen instead since the reclaimed components will be in better state and of higher quality (Güngör, 2006). This improves the potential for higher R-strategies.

The terms ‘fastener’ and ‘connection’ or ‘connector’ are interchangeably used in different literature. Although exact difference is not described, a fastener can be seen as a subset of a connection. Where ‘connection’ in most literature is used in broader context, ‘fastener’ is mostly used to refer to a mechanical fixing.

“A fastener or connector is described as a component employed between connected parts, which holds the mated parts together and establishes relative part location, alignment and orientation, transfers loads, and absorbs tolerances between the parts to prevent vibrations.” (Güngör, 2006)

One of the more comprehensive studies on connectors is done by Sonnenberg (2001). This research states that the disassembly process of connections depends upon:

- The type of fastener
- Type of connection
- Geometrical shape
- Size and material of fastener
- Variability of damage to fastener
- Arrangement of the fastener in any assembly

The research classifies connectors in five different categories:

1. *Discrete fasteners*: a discrete fastener is independent from the components it connects. It can consist of multiple parts and can be completely removed from the components it connects. Examples are nails, screws, bolts and nuts, rings or springs.
2. *Integral attachments*: integral attachments are connections which are integrated in the connected components which can be fastened by using a particular motion. This motion makes a certain interlocking or joining possible. These connectors don't always need tools for (dis)assembly.
3. *Adhesive bonding*: adhesive connections will use the principle of chemical reactions as method. As an advantage it can offer a more minimalist aesthetic, and in some instances, enable composite action between connected components. Although currently new technologies emerge where debonding of adhesives is tested, most used adhesives nowadays are not designed for reversible actions.
4. *Energy bonding*: energy bonding includes soldered or welded connections where the joints are melted or plasticized with an external energy source, for example inductive heating.
5. *Other connectors*: some types of fastening might not completely fall in one of the first four categories.

(Sonnenberg, 2001) (Güngör, 2006)

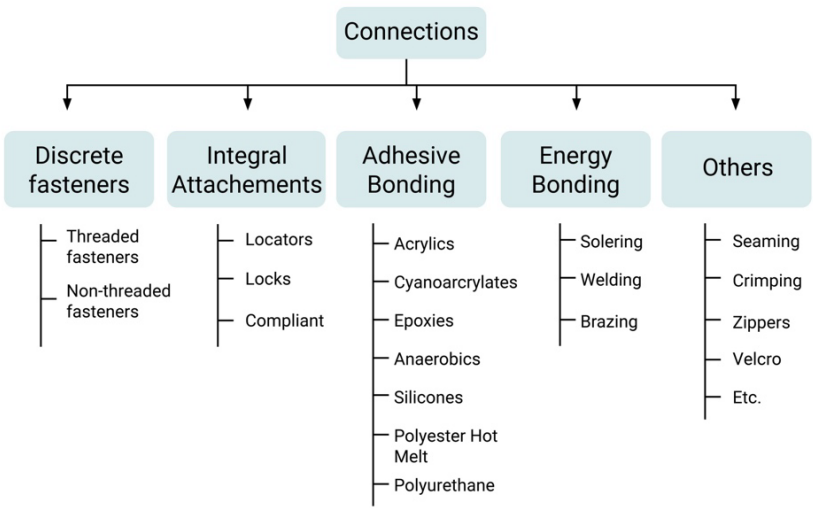

Figure 13: The different categories of connections (Sonnenberg, 2001) (adapted by author).

There are two different ways for the unfastening of these connection types written above:

1. Removal of fasteners, this process mainly appears in the first category of discrete fasteners.
2. Detachment, this mainly appears in the second group of integral attachments.

Both of these disassembly or 'unfastening' methods come with several barriers and issues. Using the method of complete removal of a fastener, the potential of disassembly

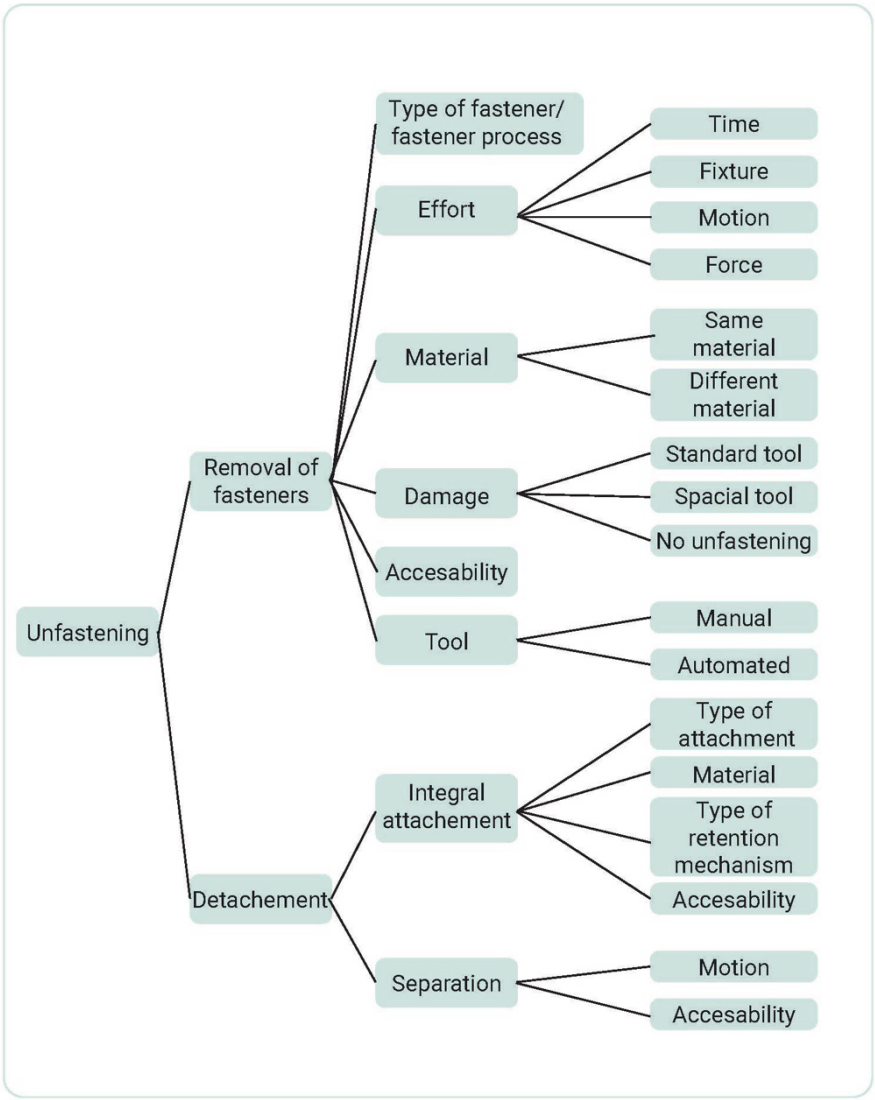

Figure 14: Ways for unfastening and their associated issues (Sonnenberg, 2001) (Image adapted by author)

mainly lays in the type of connector that is applied. Where a screw is designed for a reversible motion, a small nail is only designed for fastening and can only in certain situation, using force, be unfastened. Which bring focus to the second issue which is the needed effort. The needed effort for unfastening is dependent on how much time it needs, the strength of the fixture or difficulty of the motion and how much force needs to be applied. The type of material of a fastener also plays an important role and can have impact on the potential for disassembly next to that it has influence on the next issue which is the damage. In many cases connections are exposed to a lot of environmental

factors. In the case of façade systems, the weather conditions have crucial impact on the materials in a system. This can cause problems like corrosion or UV degradation. This can make non-destructive unfastening of connections more difficult. More force may be required, which can result in more damage like broken screwheads, which then requires the use of special tools. The type of tools is quite related to the accessibility of the connections.

The second method of detachment consist out of two types where the first one is separation. This can just be the simple lifting of sliding out of the fastening component. The other method is the unfastening of integrated parts. An example of a used integral attachment method is a so-called 'snap-fit' connection. These connections are popular because they reduce the number of parts in a system which reduces cost and assembly time.

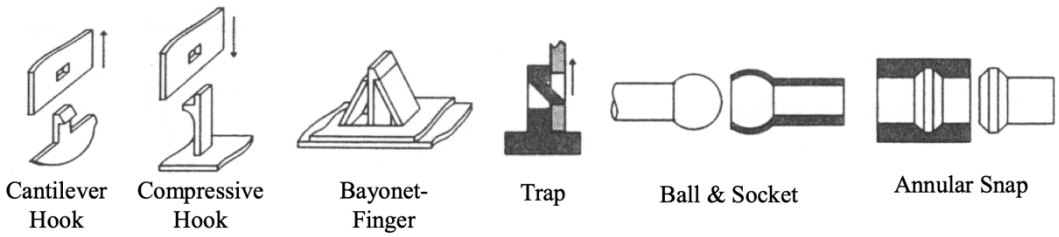

Figure 15: Examples of snap-fit connections (Shalaby, 2008).

Although Design for Disassembly focusses a lot of attention on the disassembly phase of a product, it is still important to give enough attention to the ease of assembly but also to the performance and durability of the design (Güngör, 2006).

3.3 DfD techniques

According to Abuzied et al. (2020) divides DfD techniques into two categories. The techniques described by Sonnenberg mainly consist of so-called *disassembly embedded design*. This category focusses on incorporating a mechanism specifically designed to facilitate the disassembly of a product.
The other category is called *Active Disassembly* (AD). Active disassembly allows for the separation of assemblies by utilizing smart materials or structures within the product that can be activated through one or more external stimuli. Through the use of these stimuli or external triggers like temperature, magnetic force or pressure, the connections in a product or system can be disconnected.

Disassembly Embedded Design can offer great time reductions during the disassembly phase. However, some drawbacks include the additional time and expertise required from designers during the design phase, the limitation of having to unfasten one connection at a time, and the need to develop multiple designs for all the different components. Next to that the accessibility is harder to achieve. In some of these situation

Active Disassembly may be a solution. It can allow a single technique in different situations. Next to that it can unfasten multiple connections at the same time. In theory it is possible to disassemble or disconnect a complete system at the same time by using one single trigger. For example, when using Disassembly Embedded Design techniques, disassembly typically requires a specific tool or motion to unfasten each connection individually. However, if it were possible to place an entire subset of components in -for example- warm water, all connections can be triggered and released simultaneously. This eliminates the need for different tools or large physical efforts and reduces the needed time (Abuzied et al., 2020).

The field of research about Active Disassembly (AD) is emerging recent years and is based on the use of Shape Memory Alloys (SMA) or Shape Memory Polymers (SMP), which can revert to their original shape when exposed to specific conditions, using *active disassembly devices* (Abuzied et al., 2020).
SMA and SMP are both so-called 'smart materials'. These materials have the ability to transform their dimensions in different environmental stages. Both of these materials have two different phases, a low temperature phase (martensite) and a high temperature phase (austenite). When these smart materials are heated above a certain temperature it will transform back to an original shape. Therefore, these materials can be used to produce these active disassembly devices. These devices can exist out of different shapes. SMA has a quite low deformation in heated conditions and can be produced in the shape of tube, cotter pin, splint pin, coil- spring, ribbon and rivets. SMP has a larger deformation because it loses its mechanical strength during heating. This can be used for rivets, snap-fits, washers, and screws. These devices can lead to two types of AD techniques for joints to initiate disassembly: joints based on material properties, and joints based on structural properties (Abuzied et al., 2020). Figure 16 shows some examples of these type of joints.

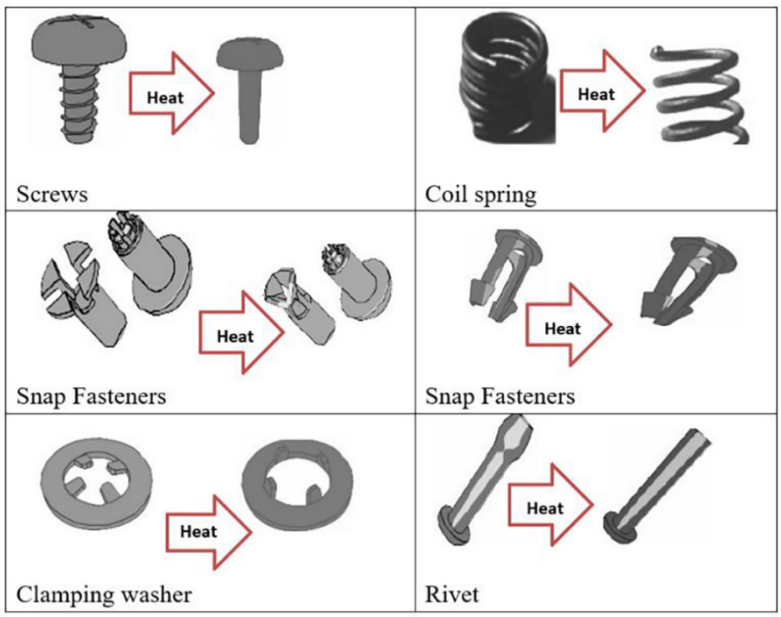

Figure 16: Different forms of SMA/SMP active joints (Abuzied et al., 2020).

Where material-based joints will change their shape to as an effect of a specific temperature trigger to initiate disassembly, a joint based on structural properties uses a specific geometry or shape to initiate disassembly. Shalaby (2008) designed a snap-fit connection in which the geometry changes after applying a certain temperature, resulting in removing the interlocking part. This way the two parts can be separated from each other and be dismantled.

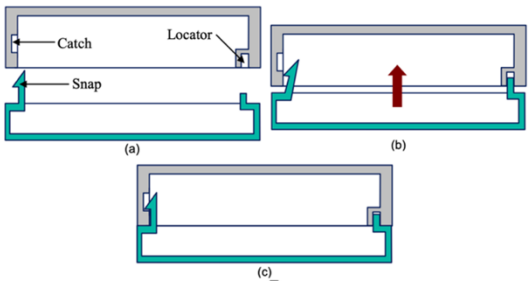

Figure 18: assembly of 'locator-snap system (Shalaby, 2008).

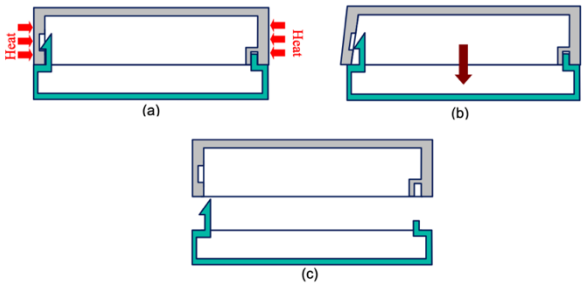

Figure 17: Disassembly of locator-snap system using heat (Shalaby, 2008).

3.4 Guidelines for DfD

Literature about DfD shows that in the past two decades several guidelines and frameworks have been assembled which can help during the design process of certain products. No frameworks have been created in which the specific unitized façade system and in particular the connections and fasteners in a system should be designed for disassembly. Therefore, a guideline should be used which also focusses on the on the DfD principles of a product in which similarities can be found. Although this framework cannot be applied directly to the design process of a façade unit, it can help with applying certain principles and strategies during research. A general disassembly framework for enhanced reclamation of façade components has been created by Droste (2023). This research gives an overview of how reclamation potential, disassembly potential and a user output could be combined to increase potential for material recovery.

A comprehensive framework or 'map' has been created by De Fazio et al. (2021). The so-called 'Disassembly Map' is created to guide the design phase of products and shows different routes to target components in a system. And however it is created to focus on increasing the potential of repairability, it does not mean that it can't be used in achieving any of the other R-strategies mentioned in Chapter 2. As the research states, it can be used in targeting components with high failure rate, high embodied carbon, or economic value. The research uses elements based on the ease of Disassembly Metric (eDiM) (Peeters et al., 2018) and the Maynard Operation Sequence Technique (MOST) (Zandin, 2002). These will be further explained in Chapter 3.
The method uses four parameters to create the disassembly map:

- Disassembly depth/sequence
- Disassembly time
- Type of tools
- Fasteners reusability

The method developed by De Fazio et al. consists of seven key features for visualizing and analyzing disassembly processes. These include:

1. **Logic Representations** – Defines disassembly dependencies (sequential, independent, or multiple).
2. **Cluster Blocks** – Groups components with similar end-of-life or failure characteristics to simplify disassembly.
3. **Alternative Sequences** – Maps multiple possible disassembly routes.
4. **Action Blocks** – Indicates the type of motion and force required for disassembly actions.
5. **Action Block Coding** – Categorizes motions (hand, single-tool, or multi-tool) and force levels (low, moderate, high) with color-coded symbols.
6. **Disassembly Penalties** – Identifies design challenges such as hidden connectors, uncommon tools, or non-reusable parts.
7. **Target Component Indicators** – Highlights components critical for replacement or recycling.

The framework enables a clear visualization of the full disassembly process and was validated through the redesign of a vacuum cleaner visible in Figure 19.

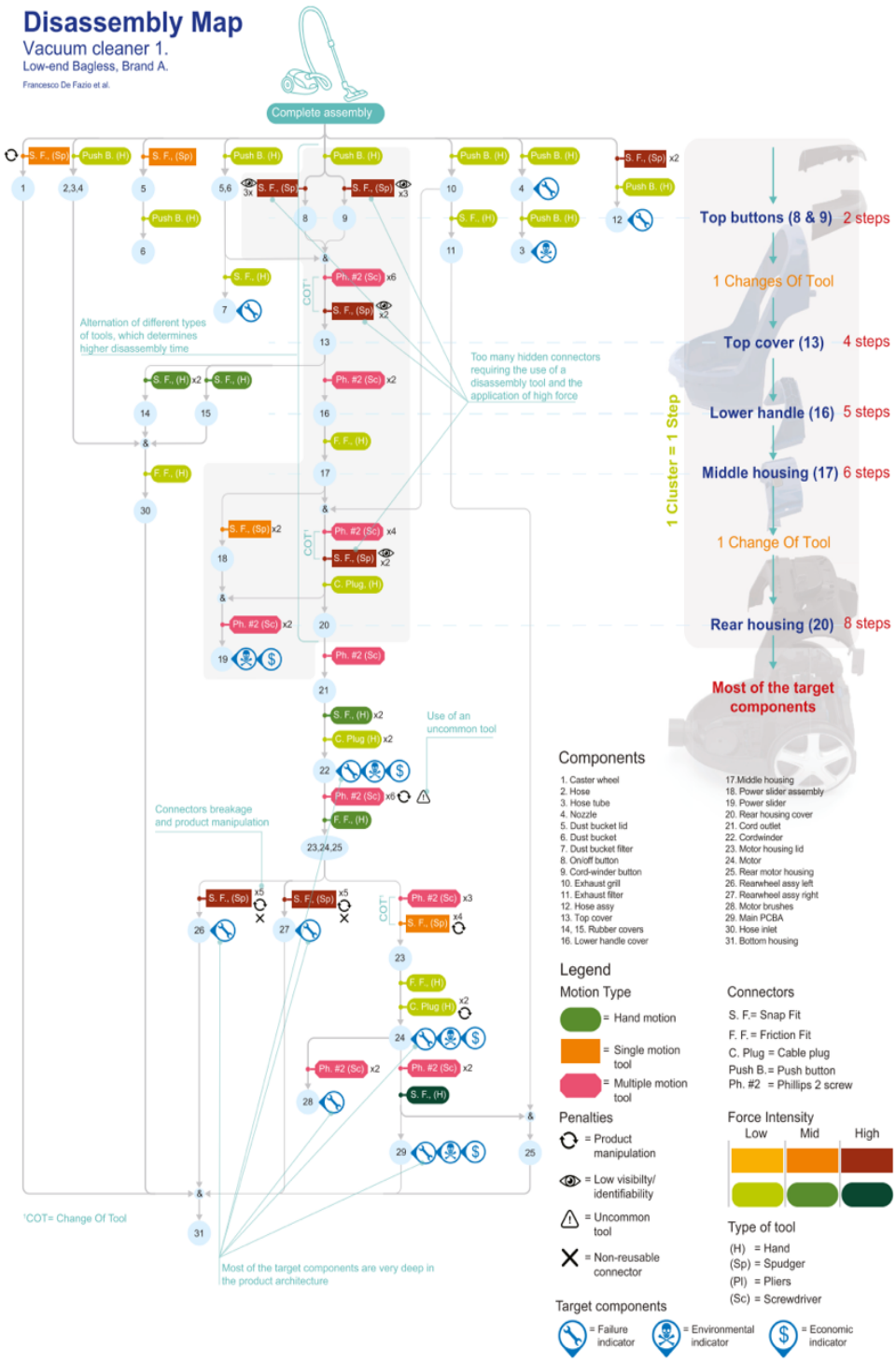

Figure 19: Disassembly Map of original design of vacuum cleaner by De Fazio et al. (2021).

3.5 Applications of DfD techniques in other industries

To get a better understanding of the practical application of DfD principles in products and systems it is possible to look beyond the market and industry of the built environment. The low rate of application of DfD principles in current building and façade design does not necessarily apply to other design fields. Other industries already started applying DfD several years ago. Principles in connections from these industries could be interesting for the design of connections in facades as well.

Automotive industry

One industry applying DfD as well is the automotive sector. Rising productions of vehicles in the past decades raised the concerns about the environmental impact. The joining solutions with the characteristic off rapid disassembly is considered as key technology driver (Lu et al., 2014). The automotive manufacturers are, like façade manufacturers, facing challenges of connecting dissimilar materials while trying to maintain mechanical and durability requirements, especially in structural applications. Adhesive bonding is used in greater extend due to its advantages like weight savings, prevention of corrosion, uniform distribution of stress larger applications of various materials and relatively high impact resistance. Applications of these adhesives reach several fields of the manufacturing process of vehicles which can be divided to:

- Sealants for body joints
- Spot welding sealants and tapes
- Anti-flutter bonding and structural adhesive bonding
- Hem flange sealing

This also increased the research for methods for disassembly of adhesives bonded joints.

Lu et al. (2014) describes the rising research to thermally removable adhesives. Also, it describes the research to electrochemical reduction of an adhesive. Which can be applied by adding certain polymers to an adhesive. Adding an electric current to this adhesive will lead to scission of the polymer and therefore lead to degradation. One of the prominent names in this field of research is called ElectRelease and exist of a series of structural epoxy adhesives that can be dismantled quite easily by applying an electric current of 10-50V. This is achieved using a metal conductor along the joint. This development has triggered interest in research for electrically assisted debonding adhesive techniques and its potential in the automotive industry.

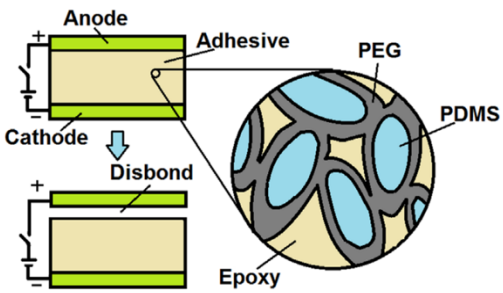

Figure 20: microscopic structure of ElectRelease principle (Lu et al., 2014).

Earlier in this chapter the use of so-called smart materials like SMA and SMP was mentioned. Jones et al. (2002) investigated the possibility to use smart materials to disassemble glazing from automotive vehicles. By integrating actuators into a host product, the product casing can be designed to separate upon activation by a heat trigger, enabling the recovery of internal components. SMAs, like Nickel Titanium (NiTi), can be fashioned into compact actuators without additional moving parts. For instance, when shaped like a coiled spring, they remain completely inactive within the product casing but can extend when a specific temperature stimulus is added. Both the use of SMP and SMA was investigated. The disassembly method using SMA was found a success, where the glass was placed in a channel and clipped using SMA clips. These clips would unroll and drop off the assembly when they were heated, making it possible to release the glass window (Jones et al., 2002).

Electronic devices industry

Shalaby (2008) describes an example of the use of smart materials in electronics. Products like an LCD Display could be designed by integrating Smart Memory Alloy in order to use heat for disassembling components. In Figure 21 a washer is designed to expand when it is heated. Releasing the screwhead and therefore make it able for two parts to be separated. This technique was used in LCD displays and TV's.

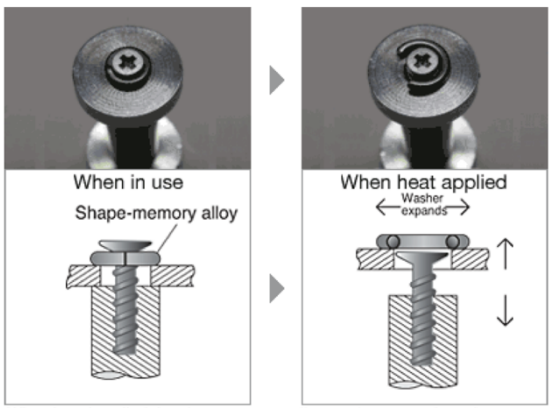

Figure 21: Shape memory alloy concept (Shalaby, 2008).

Adhesives

Adhesives are made from polymers to give them their flexibility. The positive side of adhesives is that they can be used for joining a wide variety of materials and a combination of different materials. Next to that adhesives are lighter and are mostly cheaper than mechanical connections. But also, in the field of adhesives there is a need to create a reversible product. Adhesives can be divided in two types:

1. *Permanent adhesives* are adhesives which are mainly used in a structural bonding. This means that the success of the assembly depends on the strength of the bond. These adhesives are challenging to disassemble and also are hard to use during repair situations where humidity and temperature can't be regulated that easily.

2. *Debondable adhesives* are not as strong as structural adhesives but can be used to bond delicate materials.

Bibi et al. (2023) gives several examples of debondable adhesives:

- Photo-debondable adhesives
- Thermally debondable adhesives
- Adhesives with magnetic debonding
- Ultrasonic debondable adhesives
- Electrically debondable adhesives

This research mentions the possibility for especially electrical debondable adhesives as a way to promote recycling and lower the amount of waste. This mainly because it can be triggered remotely without the need for direct access to a connection.
In the end practically every adhesive is debondable because all polymers will decompose because of heating. But at the same time this may be a weakness during the service life of a complete system when this stimulus will be used as debonding technique. A lot of studies focus on photo-debondable adhesives(Bibi et al., 2023) (Mulcahy et al., 2022).
For the same reason as mentioned for thermally debondable adhesives, this type of stimuli can be a problem. Most debondable adhesives are based on the current techniques for adhesives by using modified monomers or additives. These approaches typically require minimal alterations, have limited impact on adhesion performance. Therefore, these techniques are not so expensive compared to existing adhesives. The further development of these adhesives will certainly play a role in the recyclability of future products (Mulcahy et al., 2022).

3.6 Measurement methods

When designing a product or system using DfD principles it can be hard to prove the complete design is easier to disassemble than the previous design. Measuring requirements like thermal performance, acoustic performance or water tightness, a simple test can be conducted where electronic devices or sensors can be used to give a clear output which can be compared with the previous output. To evaluate a product in its ease to be disassembled special measurement or evaluation methods need to be used. These methods need to make it able to give certain connection methods a clear rating so these can be compared with another connection method. As been stated before, ease of disassembly depends on a variety of different factors. Therefore, an evaluation method is needed which includes various factors and combines these with each other to create a clear single output. Over the years several of these methods have been created. Although specifically in façade systems no measurement methods for DfD could be found yet, also methods design for other industries, like ones mentioned before may be used. For this research two have been reviewed which could help on validating disassembly of connections in particular.

3.6.1 DGBC method

The first measurement method described is created by the Dutch Green Building Council and publicized in (van Vliet et al., 2021). This report describes a way to measure the potential for physical disassembly. It uses the basic principles of connections and fasteners also described by Sonnenberg (2001). Disassembly potential of connection (DPc) in this research uses several factors. For the connections itself it uses:

- Connection type
- Accessibility of connection

For compositional disassembly potential (DPcp), which focusses on how easy a complete product can be disassembled it uses:

- Independency
- Geometry of product edge

These factors play a vital role in the existing situation of a component when it needs to be disassembled unexpectedly or at the end-of-life. These basic factors can create a complete score or ranking for disassembly of the total product by combining them.

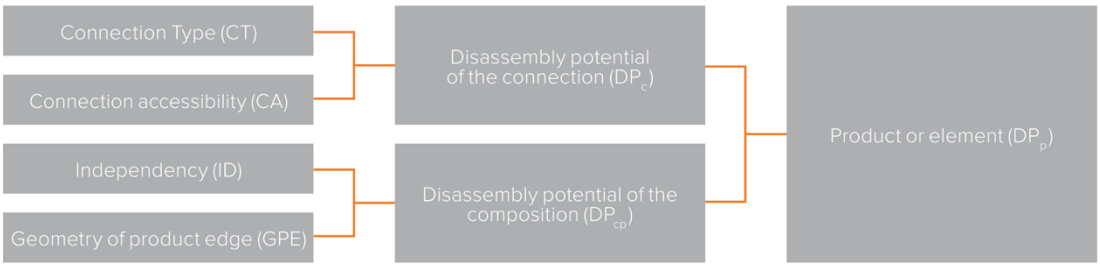

Figure 22: step-by-step plan for assessing disassembly potential of product (van Vliet et al., 2021).

First the *connection types* are ranked. These connection types are also divided in five different categories in which the types can get a score between 0 and 1. These are then expanded by describing most common fasteners used in the construction industry. If a system contains a connection that has not been mentioned in this table, it can be evaluated using an equivalence principle. Next to that new techniques can create ways in which a chemical connection may be disassembled as easy as a dry connection. In that case the technique may be rated using the same equivalence principle.

Secondly the accessibility of a connection is ranked. Accessibility plays a role in the possibility to reach the connection by hand or tool. If accessibility is good, the connection is easily reachable without the need to damage other parts. Again, accessibility has been ranked in several categories.

Connection type (CT)		Score
Dry connection	Loose (no fastening material)	1,00
	Click connection	
	Velcro connection	
	Magnetic connection	1.00
Connection with added elements*	Bolt and nut connection	0,80
	Spring connection	
	Corner connections	
	Screw connection	
	Connections with added connection elements**	
Direct integral connection	Pin connections***	0,60***
	Nail connection	
Soft chemical connection	Caulking connection	0,20
	Foam connection (PUR)	
Hard chemical connection	Adhesive connection	0,10
	Dump connection	
	Weld connection	
	Cementitious connection	
	Chemical anchors	
	Hard chemical connection	

Figure 23: connection types and score according to Van Vliet et al. (2021).

Connection accessibility (CA)	Score
Freely accessible without additional actions	1.00
Accessible with additional actions that do not cause damage	0.80
Accessible with additional actions with fully repairable damage	0.60
Accessible with additional actions with partially repairable damage	0.40
Not accessible - irreparable damage to the product or surrounding products	0.10

Figure 24: Accessibility of connections (van Vliet et al., 2021).

By using these two factors the disassembly potential of a connection can be calculated using:

$$DPc_n = \frac{2}{\frac{1}{CTn} + \frac{1}{CAn}}$$

In which:
DPc_n = disassembly potential of the connection of n product or element n:
CT_n = type of connection of product or element n;

CA_n = accessibility connection of product or element n.
The third factor, independency, focusses on the fact if a part or component is integrated in another element. Large integration can lead to more needed actions for disassembly and can lead to disassembly of other parts. Independency is ranked by van Vliet et al. in three categories.
Lastly the geometry of a component plays a role in the disassembly potential. van Vliet et al. describes it as the ability of a component to interlock itself in the surrounding parts using the shape of its edges. Interlocking of components can have large impact on the total disassembly potential and is described as GPE (Geometry of Product Edge). It is ranked in three different categories.

Independency (ID)	Score
No independency - modular zoning of products or elements from different layers.	1.00
Occasional independency of products or elements from different layers.	0.40
Full integration of products or elements from different layers.	0.10

Figure 26: valuation of independency (van Vliet et al., 2021).

Geometry of product edge (GPE)	Score
Open, no obstacle to the (interim) removal of products or elements.	1.00
Overlapping, partial obstruction to the (interim) removal of products or elements.	0.40
Closed, complete obstruction to the (interim) removal of products or elements.	0.10

Figure 25: Geometry of product edge valuation (van Vliet et al., 2021).

Figure 27: Schematic view of geometries interlocking, leading to obstruction of removal (van Vliet et al., 2021).

In Figure 27 examples of how geometries can play a role in interlocking of parts which may lead into the need for disassembling multiple parts, leading to a decrease of the score of the DPc_n and therefore the total disassembly rating.
The disassembly potential of composition DPcp can now be calculated using:

$$DPcp_n = \frac{2}{\frac{1}{IDn} + \frac{1}{GPEn}}$$

In which:
$DPcp_n$ = disassembly potential of the composition of element n:
ID_n = independency product of element n;
GPE_n = geometry of the product edge of element n.

The total formula of the measuring of disassembly potential can then be written as:

$$DPp_n = \frac{4}{\frac{1}{IDn} + \frac{1}{GPEn} + \frac{1}{CTn} + \frac{1}{CAn}}$$

3.6.2 eDim method

Another measurement method is a method created by Kroll & Hanft (1998). This method focusses on objectively quantifying the ease of disassembly of products. Although this research uses the example of the industry of electronic devices, it states that the method also could be used in other industries.

- *Accessibility:* Accessibility refers to the location of a part in the system and measures the ease a part or component can be reached by hand or tool.
- *Positioning:* the degree of precision is needed to reach a product with a tool or hand. Reaching a small screw for example can be more difficult than grasping a large part.
- *Force:* the amount of force that is required to perform a task.
- *Base time:* the time that is needed to perform a task.

The method has been developed into the so-called 'Disassembly evaluation chart'. In this chart the different tasks during the disassembly process can be sequentially recorded and assessed on different rows.
Providing quantitative design feedback was determined to be essential according to Kroll (1996). Ranking the ease of a task with a scale of 'good – moderate – bad' for example would not be sufficient when considering different difficulty factors. For example, if the required force is low but accessibility is poor, what would the average score be? That is why time has been chosen as the difficulty score. After all, difficulty in positioning or reaching a component takes more time, as does applying more force.
There are two different ways of calculating the disassembly time. The first way is to measure the exact time during practical disassembly processes. This however was found to be difficult and not always possible. Therefore, several methods were created to rating ease of disassembly by calculating the efforts needed to disassemble a product and extracting components (Vanegas et al., 2016).

The principle of Kroll and Hanft in the 1990s led to a new measurement system created by Vanegas et al. (2016), later referred to as 'ease of Disassembly metric' or 'eDim' (Peeters et al., 2018). This measurement method is based on the same difficulty ratings and uses **MOST: Maynard Operation Sequence Technique.** MOST is a measurement technique that is widely accepted in a large variety of industries. MOST is based on activities which are so-called 'standard sequences'. These sequences are divided in a basic set of motions which are given a letter.

A refers to a horizontal action of gaining control
B refers to a physical move in vertical direction
G refers to gaining control

P refers to the action of placement
L refers to the action of loosening

To each letter a numerical index is added which designates the performance time of this 'sub activity'.

A basic 'remove' task can then be created by the sequence A_1 B_0 G_1 A_1 B_0 P_1 A_1

A_1 = moving to loose part with hand
B_0 = no body movement needed
G_1 = gain control of the part
A_1 = move the part to another location
B_0 = no body movement needed
P_1 = place the part on new location
A_1 = return hand(s) to assembly

Once the sequence is completed the performance time in TMU (time measurement units) can be calculated. MOST method defines 1 TMU = 0.036 seconds. The total time performance can then be calculated by summing up all the indices of the different parameters and multiplying by 10:

(1+0+1+1+0+1+1) * 10 = 50 TMU

50 TMU * (0.036 s/TMU) = 1.8 seconds

The same way a basic sequence for tool use can be created which is described in Figure 28.

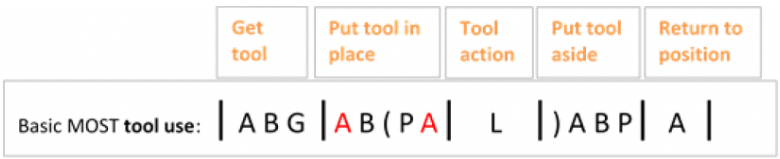

Figure 28: Basic sequence for tool use using MOST (Vanegas et al., 2016).

In the table in Figure 29, the different indexes are elaborated based on the range of steps that is needed within the sub activity.

General Move (A B G A B P A)					
Action distance (A)	**Body Motion (B)**	**Gain Control (G)**	**Placement (P)**	**Index**	**Time (s)**
< = 5 cm			Pickup / Toss	0	0
Within reach		**Grasp** Light Objects (simo^2)	**Put**: Lay aside / Loose fit	1	0.36
1-2 steps	Sit / Stand / Bend and Rise 50%	**Get** Light Objects Non-simo / Heavy or Bulky / Blind or Obstructed / Disengage / Interlocked / Collect	**Place:** Loose fit blind or Obstructed / Adjustments / Light Pressure / Double Placement	3	1.08
3-4 steps	Bend and Rise		**Position:** Care or Precision / Heavy Pressure / Blind or Obstructed / Intermediate Moves	6	2.16
5-7 steps	Sit or Stand with Adjustments			10	3.60
8-10 steps	Stand and Bend / Bend and Sit / Climb On or Off / Through Door			16	5.76

Figure 29: General move card, (vanegas et al., 2016).

Based on previous studies and observation of manual disassembly processes, the eDim method identifies six basic disassembly tasks:

- **Tool change:** picking up a tool and putting it back.
- **Identifying connectors:** refers to the needed time to identify the location of a fastener and to decide which type of tool needs to be used. The ease of identification is also related to manipulation requirements of the product.
- **Manipulations of product:** does the product need to be turned or do other components need to be removed to access certain connections.
- **Positioning:** the action of positioning a tool at a connection before starting the disconnection task.
- **Disconnection:** time for disconnecting a fastener.
- **Removing:** time to remove separated component and replace it to new location.

Vanegas states that the proposed categorization does not consider inefficiencies in the disassembly process, such as time lost on failed disconnection attempts or unnecessary actions. Since these actions are neither standardized nor repetitive and vary by individual, they are linked to the process rather than the product itself.

All of these six basic disassembly tasks are modelled using MOST to determine the needed time. For this model some assumptions should be made regarding the starting position, setup, pre-defined sequence, and availability of the tools.

An example of a table with reference time created by Vanegas is shown in Figure 30.

Disassembly task	Description	Sequence	TMU	Time (s/task)
Tool Change	Fetch and Put back	|A1B0G1|+|A1B0P1|	40	1.4
Identifying	Localising connectors			
	Visible are > 0.05 mm^2			0
	Hidden: visible are < 0.05 mm^2	|T10|	100	3.6
Manipulation	Product handling to access fasteners	|A1B0G1|+|L3 |	50	1.8
Positioning	Positioning tool onto fastener	|A1B0P3A0|	40	1.4
Removing	Removing separated components	|A1B0G1| + |A1B0P1|	40	1.4

Figure 30: Example of reference time for different disassembly tasks for small electronic products (Vanegas et al., 2016).

After this, a table need to be created in which each disconnection method for different fastener is given a sequence (example in appendix 2.4). Lastly a calculation sheet can be filled in, from which the total score can be derived and the ease of disassembly of two systems can be compared.

3.7 Conclusion

This chapter gives insight in the principles of DfD techniques. DfD focusses on simplifying deconstruction processes by thoughtful planning and design. The targets of DfD are to increase the possibility of recovering materials and components by simplifying the de-manufacturing process and reducing its needed time and costs. DfD principles should be implemented in an early stage of designing a system. Using thoughtful designs for connections can help reaching DfD principles. Several types of fasteners and connections are reviewed and listed which gives an overview of available options when designing to combine components. This list brings two ways of unfastening which are complete removal of connections or detachment. It shows that several issues can play an important role, like the accessibility of a connector, the needed effort or the required tools. There are two techniques in DfD which are *disassembly embedded design* and *active disassembly*. Active disassembly opens the way to the use of smart materials. Since these are dependent on heat as stimuli, they are not always applicable. A guideline from De Fazio et al. (2021) is reviewed and gives an overview of how a system can be visualized in terms of disassembly potential. Although this framework uses electronic devices as case study, it shows how the barriers in a system can be identified and offers the overview of where potential improvements can be made. The automotive industry and electronics industry are examples of where also DfD principles are implemented. Although these industries have a completely other character than the façade industry, they both focus on investigating new techniques to increase the potential of disassembly.

It is important to state that this research and the redesign described in later chapters is using the method of *disassembly embedded design*. The reason for this is mainly the fact that most applications of smart materials are primarily focusing on research purposes. Therefore, smart materials nowadays are hard to come by and might be expensive to apply in large scale projects. For this reason, in holistic research like this it is hard to aim for *active disassembly* options since the exact connections to target are not yet completely clear. However, future research involving the potential of smart materials in all fields of disassembly to improve reclamation potential of components, also in facades, is recommended. Future research could focus on a specific, predefined connection and adopt a more linear research approach, rather than a holistic one.

Finally in this chapter, two different methods for measuring the ease of disassembly are reviewed. The first method, developed by DGBC, is relatively simple and uses predefined tables to assign scores based on different difficulty levels. Due to its simplicity, its effectiveness in comparing complex systems, such as façade units, remains uncertain. Moreover, the method is demonstrated using relatively basic construction examples, which may not reflect the complexity of real-world façade systems. The second method, known as eDim, is more detailed and focuses on the actual time required to perform specific disassembly tasks. It is based on the MOST (Maynard Operation Sequence Technique) system, which calculates precise Time Measurement Units (TMUs). Because of its higher level of detail, eDim may be better suited for assessing more advanced systems like façade units. However, it also demands significantly more time and effort to apply. Both methods could be relevant to this research. Their actual applicability to façade design will become clearer during practical implementation.

C. PRACTICAL RESEARCH

4. CASE STUDY: ABN AMRO FAÇADE PANEL

Chapter 4 shows the case study used in this research which is the design of the façade of ABN AMRO building located in Amsterdam. As mentioned in the research framework, a real-life design process could help for identifying key challenges for improving reclamation potential. An introduction about the system is given after which the service life of the different components is analyzed. Then the disassembly potential of components is determined after which the reclamation potential of different components is further investigated. Finally, the experiment of the practical disassembly process of this panel is described and conclusions are drawn from it.

4.1 Introduction ABN AMRO facade

In order to find ways to higher the reclamation potential of components and to increase the possibilities for disassembly, this research, in collaboration with Scheldebouw, uses an existing façade as case study. The aim is to find out how the current panels can be adapted in order to make reclamation of components possible and to investigate how connections can (re)designed in a way that future disassembly and therefore adaptability and reclamation is possible. The façade is currently attached on the building of ABN AMRO headquarters located in Amsterdam, The Netherlands. The façade is designed and built in the 1990s and was one of the early designs of a so-called 'active wall' in which air flow is possible through the cavity inside the panel. The purpose of this design is the possibility to take the air inside the office in at the bottom of the panel and return the air at the top of the panel to the climate system. This way the energy demand of a building will decrease. Sun shading (venation blinds) is incorporated into the internal cavity. The sun shading is therefore significantly less exposed in comparison to being placed at the facade exterior leading to reduced maintenance requirements.
The panel is now over 25 years old, meaning some components may be reaching the end of their service life, while others may still be functional. Next to that the panels aesthetics could be considered outdated in contemporary building designs.

Figure 31: Facade of ABN Amro building (image by author).

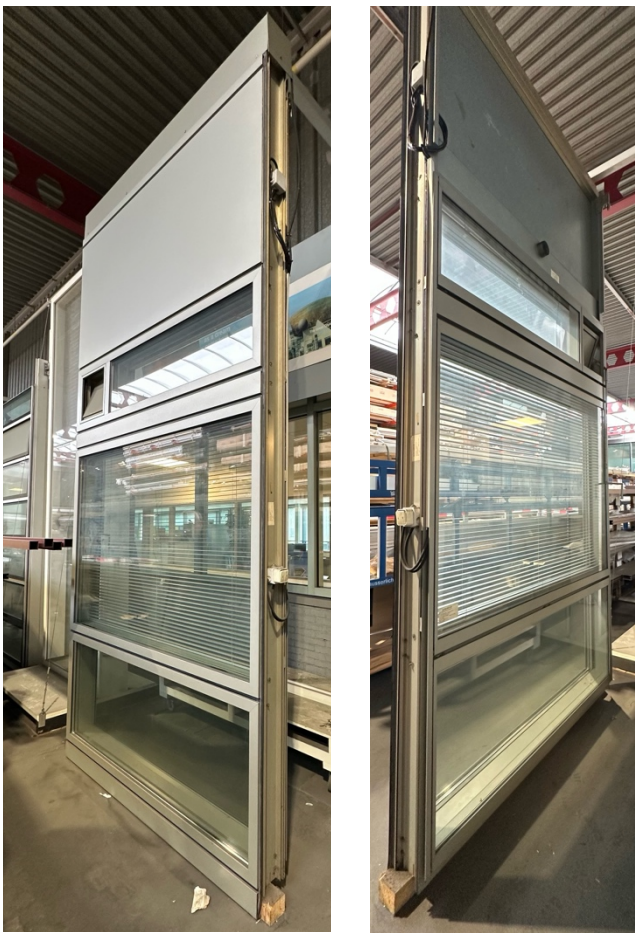

Figure 32: Outer side (left) and inner side (right) facade panel ABN Amro (image by author).

Although this panel has been assembled 30 years ago, the ways of connecting components can be considered the same as contemporary systems. Geometry of

extrusion types, types of screws and aesthetical decisions may be different from the systems Scheldebouw builds today, but most assembly methods have not been changed over the last two decades.

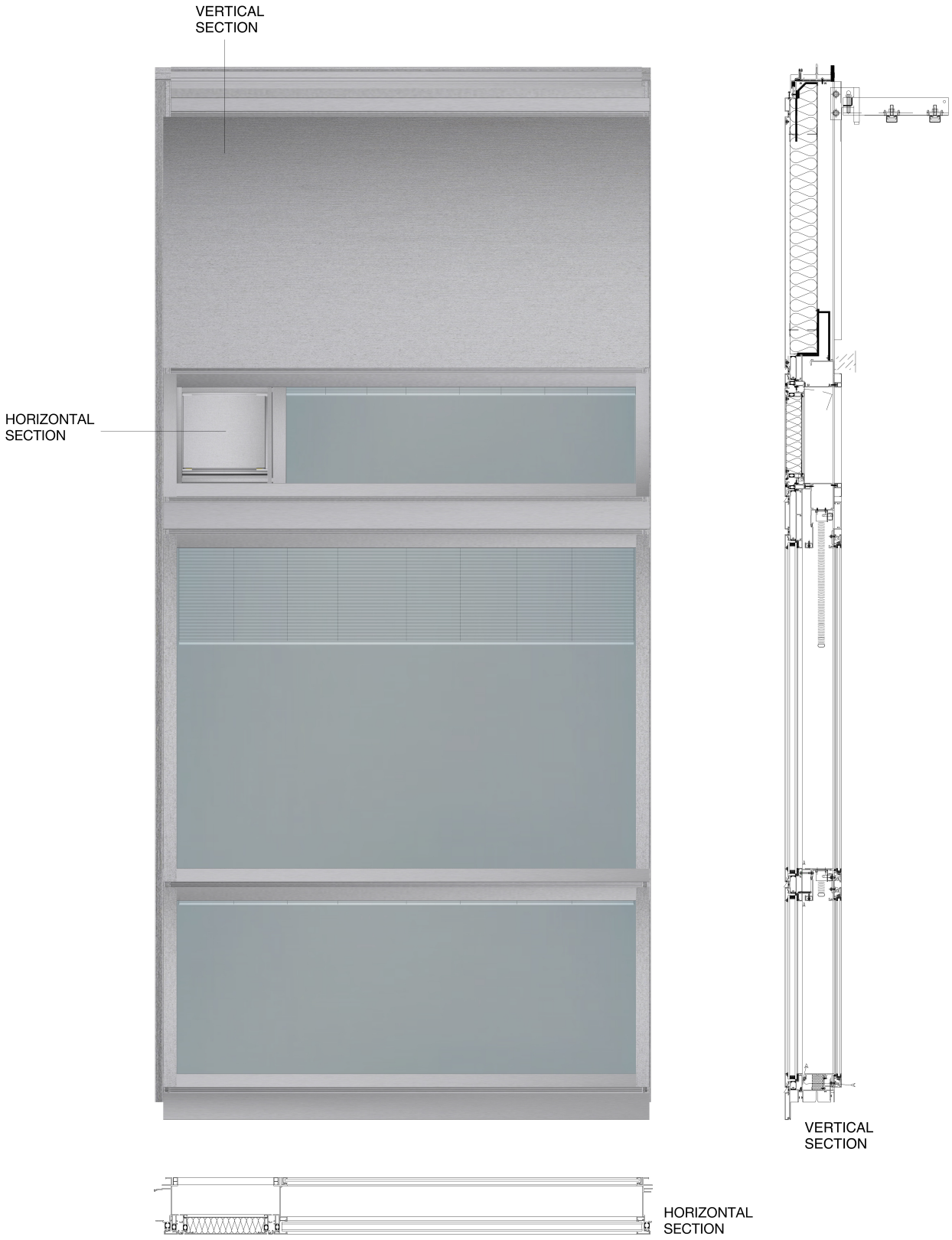

Figure 33: Section 1:20 existing ABN AMRO panel (image by author and adapted from Scheldebouw).

In Figure 33 a 1:20 section of the panel is shown in which the cavity, provided with sun shading is visible. See appendix 1.1 for 1:5 details. The panel has three transparent sections in which three separate insulated glass units are installed. These are connected to an aluminum frame with silicone sealant and clamped by aluminum cover caps. The opaque section exists from a steel sheet on the inside and an aluminum sheet on the outside and Rockwool insulation in between. Next to the upper IGU there is a small openable panel which allows some natural ventilation into the building. On the inside of the panel single glass windows are installed. These single glass plates are interlocked with sealant in aluminum window frames. All three of these windows are fitted with steel hinges and locks that are installed on the bottom or top side of the window frames, in order to make cleaning and maintenance inside the cavity possible.
The buildup of this panel can be divided in separate parts. First of all, the aluminum frame is assembled with the use of screws and silicone sealant, further specified in Chapter 5. The frame exists of several different extrusion types. Two extrusions, a male and female profile, are used as mullions. The frame has five transoms which are all different and exist out of different profiles. These transom profiles are fastened to each other by interlocking and screw connections.

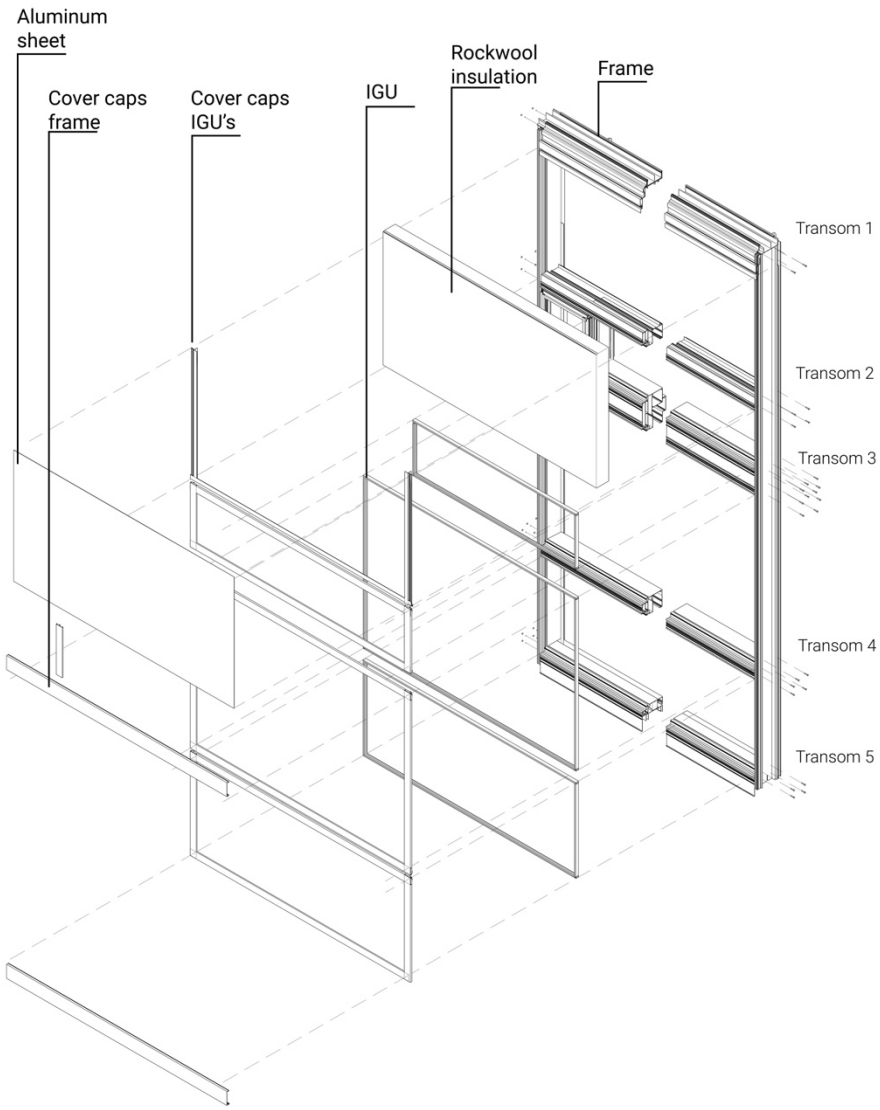

Figure 34: Exploded view panel from outside (image by author).

From the back side of the panel the steel sheet can be connected with to the transoms the use of bolt-nut fastener and are also fastened to the mullions with screws. From the inside, glazing beads are installed in a snap-fit connection with the mullions.
The different insulated glass units are connected from the outside of the panel by applying silicone sealant on the glazing beads. After this, the cover caps can be installed using a snap-fit connection with the transom profiles, clamping the IGU's in place. Gaskets are the applied to keep these in place and to secure weather tightness.
The aluminum profiles for connecting the aluminum sheet are attached to the mullions using screws after which the sheet can be connected through an interlocking geometry. The sheet is then secured on the top by screws.

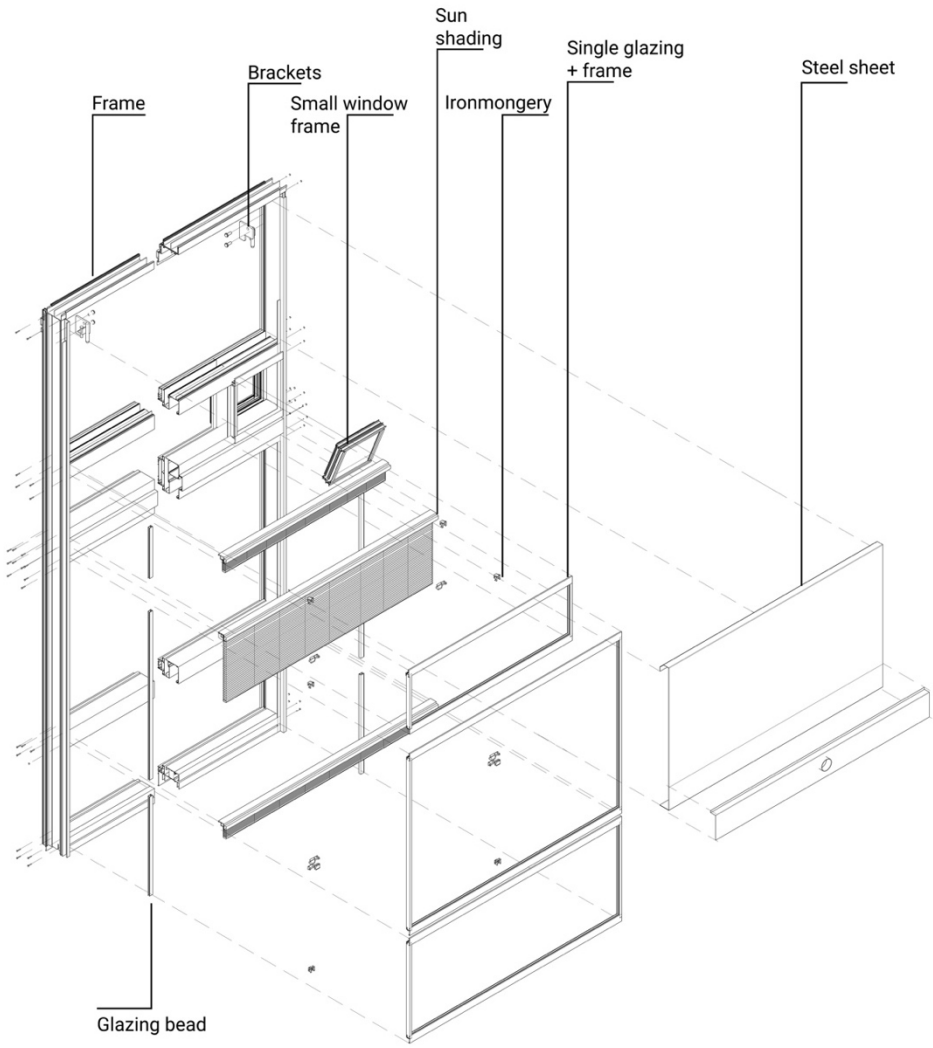

Figure 35: Exploded view ABN AMRO panel from inside (image by author).

From the inside of the panel the hinges and locks for the single glass units can be fastened to the frame with screws. Sun shading can be installed with screws and bolts. After the frames are assembled, the single glass plates are assembled inside with the use of structural sealant. These units are then be assembled to the hinges on the frame using screws.

After assembling the small openable window frame, it can be attached to the hinges on the frame.

4.2 Service life components

The components in this system are all connected in different ways and are made from different material types of which the service life span is far apart from each other. To find out what the different reclamation options are, and which type of R-strategy can be applied to different components, an analysis of the service life is needed. In the analysis underneath, the different expected service life spans of components are stated which are based on previous projects of Scheldebouw, Scheldebouws own estimation, and the estimation of manufacturers of the separate components. Next to the expected service life, the number of current service years is noted and the warranty on the component given by Scheldebouw to the client is noted.

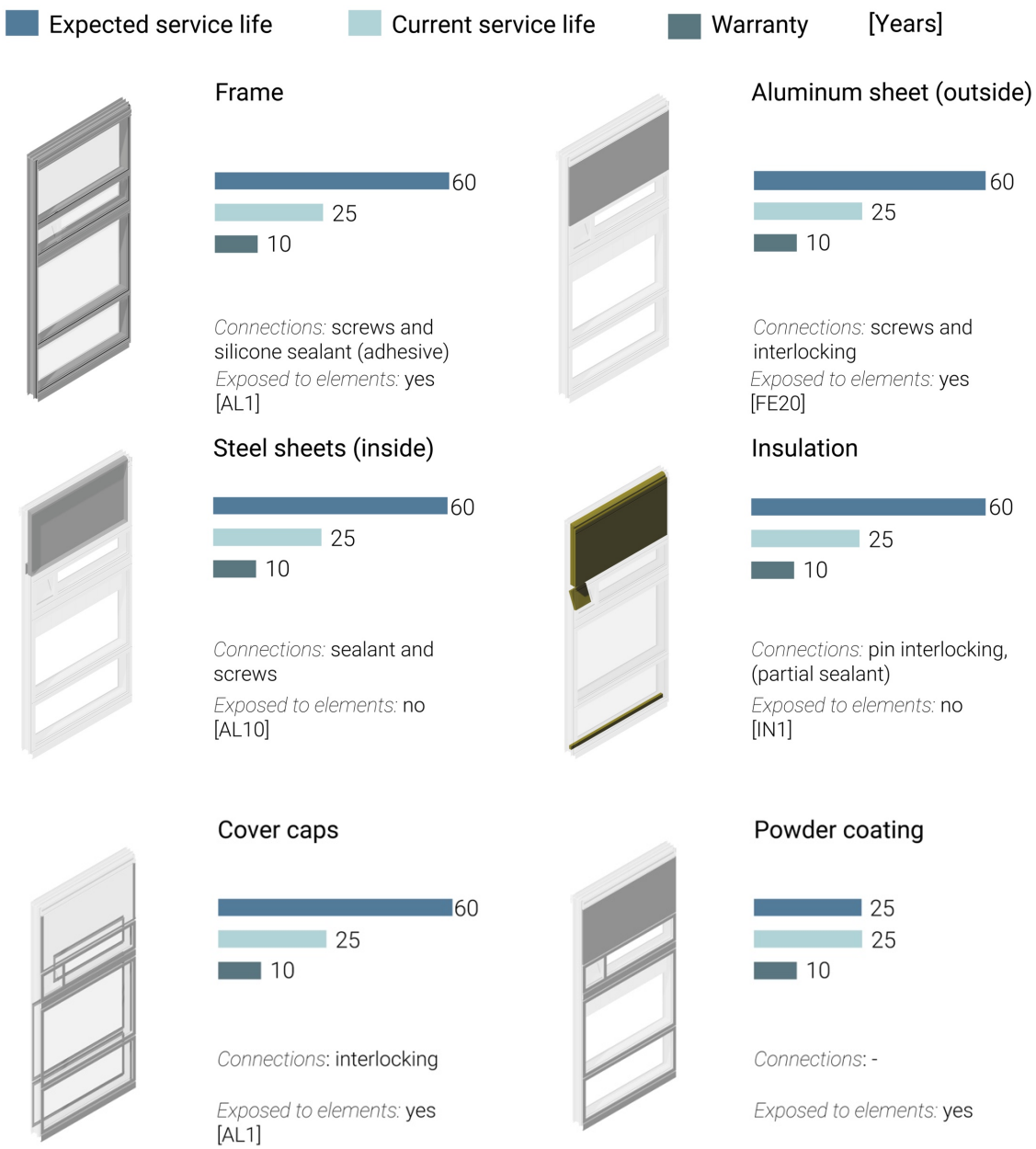

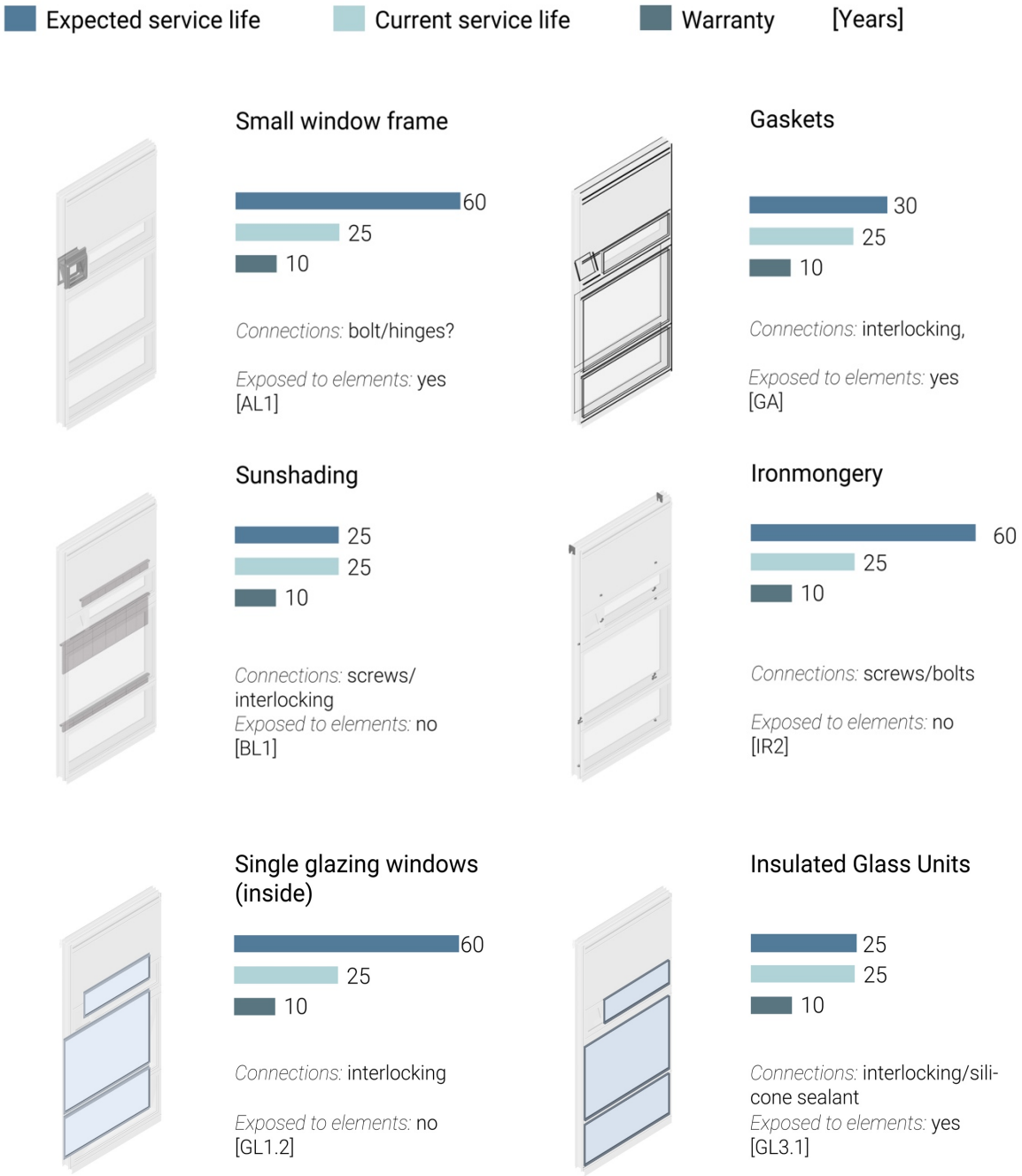

To reach high reclamation potential, the low life components need to be separated from the long-life components. In this case the frame and steel sheet on the backside has not yet reached half of their estimated service life span. This is also the case for the Rockwool insulation which, if not exposed to weather conditions, can serve for 35 more years. The aluminum cover caps and the aluminum sheet on the outside are fitted with a powder coating. This coating will last between 20 -25 years until color changes, gloss reduction and scratch/weather/chemical resistance will no longer satisfy. For this reason, the powder coating must be seen as a separate material, since applying a new powder coating the service life expectancy of the aluminum profiles can then be extended. The single glazing on the inside of the panel, surrounded by an aluminum frame are not exposed to the elements. Therefore, the sealant has not suffered long weather conditions

and the hinges and steel locks on the inside will still be operatable. The insulated glass units on the outside, however, have been exposed to the elements for 25 years and are currently at their end of life. Most important reason is the degradation of the sealant around the spacer bar in-between the glass panes (Wolf & Waters, 1993)(Likins-White et al., 2023). In addition, these IGUs do not meet current thermal performance standards due to their low insulation capacity, primarily resulting from the absence of low-e coatings, outdated spacer designs, and unfilled (non-argon) cavities. The IGU's therefore do not comply with current standards. The small openable window frame can be considered to have the same lifespan as the complete frame. The gaskets however are all at end of life and after 25 years do not have the guaranteed stiffness (e.g. Young's modulus) and water resistance. The sun shading systems also will have reached their end of life and the electrical mechanisms are not reliable to serve another 35 years.

4.3 Disassembly potential

To reclaim the components of this panel to increase circularity of the system the connections between components need to be rated in terms of ease of disassembly. The measurement methods described in Chapter 3 can be used to give an objective score. This can then later be compared with the new design options. At the same time this offers

Component name	Material	Components ID	CT	CA	ID	GPE	DPp
Sun shading	[mixed]	BL1	0,8	0,8	1	1	0,89
Gaskets	EPDM	GA	1	0,8	1	1	0,94
Mullion 1	Aluminum	AL1	0,1	0,1	1	0,1	0,13
Mullion 2	Aluminum	AL1	0,1	0,1	1	0,1	0,13
Transom 1	Aluminum	AL1	0,1	0,1	0,1	0,1	0,10
Transom 2	Aluminum	AL1	0,1	0,1	0,1	0,1	0,10
Transom 3	Aluminum	AL1	0,1	0,1	0,1	0,1	0,10
Transom 4	Aluminum	AL1	0,1	0,1	0,1	0,1	0,10
Transom 5	Aluminum	AL2	0,1	0,1	0,1	0,1	0,10
Aluminum sheet (outside)	Steel	FE20	0,8	0,8	1	1	0,89
Steel sheet large	Aluminum	AL10	0,1	0,1	1	0,1	0,13
Steel sheet small	Aluminum	AL10	0,6	1	1	1	0,86
Insulated Glass Units	Mixed	GL3.1	0,1	0,4	0,4	0,1	0,16
Single glass panes (inside)	Glass	GL1.2	0,1	0,1	0,1	0,1	0,10
Window frame (insde)	Aluminum	AL10	1	1	0,1	1	0,31
Insulation	Rockwool 211	IN1	0,8	0,6	1	0,4	0,62
Hinge window	Steel	IR1	0,8	0,8	1	1	0,89
Hinge transom	Steel	IR2	0,8	0,8	1	1	0,89
Cover caps frame	Aluminum	AL1	1	1	1	1	1,00
Cover caps IGU's	Aluminum	AL1	0,8	0,4	1	0,4	0,55
Glazing beads (inside)	Aluminum	AL1	0,6	0,4	0,4	1	0,52

Table 1: DGBC calculation table for disassembly score of components from ABN AMRO panel (author).

the possibility to find out if these measurement methods can be used in unitized façade systems and if they satisfy the different types of actions required.
Using the DGBC measurement method for the current design, it can be derived that the most difficult parts to disassemble are the different aluminum parts which together create the frame of the panel. To disassemble the transom profiles from the mullions will be hard because of the sealant applied on all locations including the screw heads. Removing of the transoms will not be possible without use of excessive force and damaging the materials. The same conclusion can be given for the large steel sheet on the backside of the panel which has been sealed and screwed from different directions to the mullions. Other components with a low rating are the insulated glass units which are attached to the frame with the use of sealant. Because this sealant is applied in a L-shape, on both the back and sides of the IGU, it will be hard to access. When disassembling an IGU on site it will be necessary to cut the sealant from inside the building but also from the outside. When the panel needs to be disassembled on an external location, the panel need to be turned just to remove the IGU which will make the total process more difficult and more time consuming. Next to that the IGU's are interlocked by the cover caps on the outside which are harder to disassemble because they are miter cut on the corners and interlocked with a small aluminum plate on the backside. Making the simple snap-fit mechanism harder to initiate.
Also, an inner glazing pane is hard to disassemble because it is a subassembly in which the glass plates are connected to the aluminum window frame with sealant. However, the disassembly of these window frames from the panel frame can just be done by opening the locks and lifting them from the hinges. No additional tools are required.

The measurement method of DGBC creates a possibility to do quick calculations to select components, in an objective way, which could be targeted for disassembly. However, the simplicity of the method comes with some limitations like the low range of the scores that can be given for the different difficulties. Therefore, comparing two systems with each other will be hard and because of that, the validation of a redesign should be conducted using a more complex and detailed method like eDim, which is also described in Chapter 3.

4.4 Reclamation potential

To select which materials eventually will be reused and what material can fulfill a function in a future façade depends on the design and requirements of the future façade. This practice, however, does not yet have an aimed design or function and therefore all materials and components can be considered to fulfill a new function.

Looking to the service life of components and to the disassembly potential a conclusion can be made which materials have large potential to reclaim for future use. From the service life analyses we can conclude that the aluminum frame has an estimated service life of 35 years left until it is considered end of life. This is also the case for the steel sheet on the back of the panel and the insulation inside the panel. The aluminum cover caps and the aluminum sheet on the outside of the panel could serve for 35 more years, however, the powder coating on the material is considered end of life and should be renewed, therefore all these materials should be disassembled. The insulated glass units on the outside are considered to be end of life and are not reaching current standards for thermal performance and should therefore be renewed. On the inside of the panel the single glass windows including the frames have a remaining lifespan of 35 years and can therefore be disconnected as subassemblies. This way the sun shading can be disassembled and therefore the inside of the IGU seal can be accessed. For the steel plates on the back only the small, connected by rivets, needs to be disassembled.

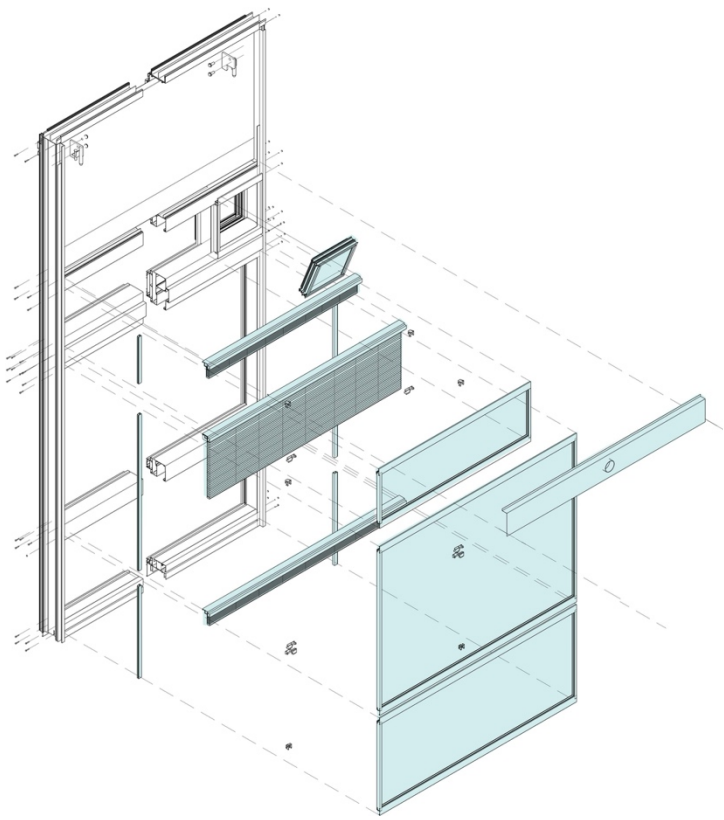

Figure 36: components that need to be disassembled from back side panel (image by author).

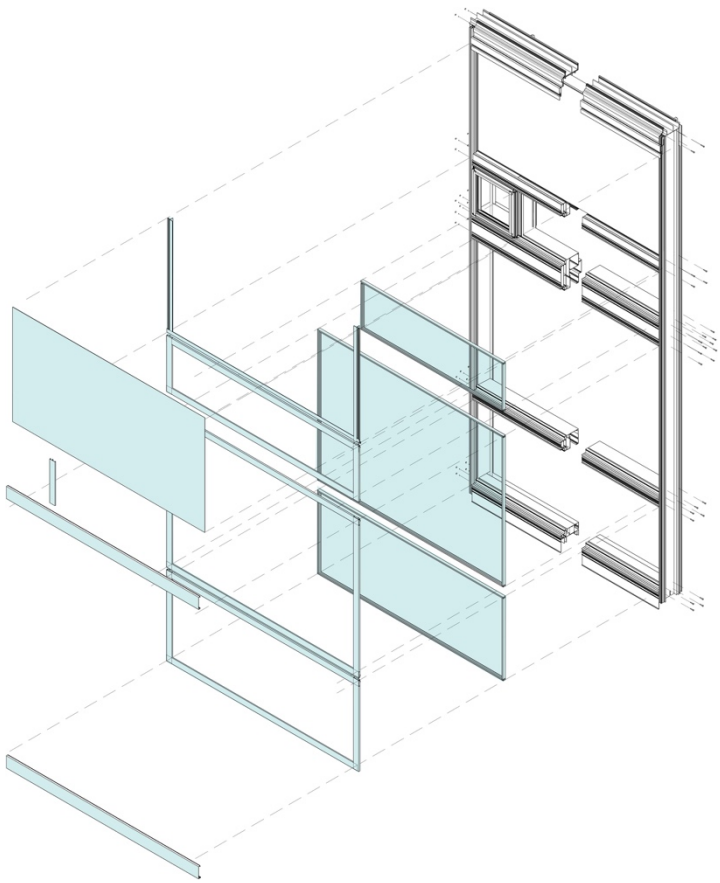

Figure 37: Components that need to be disassembled from front side of panel (image by author).

When considering the reclamation potential of long-life components, it is important to find out in which way the component can achieve the highest R-strategy. Starting with the aluminum extrusions.

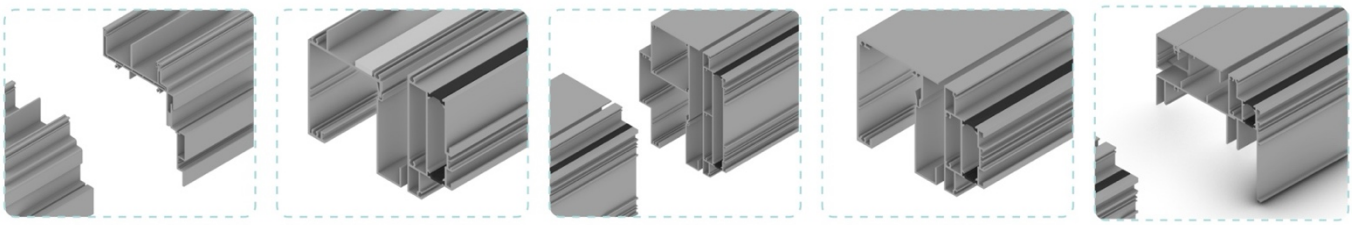

Figure 38: Different transom assemblages ABN AMRO panel (image by author).

Visible in Figure 38 is that all transoms in the ABN AMRO panel are very different from each other all exist out of a composition from different aluminum profiles. These profiles are all highly specific and only used in this particular project. When trying to design for circularity, this creates several problems. Firstly, because these aluminum extrusions are not standardized and therefore not reusable in other façade projects. Their geometry and dimensions limit the use in new façade frames. Standardization of profiles, however, limits the freedom of design for new systems. For this reason, when the profiles would be disassembled from each other, the highest possible R-strategy would be recycling of aluminum. When focusing on recycling materials, the way of disassembly does not always need to be a non-destructive way.

This would not be the case when the complete frame would be considered of being a component. When looking at the frame of an aluminum unitized façade system, it exists of the *aluminum mullions* and the *aluminum transoms* which are connected with each other by screws and sealant. Attached to it on the back is mostly a *steel sheet*, connected with rivets and sealant.
All the components, mostly the same, in this larger component will have the same life span and therefore will probably all be considered end of life at the same time. For this reason, designing for a higher R-strategy should focus on the reclamation of the complete frame. This will also bring limitations in future use. The panel will keep its original height and width and therefore won't be applicable in every load bearing structure due to different height in floor levels. These limitations, however, will be easier to overcome than finding ways to make a large number of different separate profiles applicable.

The focus on the reclamation of the frame as a whole has several limitations. The geometry of the outside of the different transoms and mullions is not standardized. Which means that the adaptability of the frame is limited. Adapting the frame to new standards can be crucial in order to reach new performance or aesthetical requirements.

One of the most important connections creating this barrier for adaptability is the inserted thermal break which will be further addressed in the following chapters. Older systems have a very small thermal break compared to current systems (see Figure 39). To upgrade old systems to meet current thermal performance standards, the thermal break needs to be enlarged to reduce heat transfer through the profiles.

Additionally, the ability to adjust the depth of the thermal break allows for the insertion of thicker IGUs, such as triple glazing, which offer improved thermal insulation. Currently, the method used to insert the thermal break into the aluminum extrusion is not reversible. As a result, neither the depth of the thermal break nor the geometry of the front face of the aluminum profile can be modified.

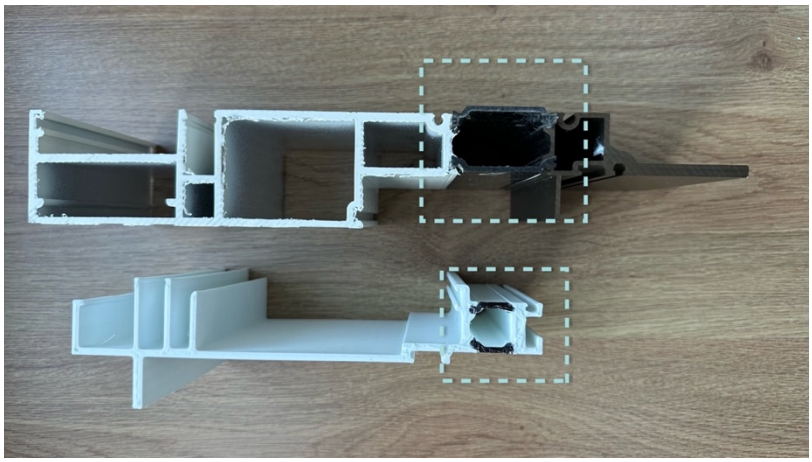

Figure 39: Aluminum profile with current thermal break size 4cm [above], compared to old profile thermal break size 2cm [under] (image by author).

To understand the problem of the non-reversible thermal break it is important to first understand the current assembly process. As has been stated before, the thermal break normally exists of Polyamides like PA-6.6 often reinforced with glass fibers. Systems from Scheldebouw often use the glass fiber reinforced polymer (GFRP). The geometries of the thermal breaks are made by these materials using pultrusion technology.

After designing the new profile, the aluminum is extruded in two parts, one (often larger) part for the interior and one for the exterior side. Both have a groove designed to insert the thermal break. These thermal breaks are toothed or grooved to allow mechanical interlocking. After the GFRP is inserted in the groove, the assembly is passed through a rolling machine which uses rollers to deform the aluminum and bending it around the thermal break. This way it gets locked into place without damaging the material. Basically, the clamping of the deformed aluminum creates the shear strength between the two aluminum profiles and the thermal break.

Figure 40: Rolling thermal break process, front view (Sinon, n.d.).

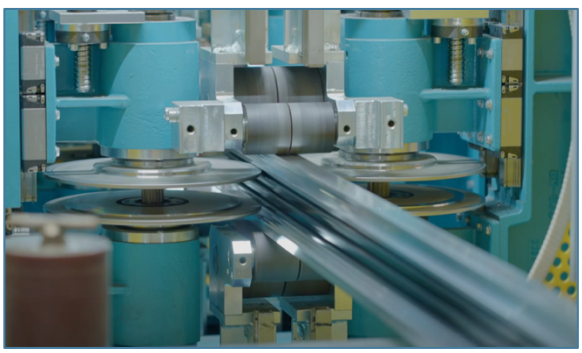

Figure 41: Rolling thermal break process, side view (Sinon, n.d.).

The problem in this case is that there is currently now machine or method available to remove the thermal break in a non-destructive way. Next to the fact that, the removal will also be difficult when the profiles are assembled as a frame. Large frames are harder to modify since they won't fit through an automated machine like in the assembly process. This means that the clamping mechanism is not reversible. If this design would be adjusted in a way that fastening is redesigned for reversibility, the key challenge to address would be overcoming the vertical shear force between the aluminum and the thermal break.

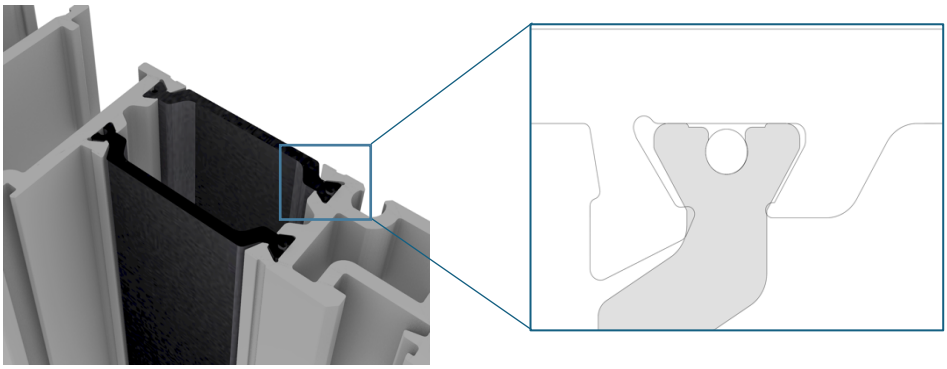

Figure 42: Schematic view of aluminum hook clamping thermal break (image by author).

4.5 Disassembly experiment

4.5.1 Objectives

To assess whether disassembly tasks are as straightforward in practice as they appear in technical drawings, a disassembly experiment was conducted using the ABN AMRO panel. This took place at the Scheldebouw test lab in Middelburg.
The primary objective of the experiment was to identify the basic disassembly tasks involved in dismantling a façade unit. Based on this information, a sequence table can be developed using the MOST and eDim measurement methods described in Chapter 3. As stated in that chapter, no specific method currently exists to measure the ease of disassembly of unitized façade systems. Therefore, another purpose of the experiment was to evaluate whether existing measurement methods for disassembly potential are accurate and reliable enough to serve as validation tools for such systems.
An additional objective was to determine whether the targeted components, outlined in the previous paragraph, could be disassembled without damage, and whether the frame could be reused. Throughout the experiment, special attention was given to the criteria outlined in the measurement methods. These included accessibility, tool positioning, the number of tools required, the amount of force and time needed, and the types of connections used.

The process was conducted by experienced workers in façade assembly and testing. However, they were not trained for the specific disassembly tasks as these tasks are not conducted very often by Scheldebouw. Next to that it is important to mention that this panel has been inside the manufacturing hall since 1996 and has never been exposed to the elements. For this reason, the components in this system have not suffered much.

Previous research by Scheldebouw showed corrosion between the stainless-steel bolts and aluminum. Also, moisture and debris had accumulated in the interstitial spaces. The biggest problem during this disassembly experiment was the issue of broken screws and stripped screw heads due to the corrosion. Since the ABN AMRO element has almost no screws which can be exposed to the elements, this should not be a large issue within this case study.

Figure 43: Corrosion of bolts (left) and debris (right) during disassembly experiment of CitiBank unit, conducted by Scheldebouw (image by Scheldebouw).

However, it is not possible within the scope of this research to exactly state what the difference in disassembly time would be between this panel and one which was exposed to the elements.

4.5.2 Setup

The panel was first placed on the front to disassemble the components on the backside first, after which the panel was turned to disassemble the components on the front side. For the complete process the following tools were used:
- Gloves
- Drill
- Plier set (cutting and gripping pliers)
- Stanley knife
- Allen keys
- Screwdriver set (Phillips, flathead, and Torx)
- Small mirrors
- Crowbar
- Hammer
- Silicone corner knife
- Fein multitool with attachment blades
- Cleaning items
- Vacuum lifter
- Cable lifting system

During the process pictures were taken of the different steps of the disassembly process. Additionally, important observations were recorded from which the most important findings could be derived later.

Figure 44: (image by author).

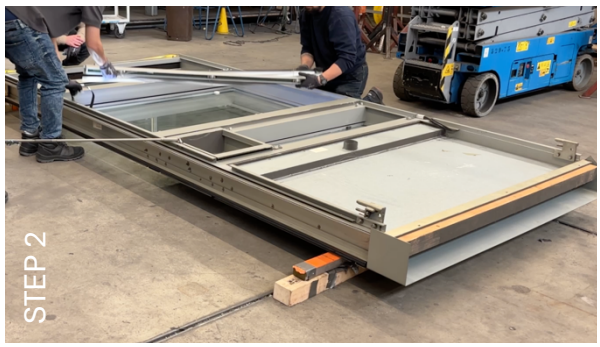

Figure 45: (image by author).

The first step of the process was the disassembly of inner window frames by lifting from half hinges. After that the sun shading was disassembled by unscrewing the interlocking system from the transom (Figure 45). This took more time than expected because of poor visibility and accessibility of the screws.

Figure 46: (image by author).

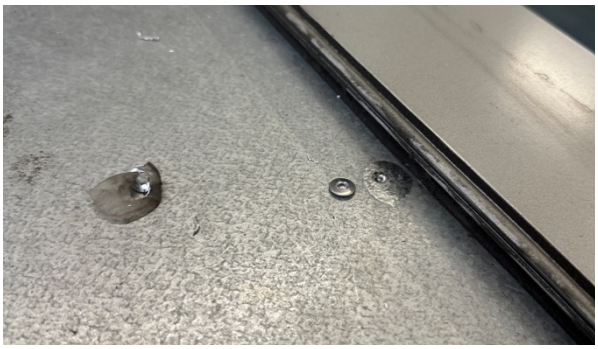

Figure 47: (image by author).

Thirdly the small stainless-steel plate of the air channel needed to be removed. It was tried to remove the sealant from the rivet heads which was applied for airtightness, unfortunately this was too hard and time consuming. The aluminum rivets could be unfastened from the small metal sheet by drilling through the middle of the head after which the head would separate (Figure 47). The spinning of this head would debond the small amount of adhesive on top of it.

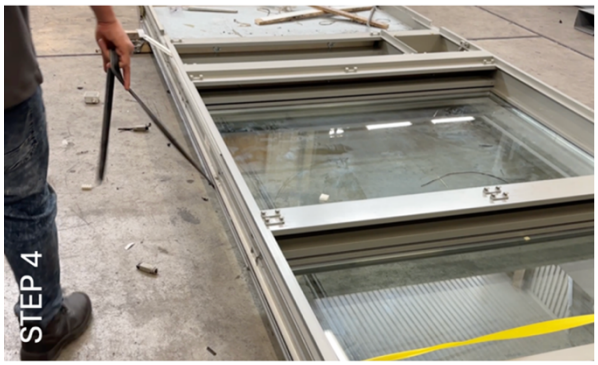

Figure 49: (image by author).

Figure 48: (image by author).

In the fourth step the gaskets were removed. For the disassembly of the glass, it was tried to remove the inner gaskets between the glazing beads and the glass. This was found to be impossible because of the strong bond between the silicone sealant and the gaskets.

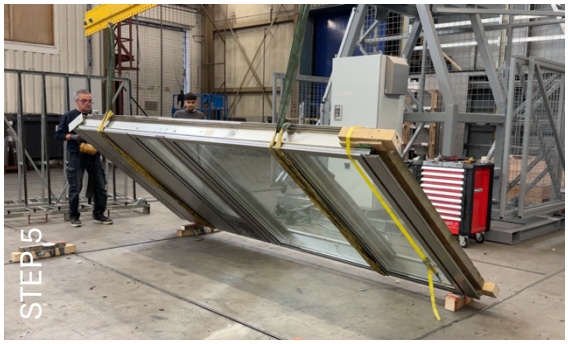

Figure 50: (image by author).

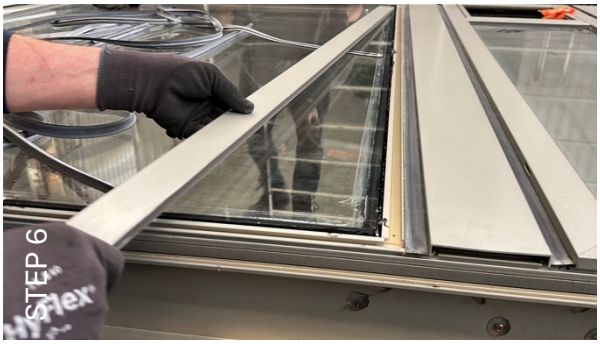

Figure 51: (image by author).

To remove the glazing, it needs to be accessed from the front. Therefore, the complete panel needed to be turned using a crane (Figure 50). After removing of the gaskets, the cover caps could be removed by lifting the snap-fit connection.

Figure 53: (image by author).

Figure 52: (image by author).

Because the panel was turned it was possible to access the silicone sealant from the frontside, this was done using a special L-shaped knife tool to cut through sealant. This was found to be very time consuming and labor intensive. Because the L-shaped knife turned out to be unsuitable for this task a multitool was needed to cut through the sealant. The multitool was later used to cut through the gasket and sealant on the inside since it was not capable of reaching it from the frontside of the panel. Accidental hitting of the glass with the multitool leads to damage of the glass as small pieces come off (Figure 55).

Figure 54: (image by author).

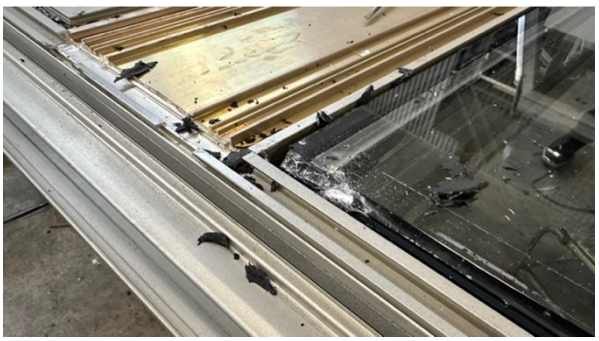

Figure 55: (image by author).

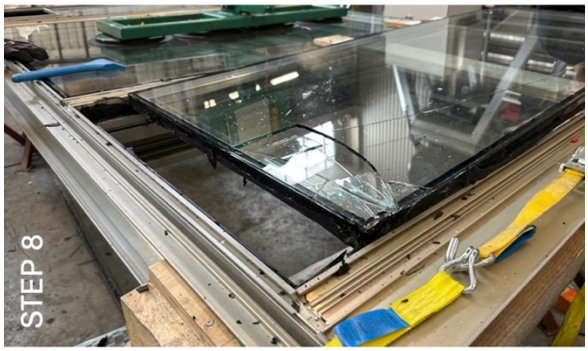

Figure 56: (image by author).

Figure 57: (image by author).

When sealant on all sides was assumed to be cut through the glass could be lifted using vacuum lifter. The inability to see whether the sealant was completely cut and not knowing if the glass was still attached at certain points caused the corners to bend while lifting the glass. This led to the breaking of all three glass units (Figure 56). After removing of the IGU's the left sealant needed to be removed from the frame (Figure 58).

Figure 58: (image by author).

4.5.3 Findings derived from experiment

The disassembly experiment revealed several important findings that were not clear from the drawings alone. Several key findings are outlined:

Key Challenge / Observation	Description	Main Takeaway
1. Measuring task time was not possible	Disassembly steps were tracked, but unclear tasks, missing tools, and lack of predefined procedures (e.g., for cutting glass) caused delays. Workers had to experiment and interpret drawings.	Standardizing procedures and allowing for training would enable accurate task timing and improve efficiency.
2. Sealant between glass and frame	Silicone or structural sealant caused long disassembly times. Difficult to cut completely, especially in L-shapes and hard to verify complete cut-through. Risk of glass breaking and additional time needed for cleaning residue.	Sealant-based connections should be avoided for circular design; they significantly hinder disassembly and increase risk of damage.
3. Use of electrical tools around glass	Multitools damaged frame parts and glass edges, compromising component reusability (e.g., glazing can't be reused by HEGLA, mentioned in Chapter 2).	Avoid the need for high-impact tools near sensitive components; prioritize methods that preserve material integrity.
4. Safety risk of annealed glass	Older panels used annealed IGUs that break into dangerous shards. Lack of tempered layer is a hazard.	Apply safety foil to prevent injuries by keeping broken pieces in place.
5. Sun shading cables not detachable	Electrical sun shading cables were not designed for easy removal and had to be cut.	Improve cable management and use detachable cable heads to support future disassembly of electronics.
6. Difficulty interpreting drawings	Fastener types (e.g., for sun shading) were not described clearly, requiring visual verification that was hindered by poor access.	Include detailed, disassembly-focused drawings/descriptions to reduce delays and support effective dismantling.

An overall conclusion of several of these findings could be that a certain *'disassembly manual'* for units would be created during the design and assembly process. This disassembly manual could show clear instructions and needed preparations for workers. This will reduce the required time during the disassembly process. A manual will line out the required tools and additional materials, in this case for example a protective foil over the glass. Also estimated time required for different disassembly tasks might be included in a certain manual.

4.6 Conclusion

In conclusion, this chapter outlines the full process of evaluating a system's disassembly and reclamation potential, and demonstrates its application through the practical disassembly of a façade unit. The service life analyses in section 4.2 shows that in the case of the ABN AMRO panel the sun shading, gaskets, insulated glass units, and powder coating can be considered end-of-life. The other components can therefore be considered as 'long-life components'.
From the calculation sheet in section 4.4 the components with lower and higher disassembly potential can be identified. As stated, the different aluminum profiles in the frame are hard to disassemble due to their connections. Also, the IGU's are hard to disassemble because of the use of sealant and the bad accessibility. Next to that it is concluded that the DGBC measurement method can be used for quick objective selection of materials which could be relatively easy disassembled. However, it does not support detailed rating of specific high-tech structures as unitized façade systems. To compare different systems with each other a more detailed approach like eDim is required.
In section 4.4 a selection is made which components should be disassembled from the current ABN AMRO panel. It was found that, due to the highly specific extrusion designs used in unitized façade systems, disassembling these profiles offers little added value for reuse or refurbishment, and is primarily beneficial only for material recycling. It is therefore stated that the frame (transoms, mullions and steel back sheet) should remain connected since all these materials have the same long-term life span. During the disassembly experiment of the ABN AMRO panel, described in section 4.5, it was again concluded that the use of sealant to connect the glass to the frame was lowering the circularity potential of the system. Several practical conclusions were made for future disassembly projects. The creation of a 'disassembly manual' for future projects is stated to be beneficial for workers to quickly understand the required task and tools, reducing the overall disassembly time.

5. CONNECTION TYPES IN UNITIZED FAÇADE SYSTEMS

Using the information from the previous chapter and by observing ongoing building processes of new systems a list can be created of current connections in unitized systems. The MOST measurement method described in the literature research can be used for the validation of the separate connections.

5.1 Current connections and fastening methods

In the facades designed and manufactured by Scheldebouw, different connections and fastening methods can be found. By listing these different connection types, the reclamation potential of different materials or different assemblies of components can become clearer. Several of the fastening methods described in this chapter are derived from the instructions which are used by the construction workers in the factory. Although the geometry or design of used components may be different in Scheldebouws projects, the type of materials and components and the ways of connecting will be very similar. For example, the aluminum extrusions of the frame will be different in every project or even in the same project. At the same time all these projects use the same screw connection and adhesive to fasten the extrusions together.

Figure 59: Applying Silicone Sealant on top side of aluminum profile (image by Scheldebouw).

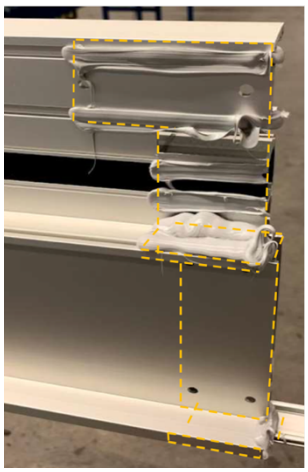

Figure 60: Sealant on seams of mullions (image by Scheldebouw).

Figure 61: Inserting screws in aluminum profiles (image by Scheldebouw).

The first step during the process of façade systems mainly consists out of the assembly of the aluminum frame. The strength and structural performance of the complete unit will depend mostly on how the mullions (vertical profiles) and transoms (horizontal profiles) are connected. For this connection a layer of silicone sealant is applied on the top side of the profile to secure weather tightness.
In the assembly process of unitized facades two types of sealants are used: a two-part silicone sealant for structural glazing application (*structural sealant*) and a one-part silicone sealant for glass and weather sealing (*silicone sealant*).

After applying the adhesive, screws are placed through the inner aluminum plate and the transom. The aluminum profiles are highly specific. The exact location of screws and sealant will depend on the design of the extrusion.

Next to the fact that most extrusions are very specific and only usable in combination with project related components, the extrusions also need to be adjusted by drilling holes or partial cuts in order to make connections between components possible.

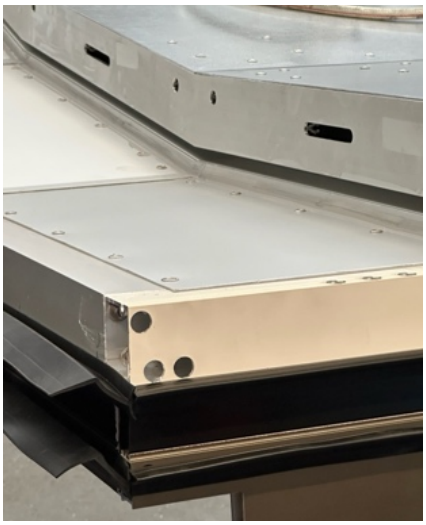

Figure 62: Holes drilled in aluminum profiles for screw accessibility (image by author).

Figure 63: Thermal break (GFRP) in aluminum extrusion (image by author).

Within the aluminum transoms and mullions itself there is also a connection which is the fixing of the thermal break (Figure 63) in the aluminum extrusion further described in section 4.4. Although this connection is ‘dry’, it is not reversible and the only way to remove the thermal break is to cut through the profile.

The next part in the assembly process most of the time contains of placing metal sheets on the frame. These metal sheets are most of the time fastened with the use of rivets. For fastening a rivet it only needs to be accessed from one side and can be fastened using a rivet gun. This will create a knot on the back side of the underlaying extrusion and this way keep the two surfaces together. This interlocking principle has a higher strength (in the direction of the rivet axis) than a normal screw where the only interlocking will come from the screw wire. Therefore, the rivet is assumed to be a better fastener during the assembly process. However, it is less reversible than a screw since there is no reversed motion possible. The rivet can be unfastened by drilling a drill with the diameter of the knot through the middle of the rivet. The rivet won't be usable after, but the components connection can be disassembled using this removal method of these, described by Sonnenberg (2001), 'discrete fasteners'.

Figure 64: Making small hole for location of rivet (image by Scheldebouw).

Figure 66: placing all rivets on steel sheet (image by Scheldebouw).

Figure 65: Inserting rivet using rivet gun (image by Scheldebouw).

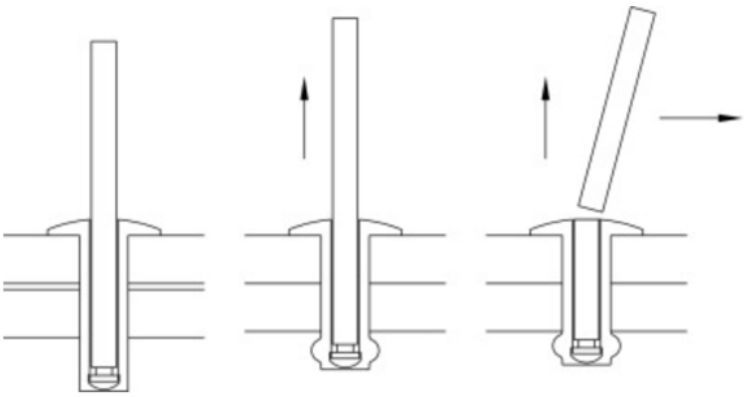

Figure 67: Schematic drawing of rivet principle (Megson, 2018).

The next process contains of applying a lot of sealant through all seams in the construction which are mainly visible between the metal sheet and the aluminum extrusions. This sealant is mainly used to insure the weather and water tightness of the system.

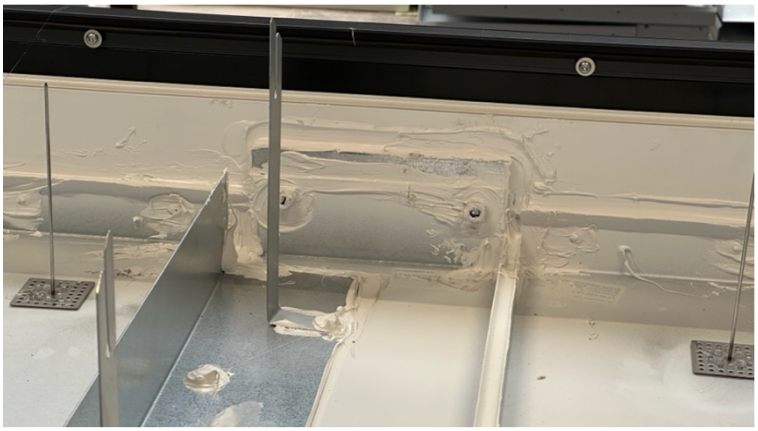

Figure 68: sealant applied in the seams of the aluminum extrusions and metal sheets (image by author).

Figure 69: sealant applied in corner (image by Scheldebouw).

The sealant is also applied on the screw holes to seal the location of the screws. In Figure 70, the L-shaped profile is placed to hold the fire barrier insulation in place. This is also sealed for maximum performance.

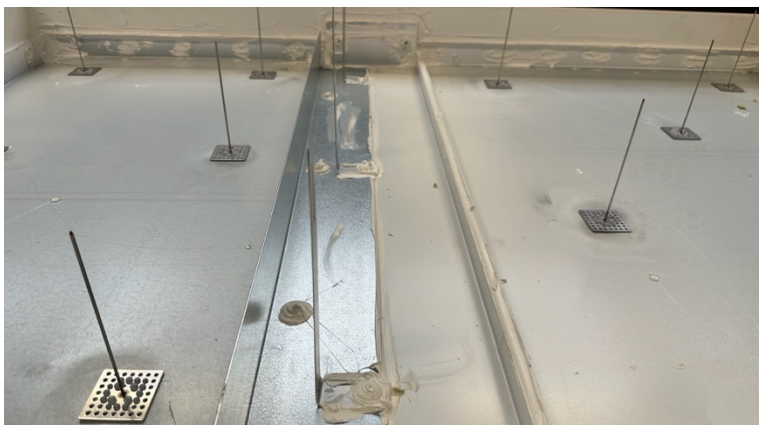

Figure 70: L-profile for floor stop (image by author).

Figure 71: Sealant on screws mullions-transoms (image by author).

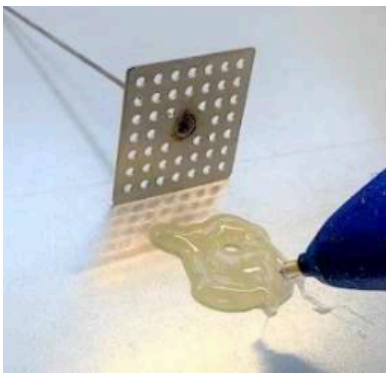

Figure 72: Using adhesive to connect pin to metal sheets (image by Scheldebouw).

Figure 74: placing insulation on metal pins (image by Scheldebouw).

Figure 73: Metal ring on pin for interlocking (image by Scheldebouw).

In order to keep the insulation in place, metal pins are glued or welded on the steel plate. Insulation is placed over it and interlocked by a metal ring on the pins.

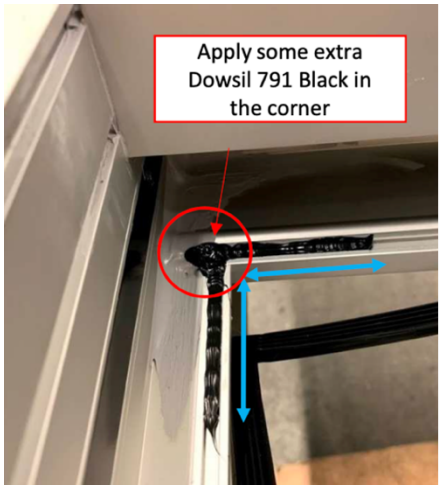

Figure 75: Sealant in corner for EPDM gaskets (image by Scheldebouw).

Figure 76: EPDM gaksets placed in aluminum profile (image by Scheldebouw).

Next to sealant several different EPDM gaskets in the system are applied to make the design weather tight. The aluminum extrusions are designed to interlock the geometry of these gaskets. For that reason, they can by dry assembled. Nevertheless, during the assembly process, a small amount of sealant is applied in the corners to secure the placing of the gaskets.

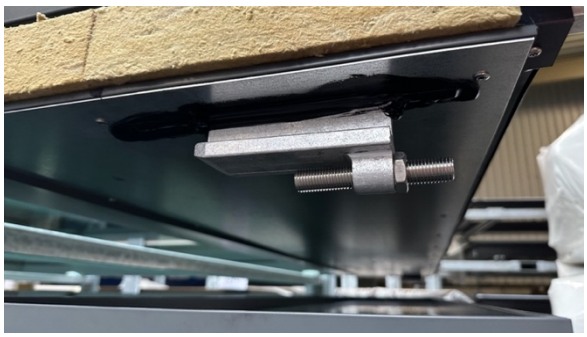

Figure 77: Sealant on bracket on outside of panel (image by author).

Figure 78: Connection of brackets on inside of panel (image by Scheldebouw).

The brackets, required to hang the system on the main structure of the building are attached to the mullions of the unit using screwed connections. After this, the sealant is applied on the in- and outside.

Figure 79 shows the assembly process of an IGU into the aluminum frame. There are two ways of connecting an IGU with the frame.

Figure 79: Placing of IGU (image by Scheldebouw).

Figure 81: Placing window profiles (image by Scheldebouw).

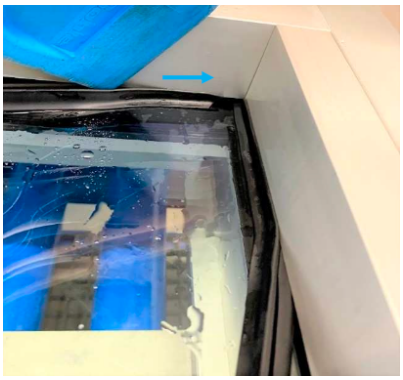

Figure 80: Placing EPDM gaskets (image by Scheldebouw).

In Figure 82 a drawing of structural glazing (left) and dry glazing (right) is shown. In structural glazing, the glass is placed onto a glazing gasket. This gasket is significantly harder than the glazing gaskets used in dry glazing and must be compatible with the structural silicone used. The gasket in SG systems consist of four separate parts, and the system's sealing is provided by the silicone. In DG systems, the sealing is ensured by the vulcanized glazing gasket, which is softer due to the "flaps" and formed as a single pre-produced frame. The wedge gasket applies pressure on the glass and thereby also on the sealing glazing frame. This wedge gasket also consists of four separate parts and therefore will not be watertight.

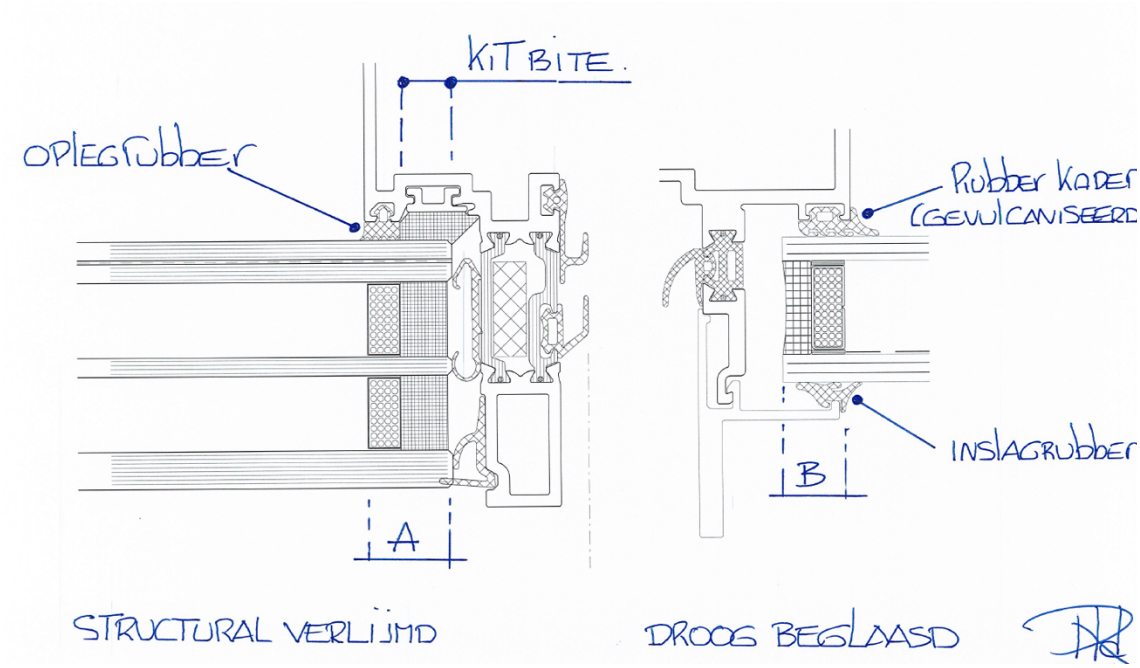

Figure 82: Drawing of structural glazing method (left), and dry glazing method (right) (image by Scheldebouw).

Figure 83: Machine for applying sealant for structural glazing (image by Scheldebouw).

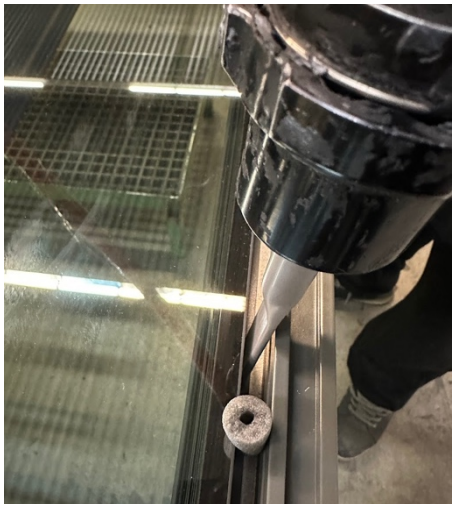

Figure 84: Inserting structural sealant against inner gasket (image by Scheldebouw).

The floor stop insulation is applied on the outside of the mullions and fastened using non-combustible glue.

Figure 85: applying non-combustable glue on mullion (image by Scheldebouw).

Figure 86: Placing floor stop insulation (image by Scheldebouw).

Cover for transoms and window frames can in some situations be designed with using a snap fit connection. This connection relies on smart geometries of aluminum extrusions and can be used to hide screw connections underneath. This is a reversible connection which is easy to (dis)assemble.

Figure 87: example of aluminum cover cap connected by using snap-fit principle (image by Scheldebouw).

5.2 Validating ease of disassembly of connections

Now the most used connections are listed, these can be quantitatively evaluated for their ease of assembly using the MOST sequences described in Chapter 3. To apply this measurement method, it needs to be shaped for the process of large façade panels. The eDim method described by Vanegas et al. (2016) is presented and validated using smaller electronic products. The basic sequences during the (dis)assembly process of large-scale structures like façade elements are different from electronic products. The sequences can be determined by using the MaxiMOST system instead of the BasicMOST system used by (Vanegas et al., 2016).
The first step is to create a Time Reference sheet which focusses on the basic sequences during (dis)assembly processes of unitized façade elements. Secondly a Sequence Calculation sheet needs to be created in which the different connections are listed. These two tables show the calculated Time Measurement Units and the needed time for every sequence.
The tables presented in this chapter are composed with the available information of the previous observed connections and the experience and observation of the disassembly process of the ABN AMRO panel. Therefore, these tables may not include all possible connections or (dis)assembly tasks. Additional research would be necessary to find out if more connections or tasks should be added.
All sequences in both sheets are determined using the tables and instructions in **MOST® Work Measurement Systems** by Zandin (2020) and the used tables can be found in appendix 2.3. The Time reference sheet shows the needed time, calculated after determining MOST sequence for several basic tasks that were observed during the disassembly experiment described in Chapter 4.

The tasks:

- Tool change: changing of required tools by walking to a trolly.
- Identifying: determining the location of the connector
- Manipulations: need to replace complete element with crane or remove parts before accessing connection
- Positioning: positioning of hand or tools to disassemble fastener.
- Removing: removing of disassembled objects from panel.

Table 2: Time Reference sheet of disassembly tasks in unitized facade element, based on MaxiMOST sequence (by author).

Disassembly task	Description	Sequence	TMU	Time (s/task)
Tool change	Fetch and put back on tool trolley (2-3m)	|A1B1P1|	300	10.8
Identifying	Localizing and determining connection type			
	Visible			0
	Hidden	|T16|	160	5,76
Manipulation	Component handling to access fasteners	|A1B1P3|	500	18
	Turning element to other side	|A6T10K32T10P16T3A1|	7800	280,8
Positioning	Positioning tool onto fastener			
	Reachable fastener positioning (screw)	-	-	-
	Hidden fastener positioning (sealant)	|A1B0P1A0|	200	7,2
Removing	Removing separated components and walking to storage place (2-3m)	|A3B0P1|	400	14,4
	Sealant removal	|A1B0T6|	700	25,6
	IGU removal (crane)	|A6T10K6T10P3T3A1|	3700	133,2

On the next page the connections described in paragraph 5.1 and Chapter 4 are given a MOST sequence after which the TMU can be calculated. In this Sequence calculation sheet the connectors screw, snap-fit, sealant, rivets and gasket interlocking are included. All connections are divided in sub-types to specify the exact type of fastener or used tools.

Table 3: Sequence Calculation sheet of listed connections in facade unit (by author).

CONNECTORS	CONNECTORS CHARACTERISTIC	TOOL	MOST SEQUENCE	TMU	TIME (S)
SCREW					
TYPE 1	Screw L<= 50mm	Screwdriver	|T10|	1000	36
TYPE 2	Screw L<= 100mm	Screwdriver	|T24|	2400	86,4
TYPE 3	Screw D <= 50mm	Power tool	|T6|	600	21,6
TYPE 4	Screw L<= 100mm	Power tool	|T6|	600	21,6
SNAP-FIT					
TYPE 1	Snap-fit by hand	Hand	|T1|	100	3,6
TYPE 2	Snap-fit + (corner) interlocking	Hand	|T3|	300	10,8
TYPE 3	Snap-fit by tool	Pry tool (flat screwdriver)	|T3|	300	10,8
SEALANT					
TYPE 1	Silicone sealant [per cut 0.5m]	Knife Multitool Cutting wire	|T3| |T3| |T3|	300 300 300	10,8 10,8 10,8
TYPE 2	Structural sealant [per cut 0.5m]	Multitool	|T3|	300	10,8
RIVETS					
TYPE 1	Aluminum rivet	Power tool	|T1|	100	3,6
TYPE 2	Stainless steel /multi grip/sealed rivet	Power tool	|T3|	300	10,8
GASKET INTERLOCKING					
TYPE 1	Gasket [glazing cap]	Pliers Screwdriver	|T3|	300	10,8
TYPE 2	Gasket [mullion/transom]	Hand	|T1|	100	3,6
TYPE 3	Gasket-to-sealant (window inside) [per 0.5m]	Multitool	|T3|	300	10,8
GENERAL INTERLOCKING					
TYPE 1	Interlocking geometry	Hand	|T1|	100	3,8
TYPE 2	Interlocking fastener	Screwdriver Pry tool	|T3|	300	10,8

6. TARGETING CONNECTIONS

Chapter 6 uses the research and finding described in Chapter 4 and 5 to select the different connections which could be redesigned to increase the reclamation potential.

6.1 Identification of key connections for redesign

The research described in the previous chapters shows that several connections between components are barriers in the disassembly potential, and therefore circularity potential, of unitized façade systems.

6.1.1 Façade frame

As been stated before, the connections between aluminum profiles used as transoms and mullions and together creating the frame of a unitized façade panel are not easy to disassemble. This is mainly because of the use of silicone sealant. The sealant is applied in large quantities to create optimal weather resistance. The sealant is also applied on and around the screwheads which makes them harder to access and therefore losses their reversible capability. For this reason, the frame can only be disassembled in a destructive way. Making recycling of the aluminum material the highest possible R-strategy to reach. This is still an important strategy to accomplish when the frame reached its end of life. At the same time weather resistance and durability is crucial to guarantee the performance of the system and also to secure its expected service life span. It is therefore important to find out if the sealant applied on frame parts can be applied in a way that makes removal and accessibility of screws easier. Research will need to be conducted with various practical tests focusing on the disassembly potential of all components within the frame. This research may determine whether the method of applying sealant can be adjusted and whether the type of sealant can (partially) be replaced with a less strong but equally waterproof alternative. By identifying the challenges in disassembling the components, the assembly process can be adjusted accordingly. It is also important to consider the requirements for the optimal recycling of the material.

6.1.2 IGU connection

As shown in the service life analyses, the component with the longest service life is currently the aluminum frame and the component with the shortest life the insulated glass unit. Since these components are connected with each other this connection can create a barrier in the reuse of the frame if the IGU cannot be disassembled in an easy and non-destructive way. A poorly accessible connection can make on-site disassembly difficult or even impossible. Creating large efforts in terms of time and costs. In the case of the ABN AMRO panel the sealant is applied in a way in which is hard to access with a tool. Next to that, the design of the frame does not allow the assembly of smaller or thicker IGU's than the original size. Which results in low adaptability for future designs where the thickness of IGU's might be thicker or thinner, looking at innovations in triple glazing as well as vacuum glazing.

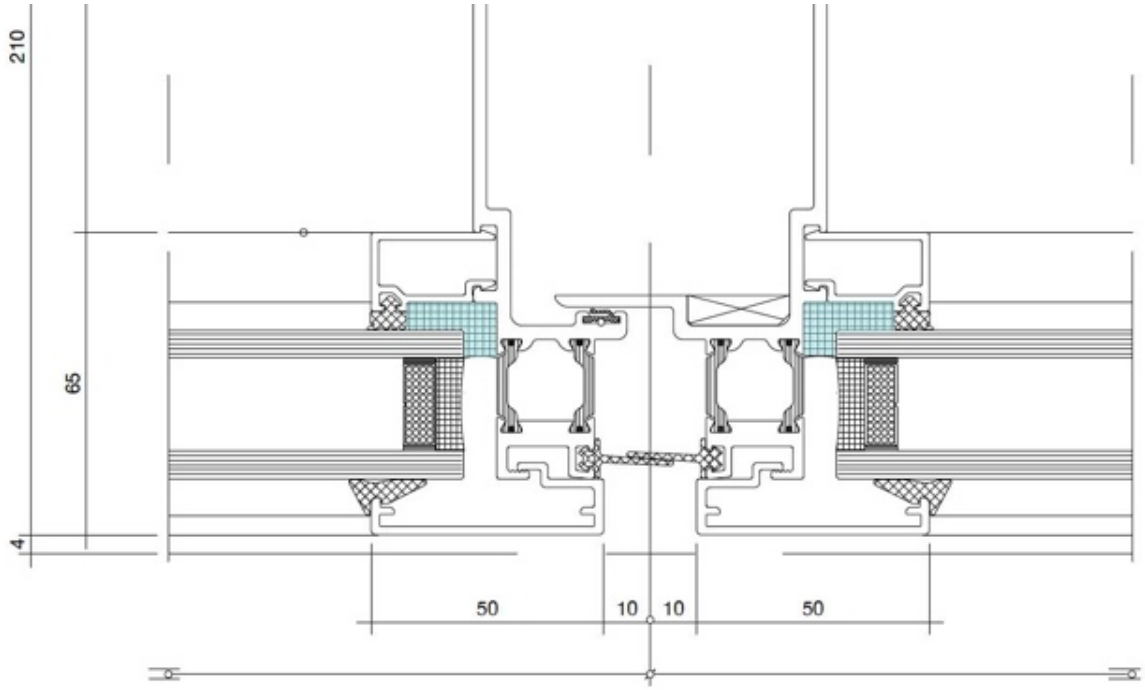

Figure 88: horizontal section mullions-insulated glass unit, hatched is the sealant applied in a L-shape (drawing by Scheldebouw, adapted by author).

6.1.3 Thermal break

As been stated, the polyamide thermal break inside an aluminum extrusion is clamped in a non-reversible way.
The manufacturers of these extrusions use this same method for all different extrusions, and with doing so, they minimize the required space and material for the assembly. Scheldebouw as façade manufacturer saves time during the assembly of new panels. However, the thermal break connects a crucial part of the aluminum profiles, and therefore the complete façade frame, which is the outer part of the mullion and transom. This outer part is mainly used and designed in a way to hold the IGU. Because this part is not adaptable due to the non-reversible connections in the aluminum extrusion, it can be seen as a barrier for future reuse or refurbishment.

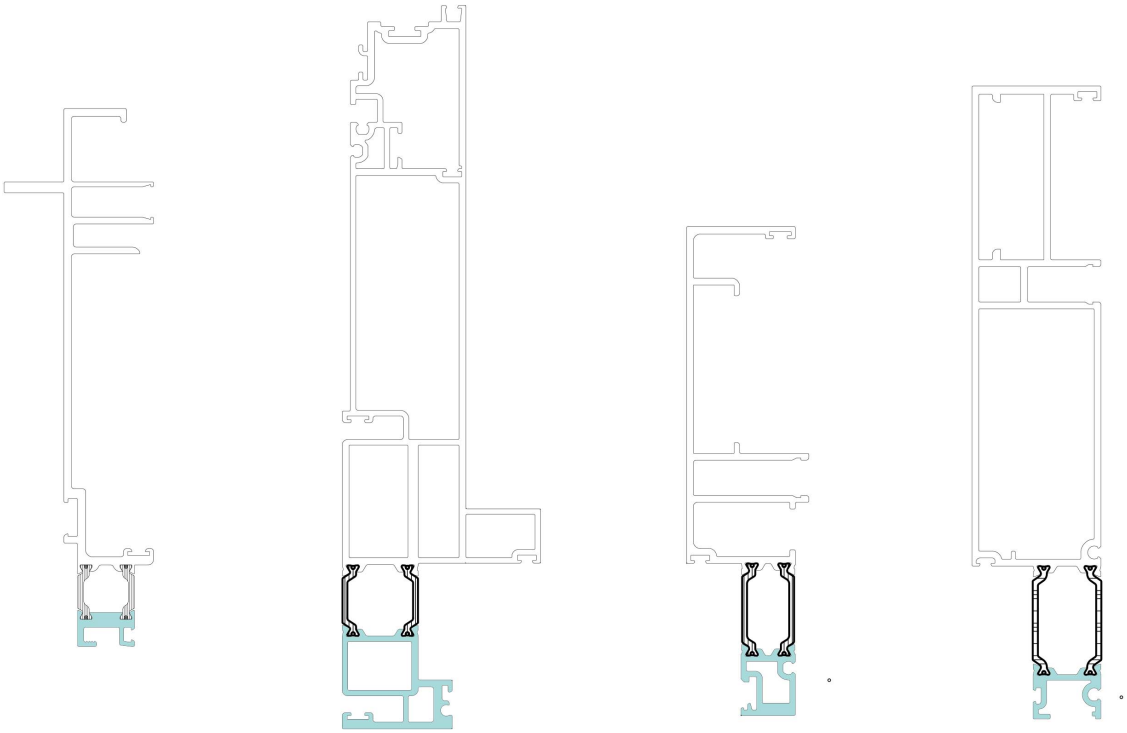

Figure 89: Different aluminum extrusion designs used as mullions, hatched is the various types of aluminum parts of the profiles which are connected to the thermal break (drawings by Scheldebouw, adapted by author).

In Chapter 2, the research by Hartwell et al. (2021) was described in which lack of standardization was mentioned as one of the important reasons for low reclamation potential in facades. Even though this thermal break can be seen as a barrier in the adaptability of old frames, it can also be considered as being a universal part which is used in most systems and therefore a possibility for standardization. When this specific part could be replaced, and a new frame can be assembled with use of the old. Redesigning the connection of thermal break in a way that makes disassembly possible can increase reclamation potential but also will come with limitations. Like the possible amount of space to create a reversible connection. Next to that, it needs to match the strength performance of the original connections to be able to carry the weight of the IGU and outside framing and cladding material. By using the existing geometry of the outside part of an extrusion, a new outer framework can be connected to create the adaptability for future use.

6.2 Conclusion

In conclusion, this chapter gives an overview of the connections in a facade which found to have an impact on the overall reclamation and adaptability of a unitized facade system.

Disassembling aluminum frames in unitized façade panels is difficult due to heavy silicone sealant use. As a result, recycling is the main end-of-life strategy. Research is needed to explore alternative sealant methods or materials that maintain performance while improving disassembly for recyclability.

The long-lasting aluminum frame is hard to reuse due to its fixed connection with the shorter-lived IGU. Poor sealant access and a rigid frame design limit disassembly and adaptability to future glazing types.
The thermal break in aluminum extrusions is non-reversibly clamped, aiding efficient assembly but limiting future reuse and adaptability of façade frames. While this poses a barrier, its widespread use offers potential for standardization. Redesigning the connection for disassembly could improve reclamation but must meet space and strength requirements.

D. DESIGNING AND VALIDATION

7. REDESIGNING OF CONNECTIONS

Chapter 7 shows the redesign for the three targeted connections in Chapter 6. Improvements for the connections of the frame are proposed, and a new carrier frame principle is introduced using the ABN AMRO system. Lastly a new reversible standardization method is introduced for the thermal break and internal fixation to the exterior of aluminum profiles which can improve adaptability of systems.

This chapter shows different redesigns for three different connections in unitized façade systems and shows possibilities to improve the reclamation potential of components.

1. Section 7.1 starts with an adaption and short recommendation for the potential reconfiguration of the connection between aluminum mullions and transoms of current façade systems.
2. Section 7.2 focuses on the redesign of the ABN AMRO façade, which helped to identify the barriers of reclamation during a real design process.
3. Section 7.3 will show a potential redesign of the thermal break in aluminum profiles and the future reclamation possibilities.

7.1 Improvements frame connection

A

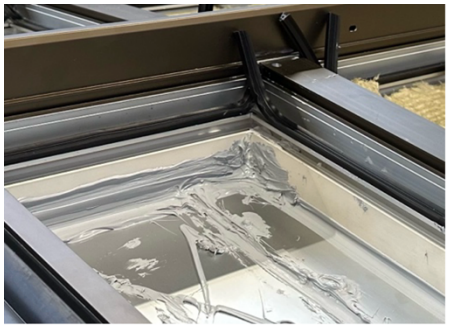

Figure 90: Observation of worker applying sealant (1) (image by author).

B

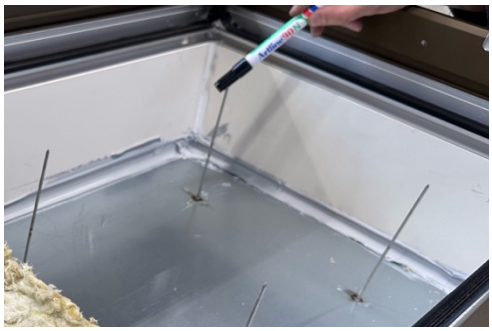

Figure 91: Observation of worker applying sealant to frame (2) (image by author).

During observation of the production process, it became apparent that the amount of sealant applied by the workers varies significantly. In Figure 90 and Figure 91 two different situations are shown. Situation A uses visibly more sealant than B while the performance requirements are the same. Although the location of application and the handling of the sealant gun are consistent, there is a high degree of variation in the final result between different units. As described in Chapter 6, research should be conducted to assess the performance differences resulting from varying amounts of applied sealant. This research can determine the optimal quantity of sealant required and identify the most efficient application method. The findings could help reduce the amount of sealant needed, which would enhance the product's disassembly potential.
The current method of assembling a frame, which has been elaborated in Chapter 5, consists of applying sealant on the top of the transom profile, placing the mullion profile on top of it, and screwing screws through the mullion in the extruded screw holes in the transom. During this process a large amount of sealant is used.

Figure 92: Applying sealant on top of transom profiles (image by

Figure 93: Attaching mullion to transom using screws (image by Scheldebouw).

Instead of applying sealant between the profiles, it may be possible to replace it with a waterproof foam, as illustrated schematically in Figure 94. By applying foam to the head of the transom, the need to apply sealant to this surface is eliminated. The application of a small sealant bead around the seam could be considered. The addition of a thin foam layer may affect the finish and aesthetic quality and should therefore be applied with care.

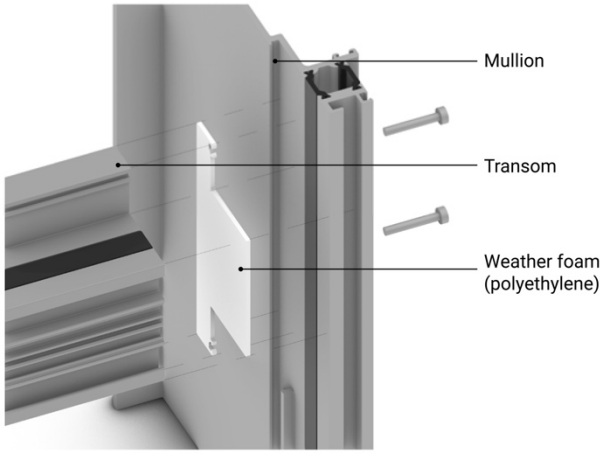

Figure 94: inserting foam for weather sealing between transom and mullion (image by author).

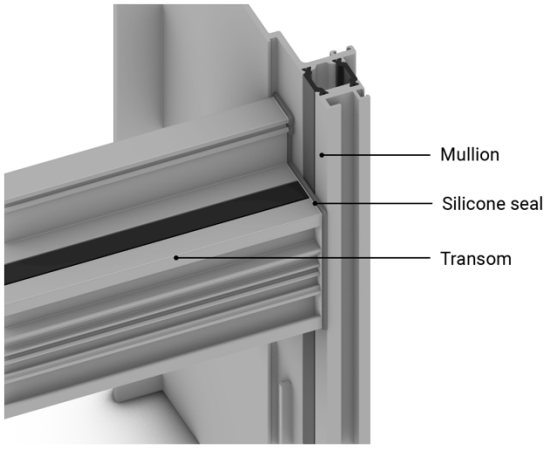

Figure 95: Applying small sealant bead around seam (image by author).

An example in terms of material could be a thin layer of polyethylene foam, which has good durability in terms of water and UV radiation. Further research needs to be applied to determine an exact material to achieve maximum performance and aesthetic satisfaction. As been stated before in Chapter 6, this type of redesign will primarily focus on the possibility for recycling since reuse of the aluminum extrusions in other systems will be hard because of their highly specific geometry. At the same time a redesign of this connection or additional research in the application of the sealant may influence the overall carbon impact of the system since less silicone sealant is needed. The exact type and carbon footprint of the foam should be determined to accurately assess the overall environmental impact.

7.2 New carrier frame principle for old frame units

The ABN AMRO panel forms the basis of a representative case study to examine the exact technical challenges encountered, associated with disassembly, when attempting to redesign an existing façade unit. By identifying the challenges faced during the design process, conclusions can be drawn about which connections need to be modified in order to increase the reclamation potential. Redesigns of these connections can contribute to greater adaptability of the systems and thereby improve the reclamation potential.

Additionally, a redesign of the ABN AMRO system offers the opportunity to compare two systems in terms of disassembly potential. The question then becomes whether the redesigned system is indeed easier to disassemble than the previous design. This creates an opportunity to test the described measurement methodology of eDim, as outlined in Chapter 3, in practice for façade systems. Based on this, conclusions can be drawn

about whether eDim and MOST can serve as viable measurement techniques to be implemented in the practical design process of all systems.
For this project, it was decided by Scheldebouw that the new design should have a more smooth and simplistic design, in order to create a more modern look. This could be done by eliminating the middle transoms from the outer view. This could be created by applying a new sub frame to the existing outer frame structure of the mullions and transoms. This sub frame would make easy assembly and disassembly of the new IGU possible and creates a 'cluster block' design which was described by the framework of De Fazio et al. (2021) described in Chapter 3. This approach makes it possible to disassemble a group of components either for removal or to provide easier access to another component. Also, the on-side assembly and disassembly options become more feasible.

Figure 96: Design inten for ABN AMRO panel (left old, right new) (image by author).

This redesign aimed to reuse the components described in the previous chapter; the frame, aluminum sheet, external cover caps and insulation. Primary focus is placed on assessing the adaptability potential of the existing frame. One of the most important problems to overcome during the detailing of a new design was to modify the depth of the thermal break. Modifying the depth allows for the use of insulating glass units (IGUs) of varying dimensions, which could help improve the overall thermal performance of the system.
The total set of new details (scale 1:2) as well as the old details of the ABN AMRO panel are available in the **appendix 1.2.** The most important sections are pictured underneath in which the red lines show the added components and materials and the black lines the original components which have been left in place.

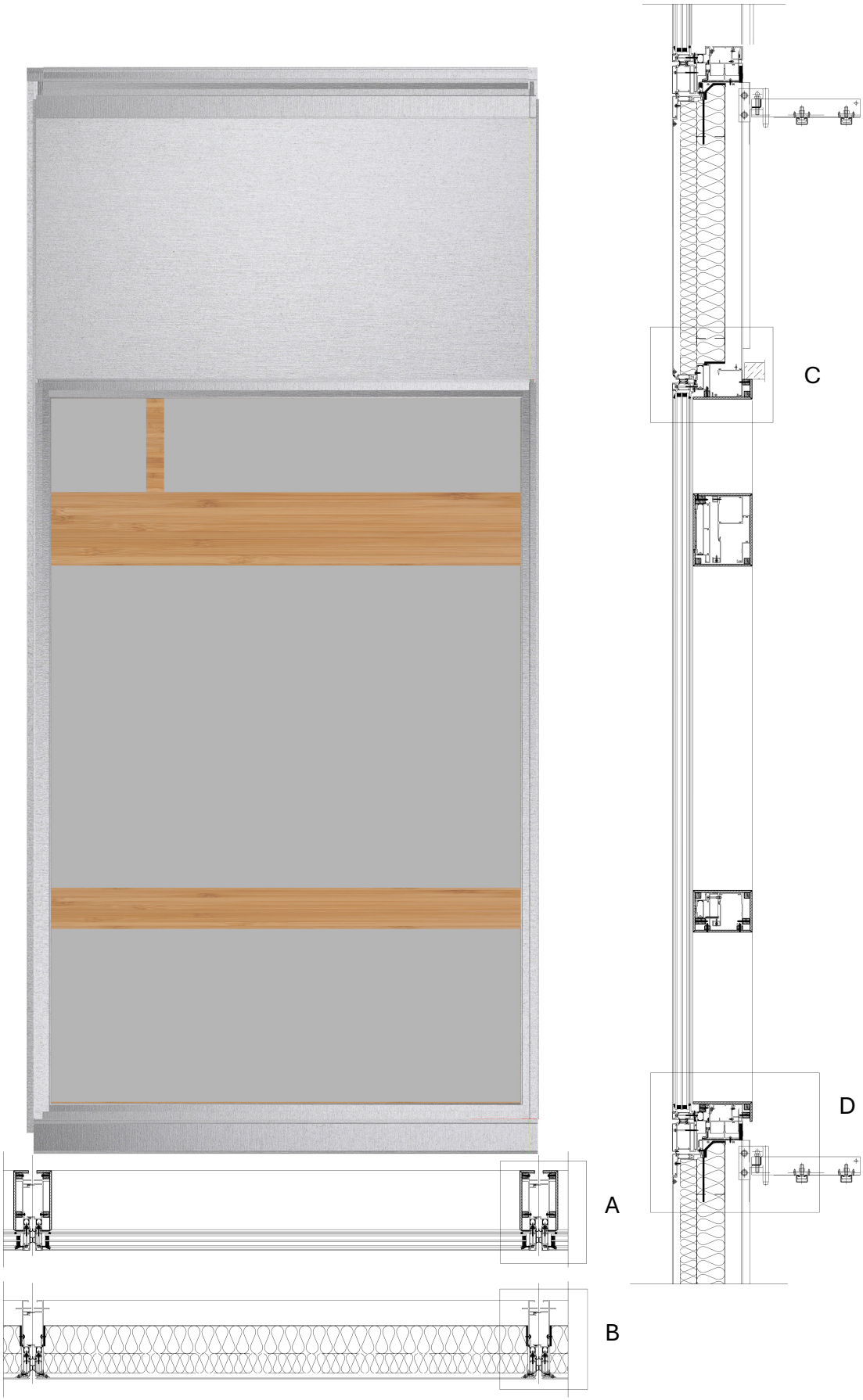

Figure 97: Section 1:20 new design ABN AMRO panel (image by author).

In the drawing in Figure 98 the new detail of the horizontal section of the male-to-female mullion section is visible. A new *carrier frame* has been designed which exists of two vertical and two horizontal aluminum profiles. Within this frame a new insulated glass unit can be inserted and clamped in a dry way (without sealant) with the use of EPDM gaskets and glazing cover caps on the outside. The frame is attached to the existing mullion using screws. The new frame has a new GFRP thermal break with a total depth of 40mm, which is twice as much as the existing thermal break of 20mm. An EPDM gasket over the complete length of the existing profile is placed within the existing geometry to secure weather tightness. On the outside of the carrier frame cover caps are placed to hide the screws. Because this cover cap is separate from the one securing the IGU, it is possible to disassemble the entire carrier frame with the IGU still in place. The interior of the existing frame has a new wooden finish to create new aesthetics.

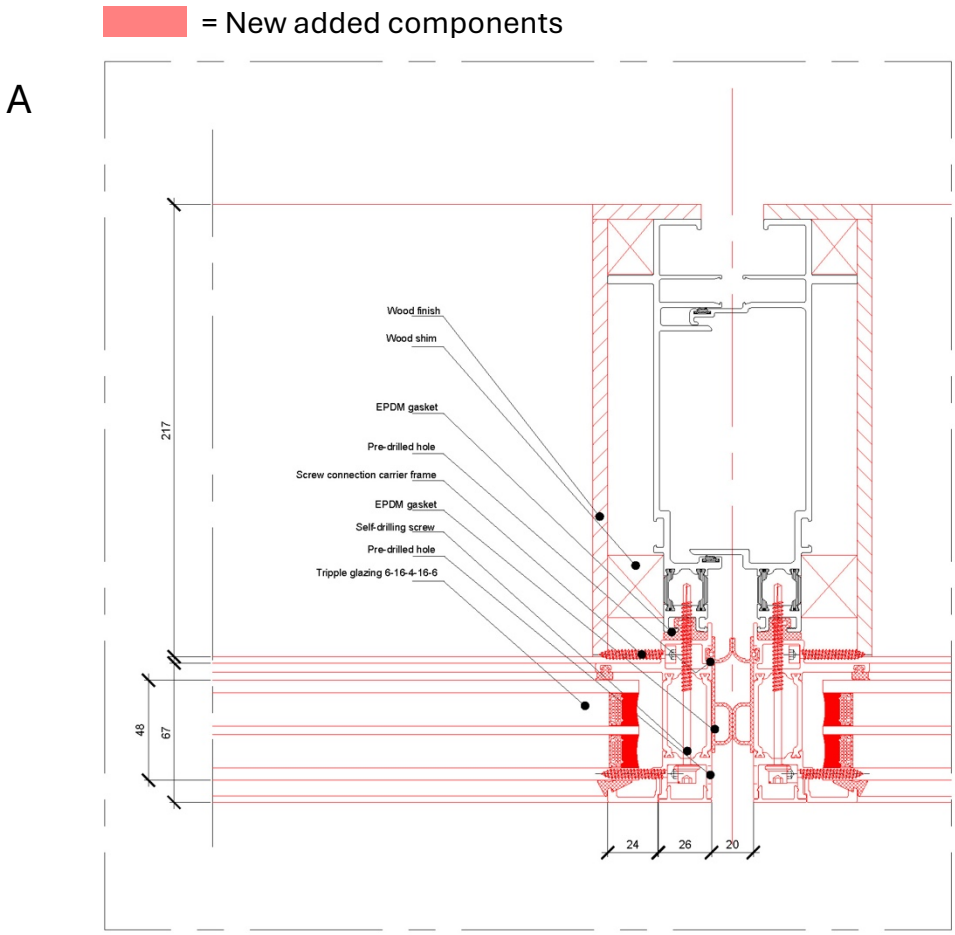

Figure 98: horizontal section mullion-carrier frame (drawing by author).

B

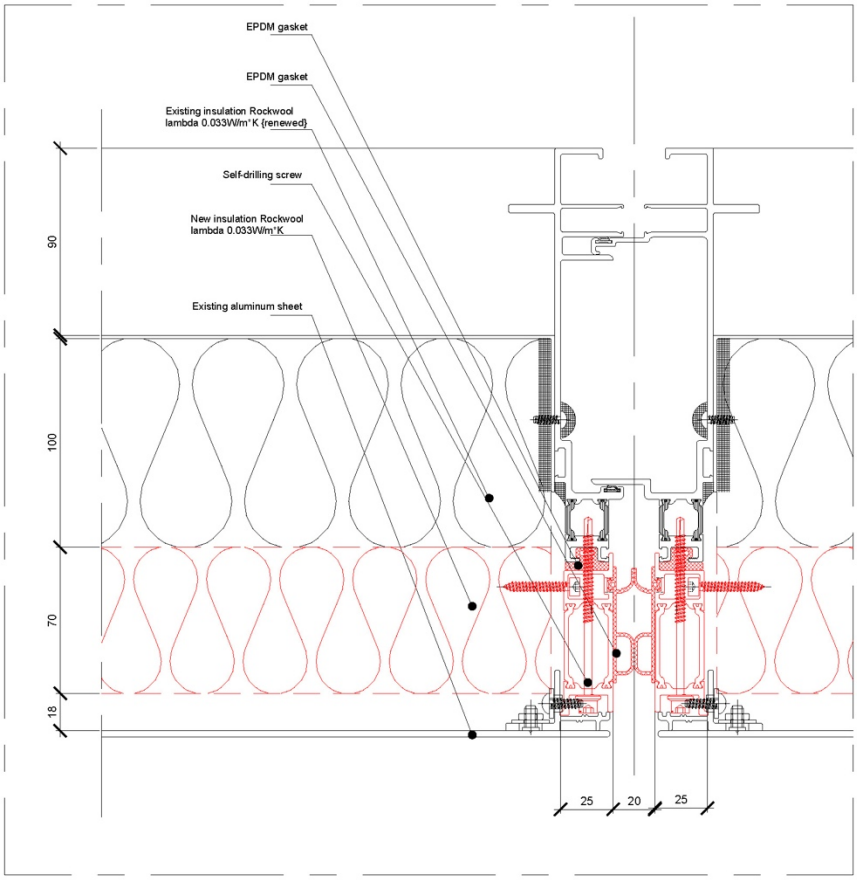

Figure 99: horizontal section mullions, opaque section (drawing by author).

In Figure 99 the horizontal section of the opaque part of the panel is visualized. The same principle of a new frame has been applied in which the vertical profile has the same geometry to insert an EPDM gasket over the complete length. The existing aluminum sheet on the outside is reused and connected in the same 'keylock' principle to the new frame. An additional 70 mm of Rockwool insulation is added in the created space.

= New added components

C

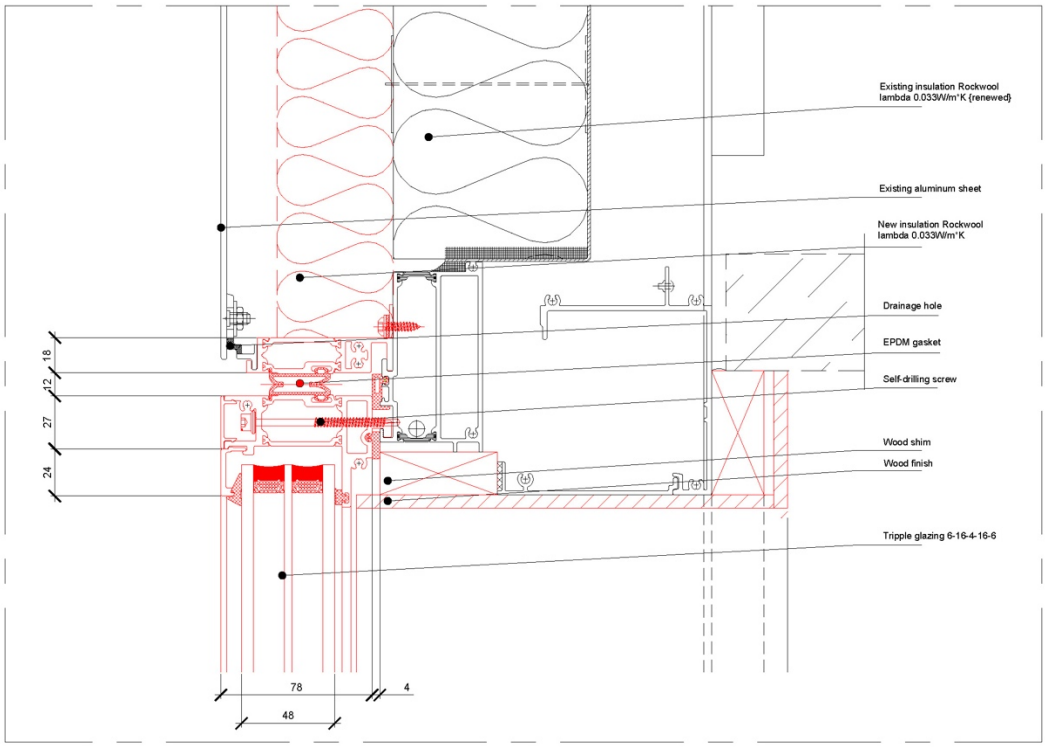

Figure 100: vertical section top connection carrier frame (drawing by author).

The vertical section of the top part (Figure 100) shows the new carrier frame interlocking in the old transom which creates easier positioning during the assembly process. The same method is used for the new frame of the opaque section. The weather tightness is secured using two gaskets of which one is inserted in the frame and one in the existing transom.

Figure 101 shows the the gap between the new carrier frames of the IGU and the opaque section is filled using an additional profile on which the existing cover cap can be reused. The top profile attached to the existing aluminum sheet has been removed and replaced by a new one to make attachment to the new frame possible using screws. These screws secure the sheet for extra safety and are hidden by an additional cover cap.

= New added components

D

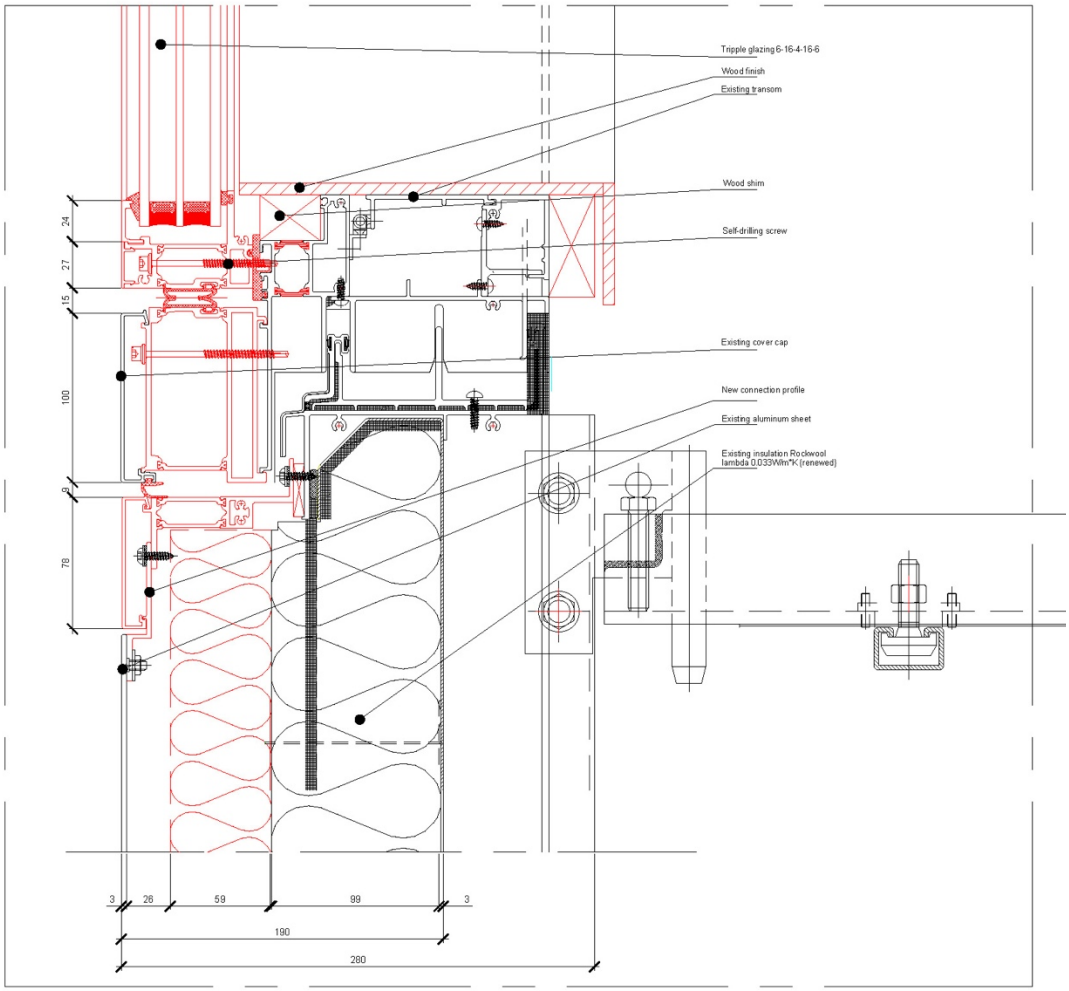

Figure 101: vertical section bottom connection carrier frame (drawing by author).

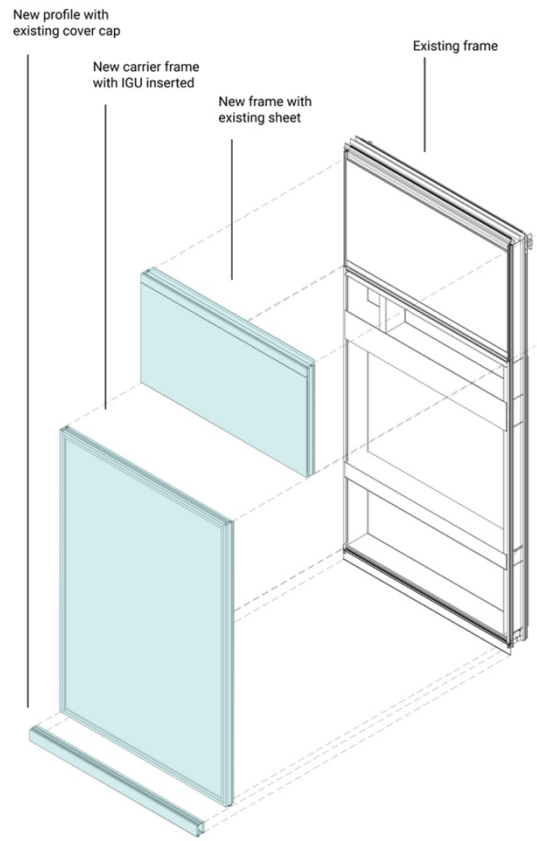

Figure 102: Exploded view total system (image by author).

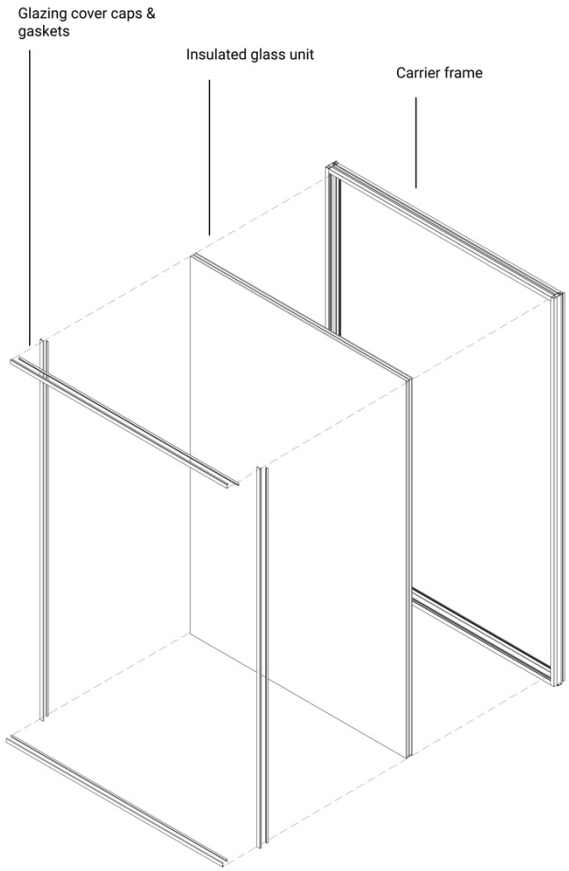

Figure 103: Exploded view new carrier frame (image by author).

Figure 102 and Figure 103 show a schematic view of the new designed panel. In Figure 103 the carrier frame with the IGU shows the possibility to replace the IGU without the need to disassemble the carrier frame from the main frame. At the same time the complete carrier frame can be assembled with the IGU inserted reducing the total assembly time and making on-side assembly or disassembly of this system feasible. This way a 'cluster' of components is implemented in the façade system, which could simplify a possible disassembly map as has been described in Chapter 3 introduced by De Fazio et al. (2021).

The design principle of a carrier frame creates the possibility to adjust the existing frame of a unit and therefore the ability to change the aesthetics and the performance. The thermal performance is upgraded by inserting a new IGU and by extending the thermal break. However, the possibility to use the carrier frame in the future with a different glass thickness is still limited. Next to that, the new frame adds material and therefore also carbon to the new system. Chapter 8 will give an indication on the additional environmental impact in terms of global warming potential (GWP), measured in carbon dioxide equivalent, compared to the existing and reused part.

Figure 105: 3D detail of top section carrier frame (image by author).

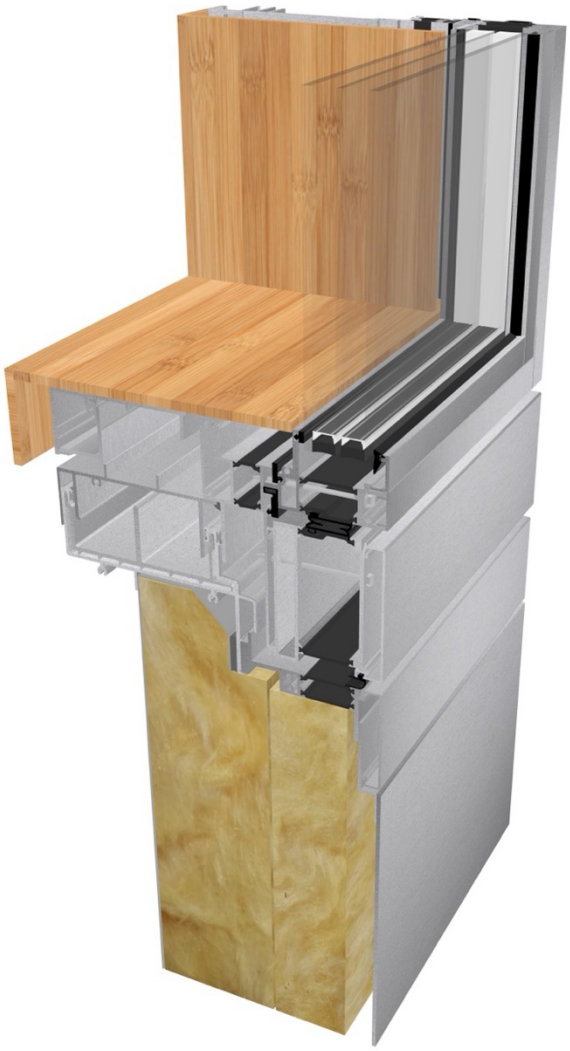

Figure 104: 3D detail op top-bottom section panels (image by author).

Figure 106: 3D detail of bottom section carrier frame (image by author).

Although it can be assumed that new reclamation projects based on this carrier frame principle will save more carbon than designing completely new systems, the amount of material that needs to be added should be lowered to a minimum amount. The next question is in which way current system designs can already be prepared for future adaptability of this carrier frame principle. During the design of the carrier frame presented for the ABN AMRO panel, there was no flexibility to alter the geometry of the existing frame profiles (mullions and transoms) in a non-destructive way. Therefore, the only way to increase the depth of the thermal break in the system was to add an element with a larger thermal break on top of the old. If the old thermal break could be removed and changed for a new adapted thermal break the amount of new frame material could be reduced. Section 7.3 will show a possible solution to make future systems more adaptable at the end of life.

Figure 107: Corner section of new carrier frame attaching to existing frame (image by author).

Figure 108: Exploded view carrier frame design ABN AMRO panel (image by author).

One of the challenges identified in previous disassembly research by Scheldebouw, on the old panels of the CitiBank Tower (as discussed in Chapter 4), was the issue of corrosion. The study revealed that stainless-steel screws used in combination with aluminum profiles could suffer from corrosion. This corrosion complicated the unscrewing process, as screws frequently broke or screw heads became stripped. Consequently, Scheldebouw decided to use Torx screws in future systems instead of Phillips screws to overcome these issues. In the new design, it is assumed that the highest risk of moisture penetration will be from the front, as there will be no flowing water between the carrier frame and the main frame. Although completely preventing screw corrosion may be unfeasible, applying a protective foam layer over the screw heads could offer a viable solution by limiting water ingress. This improvement involves adding a small, foam layer that can be easily removed, enhancing the disassembly potential compared to the use of sealant on and around the screw heads.
The specific material to be used for this weather-sealing foam should be selected and evaluated through testing prior to implementation.

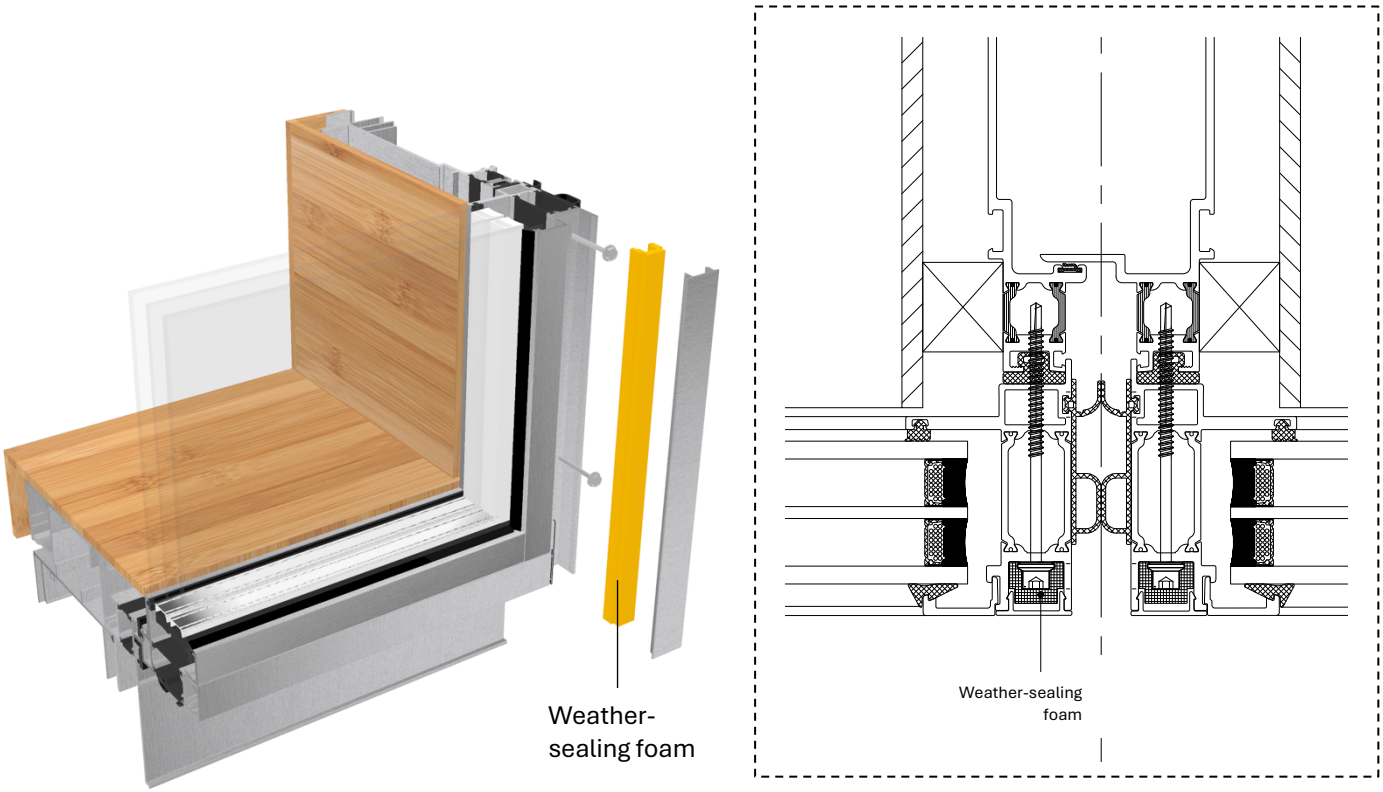

Figure 109: Option for applying foam to prevent corrosion on stainless-steel screws in carrier frame (image by author).

7.3 New thermal break design

In Chapter 4.5 the problem of the non-reversible connection of the thermal break is explained. As shown, the clamped aluminum around the GFRP can not be removed in a non-destructive way. The only existing available method would be cutting or sawing through the aluminum. The main challenge in redesigning this connection is creating enough shear resistance to allow forces on the aluminum front part.

7.3.1 Design considerations

During the design process multiple options were considered in order to overcome the problem of distributing the shear force. Outlined are several sketches in which an additional reversible fastener is used that can be removed when the thermal break needs to be removed.

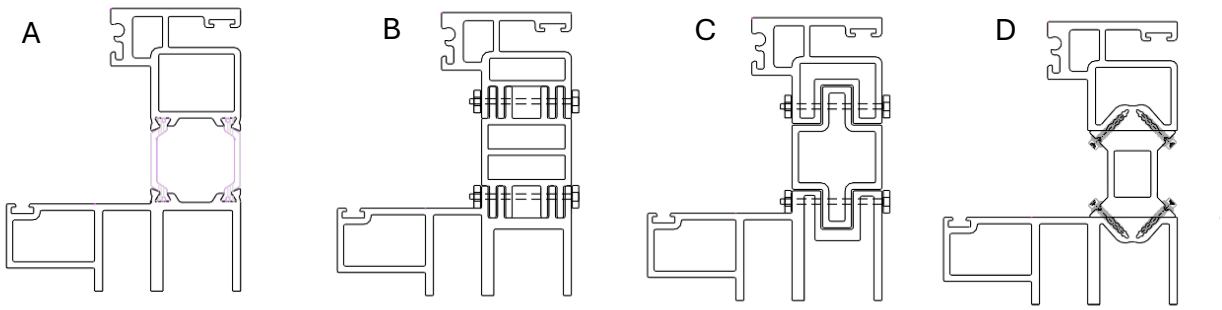

Figure 110: Design considerations for connecting thermal break (image by author).

Above several design options are shown of a section of the front part of an aluminum mullion profile. Drawing A in Figure 110 shows the original current design in which the thermal break is clamped in the aluminum profiles. The first design option considers the possibility of distributing the shear force using a screw in horizontal direction. This would need an adjustment of both aluminum parts to create a surface for positioning the screw. This option has several limitations. The possibility to create enough space for the thermal break geometry highly depends on the mullion design. It is most likely that the needed space will have an influence on the size of the thermal break and therefore on the thermal performance of the profile. The same arguments can be made in second design. This design however makes complete disassembly of the thermal break possible, and reuse of this part could be feasible. The third design considers the possibility of screwing the thermal break into a pre-extruded screw channel in the aluminum profiles. The design however would require a large number of screws which are hard to position, depending on the geometry of the designed mullion.

7.3.2 Final redesign

The final redesign of the connection focusses on the possibility to remove the front part of the profile, as identified in Chapter 6, with the thermal break inserted in the original

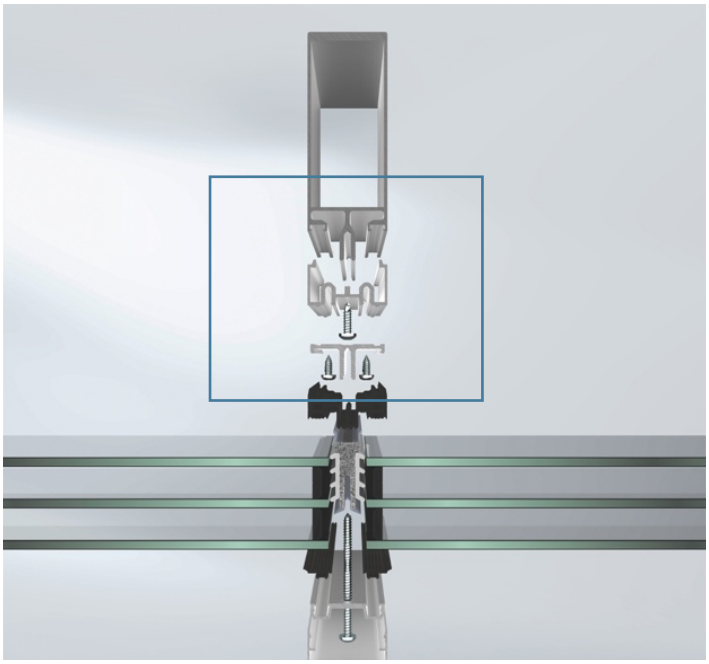

Figure 111: Schüco AOC 50 / 60 Reno, example of use of pre-extruded screw holes (Schüco, 2025).

way. If this part as a whole could be removed from the main aluminum profile, the front part becomes adaptable and another top part can be assembled for new aesthetics or new performance requirements. By keeping the original method of rolling in the thermal break unchanged on one side, only the connection between the thermal break and the main aluminum profile needs to be redesigned. For this connection an existing way of fastening is used as a reference, in this case a connection principle by Schüco in which a screw hole is pre-extruded in the aluminum profile, making it possible to insert screws over the complete length of the profile.

Underneath the new design for attaching the thermal break is shown. The design has been developed in such a way that only minimal adjustments to the aluminum profiles are necessary. The only two modifications in the extrusion of the larger part are the added screw channel and a small circular opening. The new thermal break will exist of one piece instead of two and will be connected with to the larger aluminum part with screws in a 65-degree angle. The small aluminum part will be connected in the original way.

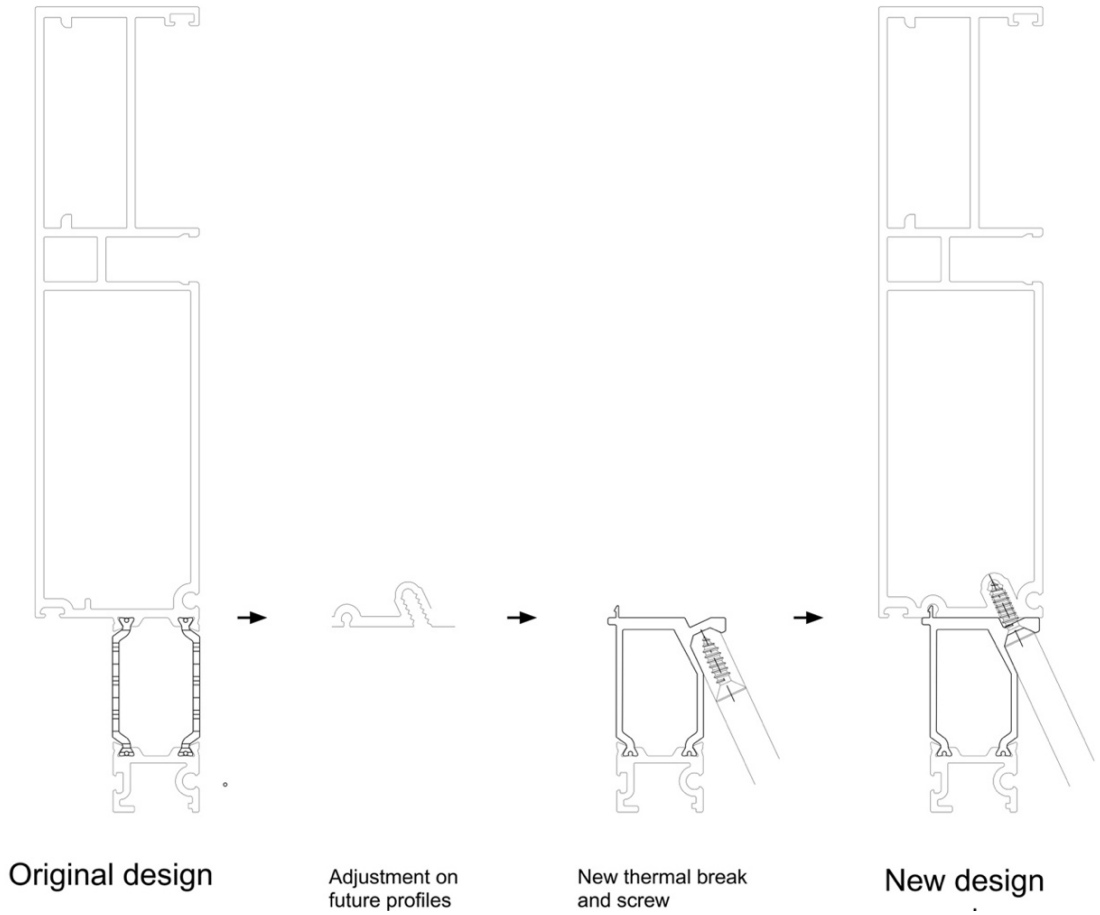

Figure 112: Adjustment to aluminum profile for new thermal break assembly (image by author).

On the right, a detailed view of the new connection is shown, clearly displaying the clip on the left. This clip will make positioning of the thermal break possible and prevents buckling in the left direction and therefore makes it possible to use a single screw connection. The angle of the screw makes it easier accessible from the front. Next to that the force of the screw will push the clip on the right in place, locking movement in the X-direction. A small V-shape in the center of the screws location will make positioning of the screw easier. The exact number of screws per profile depends on the length of the profile. To reach the same shear strength as the current clamped connections, the current shear resistance should be divided by the shear strength of one screw to determine the exact number of screws.
Below several mullion designs, used in previous projects of Scheldebouw, are adjusted to fit the new designed thermal break. It shows the possibility of applying this connection in multiple designs.

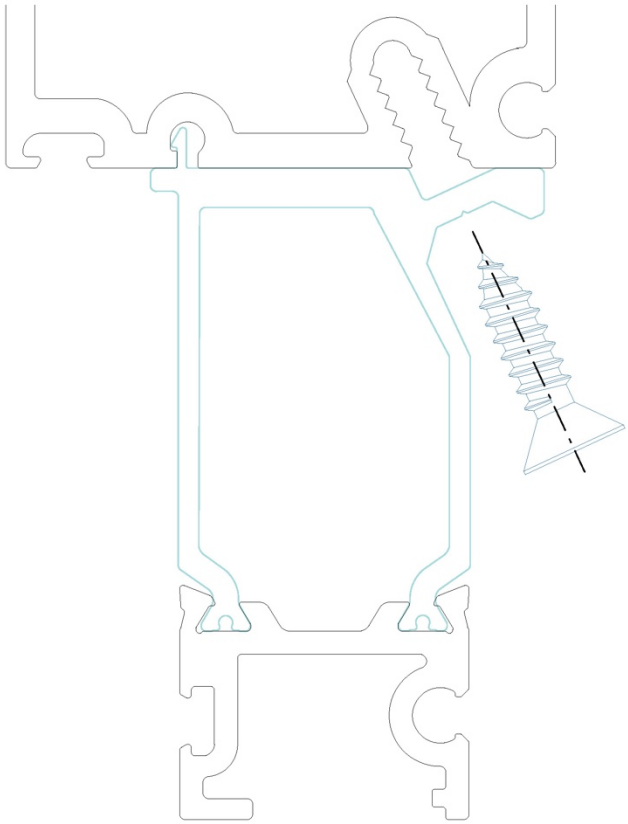

Figure 114: Detailed view of thermal break connection (image by author).

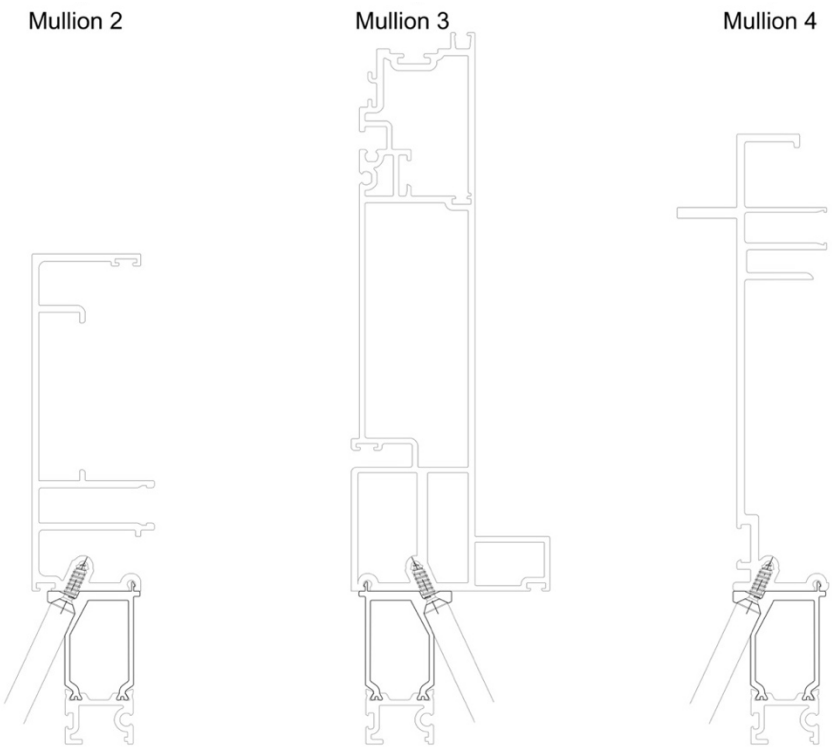

Figure 113: Different mullion designs using the same front part with new standardized thermal break connection (image by author).

By keeping the connection in the exterior aluminum part (B) on the front the same, the geometry won't need a larger surface. This makes the complete disassembly of the thermal break material not possible. However, reusing the complete aluminum component (B) with the thermal break already inserted remains feasible, as it can be mounted onto new profiles as a single unit. On the right different mullion profiles are shown when fitted with different front parts using the exact same design for the thermal break connection. This shows the interchangeable potential of these parts and the idea of standardization in the complete design of the frame of a unitized façade.

There are some limitations in this design like the small extra surface that is needed to extrude the screw channel. Also, this method of connecting adds an extra step in the assembly process of the façade system and might therefore have financial consequences for façade manufacturers like Scheldebouw which would normally purchase profiles in which the thermal break is already inserted.

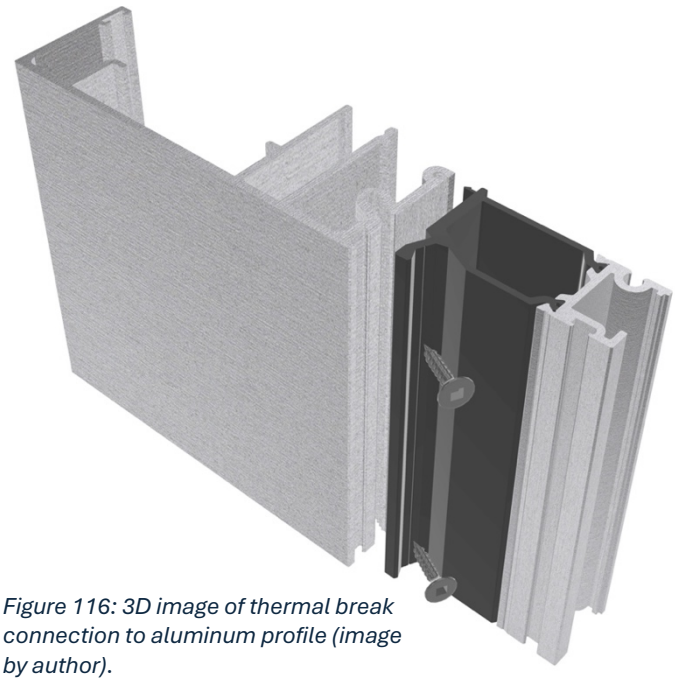

Figure 116: 3D image of thermal break connection to aluminum profile (image by author).

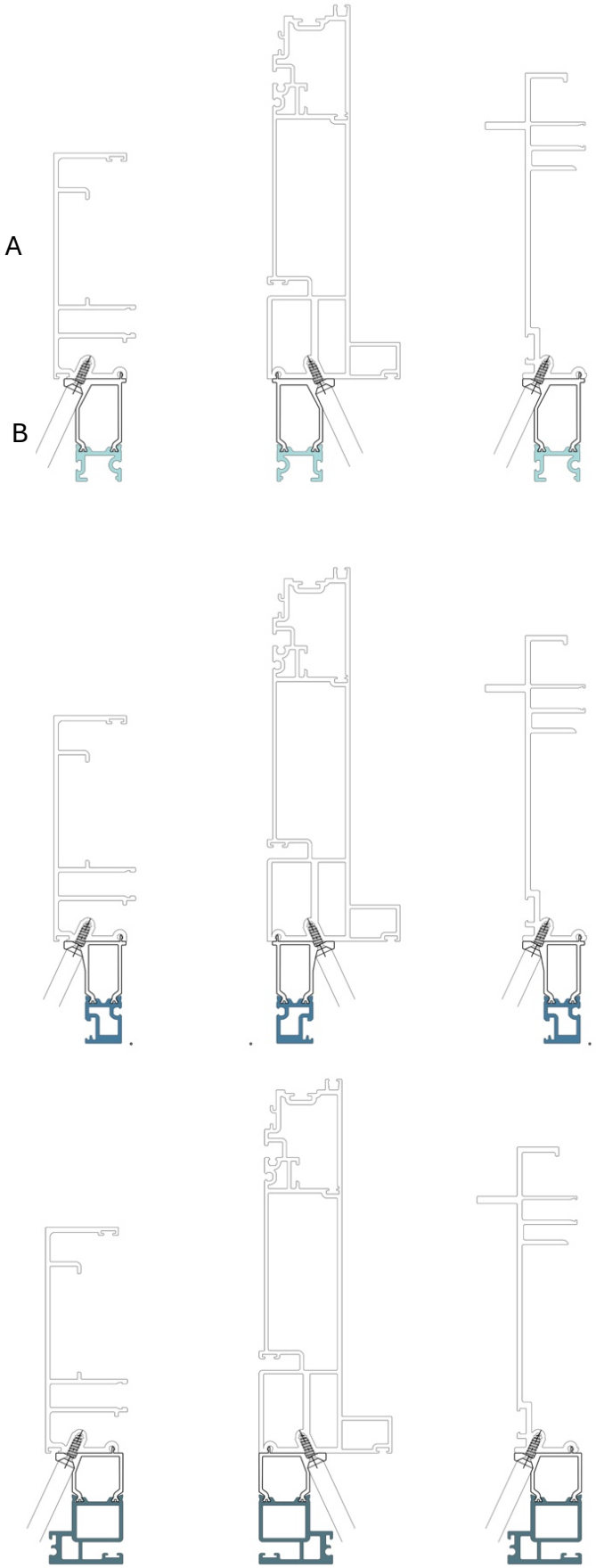

Figure 115: Interchangability of thermal break between different mullions (image by author).

Another limitation of this design would be the weather resistance of the connection. This can be overcome in different ways depending on the requirements the manufacturer has. A small line of silicon sealant on the outside which is easily accessible and can be cut through with a single stroke might secure weather tightness. Another option would be to fit the new thermal break with a small hole to insert a small thermal gasket. Both options are drawn in Figure 117. Requirements should be determined, and practical tests should be conducted to determine the detailed adjustments to the connection for optimal weather resistance.

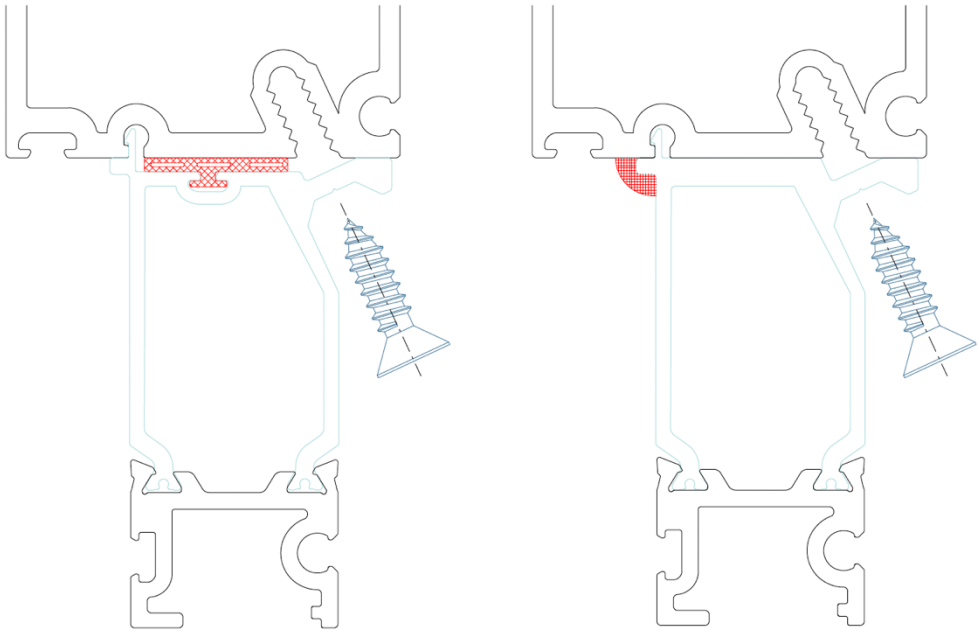

Figure 117: Possible adjustments to thermal break connection to secure weather tightness (image by author).

In the examples shown in the drawings, the width of the thermal break is kept the same because all mullion designs allowed the same size. However, if some mullions require a wider or smaller thermal break, it could be useful to standardize the geometry in multiple widths. This will mean that the screw hole and the clip will be further from, or closer to each other. To keep the advantage of standardization, these different sizes should be determined from the start of the implementation of this new design.

7.4 Conclusion

Chapter 7 shows the possible redesigns of the targeted connections described in Chapter 6. First the redesign of the frame connections. Observations of the production process reveals significant variation in sealant application. The current sealant assembly method limits disassembly and recyclability. Replacing sealant with a durable, waterproof foam, such as polyethylene, offers a promising alternative that could simplify assembly, improve recyclability, and reduce carbon impact. However, further research is needed to assess the performance, aesthetics, and suitability of such materials. Redesigning this connection supports recycling efforts, particularly given the limited potential for direct reuse of the aluminum profiles due to their specific geometry. Next tot that it offers the possibility of reducing the amount of needed chemical sealants what will also save costs and carbon emissions.

Secondly a new principle for unitized system is introduced as the so-called *carrier frame principle*. In this design the short life materials like the IGU are hold together in a lightweight sub-frame which can be disassembled from the main frame of the unit. This makes on-site disassembly possible while still allowing the possibility to replace the IGU separately. This carrier frame principle is a design that can be used for refurbishment of old facade systems. Although the possibility of applying a carrier frame is dependent of the existing mullion and transom, the only specific parts in the ABN AMRO design is the interlocking geometry on the top of the frame, and the 90-degree angle in the vertical profiles, both designed for easy positioning during assembly. It is therefore assumed that this principle is not only possible in the ABN AMRO panel but could be a solution for future projects.
Although the overall number of components that need to be disassembled is reduced, it does not mean that the overall disassembly potential also increases. In the next chapter the eDim method based on MOST is used to create a score for both systems to validate if this carrier frame principle will improve the overall disassembly potential of materials.

The third design presented shows a possible redesign of the current thermal break in aluminum profiles. In this design process the hardest part to overcome was to find an alternative way to transfer the shear force which is currently created by clamping due to deformation of the aluminum part. The new design is based on existing methods used, among other, by companies like Schüco. In this design the larger aluminum part is designed with a pre-extruded screw hole over the total length. This creates the opportunity to fasten the new thermal break geometry in a reversible way by the use of screws. The front part of a mullion and transom will therefore be demountable, increasing the overall adaptability potential of the frame. Two options for achieving requirements for weather tightness are given.

8. VALIDATION OF REDESIGN

Chapter 8 validates several aspects of the proposed designs in Chapter 7. The disassembly potential of the old ABN AMRO system is compared with the new design using the eDim and MOST measurement methods. After that the improvement of thermal performance of the new design is calculated and a partial structural verification for the frame is provided. Finally, the proposed redesign for the new thermal break connection is fictively implemented in two details of the ABN AMRO panel to show the possibility.

8.1 Validation of designed products

In Chapter 3 the validation method for determining the disassembly potential of products is described. The first method designed by DGBC is already used and filled in in Chapter 4 to decide which components of the ABN AMRO panel could be removed. However, the measurement method of DGBC is not able to give a detailed score in disassembly potential of two designs to compare them with each other. Therefore, this chapter will use the previous described eDim measurement method to compare the new carrier frame design with the existing design. Next to that, the thermal performance of both systems is calculated using BISCO Physibel software. Thirdly, an estimation is made to determine maximum deformation of the glass to see if during bending it will collide with existing transoms.

8.2 Calculating disassembly potential

The eDim measurement method and the funding MOST Work Measurement systems are both described in Chapter 3.
The needed Time Reference sheet and the Sequence Calculation sheet, in which the different (dis)assembly tasks and connections in unitized façade systems are listed are described in Chapter 5. These two tables show the calculated Time Measurement Units and the needed time for every sequence.
For the time reference sheet an example of a calculation can also be found in appendix 2.4. All sequences in both sheets are determined using the tables and instructions in **MOST® Work Measurement Systems** by Zandin (2020) and the used tables can be found in appendix 2.3.

After composing these tables, the eDim table can be filled in to determine the total score of the assembly. Although for this research the complete systems are calculated, it can be considered 'unfair' because the old design includes more IGU's (3) than the new (1) which could have been an aesthetic decision at that time. Therefore, the single IGU and carrier frame parts are also compared with each other. The complete tables of the IGU removement and carrier frame disassembly can be found underneath. The calculation tables of the complete panels can be found in appendix 2.1 and 2.2.

Some important statements about the use of this method; The current method was not completely designed for the task of sealant removal for IGU disassembly. In real life the sealant cutting and determining if it is cut all trough is hard as is described in Chapter 4. The total number of strokes per IGU side (left, right, top, bottom) is set to three strokes (12 in total), with a normal knife, till complete unfastening of the sealant from the IGU. In real life this would be number would be higher but very diverse in different situations.

Table 2 shows the disassembly time of the one IGU of the old design. The tasks which take the most time are the cutting of the silicone sealant and the removing of the remaining. Also, the need to turn the element because the IGU needs to be accessed from two sides takes a relatively long time. Resulting in a total theoretical time of 1126 seconds (18.8 minutes).

Disassembly sequence of components	Disassembly sequence of connectors	Number of connectors	Number of product manupilations	Identifiability	Tool Type	Tool Change (s)	Identifying (s)	Manupilations (s)	Positioning (s)	Disconnection(s)	Removing (s)	eDiM(s)
IGU (middle)	gasket-to-sealant	12	0	0	Multitool	0	0	0	0	129,6	0	129,6
IGU (middle)	Sealant inside	12	0	0	Multitool	0	0	0	0	129,6	0	129,6
			1	0	Crane	14,4	0	280,8	0			295,2
Gasket [glazing cap] (lower 1)	Gasket interlocking type 1	1	0	0	Pliers	14,4	0	0	0	10,8	14,4	39,6
Gasket [glazing cap] (lower 2)	Gasket interlocking type 1	1	0	0	Pliers	0	0	0	0	10,8	0	10,8
Gasket [glazing cap] (lower 3)	Gasket interlocking type 1	1	0	0	Pliers	0	0	0	0	10,8	0	10,8
Gasket [glazing cap] (lower 4)	Gasket interlocking type 1	1	0	0	Pliers	0	0	0	0	10,8	0	10,8
Glazing cap (lower 1)	Snap-fit type 1	1	0	0	Hand	14,4	0	0	0	3,6	14,4	32,4
Glazing cap (lower 2)	Snap-fit type 1	1	0	0	Hand	0	0	0	0	3,6	14,4	18
Glazing cap (lower 3)	Snap-fit type 1	1	0	0	Hand	0	0	0	0	3,6	14,4	18
Glazing cap (lower 4)	Snap-fit type 1	1	0	0	Hand	0	0	0	0	3,6	14,4	18
IGU (middle)	Sealant type 1	12	0	0	Knife | multiotool	10,8	0	0	7,2	129,6	133,2	280,8
IGU		0	0	0			0	0	0	0	133,2	133,2
					TOTAL	54	0	280,8	7,2	446,4	338,4	1126,8

Table 4: eDim table of disassembly of single IGU of old design (author).

Table 2 shows the disassembly of an IGU in the new design. Eliminating the silicone sealant and the need to turn the element during the process eliminates almost 2/3 of the needed time. Resulting in a total theoretical time of only 291 seconds (4.9 minutes).

Disassembly sequence of components	Disassembly sequence of connectors	Number of connectors	Number of product manupilations	Identifiability	Tool Type	Tool Change (s)	Identifying (s)	Manupilations (s)	Positioning (s)	Disconnection(s)	Removing (s)	eDiM(s)
Gasket [glazing cap] (lower 1)	Gasket interlocking type 1	1	0	0	Pliers	14,4	0	0	0	10,8	14,4	39,6
Gasket [glazing cap] (lower 2)	Gasket interlocking type 1	1	0	0	Pliers	0	0	0	0	10,8	0	10,8
Gasket [glazing cap] (lower 3)	Gasket interlocking type 1	1	0	0	Pliers	0	0	0	0	10,8	0	10,8
Gasket [glazing cap] (lower 4)	Gasket interlocking type 1	1	0	0	Pliers	0	0	0	0	10,8	0	10,8
Glazing cap (lower 1)	Snap-fit type 1	1	0	0	Hand	14,4	0	0	0	3,6	14,4	32,4
Glazing cap (lower 2)	Snap-fit type 1	1	0	0	Hand	0	0	0	0	3,6	14,4	18
Glazing cap (lower 3)	Snap-fit type 1	1	0	0	Hand	0	0	0	0	3,6	14,4	18
Glazing cap (lower 4)	Snap-fit type 1	1	0	0	Hand	0	0	0	0	3,6	14,4	18
IGU		0	1	0	Crane	0	0	0	0	0	133,2	133,2
					TOTAL	28,8	0	0	0	57,6	205,2	291,6

Table 5: eDim table of disassembly of single IGU of new design (author).

The last table shows the total amount of time that is needed to remove the complete new designed carrier frame from the system with the glass still inserted. This only consists of removing the cover caps in front of the screws, removing the screws and lifting the carrier

frame from the main frame. This takes almost the same time as removing the separate IGU leading to a total theoretical disassembly time of 264 seconds (4.4 minutes).

Disassembly sequence of components	Disassembly sequence of connectors	Number of connectors	Number of product manuplations	Identifiability	Tool Type	Tool Change (s)	Identifying (s)	Manuplations (s)	Positioning (s)	Disconnection(s)	Removing (s)	eDiM(s)
Cover cap carrier frame	Snap-fit type 1	1	0	0	Hand	0	0	0	0	3,6	14,4	18
Cover cap carrier frame	Snap-fit type 2	1	0	0	Hand	0	0	0	0	3,6	14,4	18
Cover cap carrier frame	Snap-fit type 3	1	0	0	Hand	0	0	0	0	3,6	14,4	18
Cover cap carrier frame	Snap-fit type 4	1	0	0	Hand	0	0	0	0	3,6	14,4	18
Carrier frame	Screw type 3	16	0	0	Powertool	14,4	0	0	0	30,24	14,4	59,04
Carrier frame			0	0	Crane	0	0	0	0		133,2	133,2
					TOTAL	**14,4**	**0**	**0**	**0**	**44,64**	**205,2**	**264,24**

Table 6: eDim table of disassembly complete carrier frame of new design (author).

The calculation in the appendix shows that the complete disassembly process of the old design, which is also described in Chapter 4, should take in theory 3319 seconds (55.3 minutes). The new design would only take 1674 seconds (27,9 minutes) in theory according to the eDim calculations.

In conclusion, the disassembly potential of the new system has been improved. Although the number of IGU's in the old system is not similar with the new, the carrier frame principle still shows the improvement of the ease of disassembly. Next to that it is proved in the calculations that the use of sealants for glass connections will result in a higher score compared with 'dry' connections. This is mainly because of the cutting task which is time consuming but also because of the need for modifications, in this case turning the panel which is relatively time consuming.

8.3 Calculating thermal performance

To determine if the new design of the carrier frame also improves the current performance of the system, thermal calculations are conducted. These thermal calculations have been performed at the locations in the details where thermal bridges could occur. For this purpose, both the details of the old design and the new design have been calculated at the same locations to allow comparison. Since in the new design two transoms are bypassed by the new insulated glass unit, these are not compared with the old design. Specifically, a horizontal detail of the opaque section, a horizontal detail of the transparent section, a vertical detail at the top of the carrier frame, and a vertical detail at the bottom of the carrier frame have been calculated. For these calculations BISCO Physibel building physics software is used. The detailed reports and inputs of every calculation can be found in appendix 5.2.

For the calculations the NEN-EN-ISO 10077-2 is used from which the calculation of the U-value of a frame U_f can be determined.

The formula:

$$U_f = \frac{\frac{Q}{\theta i - \theta e} - U_{panel1} L_{panel1} - U_{panel2} L_{panel2}}{W_{frame}}$$

In which:

U_f = the thermal transmittance coefficient of the frame [W/m²K]
Q = the linear thermal transmittance [W/m]
θ_i = the internal temperature
θ_e = the external temperature
U_{panel} = the thermal transmittance of the panel (adjacent to the frame)
L_{panel} = the length of the panel
W_{frame} = the width of the frame

8.3.1 Horizontal detail 01

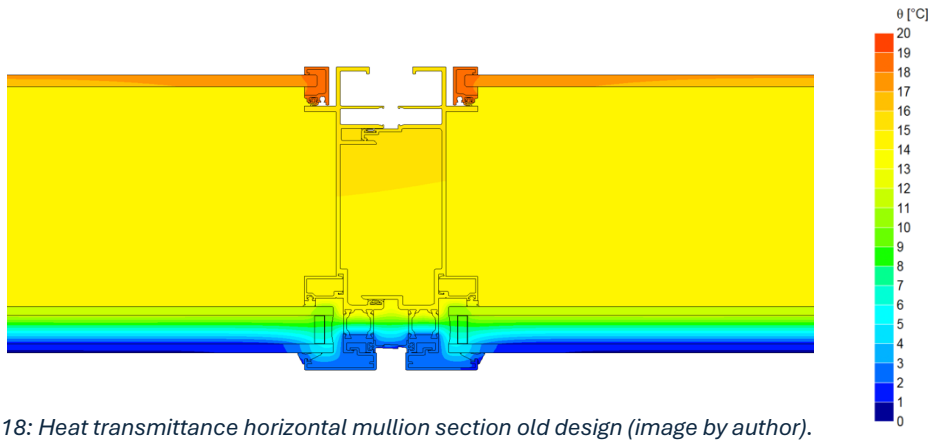

Figure 118: Heat transmittance horizontal mullion section old design (image by author).

In the detail above the thermal transmittance through the horizontal section of the mullions of the old system is shown. Visible is the old double-glazing unit without the use of argon filled cavities. The cavity of the panel is set as highly ventilated cavity with upwards heat flow. Calculating the system gives a total Uf of **4.369 W/m²K.**

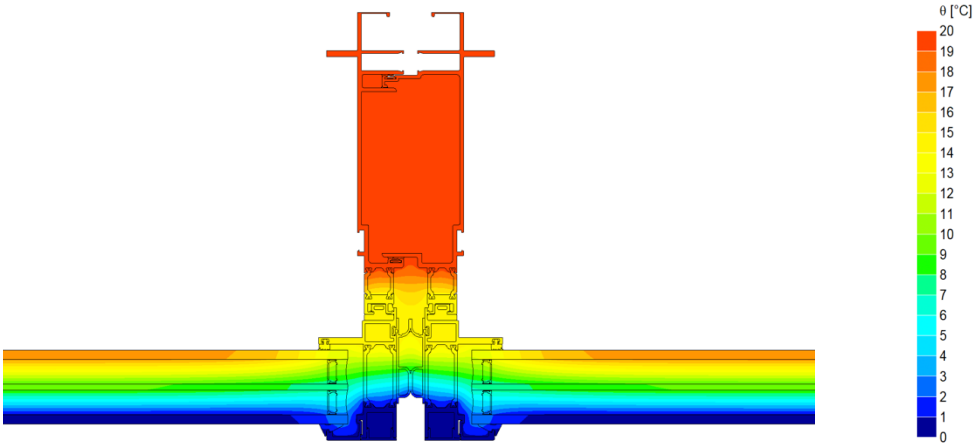

Figure 119: Heat transmittance horizontal mullion section new design (image by author).

The new design, shown above, is fitted with the new carrier frame in which new triple glazing is inserted with 90% argon filled cavities. In this detail the inner glazing is removed with the idea that the total frame will be clad with wood finish. The wooden finish is not included in the calculation. In real life there could be some influence depending on the way the wood is connected on the frame and the type of wood that is used. Since this is beyond the scope of the research the calculation is made without wood finishing. In this calculation the Uf has a value of **3.581 W/m²K** which means an improvement of 0.788 W/m²K. At the same time the installation currently extracting the air through the cavity of the façade which will lead to a reduction of overall operational energy need of the building.

8.3.2 Horizontal detail 02

The horizontal section of the opaque part of the new design shows an improvement in the thermal performance of the frame as can be seen in Figure 120. Next to the fact that the larger thermal break results in less thermal transmittance, the extra layer of 70mm of Rockwool insulation results in a better overall insulation value of the panels next to the mullions. Calculation of the total Uf of the old section gives a value of **4.090W/m²K.** The new section however has a Uf value of **1.704 W/m²K.** Which can be concluded to be a large improvement.

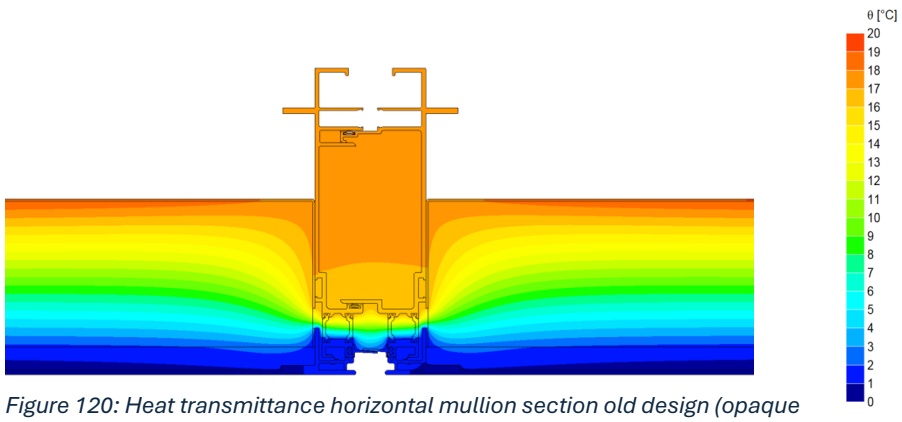

Figure 120: Heat transmittance horizontal mullion section old design (opaque part) (image by author).

The new design could potentially be fitted with extra insulation on the back if the cavity in the panel is not preserved, because the airduct can then be removed and create place for insulation. This however needs more materials and air tightening measures on the inside.

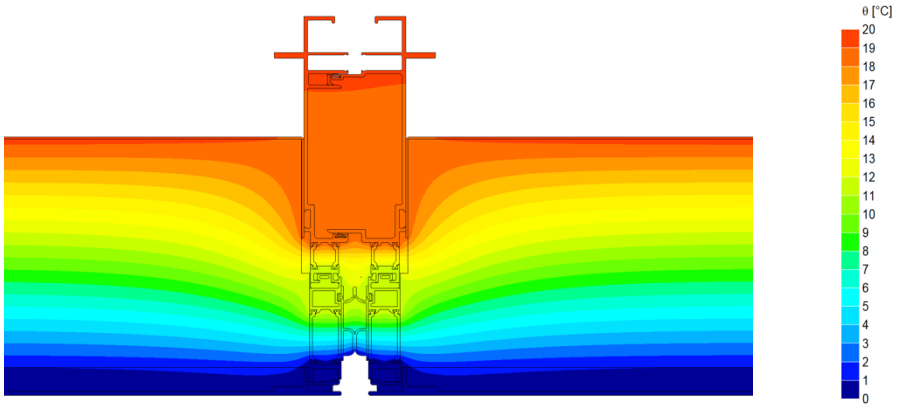

Figure 121: Heat transmittance horizontal mullion section new design (opaque part) (image by author).

8.3.3 Vertical detail 01

The vertical details above show the connection of the transparent part with the opaque part of the panel. On the left the old design, having a Uf value of **3.123 W/m²K**. On the right the new design with the carrier frame attached and the added insulation gives a Uf value of **2.546 W/m²K**. Although not as large as the other sections, the difference is still significant.

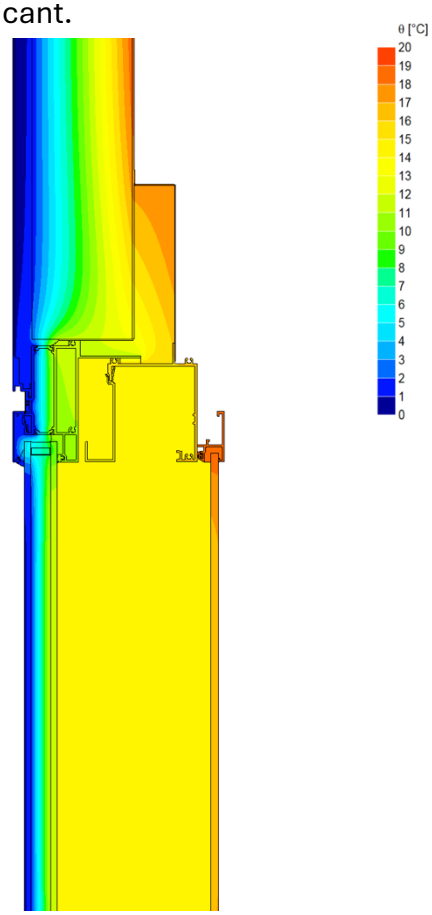

Figure 122: Heat transmittance vertical section transom 4 old design (image by author).

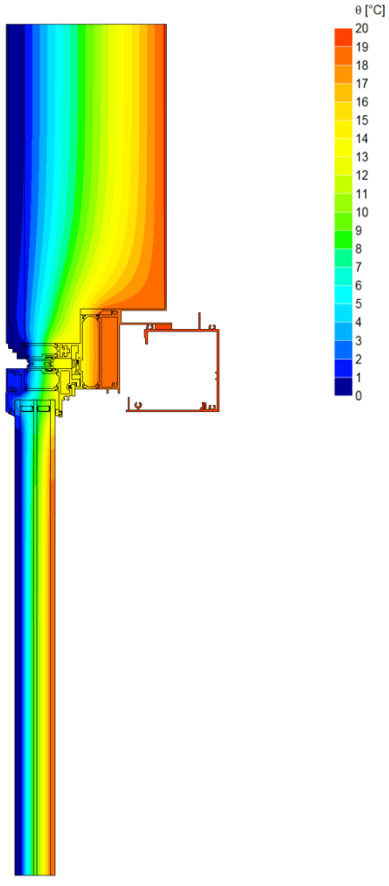

Figure 123: Heat transmittance vertical section top carrier frame new design (image by author).

8.3.4 Vertical detail 02

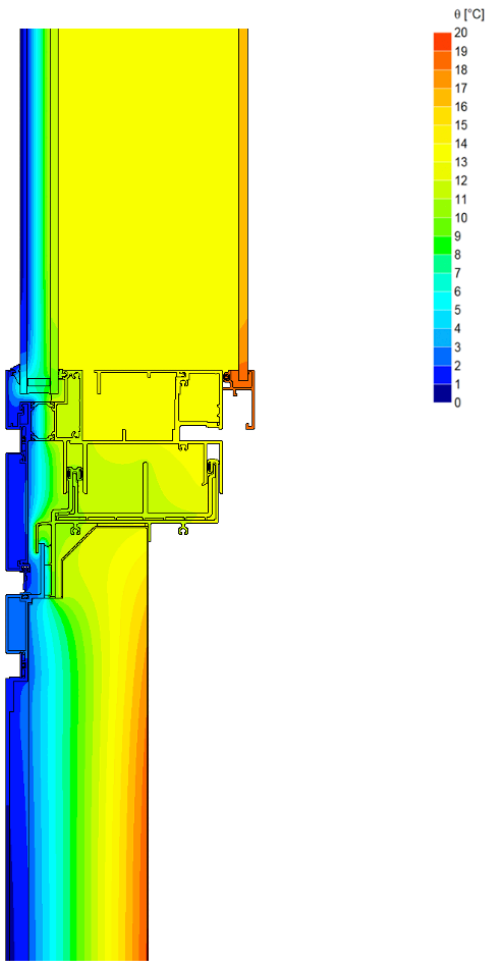

Figure 124: Heat transmittance vertical section transom 5 to 1 old design (image by author).

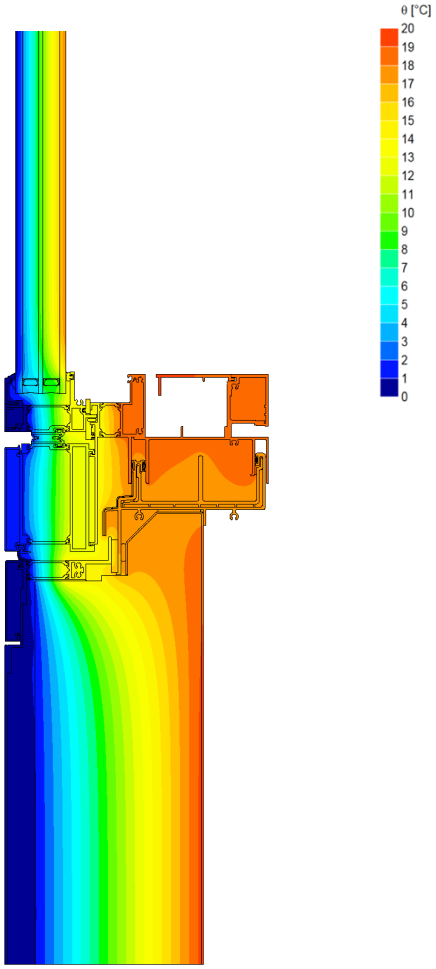

Figure 125: Heat transmittance vertical section transom 5 to 1 new design (image by author).

The second vertical detail shows the connection of the panels at the top and bottom. This detail shows the largest frame contacting the exterior. On the left the section of the old detail and on the right the section of the new design. The calculations show a Uf value of **5.668 W/m²K** for the old system. The Uf value of the new design is **3.113 W/m²K** which is significantly lower and shows the improvement made by the larger thermal barriers in the new frame.

8.3.5 Total U-value façade element

After calculating the U-value of all the frames the total U-value can be determined using the surface area of different parts. For calculating the total U-value the following formula is used:

$$Ucw = \frac{Af \cdot Uf + Ag \cdot Ug + Ap \cdot \mathrm{Up}}{Af + Ag + Ap}$$

Ucw = Total U-value of the façade unit (W/m^2·K)

Af = Frame area (m^2)
Uf = U-value of the frame ($W/m^2 \cdot K$)
Ag = Glass area (m^2)
Ug = U-value of the glazing ($W/m^2 \cdot K$)
Ap = Panel area (m^2)
Up = U-value of the panel ($W/m^2 \cdot K$)

§	Component	U [W/m^2K]	A [m^2]	U x A [W/K]	U x A [%]
	mullion 1	4.37	0.076	0.33	4
	mullion 2	4.37	0.076	0.33	4
	mullion 3	0.00	0.000	0.00	0
	transom 1	5.67	0.137	0.78	8
	transom 2	2.33	0.117	0.27	3
	transom 3	2.14	0.331	0.71	8
	transom 4	3.12	0.155	0.48	5
	transom 5	5.67	0.122	0.69	8
	glazing 1	1.23	1.157	1.42	16
	glazing 2	1.23	2.186	2.69	29
	glazing 3	1.23	0.703	0.86	9
	panel 1	0.32	1.780	0.57	6
	Total		6.840	9.15	100
	Ucw =	**1.34**	**W/m²K**		

Table 7: Calculation table U-value old system (image by author).

§	Component	U [W/m^2K]	A [m^2]	U x A [W/K]	U x A [%]
	mullion 1	3.23	0.076	0.25	6
	mullion 2	3.23	0.076	0.25	6
	mullion 3	0.00	0.000	0.00	0
	transom 1	3.11	0.137	0.43	10
	transom 2	2.49	0.155	0.39	9
	transom 3	3.11	0.122	0.38	9
	transom 4	0.00	0.000	0.00	0
	glazing 1	0.60	4.495	2.70	62
	glazing 2	0.00	0.000	0.00	0
	glazing 3	0.00	0.000	0.00	0
	panel 1	0.00	1.780	0.00	0
	Total		6.840	4.38	100
	Ucw =	**0.64**	**W/m²K**		

Table 8: Calculation table U value new system (image by author).

The calculations show an old Ucw of **1.34 W/m²K.** New design has a value of **0.64 W/m²K** which is a significant improvement of the thermal performance of the system. The improvement is a result of both the improvement of the new triple glazing over the old double glazing and cavity. Also reducing the number of transoms and the improvement of U-value of transoms and mullions has influence on the lower Ucw.

8.4 Calculation avoided carbon

To assess the performance improvement, it is essential to verify whether the total carbon emissions of the new ABN AMRO façade design are lower than those of designing and producing an entirely new façade using virgin materials. In this context, experts at Scheldebouw calculated the total environmental impact of the new design proposed in this research. Additionally, they estimated the impact that would have occurred if a similar system had been produced using only virgin materials.

By calculating the carbon impact in different stages of the LCA, the impact of the total process can be derived. In this case Scheldebouw calculated the impact for a total area of 20.000 m^2 façade. The total weight of the materials of the new design is shown in appendix 4.

As can be seen in the tables below, the total CO2 impact is compared between:

Option 0: total demolition of the façade, brought to landfill and the application of a completely new façade using virgin materials.

Option 1: the reuse of components, building the design of the carrier frame, proposed in this research.

Total area facade 20.000 m2

Total CO2.e / m2 facade

	Dismantling for waste	Transport to End of life location (Waste/Recycling)	Impact for elements that are put into recycling	Impact for elements that are put into waste	The impact of the raw materials needed	Transport of materials to production facility	(Re-) manufacturing energy	Transport elements to receiving building	Energy needed for mounting elements to receiving building	
	C1	C2	C3	C4	A1	A2	A3	A4	A5	Totaal kg CO2.e / m2
Option 0 (Demolition element / completely new unit)	0,24	2,56	12,15	45,21	244,64	3,53	31,08	1,07	0,24	340,70
Option 1 (Retain element / refurbished unit)	0,24	2,56	5,41	27,75	90,39	2,54	15,54	1,07	0,24	145,73

Option 1 (Retain element / refurbished unit) total carbon savings **57%** compared to: Option 0 (Demolition element / completely new unit)

Totaal CO2.e gevel

	C1	C2	C3	C4	A1	A2	A3	A4	A5	Totaal kg CO2.e
Option 0 (Demolition element / completely new unit)	4.800	51.161	242.917	904.102	4.892.780	70.584	621.523	21.331	4.881	6.814.078
Option 1 (Retain element / refurbished unit)	4.800	51.161	108.163	554.921	1.807.741	50.865	310.761	21.331	4.881	2.914.624

Table 9: Calculations of carbon per LCA stage (image by Scheldebouw).

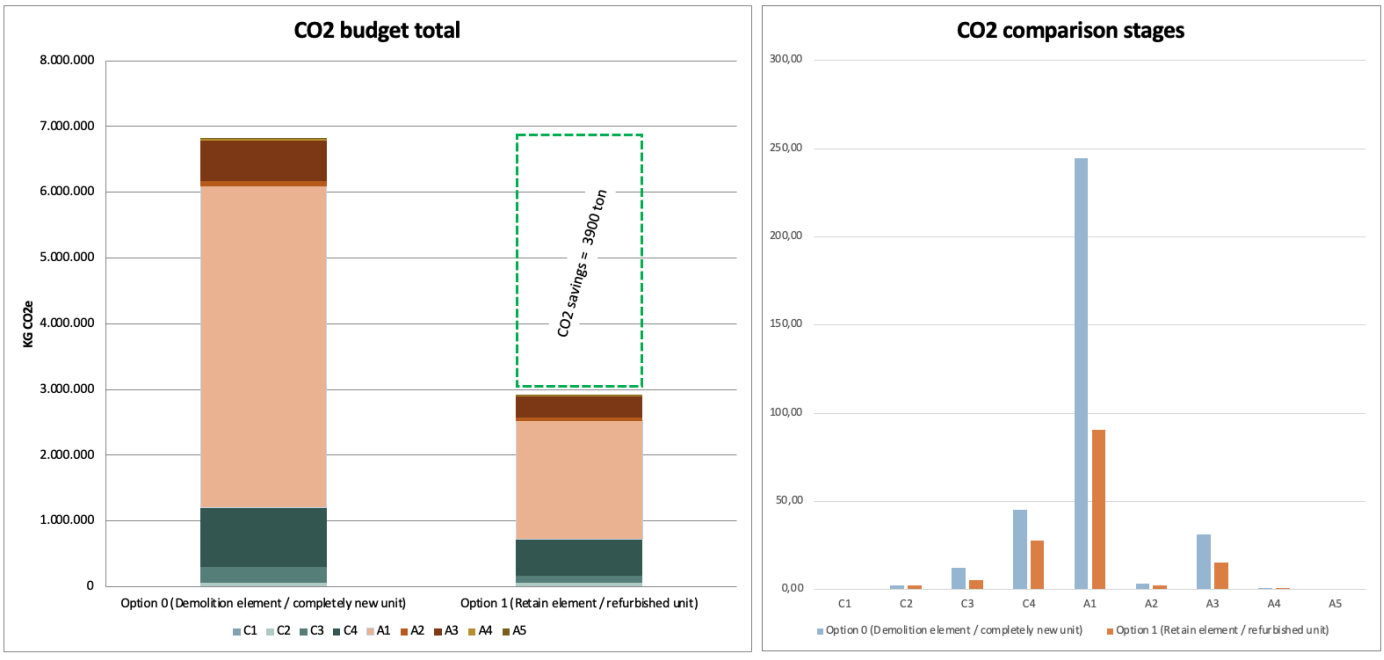

Table 10: Total budget of CO2 compared between different options (image by Scheldebouw).

The calculations by Scheldebouw show a 57% saving in emitted carbon for option 1 compared to option 0 which can be seen as a very significant impact. The largest savings are created during stage A1 in which less carbon is needed for new materials. Also, stage C4 in which the savings for waste are calculated shows a significant difference.
Within this calculation the (wooden) material for the internal finishing is not included since the exact material is not yet determined. When using a total area of 20.000m^2, the total amount of carbon savings is 3900 tons.
In conclusion it can be stated that the new design, created in this research, needs significant less carbon than when a completely new façade is used.

8.5 Structural verification carrier frame

8.5.1 Maximum bending deformation glass

Wind load can lead to bending of the IGU in the carrier frame. Because the existing transoms are located behind the IGU, deformation of the glass can lead to collision with these transoms. The maximum deformation caused by wind loads should be calculated to determine the exact size of the depth of the profiles of the carrier frame. If the rule of thumb, span/60, would be used to estimate the maximum deflection of glass panes it will result in a distance of 2525/60 = 42 mm. It can however be assumed that the maximum deformation of the third pane in a triple glass unit will show less deformation than the first, assuming that the inner and outer pane have the same thickness. The deformation of the inner glass pane depends not only on the Young's modulus of the glass but also the absorption by the first two panes and the Young's modulus of the spacer. The exact deformation can therefore only be calculated with the use of finite element software. These methods are out of the scope of this research and are therefore recommended to conduct for future projects in which the carrier frame principle is considered.

8.5.2 Number of screws

The carrier frame is connected to the main frame with screws. To determine the number of screws a simple calculation has been conducted. This calculation only takes the shear force for the screws and the maximum bearing resistance of the aluminum plate into account.

TOTAL WEIGHT FRAME + GLASS = **193.36 Kg** = 1897 N

Testing maximum shear resistance in bolt:

$$V_{bRD} = \frac{\alpha * f_u * A}{\gamma_{m2}}$$

[Eurocode 1991-1-8]

α = Reduction factor for shear (0.6) [Eurocode 1991-1-8]
f_u = Ultimate tensile strength of bolt (N/mm^2)
A = area of bolt
γ_{m2} = partial safety factor (1.25) [Eurocode 1991-1-8]

$$V_{bRD} = \frac{0.6 * 500 * 13.42}{1.25} = 3220.8\ N$$

F_{total}/F_{bolt} = 1897 / 3220 = 0.59 bolts

Testing bearing resistance of aluminum plate:

$$F_b R_d = \frac{k_1 * d * t * f_u}{\gamma_{m2}}$$

k = Reduction factor for shear (0.6) [Eurocode 1991-1-8]
f_u = Ultimate tensile strength of bolt (N/mm^2)
d = diameter of the bolt
t = thickness of aluminum wall
γ_{m2} = partial safety factor (1.25) [Eurocode 1991-1-8]

$$F_b R_d = \frac{2.5 * 4.134 * 2.5 * 111}{1.25} = 2294\ N$$

2294N > 1897N so it is satisfactory

This means that in theory the minimum number of screws is just one screw, based on the shear resistance. However, this would not be safe and satisfactory since it does not secure the stability, and the calculation does not take tensile forces into account. It is assumed that the frame should be assembled with a minimum of 10 screws.

8.6 Thermal break application

The new design for the connection of the thermal break described in Chapter 7.3 requires additional research. Calculations should show if the recommended screw connection will be satisfactory for carrying the required load of the IGU and the outside cladding of a façade element. In this case the exact calculations and practical validation of the new thermal break falls outside the scope of this research. It can however be tested if the design would have worked if an existing design like the ABN AMRO panel was equipped with a geometry proposed in Chapter 7.3 in the mullions and transoms. A design has been made to achieve the same aesthetics as the design in Chapter 7.2. The drawings below show how the mullions and lower transom of the ABN AMRO panel would look when the new thermal bridge design was used to insert triple glazing. Exact calculations of a complete design should be made to determine difference in carbon impact.

The removable front makes it able to use the same cover cap on the outside. The new glazing bead on the inside can be inserted over the complete length of the IGU. Although the design requires less new material, the carrier frame principle described in 7.2 offers the possibility to disassembly the whole frame with IGU inserted, which is not possible in the design shown below. Another limitation could be the unsymmetrical geometry which could make it harder to secure weather tightness.

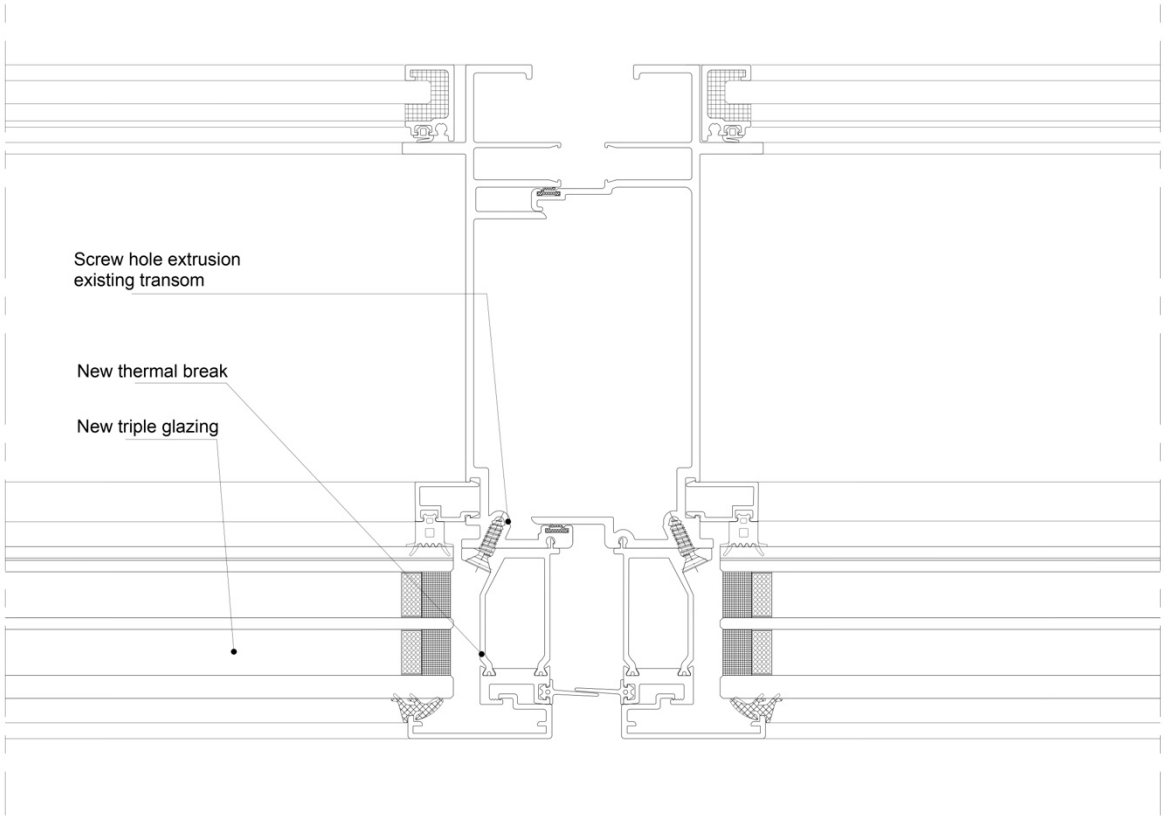

Figure 126: Fictive mullion design ABN AMRO panel, if application of standardized thermal break design would be possible (image by author).

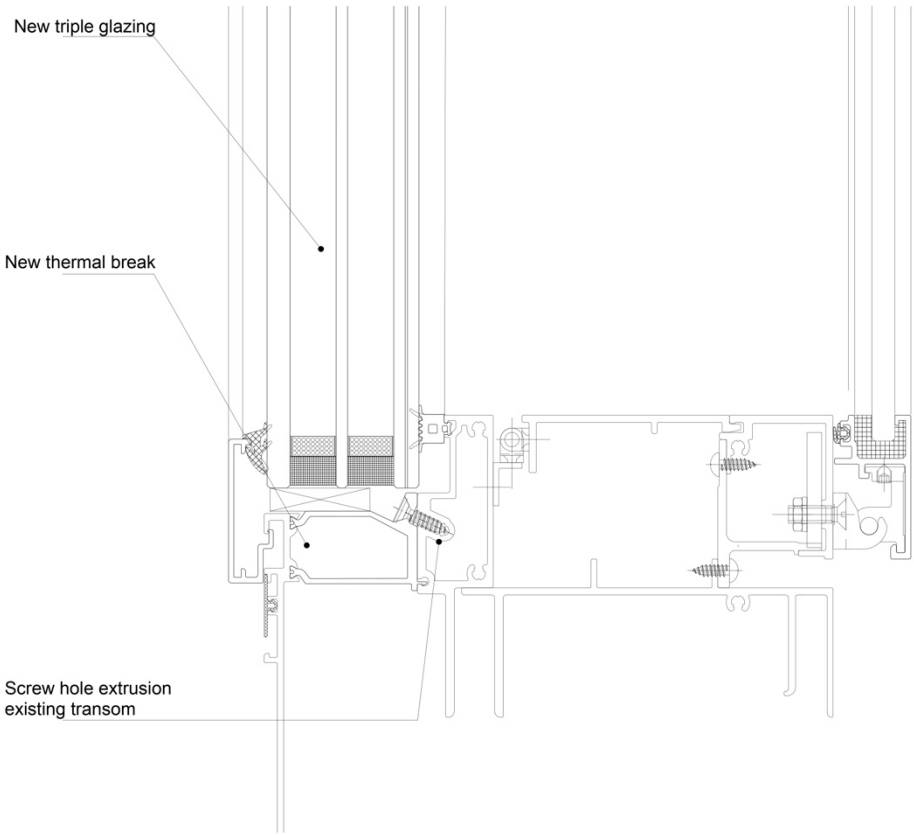

Figure 127: Fictive design lower transom ABN AMRO panel, if application of standardized thermal break design would be possible (image by author).

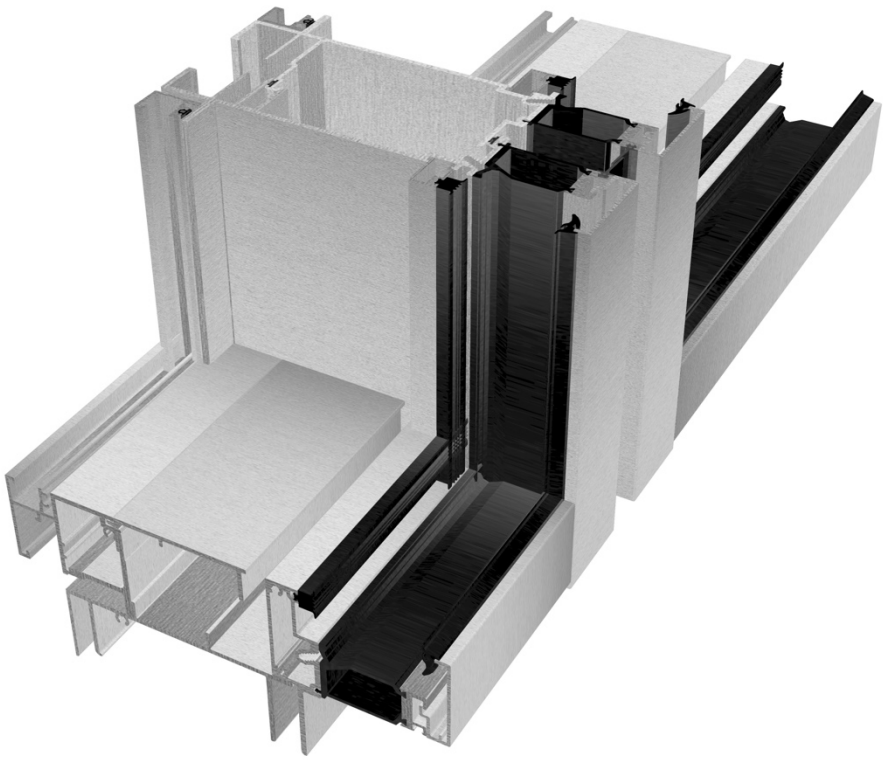

Figure 128: 3D image of corner connection of new thermal break design (image by author).

The new connection can be disassembled using a power tool to unscrew all the used screws. The existing connection would need to be sawn through along the entire length of the profile. Comparing the disassembly potential of the new screw connection with the current connection using MOST will give the same sequence:

A = Action distance
B = Body motion
T = Tool handling

A_0 B_0 T_6

Total index = 6 (see appendix 2.3)
6 * 100 = 600 TMU
600 * 0.036 = 21.6 seconds

Or

A_0 B_0 T_{10}

Total index = 10 (see appendix 2.3)
10 * 100 = 1000 TMU
1000* 0.036 = 36 seconds

In this case the only the index of the tool motion T may differ depending on the length of the profile. In any case, the current and proposed connections are not directly comparable in terms of disassembly potential, as the existing connection can only be removed by destruction, making the components unusable. In contrast, the new connection allows for full recovery and reuse of all components.

8.7 Conclusion

Chapter 8 shows different ways of validation of the designs which were presented during this research. The first paragraph shows that the new designed carrier frame principle is an improvement in terms of disassembly potential. The comparison of the IGU connection shows that the ease of disassembly has been increased by not using sealant. Next to that the option of disassembling the complete frame with IGU inserted offers a much faster disassembly process than the old design.
The thermal calculation show that the new system has improved the thermal performance by over two times. Every detail which has been calculated using BISCO software shows a lower U-value of the frame.
Next to thermal performance, small validation of the structural performance is conducted. Although the calculations for maximum shear force in screws and maximum deformation of the IGU have a positive outcome, it requires additional research and calculations to determine the exact values.

Lastly the new design of the thermal break is tested in a fictive way to find out how the new ABN AMRO panel would look like if the existing mullions and transom would be fitted with the proposed geometry from Chapter 7. It shows the opportunity of inserting a triple glazing unit in a less complicated system than with the use of the carrier frame.

E. CONCLUSION AND RECOMMENDATIONS

9. CONCLUSIONS & RECOMMENDATIONS

9.1 Conclusions

This research aimed how the environmental impact façade systems could be decreased. The main question to achieve this goal was: *"In what ways can connections in unitized façade systems be improved to make disassembly of components possible and thereby make a contribution to the circular economy in the built environment?"*. In order to answer this main question, first the five sub-questions are answered.

Sub-questions:

1. **What is the current status/view on circularity in built environment and facades?**

Circular design principles are not yet embedded enough in the façade industry. In façade systems, the integration of materials with differing life spans, without consideration of these differences during the design phase, represents a significant obstacle to achieving higher strategies on the R-ladder as defined by the Circular Economy framework. Since a complete system only lasts as long as its weakest permanent bonded connection, the concept of Design for Disassembly is found to play a key role in the increase of reclamation potential. Which focusses on simplifying deconstruction processes by thoughtful planning and design.
To objectively assess the ease of disassembly, two measurement methods were used. The first, developed by DGBC, was found to lack the necessary detail for comparing highly advanced systems like unitized façades. It is therefore best suited as a tool in the early design stages, to help select components for potential disassembly. The second method, eDim, is based on the MOST work measurement system. Although more time-consuming, it enables detailed comparison of the disassembly potential of façade systems.

2. **Which components and/or materials exhibit high potential for reclamation?**

According to the research the main two materials with large impact on the environment are aluminum and glass (Chapter 2). At the same time, aluminum frames and IGUs have an estimated lifespan difference of approximately 35 years. Although IGU's have a low life expectancy, new automated disassembly techniques for glass panes and spacers show the need for non-destructive ways of disassembling IGU's from facades.
It is found that the main frame of a facade unit has the highest reuse potential. At the same time due to the use of highly specific aluminum extrusions, the reuse potential of the separated transoms and mullion profiles is low. It is therefore stated that a higher R-strategy can be achieved when leaving the frame intact. However, when focusing on recycling, easy disassembly of the frame components could be beneficial because of the large carbon impact of the aluminum.

3. **Which types of connections are currently used in unitized façade systems, and how can they be ranked based on specific disassembly criteria?**

Although performance and technology in façade systems have significantly improved over the past decades, the basic methods of assembly have not changed drastically in the last 20–30 years. Chapter 5 presents an overview of different connections between components, revealing that the number of connection types used is relatively limited. The

MOST measurement method makes it possible to rank these connections using Time Measurement Units (TMUs). A disassembly experiment on the ABN AMRO panel contributed to the identification of basic disassembly tasks. As a result, a *time reference sheet* for these tasks and a *sequence calculation sheet* for different connection types were developed to help assess the ease of disassembly in façade systems.

4. **Which connection types currently limit the reusability or prevent the reclamation of long-life components?**

Three connection methods were targeted in this research for redesign to improve reclamation potential. Firstly, the connection between components within the main frame. The excessive use of sealant makes non-destructive disassembly of these connections nearly impossible. Secondly, the way IGUs (Insulated Glazing Units) are connected to the frame provides limited adaptability for future reuse. If IGUs with different dimensions or thicknesses are required in the future, a new type of connection will be necessary. Thirdly, the thermal break connection in aluminum frames limits adaptability and thus the reclamation potential. Although this type of connection is widely used and considered a standard method, it is not reversible, making non-destructive disassembly unfeasible.

5. **How can connections be redesigned and tested to make debonding possible and therefore increases the possibilities of the Circular Economy?**

In this research three new design are proposed. The first design is an option to use a weather foam to replace the current application of silicone sealant. This makes disassembly of aluminum profiles easier and therefore improves the recycling potential. Second, a new carrier frame principle is proposed, based on the ABN AMRO case study. Although developed for this specific façade, the carrier frame is not highly project-specific and is therefore considered a transferable design principle. This frame allows IGUs to be disassembled more easily and non-destructively. The principle also enables the simultaneous disassembly of multiple components, making on-site (dis)assembly more efficient. In addition, it supports the integration of IGUs with varying dimensions in future applications.
Third, a redesigned thermal break is introduced in which components are connected using screws. This allows the front section of a mullion or transom to be made detachable in future systems. As a result, outer profile parts become interchangeable, increasing the adaptability of façade frames. This new connection method offers a standardized, reversible solution that significantly improves reclamation potential.

In conclusion, this research identifies three redesigned connection concepts, two of which are developed in detail. The proposed carrier frame principle and a new connection method for the thermal break in aluminum profiles can improve the adaptability of unitized façade frames for future reuse. This increased adaptability enhances the reclamation potential and therefore contributes to the circular economy.

9.2 Recommendations

As the conclusion states, the redesigns proposed in this research provide practical evidence that systems can be designed for disassembly. This enhances the ability to reuse individual components and therefore reduces the environmental impact. One of the important findings during this research was that Design for Disassembly principles need to be implemented in very early stages of the design process. The disassembly experiment revealed several practical challenges for workers, including the time required for the analyzing the drawings. The implementation of a disassembly manual will support workers during the disassembly process. If created collaboratively by all designers throughout the design process, it can also raise awareness of the importance of circular design.

The redesigned connections not only offer solutions for future systems, but also demonstrate to the industry that it is possible to design for disassembly and future reuse of components.

Previous research in this field has mainly focused on theoretical challenges and the development of frameworks. In contrast, this study applies a practical approach in which a design process was developed to identify the technical barriers to disassembly and explore ways to overcome them.

Although this research proposes multiple redesigns, the holistic approach enabled a broad perspective and consideration of a wide variety of solutions. However, this approach allowed less time for validating all aspects of the proposed designs.

One element that was addressed in more detail is the testing of disassembly potential using the eDim and MOST measurement methods. While these methods provided objective outcomes, they were found to be time-consuming. This raises the question of whether the industry is willing to adopt such validation methods. Starting to develop facade-specific inventories for different connection types could speed up the process.

In addition, further research is needed to demonstrate that the proposed redesigns are applicable to other projects. Multiple tests should be conducted to prove that these solutions can be implemented across different cases. Furthermore, the redesigned connections require additional structural validation. For example, the number and type of bolts in the carrier frame should be calculated using finite element analysis, and the maximum deformation of the new IGU should also be assessed.

The new thermal break connection should be prototyped using the actual materials in order to perform practical shear resistance tests on the screws, and to compare these results with the current standard.

Moreover, it was found during this research that a gap exists between the academic research field (mostly universities) and the industry (companies such as Scheldebouw). At present, a great deal of valuable information is being collected by researchers, but much of it does not reach industry stakeholders. As a result, innovation within the circular economy is progressing slowly. At the same time, researchers often lack access to key information from production processes or design details due to confidentiality policies within companies. Strong collaboration between academic research and industry is essential to enable the implementation of circular principles.

REFERENCES

Abuzied, H., Senbel, H., Awad, M., & Abbas, A. (2020). A review of advances in design for disassembly with active disassembly applications. In *Engineering Science and Technology, an International Journal* (Vol. 23, Issue 3, pp. 618–624). Elsevier B.V. https://doi.org/10.1016/j.jestch.2019.07.003

Benachio, G. L. F., Freitas, M. C. D., & Tavares, S. F. (2020). Circular economy in the construction industry: A systematic literature review. In *Journal of Cleaner Production* (Vol. 260). Elsevier Ltd. https://doi.org/10.1016/j.jclepro.2020.121046

Bibi, I., Ahmad, H., Farid, A., Iqbal, H., Habib, N., & Atif, M. (2023). A comprehensive study of electrically switchable adhesives: Bonding and debonding on demand. In *Materials Today Communications* (Vol. 35). Elsevier Ltd. https://doi.org/10.1016/j.mtcomm.2023.106293

Bilal, M., Khan, K. I. A., Thaheem, M. J., & Nasir, A. R. (2020). Current state and barriers to the circular economy in the building sector: Towards a mitigation framework. *Journal of Cleaner Production*, *276*. https://doi.org/10.1016/j.jclepro.2020.123250

Cambier, C., Elsen, S., Galle, W., Lanckriet, W., Poppe, J., Tevernier, I., & Van der Vaeren, C. (2019). *Building a Circular Economy Design Qualities to Guide and Inspire Building Designers and Clients*.

Campos Soto, M. (2023). *Design for Disassembly Guideline*.

Circle Economy. (2020). *The circularity gap report*.

De Fazio, F., Bakker, C., Flipsen, B., & Balkenende, R. (2021). The Disassembly Map: A new method to enhance design for product repairability. *Journal of Cleaner Production*, *320*. https://doi.org/10.1016/j.jclepro.2021.128552

Droste, S. (2023). *Disassembly assessment framework for enhanced reclamation of façade systems*.

Ellen MacArthur Foundation. (2013). *Towards the circular economy: Economic and business rationale for an accelerated transition*.

European Commision. (2011). *Roadmap to a Resource Efficient Europe*.

Güngör, A. (2006). Evaluation of connection types in design for disassembly (DFD) using analytic network process. *Computers and Industrial Engineering*, *50*(1–2), 35–54. https://doi.org/10.1016/j.cie.2005.12.002

Hart, J., Adams, K., Giesekam, J., Tingley, D. D., & Pomponi, F. (2019). Barriers and drivers in a circular economy: The case of the built environment. *Procedia CIRP*, *80*, 619–624. https://doi.org/10.1016/j.procir.2018.12.015

Hartwell, R. (2019). *End-of-Life Challenges in Facade Design A disassembly framework for assessing the environmental reclamation potential of facade systems*.

Hartwell, R., Macmillan, S., & Overend, M. (2021). Circular economy of façades: Real-world challenges and opportunities. *Resources, Conservation and Recycling*, *175*. https://doi.org/10.1016/j.resconrec.2021.105827

Hartwell, R., & Overend, M. (2019). *Unlocking the Re-use Potential of Glass Façade Systems*. https://www.researchgate.net/publication/357516607

HEGLA. (2023). *Separating insulated glass: Utilising imperfect panes and end-of-life IGUs*. https://www.hegla.com/en/news/news-hegla/separating-insulated-glass-igus/

Hilbrand, L. (2012). *Embodied energy in facade design*.

Jones, N., Harrison, D., Chiodo, J., & Billett, E. (2002). *Design for Automotive Glass Removal Using Active Disassembly*.

Kishna, M., & Prins, A. G. (2024). *Uitgangspunten voor toepassing bij het PBL*.

Kragh, M. K., & Jakica, N. (2021). Circular economy in facades. In *Rethinking Building Skins: Transformative Technologies and Research Trajectories* (pp. 519–539). Elsevier. https://doi.org/10.1016/B978-0-12-822477-9.00016-4

Kroll, E. (1996). *Application of Work-Measurement Analysis to Product Disassembly for Recycling | Enhanced Reader*.

Kroll, E., & Hanft, T. A. (1998). Quantitative evaluation of product disassembly for recycling. In *Research in Engineering Design - Theory, Applications, and Concurrent Engineering* (Vol. 10, Issue 1, pp. 1–14). Springer Verlag. https://doi.org/10.1007/BF01580266

Likins-White, M., Tenent, R. C., & Zhai, Z. (2023). Degradation of Insulating Glass Units: Thermal Performance, Measurements and Energy Impacts. *Buildings*, *13*(2). https://doi.org/10.3390/buildings13020551

Lu, Y., Broughton, J., & Winfield, P. (2014). A review of innovations in disbonding techniques for repair and recycling of automotive vehicles. *International Journal of Adhesion and Adhesives*, *50*, 119–127. https://doi.org/10.1016/J.IJADHADH.2014.01.021

Metabolic, Knubbinga, B., Bamberger, M., van Noort, E., van den Reek, D., Blok, M., Roemers, G., Hoek, J., & Faes, K. (2018). *A framework for circular buildings*. www.dgbc.nl/

Mulcahy, K. R., Kilpatrick, A. F. R., Harper, G. D. J., Walton, A., & Abbott, A. P. (2022). Debondable adhesives and their use in recycling. In *Green Chemistry* (Vol. 24, Issue 1, pp. 36–61). Royal Society of Chemistry. https://doi.org/10.1039/d1gc03306a

Oluleye, B. I., Chan, D. W. M., Saka, A. B., & Olawumi, T. O. (2022). Circular economy research on building construction and demolition waste: A review of current trends and future research directions. In *Journal of Cleaner Production* (Vol. 357). Elsevier Ltd. https://doi.org/10.1016/j.jclepro.2022.131927

Patterson, M., & Vaglio, J. C. (2011). *Façade Retrofits: The Dilemma of the Highly Glazed High-Rise Facade*.

Peeters, J., Tecchio, P., Ardente, F., Duflou, J., Vanegas, P., & Coughlan, D. (2018). *eDIM: Further development of the method to assess the ease of disassembly and reassembly of products : application to notebook computers*.

Pomponi, F., & Moncaster, A. (2017). Circular economy for the built environment: A research framework. *Journal of Cleaner Production*, *143*, 710–718. https://doi.org/10.1016/j.jclepro.2016.12.055

Rios, F. C., Chong, W. K., & Grau, D. (2015). Design for Disassembly and Deconstruction - Challenges and Opportunities. *Procedia Engineering*, *118*, 1296–1304. https://doi.org/10.1016/j.proeng.2015.08.485

Shalaby, M. M. (2008). *High stiffness, lock-and-key heat-reversible locator-snap systems for the design for disassembly*.

Sonnenberg, M. (2001). *Force and effort analysis of unfastening actions in disassembly processes*. https://digitalcommons.njit.edu/dissertations

Stahel, W. (1982). *THE PRODUCT-LIFE FACTOR*.

Teeuwen, R. (2023). *Circularity of existing aluminium unitised curtain wall facades Unlocking Value from Waste*. http://repository.tudelft.nl/.

van Vliet, M., van Grinsven, jip, & tenizen, jim. (2021). *Disassembly potential measurement method*.

Vanegas, P., Cattrysse, D., Duflou, J., & Peeters, J. R. (2016). *Study for a method to assess the ease of disassembly of electrical and electronic equipment. Method development and application to a flat panel display case study*. https://doi.org/10.2788/130925

Walker, A., McAlister, S., & Grant, T. (2007). *The Environmental Impact of Building Materials*.

Wolf, A. T., & Waters, L. J. (1993). *Factors governing the life expectancy of dual-sealed insulating glass units*.

Zandin, K. B. (2002). *MOST Work Measurement Systems*. CRC Press. https://doi.org/10.1201/9781482275940

Zandin, K. B. (2020). *MOST® Work Measurement Systems* (T. M. Schmidt, Ed.). CRC Press. https://doi.org/10.1201/9780429326424

APPENDICES

Appendix 1.1

Drawings old ABN AMRO façade scale 1:5 (Drawings by Scheldebouw)

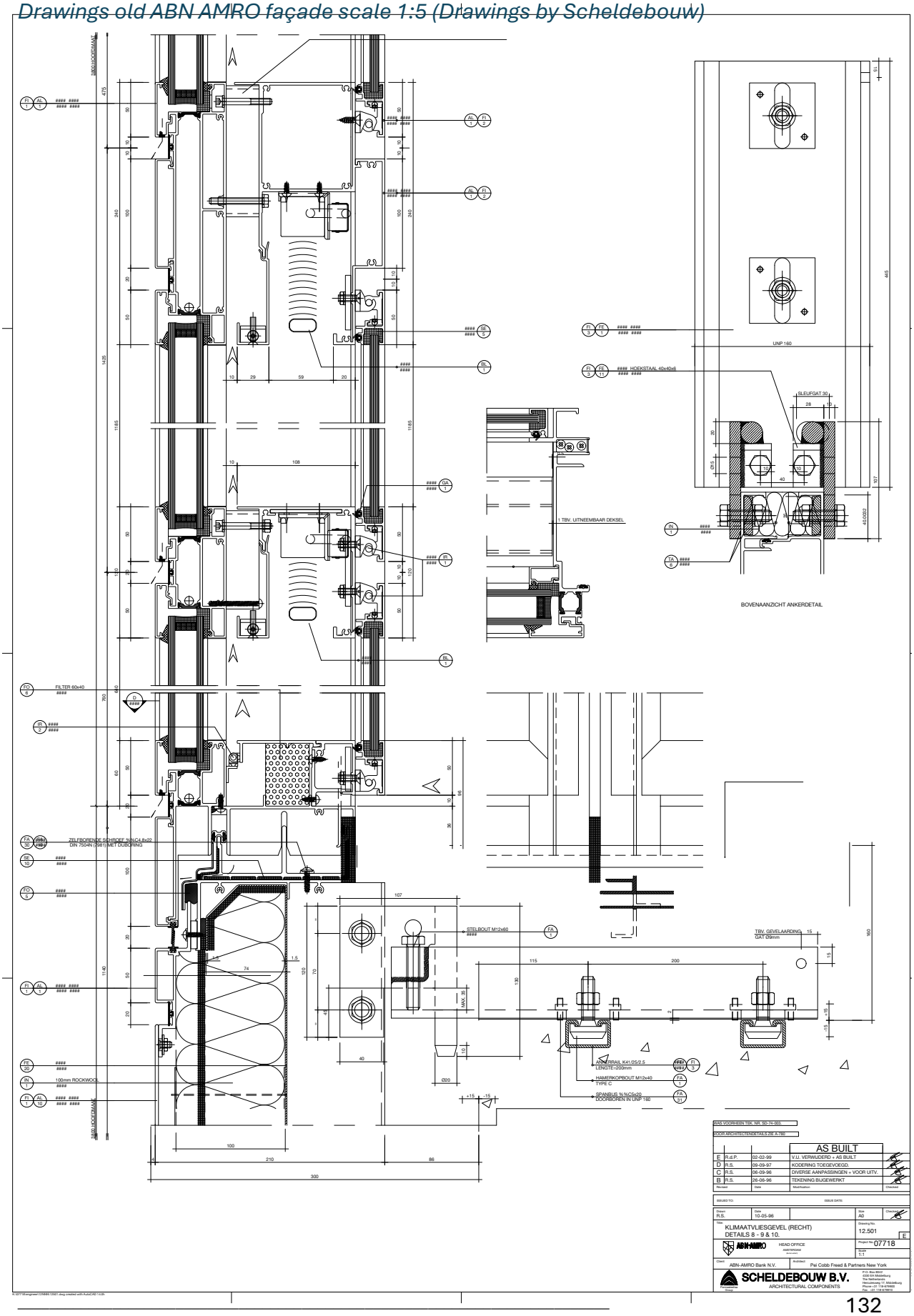

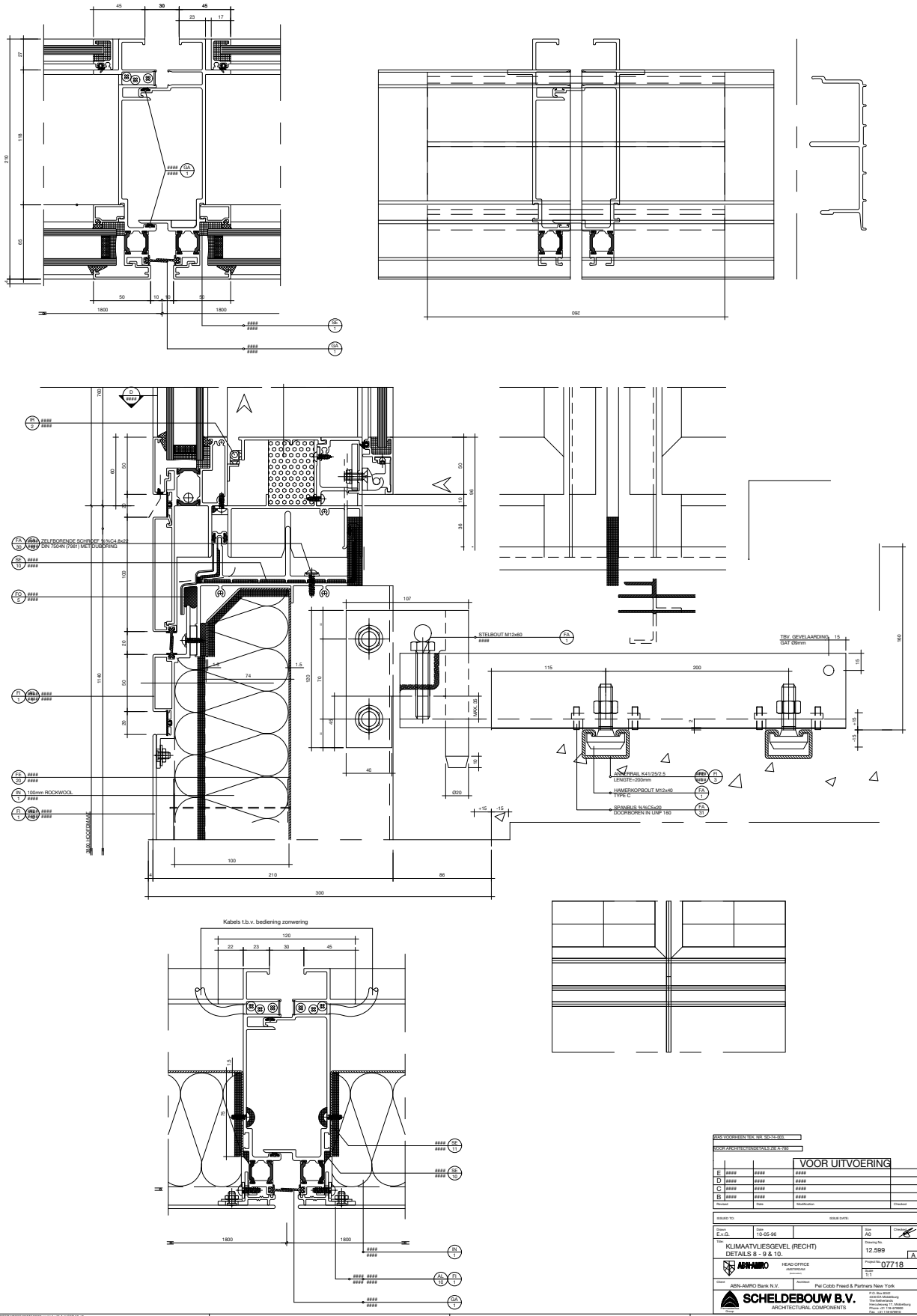
ZELFBOREND SCHROEF 5,5x1C4,8x22
DIN 7504N (7981) MET DUBDRING
100mm ROCKWOOL
300 LICHTMAAS
STELBOUT M12x60
TBV. GEVELAARDING
GAT Ø9mm
ADMERAIL K41/2S/2,5
LENGTE=200mm
HAMERKOPBOUT M12x40
TYPE C
SPANBUS 5,5x25x20
DOORBOREN IN UNP 160
Kabels t.b.v. bediening zonwering
VOOR UITVOERING
KLIMAATVLIESGEVEL (RECHT)
DETAILS 8 - 9 & 10.
12.599
07718
ABN-AMRO Bank N.V.
Pei Cobb Freed & Partners New York
SCHELDEBOUW B.V.
ARCHITECTURAL COMPONENTS

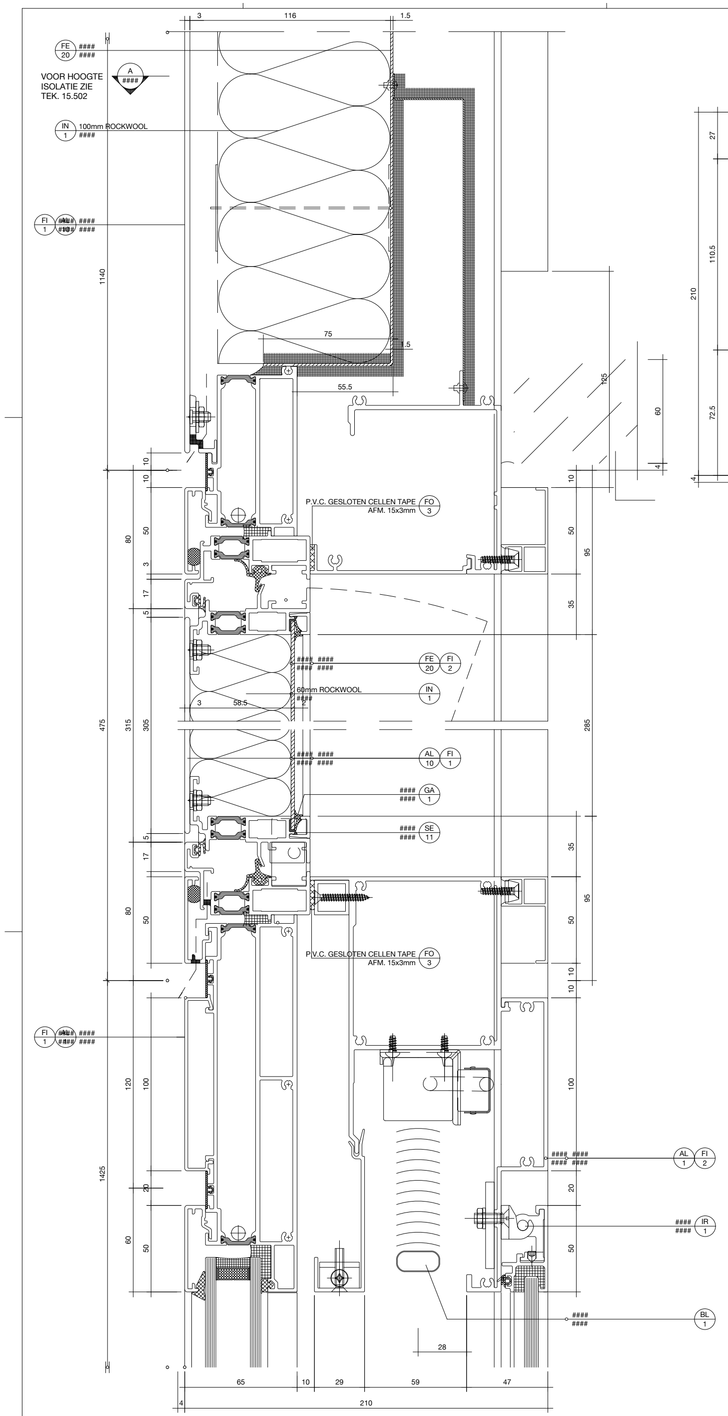

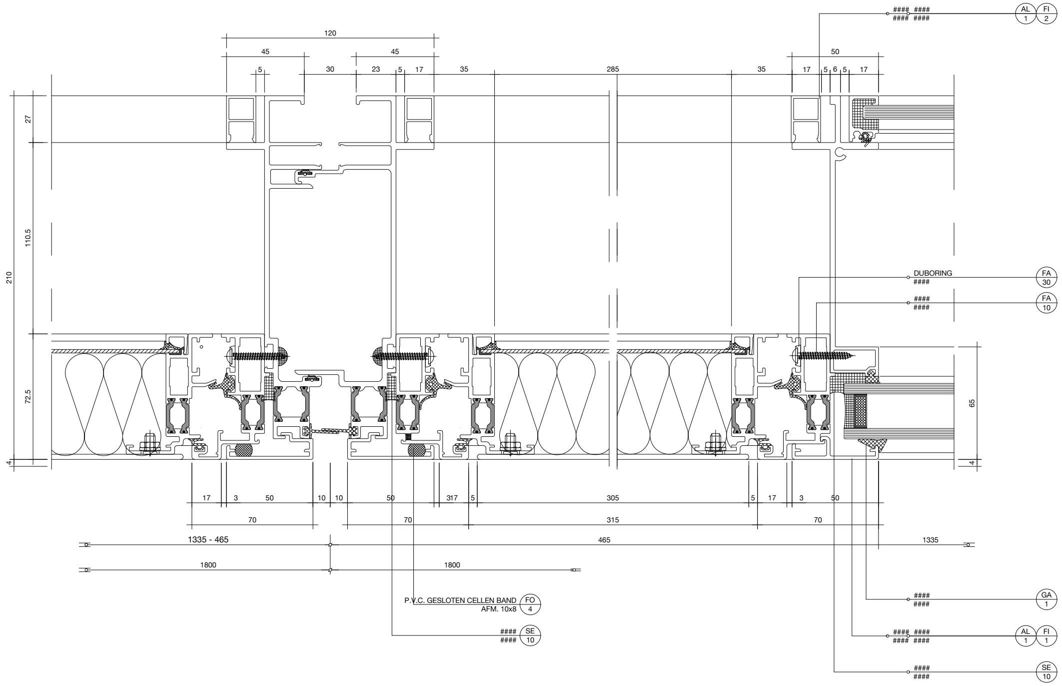

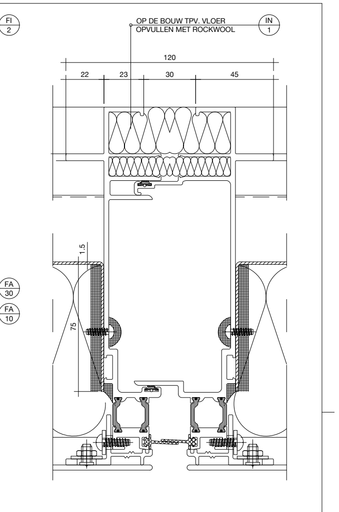

DOORSNEDE A
TPV. VLOER

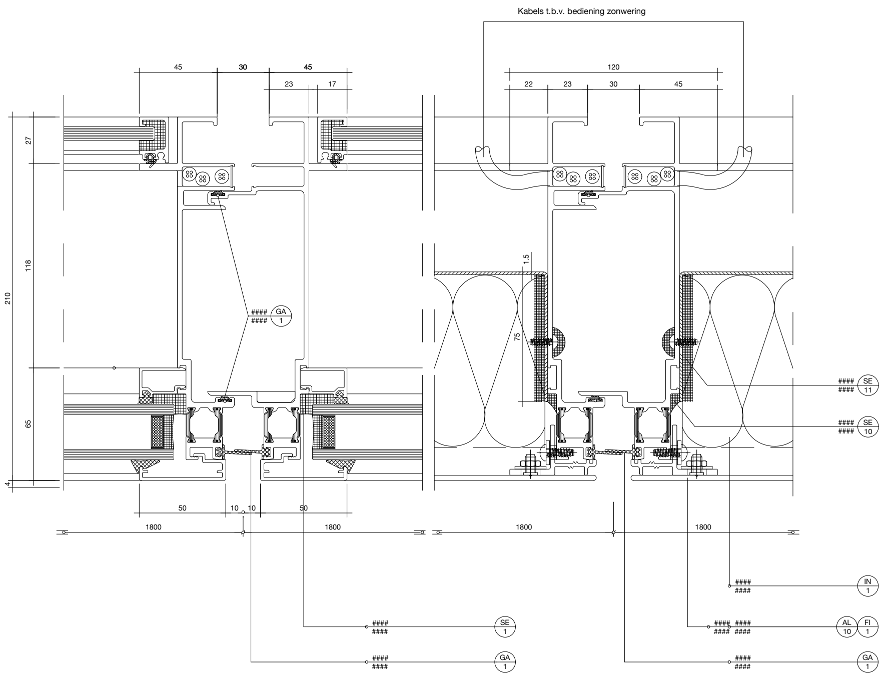

VOOR BEDIENING DRAAIDEEL ZIE TEKENING 12.503.

WAS VOORHEEN TEK. NR. SD-74-002.

VOOR ARCHITECTENDETAILS ZIE A-770 & A-780

AS BUILT

Revised		Date	Modification	Checked
E	R.d.P.	02-02-99	V.U. VERWIJDERD + AS BUILT	
D	A.N.	09-09-97	KODERINGEN TOEGEVOEGD	
C	R.S.	06-09-96	DIVERSE AANPASSINGEN + VOOR UITV.	
B	R.S.	26-06-96	TEKENING BIJGEWERKT	

ISSUED TO: ISSUE DATE:

Drawn: TH. RUTTEN — Date: 09-05-96 — Size: A0 — Checked:

Title: KLIMAATVLIESGEVEL (RECHT)
DETAILS 1-2-3-4-5 en 6

Drawing No. 12.500 — E

ABN·AMRO HEAD OFFICE AMSTERDAM

Project No. 07718

Scale 1:1

Client: ABN-AMRO Bank N.V. — Architect: Pei Cobb Freed & Partners New York

SCHELDEBOUW B.V.
ARCHITECTURAL COMPONENTS
P.O. Box 8042
4330 EA Middelburg
The Netherlands
Herculesweg 17, Middelburg
Phone +31 118-679900
Fax +31 118-679910

K:\07718\engineer\12NNN\12500.dwg created with AutoCAD 14.0h

Appendix 1.2

Drawings new design carrier frame ABN AMRO scale 1:5

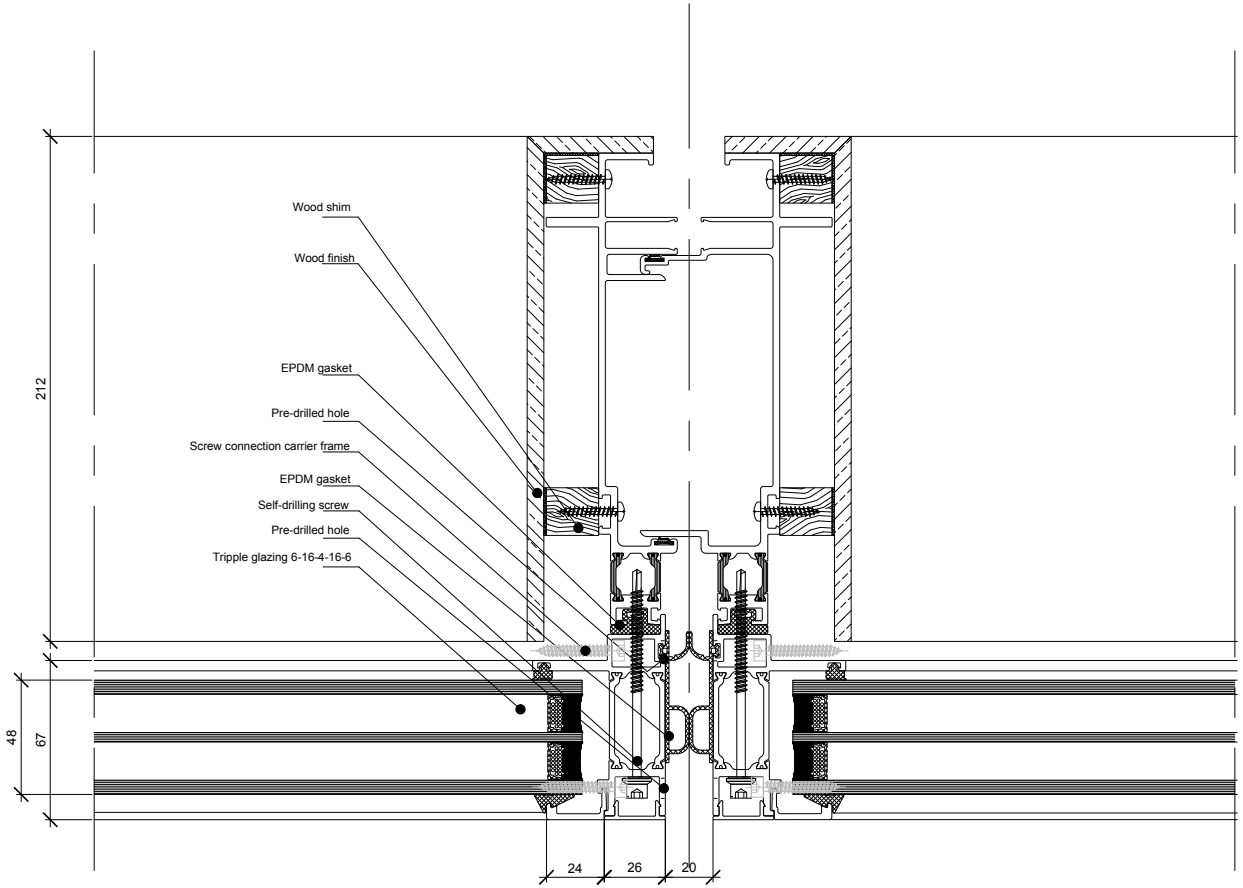

Drawn: D.B	Date: 01-05-2025		Size: A3	Checked
Title: CARRIER FRAME ABN AMRO FACADE			Drawing No.: 1	
DETAIL 1 - Mullion to mullion connection			Project No.:	
			Scale:	
Client:	Designed: Djurre Barten			
SCHELDEBOUW B.V.	TU DELFT			

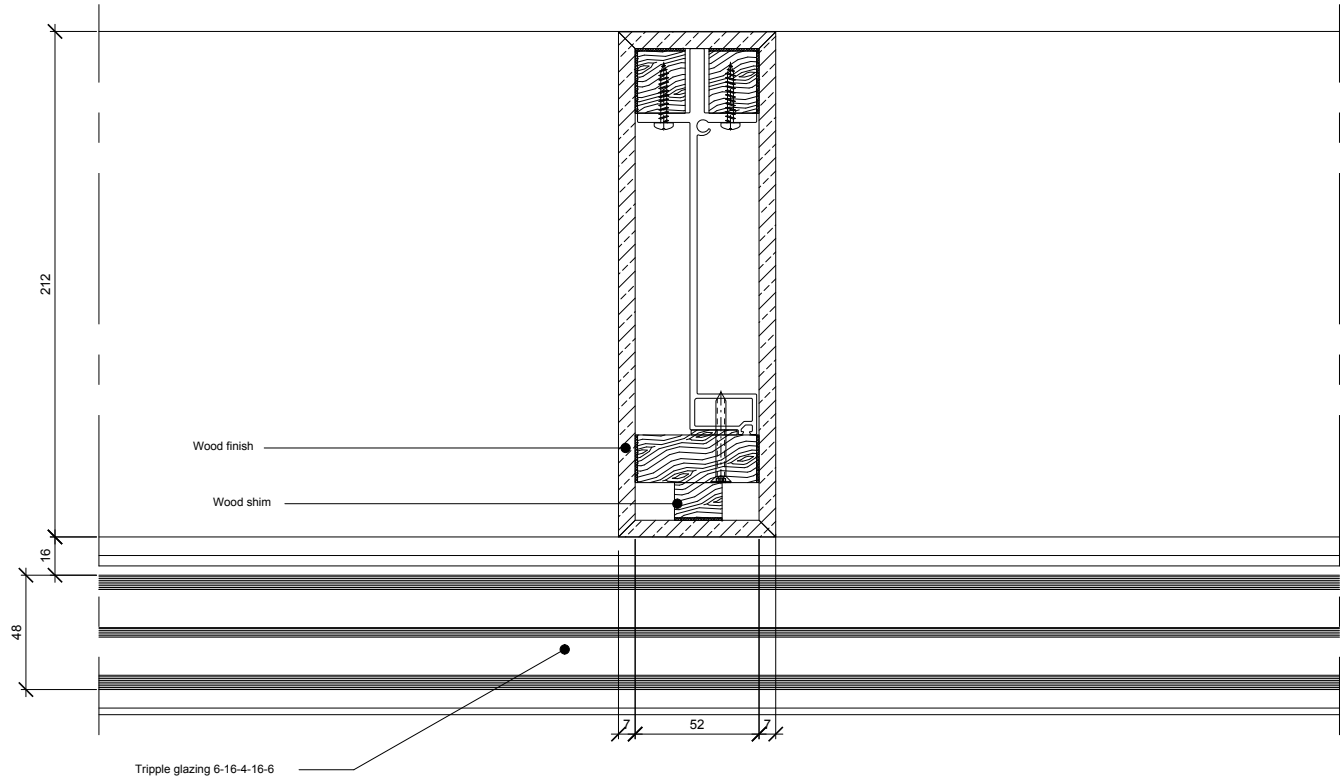

Drawn: D.B	Date: 01-05-2025		Size: A3	Checked
Title: CARRIER FRAME ABN AMRO FACADE			Drawing No.: 2	
DETAIL 2 - old window profile-IGU			Project No.	
			Scale: 1:2	
Client	Designed: Djurre Barten			

SCHELDEBOUW B.V. **TU DELFT**

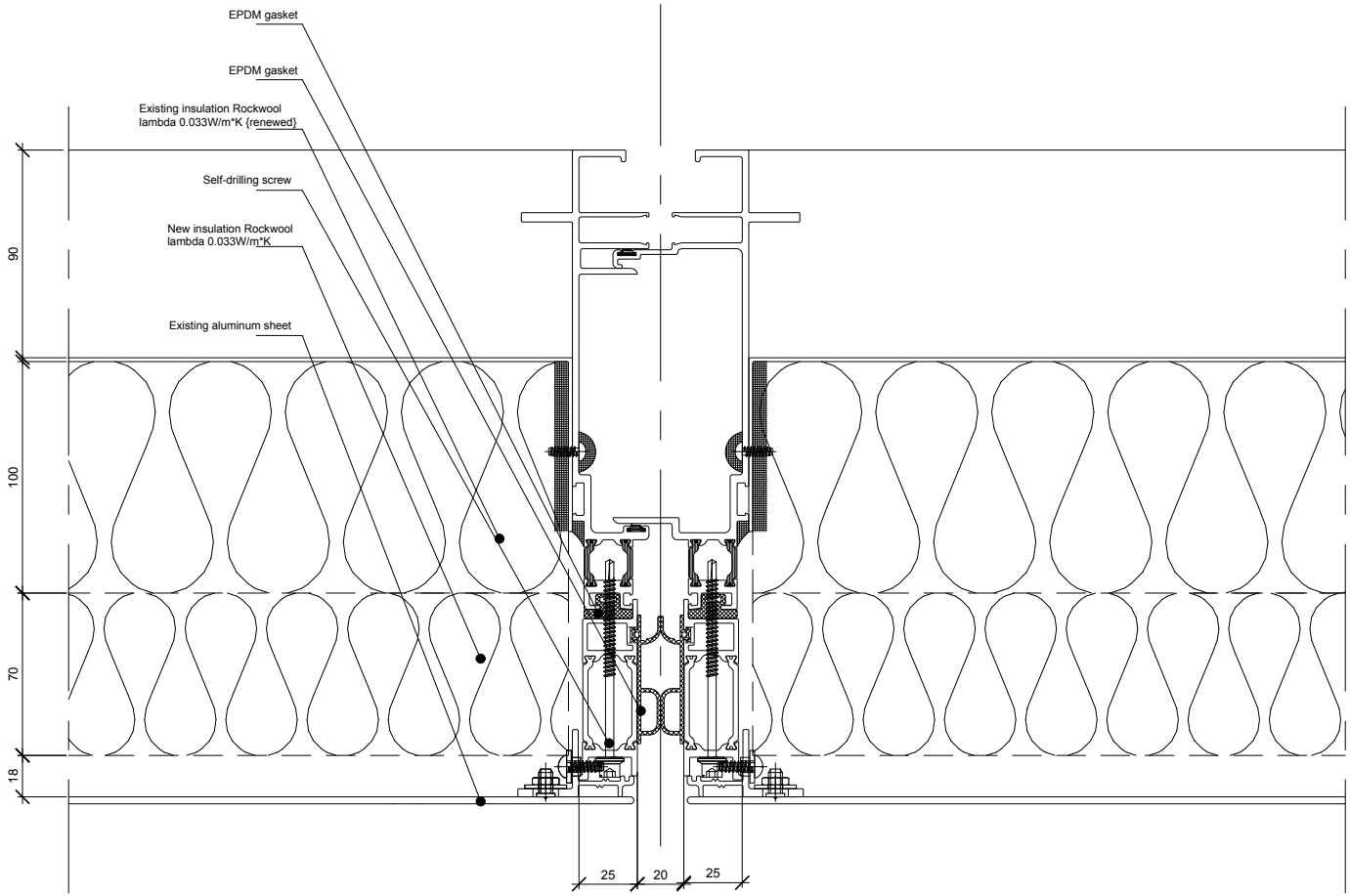

Drawn: D.B	Date: 01-05-2025		Size: A3	Checked
Title: CARRIER FRAME ABN AMRO FACADE			Drawing No.: 3	
DETAIL 3 - Mullion to mullion connection| opaque section			Project No.:	
			Scale: 1:2	
Client	Designed: Djurre Barten			

SCHELDEBOUW B.V. TU Delft

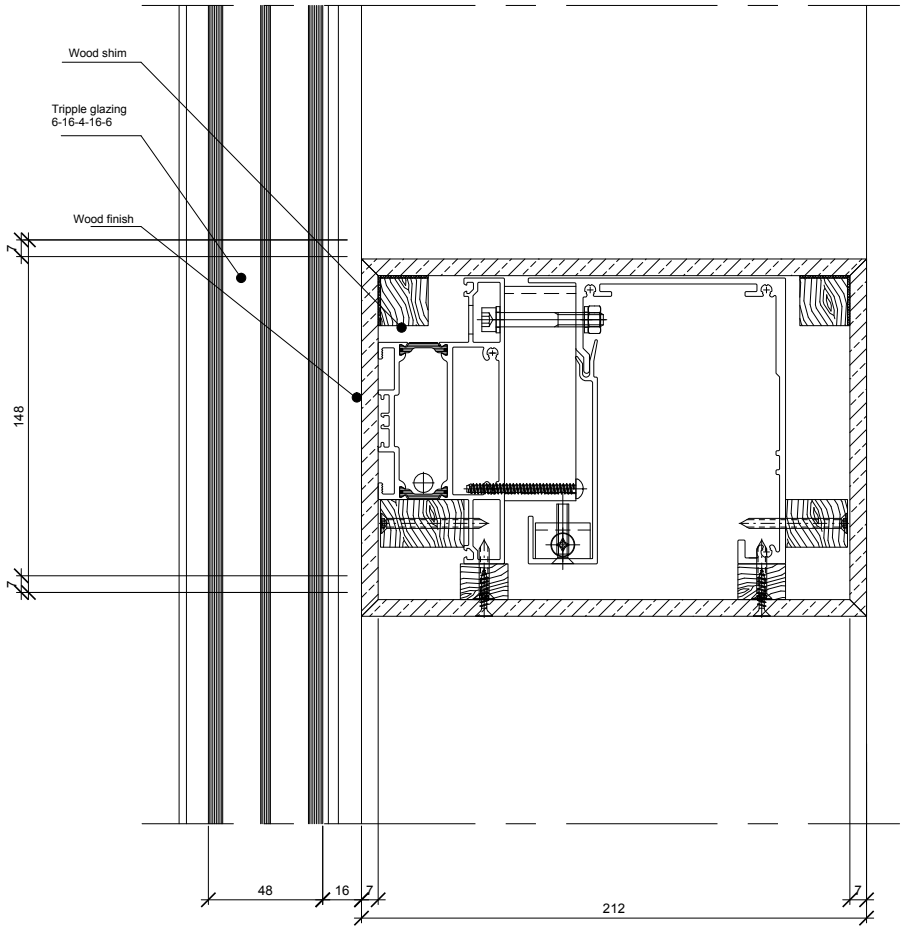

Drawn: D.B	Date: 01-05-2025		Size: A3	Checked
Title: CARRIER FRAME ABN AMRO FACADE			Drawing No.: 4	
DETAIL 4 - transom behind IGU			Project No.:	
			Scale: 1:2	
Client:	Designed: Djurre Barten			

SCHELDEBOUW B.V. TU Delft

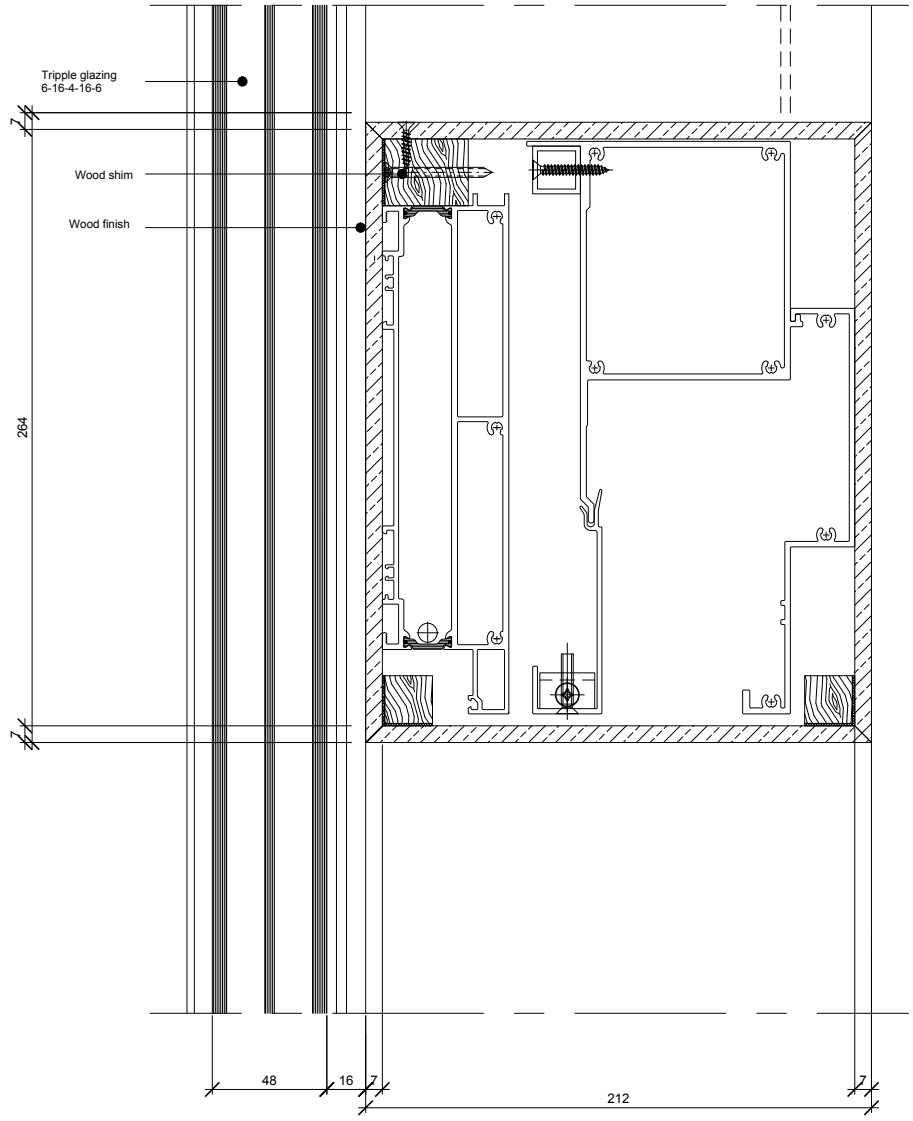

Drawn: D.B	Date: 01-05-2025		Size: A3	Checked
Title: CARRIER FRAME ABN AMRO FACADE			Drawing No.: 5	
DETAIL 5 - transom behind IGU			Project No.: Scale: 1:2	
Client	Designed: Djurre Barten			
SCHELDEBOUW B.V.	TU Delft			

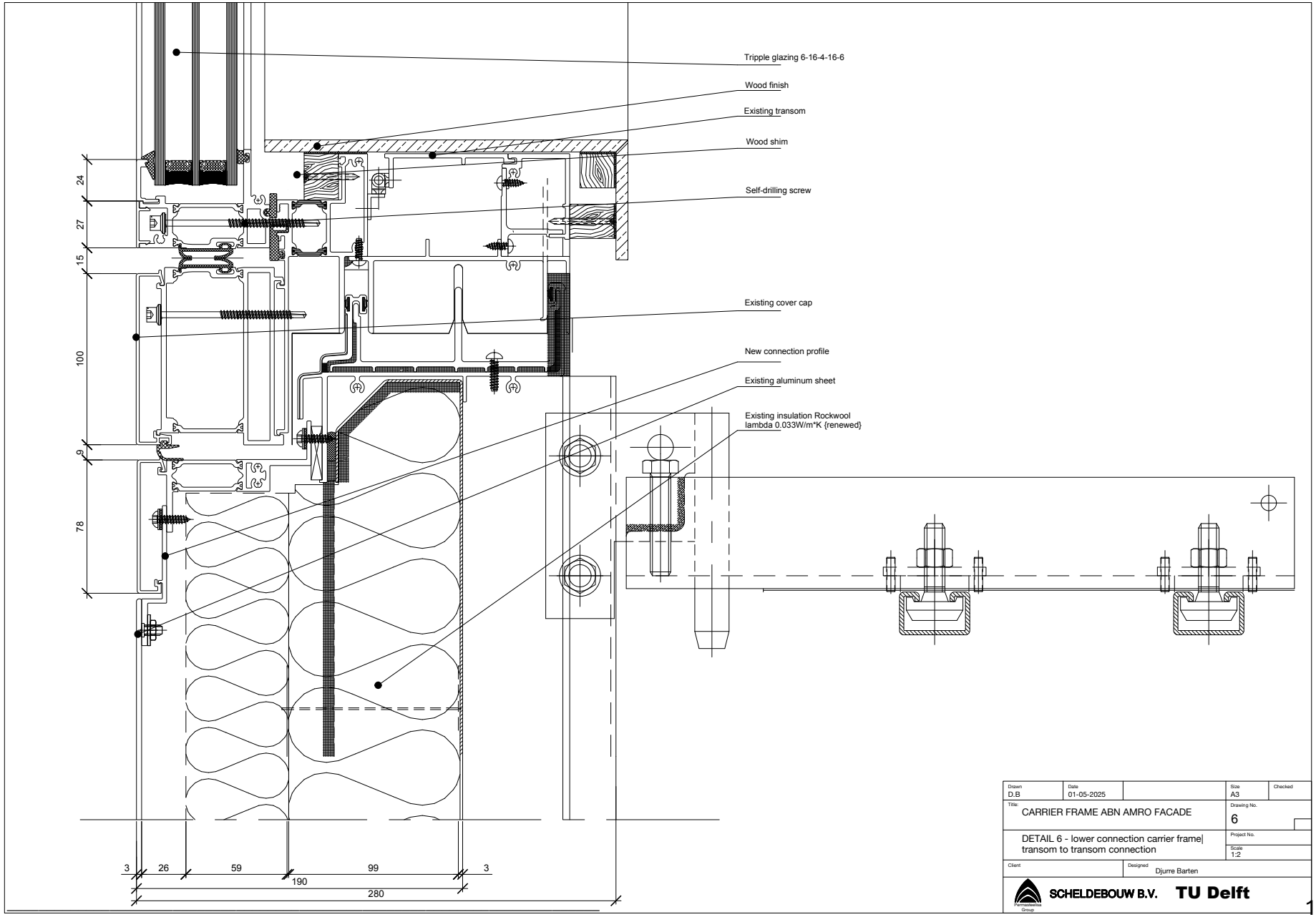

Drawn: D.B	Date: 01-05-2025		Size: A3	Checked
Title: CARRIER FRAME ABN AMRO FACADE			Drawing No.: 6	
DETAIL 6 - lower connection carrier frame| transom to transom connection			Project No.:	
			Scale: 1:2	
Client	Designed: Djurre Barten			

SCHELDEBOUW B.V. TU Delft

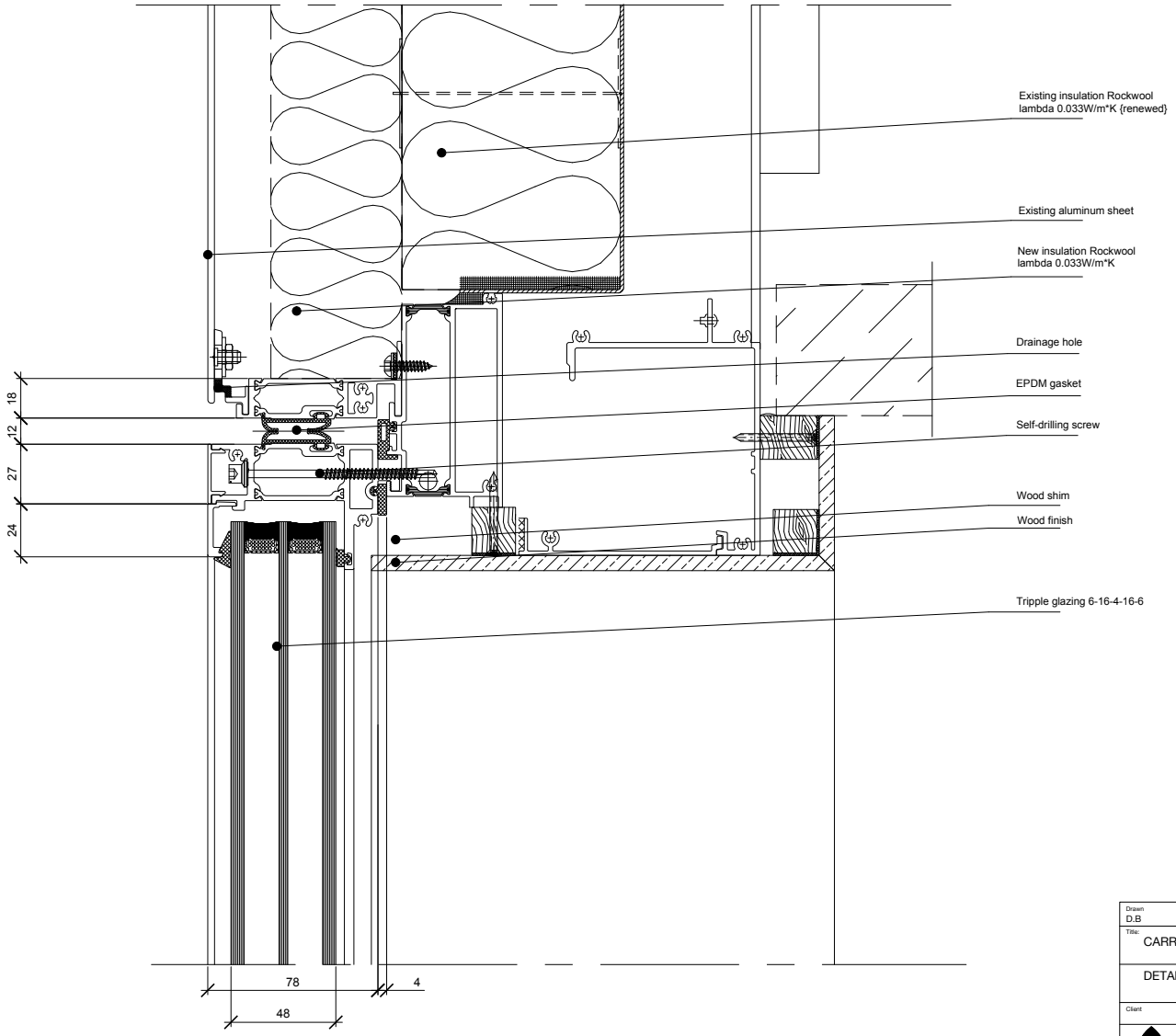

Drawn: D.B	Date: 01-05-2025		Size: A3	Checked
Title: CARRIER FRAME ABN AMRO FACADE			Drawing No.: 7	
DETAIL 7 - Top carrier frame connection			Project No.:	
			Scale: 1:2	
Client	Designed: Djurre Barten			
SCHELDEBOUW B.V.	TU Delft			

Appendix 1.3

New thermal break on ABN AMRO design

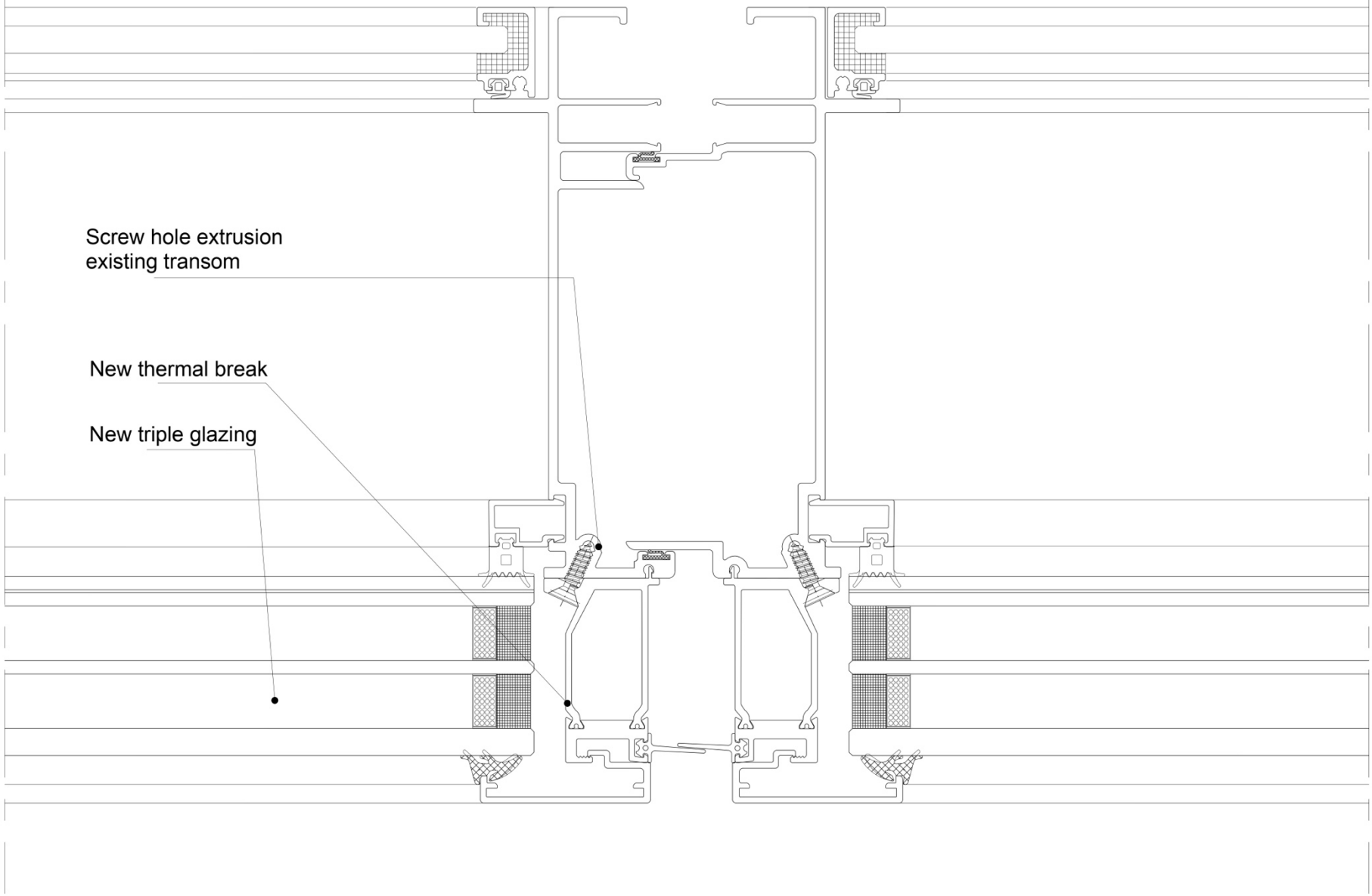

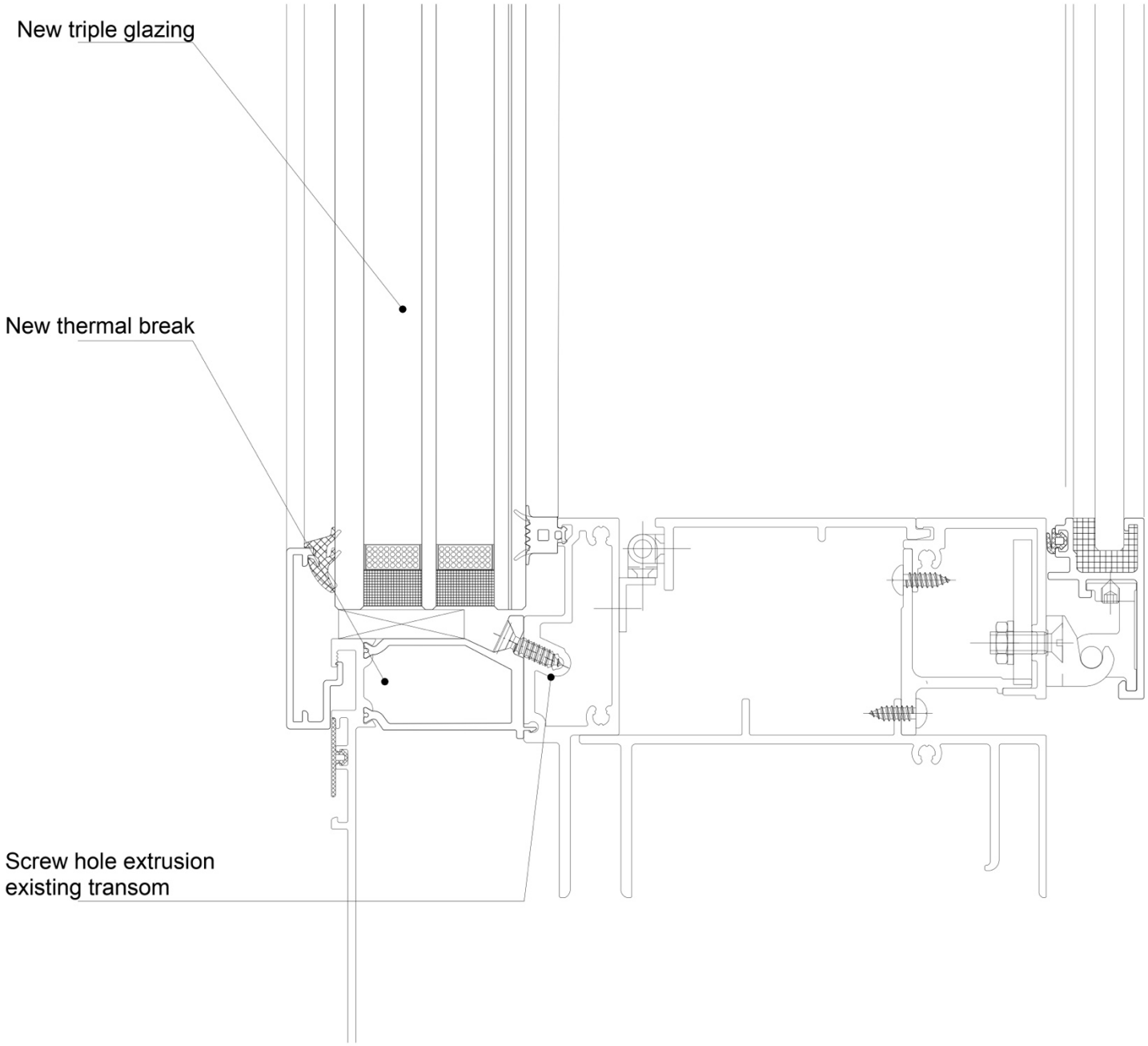
New triple glazing
New thermal break
Screw hole extrusion
existing transom

Appendix 2.1

Disassembly sequence of component	Disassembly sequence of connectors	Number of connectors	Number of product manupiations	Identifiability	ToolType	ToolChange (s)	Identifying (s)	Manupiations (s)	Positioning (s)	Disconnection(s)	Removing (s)	eDiM(s)
Inside window (lower)	Interlocking	3			Hand		5,67			3,6	14,4	23,67
Inside window (middle)	Interlocking	3			Hand		5,67			3,6	14,4	23,67
Inside window (upper)	Interlocking	3			Hand		5,67			3,6	14,4	23,67
Sun Shading (lower)	Screw type 1	3		1	Screwdriver (CH)	14,4	5,67		7,2	108	14,4	149,67
Sun Shading (middle)	Screw type 1	3		1	Screwdriver (CH)		5,67		7,2	108	14,4	135,27
Sun Shading (upper)	Screw type 1	3		1	Screwdriver (CH)		5,67		7,2	108	14,4	135,27
Small metal sheet	Rivet type 1	16			Power tool	14,4				57,6	14,4	86,4
Small metal sheet	Sealant	1			Prybar	14,4				10,8	14,4	39,6
Gasket mullion (L)	Gasket interlocking type2	1			Hand					3,6	14,4	18
Gasket mullion (R)	Gasket interlocking type3	1			Hand					3,6	14,4	18
Small window frame inside	Snap-fit type 1	1			Hand	14,4				3,6	14,4	32,4
IGU (lower)	Gasket-to-sealant	9			Multitool	14,4				97,2	0	111,6
IGU (lower)	Sealant inside	9			Multitool					97,2	0	97,2
IGU (middle)	gasket-to-sealant	12			Multitool					129,6	0	129,6
IGU (middle)	Sealant inside	12			Multitool					129,6	0	129,6
IGU (upper)	gasket-to-sealant	7			Multitool					75,6	0	75,6
IGU (upper)	Sealant inside	7			Multitool					75,6	0	75,6
			1		Crane	14,4		280,8				295,2
Cover cap (lower)	Snap-fit type 1	1			Hand					3,6	14,4	18
Cover cap (upper)	Snap-fit type 1	1			Hand					3,6	14,4	18
Gasket [glazing cap] (lower 1)	Gasket interlocking type 1	1			Pliers	14,4				10,8	14,4	39,6
Gasket [glazing cap] (lower 2)	Gasket interlocking type 1	1			Pliers					10,8	0	10,8
Gasket [glazing cap] (lower 3)	Gasket interlocking type 1	1			Pliers					10,8	0	10,8
Gasket [glazing cap] (lower 4)	Gasket interlocking type 1	1			Pliers					10,8	0	10,8
Glazing cap (lower 1)	Snap-fit type 1	1			Hand	14,4				3,6	14,4	32,4
Glazing cap (lower 2)	Snap-fit type 1	1			Hand					3,6	14,4	18
Glazing cap (lower 3)	Snap-fit type 1	1			Hand					3,6	14,4	18
Glazing cap (lower 4)	Snap-fit type 1	1			Hand					3,6	14,4	18
Gasket [glazing cap] (middle 1)	Gasket interlocking type 1	1			Pliers	14,4				10,8	14,4	39,6
Gasket [glazing cap] (middle 2)	Gasket interlocking type 1	1			Pliers					10,8	0	10,8
Gasket [glazing cap] (middle 3)	Gasket interlocking type 1	1			Pliers					10,8	0	10,8
Gasket [glazing cap] (middle 4)	Gasket interlocking type 1	1			Pliers					10,8	0	10,8
Glazing cap (middle 1)	Snap-fit type 1	1			Hand	14,4				3,6	14,4	32,4
Glazing cap (middle 2)	Snap-fit type 1	1			Hand					3,6	14,4	18
Glazing cap (middle 3)	Snap-fit type 1	1			Hand					3,6	14,4	18
Glazing cap (middle 4)	Snap-fit type 1	1			Hand					3,6	14,4	18
Gasket [glazing cap] (upper 1)	Gasket interlocking type 1	1			Pliers	14,4				10,8	14,4	39,6
Gasket [glazing cap] (upper 2)	Gasket interlocking type 1	1			Pliers					10,8	0	10,8
Gasket [glazing cap] (upper 3)	Gasket interlocking type 1	1			Pliers					10,8	0	10,8
Gasket [glazing cap] (upper 4)	Gasket interlocking type 1	1			Pliers					10,8	0	10,8
Glazing cap (upper 1)	Snap-fit type 1	1			Hand	14,4				3,6	14,4	32,4
Glazing cap (upper 2)	Snap-fit type 1	1			Hand					3,6	14,4	18
Glazing cap (upper 3)	Snap-fit type 1	1			Hand					3,6	14,4	18
Glazing cap (upper 4)	Snap-fit type 1	1			Hand					3,6	14,4	18
IGU (lower)	Sealant type 1	9			Knife | multiotool	10,8			7,2	97,2	133,2	248,4
IGU (middle)	Sealant type 1	12			Knife | multiotool	10,8			7,2	129,6	133,2	280,8
IGU (upper)	Sealant type 1	7			Knife | multiotool	10,8			7,2	75,6	133,2	226,8
Glazing bead (lower 1)	Snap-fit type 3	1	1		Prytool	10,8				10,8	14,4	36
Glazing bead (lower 2)	Snap-fit type 3	1	1		Prytool	10,8				10,8	14,4	36
Glazing bead (middle 1)	Snap-fit type 3	2	2		Prytool	10,8				21,6	28,8	61,2
Glazing bead (middle 2)	Snap-fit type 3	2	2		Prytool	10,8				21,6	28,8	61,2
Glazing bead (upper 1)	Snap-fit type 3	1	1		Prytool	10,8				10,8	14,4	36
Glazing bead (upper 2)	Snap-fit type 3	1	1		Prytool	10,8				10,8	14,4	36
Small window	Screw type 1	2			Screwdriver (AK)		5,67			36	14,4	56,07
Small windowframe outside	Screw type 3	4			Power tool	14,4				57,6	14,4	72
Small windowframe outside	Sealant type 1	4			Multitool	14,4				43,2	0	57,6

Table 11: Total eDim calculation sheet old ABN AMRO design (by author).

Appendix 2.2

Disassembly sequence of component	Disassembly sequence of connectors	Number of connectors	Number of product manupilations	Identifiability	ToolType	ToolChange (s)	Identifying (s)	Manupilations (s)	Positioning (s)	Disconnection(s)	Removing (s)	eDiM(s)
Sun Shading	Screw type 1	3		1	Screwdriver	14,4	5,67		7,2	108	14,4	149,67
Sun Shading	Screw type 1	3		1	Screwdriver (CH)		5,67		7,2	108	14,4	135,27
Sun Shading	Screw type 1	3		1	Screwdriver (CH)		5,67		7,2	108	14,4	135,27
Small metal	Rivet type 1	16			Power tool	14,4				57,6	14,4	86,4
Small metal	Sealant type	1			Prybar	14,4				10,8	14,4	39,6
Gasket mull	Gasket inter	1			Hand					3,6	14,4	18
Gasket mull	Gasket inter	1			Hand					3,6	14,4	18
												0
Cover cap (l	Snap-fit type	1			Hand					3,6	14,4	18
Cover cap (u	Snap-fit type	1			Hand					3,6	14,4	18
Cover profile (lower)												0
Cover profile (upper)												0
Gasket [gla	Gasket inter	1			Pliers	14,4				10,8	14,4	39,6
Gasket [gla	Gasket inter	1			Pliers					10,8	0	10,8
Gasket [gla	Gasket inter	1			Pliers					10,8	0	10,8
Gasket [gla	Gasket inter	1			Pliers					10,8	0	10,8
Glazing cap	Snap-fit type	1			Hand	14,4				3,6	14,4	32,4
Glazing cap	Snap-fit type	1			Hand					3,6	14,4	18
Glazing cap	Snap-fit type	1			Hand					3,6	14,4	18
Glazing cap	Snap-fit type	1			Hand					3,6	14,4	18
IGU											133,2	133,2
Cover cap c	Snap-fit type	1			Hand					3,6	14,4	18
Cover cap c	Snap-fit type	1			Hand					3,6	14,4	18
Cover cap c	Snap-fit type	1			Hand					3,6	14,4	18
Cover cap c	Snap-fit type	1			Hand					3,6	14,4	18
Carrier fram	Screw type 3	16			Powertool	14,4				30,24	14,4	59,04
Gasket winc	Gasket inter	1			Hand					3,6	14,4	18
Gasket winc	Gasket inter	1			Hand					3,6	14,4	18
Gasket winc	Gasket inter	1			Hand					3,6	14,4	18
Gasket winc	Gasket inter	1			Hand					3,6	14,4	18
Front gaske	Gasket inter	1			Hand					3,6	14,4	18
Front gaske	Gasket inter	1			Hand					3,6	14,4	18
Front gaske	Gasket inter	1			Hand					3,6	14,4	18
Front gaske	Gasket inter	1			Hand					3,6	14,4	18
aluminum s	Screw type 3	5			Power tool	14,4				57,6	14,4	86,4
Vertical prof	Screw type 4	4			Power tool					86,4	14,4	100,8
Vertical prof	Screw type 4	4			Power tool					86,4	14,4	100,8
Horizontal pr	Screw type 3	6			Power tool					86,4	14,4	100,8
Horizontal pr	Screw type 3	6			Power tool					86,4	14,4	100,8
					TOTAL	**100,8**	**17,01**	**0**	**21,6**	**941,04**	**594**	**1674,45**

Table 12: Total eDim calculation sheet new ABN AMRO design (by author).

Appendix 2.3

Activity	Sequence Model	Parameter
Part Handling	**A B P**	**A** Action Distance **B** Body Motion **P** Get and Place Parts
Tool Use	**A B T**	**T** Get, Use and Aside Tool
Machine Handling	**A B M**	**M** Operate Machine or Equipment
Powered Crane	**A T K T P T A**	**T** Transport **K** Hook-up and Unhook **P** Place Object
Powered Truck	**A S T L T L T A**	**S** Start and Stop **T** Transport **L** Load or Unload

Table 13: MOST sequence models basic activities (Zandin, 2020).

1. Vertical Motions		
Body Motion	**Definition**	**Index**
1 or 2 Bends	Bend, stoop or kneel on one knee and arise; bend with hand that may go below knees up to two bends and arise.	B_1
Kneel	Kneel onto both knees and arise.	B_1
Sit or Stand	Sit down on stool or chair with or without adjusting the position of the stool or chair **or** stand up from stool or chair with or without positioning the stool or chair.	B_1
Climb On or Off	Climb on **or** off a platform approximately 3 feet (1 m) high.	B_1
Sit and Stand	Sit on a stool or chair and arise or arise from a stool or chair **and** sit on the same stool or chair or a different one.	B_3
Crawl	Kneel and crawl on hands and knees a distance ≤ 11 feet (3 m) and subsequently arise.	B_3
Creep	Lie down on a wheeled creeper, pull in and out a total distance ≤ 13 feet (4 m) and arise from creeper.	B_3
2 Kneels	Kneel on both knees and arise. This activity is performed twice.	B_3
Climb On and Off	Climb on **and** off platform.	B_3
3–6 Bends	Bend and arise three to six times.	B_3
Climb-Object	Climb up or down three steps each 18 to 24 inches (45 to 60 cm) high and then bend or position the body carefully on the object before working, or go up or down two steps and then climb onto a platform with knees in lying, sitting or kneeling position on the object or climb off of the object the same way.	B_3
On-Floor	Lie down on the floor and arise into a standing position.	B_3
Flat-Crawl	Lie down and crawl on the stomach a distance ≤ 12 feet (3.5 m) and arise into a standing position.	B_6

Table 14: MOST Index definitions body motions (Zandin, 2020).

Action Distance		
Index Value	*Feet*	*Meters*
A_1	24	7
A_3	60	18
A_6	120	36
A_{10}	190	60
A_{16}	300	90
A_{24}	420	130
A_{32}	550	170
A_{42}	720	220
A_{54}	920	280
A_{67}	1120	340
A_{81}	1350	410
A_{96}	1590	490
A_{113}	1860	570
A_{131}	2160	670
A_{152}	2480	770
A_{173}	2820	870
A_{196}	3170	980

Table 15: MOST Index defenitions actions (Zandin, 2020).

3. Combined Body Motions		
Body Motion	**Definition**	**Index**
Bend and Sit	Bend and arise **and** sit on a stool or chair at another location.	B_1
Stand and Bend	Arise from a stool or chair **and** bend and arise at another location.	B_1
Bends and Sit	Bend and arise two to three times **and** sit on a stool or chair at another location.	B_3
Stand and Bends	Arise from a stool or chair and bend **and** arise two to three times at other locations.	B_3
Sit and Stand and Bends	Sit **and** stand from a stool or chair **and** bend and arise two to three times at other locations.	B_3
Bends and Climb	Bend and arise two to three times **and** at another location, climb on or off a platform.	B_3
Bends and Door or Hatch	Bend and arise two to three times **and** pass through a door **or** bend and arise two to three times **and** pass through a hatch.	B_3
Hatch and On-Floor	Pass through a hatch **and** lie down on the floor.	B_3
Bends and Climb On and Off	Bend and arise two to three times **and** at another location climb on and off a platform. The activity is performed twice.	B_3

Table 16: MOST Index definitions body motions (Zandin, 2020).

MaxiMOST System	Tighten or Loosen Standard Fasteners										T – Tool Use
	Screwdriver	Wrench			Ratchet		Power Tool			Hand	
Thread Diameter	All	≤ 3/4 in. (20 mm)	≤ 1 1/2 in. (40 mm)	> 1 1/2 in. (40 mm)	≤ 3/4 in. (20 mm)	≤ 1 1/2 in. (40 mm)	≤ 1/4 in. (6 mm)	≤ 1 in. (25 mm)	> 1 in. (25 mm)	≤ 1/4 in. (6 mm)	Thread Diameter
Index x 100	Fasteners										Index x 100
1	-	-	-	-	-	-	1	1	-	-	1
3	1	-	-	-	-	-	5	3	2	2	3
6	3	1	-	-	1	1	10	7	3	4	6
10	6	2	1	-	2	-	17	12	6	7	10
16	9	3	-	1	4	2			10	10	16
24	13	4	3	-	5	3					24
32		6	4	2	7	5					32
42		8	5	-	10	6					42
54		10	6	3		8					54
67			8	4		10					67
81			9								81

Table 17: MOST Tool use data card (Zandin, 2020).

MaxiMOST System	General Tools I																	T – Tool Use
	Turn By Hand			Pry	Strike						Apply Material with Tool							
					Hand		Hammer		Mallet	Sledge								
Index x 100	Finger Spins	Wrist Turns	Arm Crank	Pry Bar	Wrist Taps	Arm Taps	Wrist Strikes	Arm Strikes	Arm Strikes	Arm Strikes	Seal Gun	Grease Gun	Squeeze Bottle	Tube	Brush, Stick, Hand or Finger	Squirt Can	Aerosol Can	Tape Roll	Index x 100
	Actions		Revs.	Actions	Actions						Pulls	Lever Actions	Drops	1 in. (2.5 cm) Spots	1 in. (2.5 cm) Spots	Squirts	Sq. Ft (0.1 m²)	Foot or Strip	
1	3	4	2	3	10	5	9	4	3	-	-	-	1	-	-	-	-	-	1
3	26	15	16	16	31	15	30	16	11	4	1	4	7	-	2	8	-	1	3
6	58	31	36	34		30		32	22	10	5	14	16	6	6	20	1	3	6
10	102	53	63	60					37	18	11	28		16	12		3	5	10
16										29	19	48					6	8	16
24										43	28	72					9	12	24

Table 18: MOST Tool use data card (Zandin, 2020).

MaxiMOST System	A - Action Distance and B - Body Motion							
	A Action Distance	B Body Motion						
					Ladder		Obstructed Ladder	
Index x 100	Steps	Vertical Motions	Pass Through Openings	Combined Body Motions	Light Load	Heavy Load	Light Load	Heavy Load
					Rungs			
0	1 - 2	-	-	-	-	-	-	-
1	3 - 9	1 or 2 Bends Kneel Sit or Stand Climb On or Off	Door or Hatch	Bend and Sit Stand and Bend	-	-	-	-
3	10 - 23	Sit and Stand Crawl Creep 2 Kneels Climb On and Off 3 - 6 Bends Climb-Object On-Floor	2 Doors or Hatches Mechanical Door Manhole	Bends and Sit Stand and Bends Sit and Stand and Bends Bends and Climb Bends and Door or Hatch Hatch and On-Floor Bends and Climb On and Off	10	2	5	-
6	24 - 42	Flat-Crawl	Obstructed-Manhole		25	8	19	6
10	43 - 70		2 Obstructed-Manholes		45	16	40	14
16	71 - 108					28		26

Table 19: MOST action distance and body motion data card (Zandin, 2020).

MaxiMOST System	Assemble or Disassemble Long Fasteners												T – Tool Use
	Screwdriver		Wrench			Ratchet			Power Tool				
Length	≤ 2 in. (5 cm)	≤ 4 in. (10 cm)	≤ 2 in. (5 cm)	≤ 4 in. (10 cm)		≤ 2 in. (5 cm)	≤ 4 in. (10 cm)		≤ 2 in. (5 cm)		≤ 4 in. (10 cm)		Length
Thread Diameter	All	All	≤ 3/4 in. (20 mm)	≤ 3/4 in. (20 mm)	> 3/4 in. (20 mm)	≤ 3/4 in. (20 mm)	≤ 3/4 in. (20 mm)	> 3/4 in. (20 mm)	≤ 1/4 in. (6 mm)	≤ 3/4 in. (20 mm)	≤ 1/4 in. (6 mm)	≤ 3/4 in. (20 mm)	Thread Diameter
Index x 100	Fasteners												Index x 100
6	-	-	-	-	-	-	-	-	1	1	1	1	**6**
10	1	-	-	-	-	-	-	-	2	3	-	2	**10**
16	-	-	-	-	-	-	-	-	4	5	3	3	**16**
24	2	1	-	-	1	1	-	-	6	7	4	5	**24**
32	3	-	1	-	-	-	-	1	8	10	6	7	**32**
42	4	2	-	-	2	-	-	-	11		7	9	**42**
54	5	-	-	-	-	2	1	2			10	12	**54**
67	7	3	2	1	3	-	-	-					**67**
81	8	4	-		-	3	-	3					**81**
96	10	5	3		4	-	2	-					**96**
113		6			5	4		4					**113**

Table 20: MOST tool use card for assembling and disassembling long fasteners (Zandin, 2020).

MaxiMOST System	General Move								P – Part Handling		
	Handle Parts					Handle Parts with Adjustments					
Index x 100	Pickup or Hold and Move	Collect and Move	Put	Place	Position	Pickup or Hold and Move	Collect and Move	Put	Place	Position	Index x 100
	Small	Small, Light or Medium Size and Weight			Medium or Heavy Weight	Small	Small, Light or Medium Size and Weight			Medium or Heavy Weight	
	Actions			Objects		Actions			Objects		
1	2	2	3	2	1	2	-	1	-	-	**1**
3	17	8	10	6	3	13	6	7	4	2	**3**
6		17	18	11	6		15	16	10	5	**6**
10				18	10					10	**10**

Table 21: MOST Part handling data card general move (Zandin, 2020).

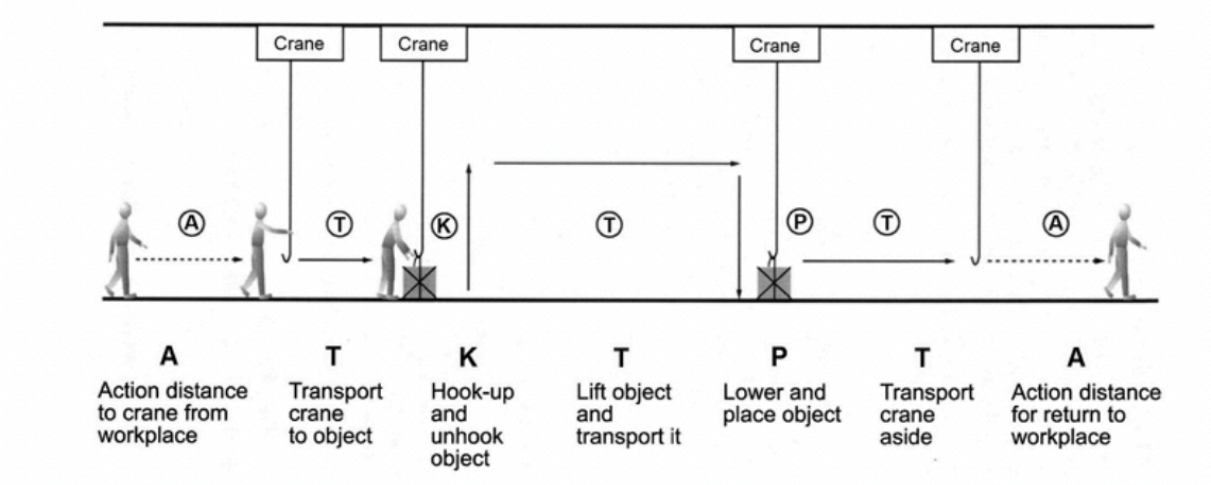

Figure 129: powered crane MOST sequence model (Zandin, 2020).

Appendix 2.4

Example of MOST sequence derivation

Scenario:
- Walking 4 meters to a toolbox
- Bending to grap a screwdriver
- Walking 4 meters back to your product
- Using screwdriver for loosening 'long fastener' screw (see Table 20 Table 20: MOST tool use card for assembling and disassembling long fasteners (Zandin, 2020).for index)

MaxiMOST sequence

|A1 B1 A1 T10|

Total index = 1 + 1 + 1 + 10 = 13

Total TMU = 13 x 100 = 1300 TMU

Convert TMU to time:
1 TMU = 0.036 seconds
1300 TMU × 0.036 = 46.8 seconds

Example of MOST sequence derivation
Manipulation; turning element on other side:

Turning element:
Grabbing belts x2
Placing belts around element x2
Attaching belts to lifter
Grabbing lifting remote
Lifting panel
Grabbing panel for right angle
Lowering panel
dismantling belts from lifting machine
removing belts from panel x2

A T K T P T A

A = action distance
T = Transport
K = hook-up and unhook
P = Placement

|A6 T10 K32 T10 P16 T3 A1|

(6+10+32+10+16+3+1) * 100 = 7800 TMU
7800 * 0.036 = 280.8 s (4min41)

Appendix 3

Small test conducted to determine ability to drill and screw through GFRP inserted in piece of aluminum.

Tests showed easy drilling of holes close to each other (1.5mm) with no sign of splitting of the material or cracks between the holes.

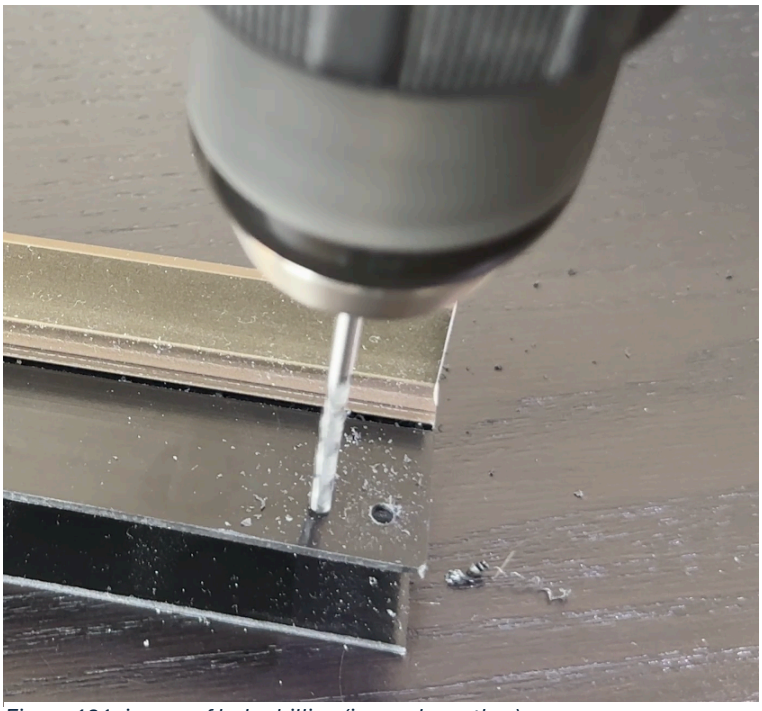

Figure 131: image of hole drilling (image by author).

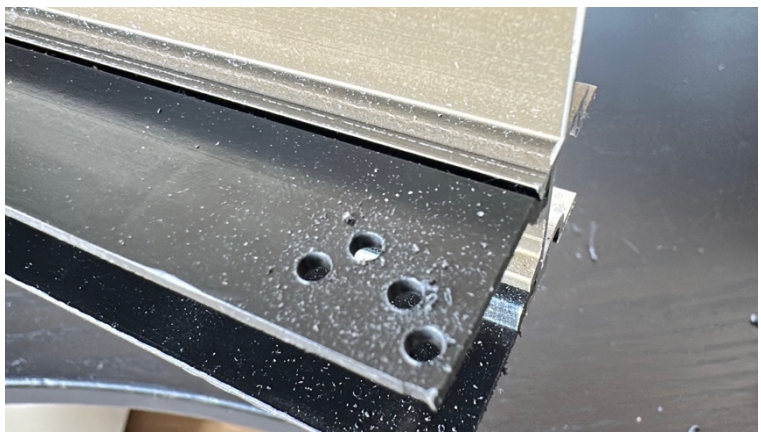

Figure 130: Drilled holes, several milimeters from each other (image by author).

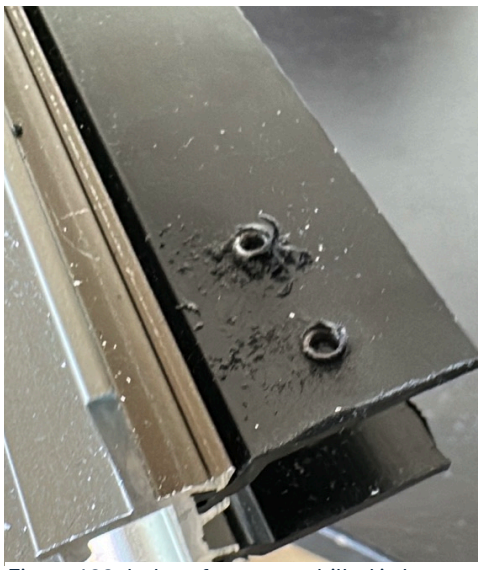

Figure 132: holes after screw drilled in/out (image by author).

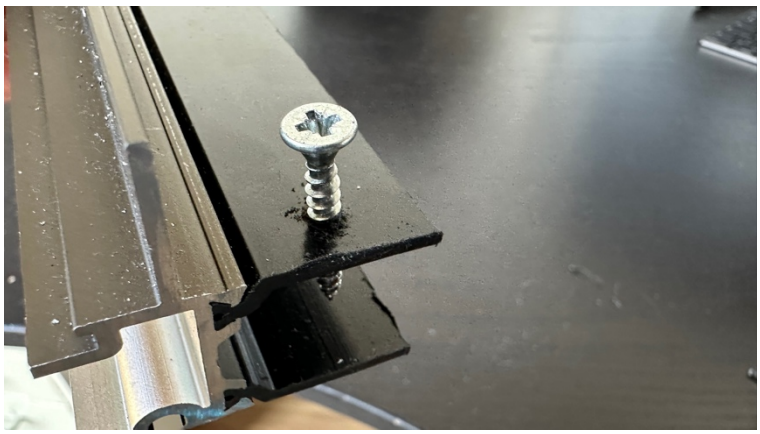

Figure 133: screw drilled through GFRP (image by author).

Appendix 4

Calculating total weight of the frame:

Aluminum (6063)
Density = 2720 Kg/m^3 [Granta design, 2023]

Horizontal parts:
Total area = 674mm^2
Length = 2647mm
Number = 2

674*2647*2 = 3568156 mm^3

Vertical parts:
Total area = 762mm^2
Length = 1800mm
Number = 2

762*1800*2 = 2743200mm^3

Total volume = 6311356mm^3
= 0.0063m^3
0.0063*2720 = 17.14 Kg

GFRP (polyamide 6.6 25% glass fiber)
Density = 1400 Kg/m^3 [Granta design, 2023]

Horizontal parts:
Total area = 200mm^2
Length = 2647mm
Number = 2

200*2647*2 = 1058800 mm^3

Vertical parts:
Total area = 200mm^2
Length = 1800mm
Number = 2

200*1800*2 = 720000mm^3

Total volume = 1778800mm^3
= 0.0018m^3
0.0018*1400 = 2.49 Kg

Total weight frame = 19.63 Kg

Glass (soda lime)
Density = 2440 m^3 [Granta design, 2023]

Width = 1.73m
Length = 2.575m
Total area = 1.73*2.575 = 4.45m^2

1.45 * 0.006 * 2(panes) = 0.0534m^3
4.45 * 0.004 = 0.0178m^3

0.0712 * 2440 = 173.73 Kg

TOTAL WEIGTH FRAME + GLASS = **193.36 Kg**

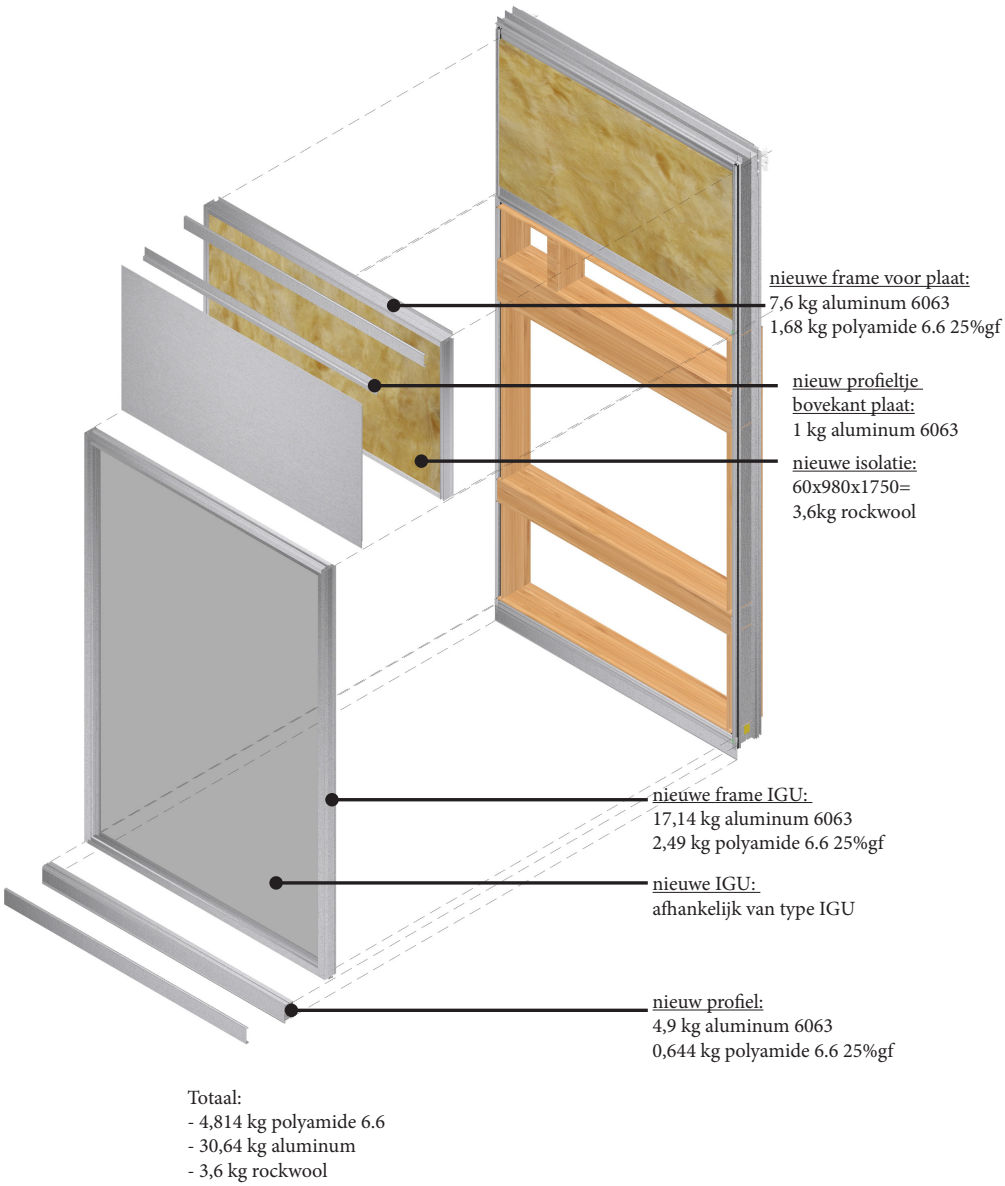

Figure 134: Weights of new materials applied in new ABN AMRO design (image by author).

Appendix 5.1

Total calculation tables Ucw value old ABN AMRO panel

Project name	ABN AMRO
Facade type:	Active wall
Date:	8/mei/25
Spacer:	

	Environmental conditions Model	Project
External temperature	0	-5
Internal temperature	20	20
Internal relative humidity		40
Dew point temperature		6.0

1) Component U_{TJ}-value by BISCO

	Component	U [W/m²K]	b_{TJ} [m]	U x b
	mullion 1	4.37	1.000	4.3700
	mullion 2	4.37	1.000	4.3700
	mullion 3			0.0000
	mullion 4			0.0000
	mullion 5			0.0000
	transom 1	5.67	1.000	5.6680
	transom 2	2.33	1.000	2.3310
	transom 3	2.14	1.000	2.1440
	transom 4	3.12	1.000	3.1230
	transom 5	5.67	1.000	5.6700
	glazing 1	1.23	-	-
	glazing 2	1.23	-	-
	glazing 3	1.23	-	-
	panel 1	0.32	-	-
		0.00	-	-

$T_{min;model}$ [°C]	$T_{min;project}$ [°C]	RH_{max} [%]	Temperature-factor
-	-	-	-
-	-	-	-
-	-	-	-
-	-	-	-
-	-	-	-
-	-	-	-
-	-	-	-
-	-	-	-
-	-	-	-
-	-	-	-
-	-	-	-
-	-	-	-
-	-	-	-
-	-	-	-
0.0	0.0	0.0	
	< 6	< 40	
	Condensation!		

2) Component Area

	Component	Quant [-]	Width [m]	Height [m]	A [m²]
		1	1.800	3.800	6.840
	mullion 1	1	0.020	3.800	0.076
	mullion 2	1	0.020	3.800	0.076
	mullion 3	0			0.000
	mullion 4	0			0.000
	mullion 5	0			0.000
	transom 1	1	1.780	0.077	0.137
	transom 2	1	1.780	0.066	0.117
	transom 3	1	1.780	0.186	0.331
	transom 4	1	1.780	0.087	0.155
	transom 5	1	1.780	0.069	0.122
	glazing 1	1	1.780	0.650	1.157
	glazing 2	1	1.780	1.228	2.186
	glazing 3	1	1.780	0.395	0.703
	panel 1	1	1.780	1.000	1.780
	Check Total		NOK		6.840

3) Curtain Wall U-value

§	Component	U [W/m²K]	A [m²]	U x A [W/K]	U x A [%]	b_{TJ} [m]
	mullion 1	4.37	0.076	0.33	4	1.000
	mullion 2	4.37	0.076	0.33	4	1.000
	mullion 3	0.00	0.000	0.00	0	0.000
	transom 1	5.67	0.137	0.78	8	1.000
	transom 2	2.33	0.117	0.27	3	1.000
	transom 3	2.14	0.331	0.71	8	1.000
	transom 4	3.12	0.155	0.48	5	1.000
	transom 5	5.67	0.122	0.69	8	1.000
	glazing 1	1.23	1.157	1.42	16	-
	glazing 2	1.23	2.186	2.69	29	-
	glazing 3	1.23	0.703	0.86	9	-
	panel 1	0.32	1.780	0.57	6	-
	Total		6.840	9.15	100	
	Ucw =	**1.34**	**W/m²K**			

Total calculation tables Ucw value new ABN AMRO panel

Project name ABN AMRO NEW

Facade type:
Date: 8/mei/25
Spacer:

	Environmental conditions Model	Project
External temperature	0	-5
Internal temperature	20	20
Internal relative humidity		40
Dew point temperature		6.0

1) Component U_{TJ}-value by BISCO

	Component	U [W/m²K]	b_{TJ} [m]	U x b
	mullion 1	3.23	1.000	3.2300
	mullion 2	3.23	1.000	3.2300
	mullion 3			0.0000
	mullion 4			0.0000
	mullion 5			0.0000
	transom 1	3.11	1.000	3.1050
	transom 2	2.49	1.000	2.4880
	transom 3	3.11	1.000	0.0000
	transom 4			3.1100
	transom 5			0.0000
	glazing 1	0.60	-	-
	glazing 2		-	-
	glazing 3		-	-
	panel 1		-	-
	-	0.00	-	-

5) Condensation assessment

$T_{min;model}$ [°C]	$T_{min;project}$ [°C]	RH_{max} [%]	Temperature-factor
-	-	-	-
-	-	-	-
-	-	-	-
-	-	-	-
-	-	-	-
-	-	-	-
-	-	-	-
-	-	-	-
-	-	-	-
-	-	-	-
-	-	-	-
-	-	-	-
-	-	-	-
0.0	0.0	0.0	
	< 6	< 40	
	Condensation!		

2) Component Area

	Component	Quant [-]	Width [m]	Height [m]	A [m²]
		1	1.800	3.800	6.840
	mullion 1	1	0.020	3.800	0.076
	mullion 2	1	0.020	3.800	0.076
	mullion 3	0			0.000
	mullion 4	0			0.000
	mullion 5	0			0.000
	transom 1	1	1.780	0.077	0.137
	transom 2	1	1.780	0.087	0.155
	transom 3	1	1.780	0.069	0.122
	transom 4	0			0.000
	glazing 1	1	1.780	2.525	4.495
	glazing 2	1			0.000
	glazing 3	1			0.000
	panel 1	1	1.780	1.000	1.780
	Check Total		NOK		6.840

3) Curtain Wall U-value

§	Component	U [W/m²K]	A [m²]	U x A [W/K]	U x A [%]	b_{TJ} [m]
	mullion 1	3.23	0.076	0.25	6	1.000
	mullion 2	3.23	0.076	0.25	6	1.000
	mullion 3	0.00	0.000	0.00	0	0.000
	transom 1	3.11	0.137	0.43	10	1.000
	transom 2	2.49	0.155	0.39	9	1.000
	transom 3	3.11	0.122	0.38	9	1.000
	transom 4	0.00	0.000	0.00	0	0.000
	glazing 1	0.60	4.495	2.70	62	-
	glazing 2	0.00	0.000	0.00	0	-
	glazing 3	0.00	0.000	0.00	0	-
	panel 1	0.00	1.780	0.00	0	-
	Total		6.840	4.38	100	
	Ucw =	**0.64**	**W/m²K**			

Appendix 5.2

Bisco report calculation files generated by Physibel Software.

See next page

BISCO Report

Project: **bisco vertical rev02**
Author: **name**
Company: **company**
Date: **27/04/2025**

Materials

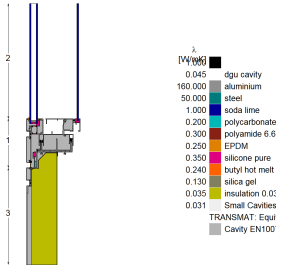

Temperatures

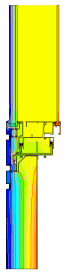

Heat flow

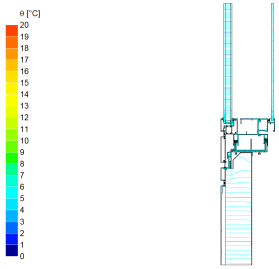

BISCO Report

Project: bisco vertical rev02
Author: name
Company: company
Date: 27/04/2025

Equivalent thermal transmittance: U_f

Equivalent thermal transmittance	U_f	=	5.668	W/m²K	= (Φ / (θ_i - θ_e) - U_1 w_1 - U_2 w_2) / w_f
Thermal coupling coefficient	L_{2D}	=	1.7548	W/mK	= Φ / (θ_i - θ_e)
	Φ	=	35.097	W/m	
	θ_i	=	20.00	°C	
	θ_e	=	0.00	°C	
	U_1	=	1.232	W/m²K	(top edge of bitmap)
	w_1	=	0.4468	m	(distance no. 2)
	U_2	=	0.311	W/m²K	(bottom edge of bitmap)
	w_2	=	0.3748	m	(distance no. 3)
	w_f	=	0.1919	m	(distance no. 1)

Materials

Col.	Name	λ [W/mK]	ε [-]
0		1.000	0.90
3	dgu cavity	0.045	0.90
8	aluminium	160.000	0.90
13	steel	50.000	0.90
18	soda lime	1.000	0.90
21	polycarbonate	0.200	0.90
44	polyamide 6.6 with 25 % glass fibre	0.300	0.90
60	EPDM	0.250	0.90
62	silicone pure	0.350	0.90
92	butyl hot melt	0.240	0.90
104	silica gel	0.130	0.90
151	insulation 0.035 W/mK	0.035	0.90
255	Small Cavities < 2 x 2 mm²	0.031	0.90
	TRANSMAT: Equivalent material (radiosity)		
	Cavity EN10077		

Boundary Conditions

Col.	Name	θ [°C]	h [W/m²K]
170	exterior	0.0	25.00
174	interior (normal) horizontal heat flow	20.0	7.70
182	indoors (reduced)	20.0	5.00
	BC_FREE: Single convective node (radiosity)		
177	highly ventilated cavity upwards heat flow		

BISCO Report

Project: **bisco vertical rev01 [2]**
Author: **name**
Company: **company**
Date: **27/04/2025**

Materials

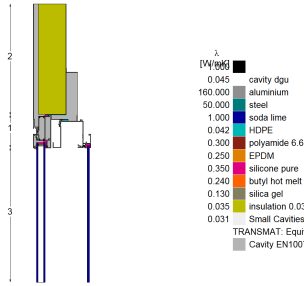

Temperatures

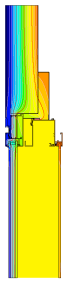

Heat flow

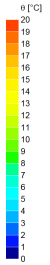

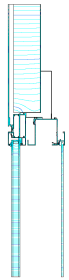

BISCO Report

Project: bisco vertical rev01 [2]
Author: name
Company: company
Date: 27/04/2025

Materials

Col.	Name	λ [W/mK]	ε [-]
0		1.000	0.90
2	cavity dgu	0.045	0.10
8	aluminium	160.000	0.90
13	steel	50.000	0.90
18	soda lime	1.000	0.90
21	HDPE	0.042	0.90
44	polyamide 6.6 with 25 % glass fibre	0.300	0.90
60	EPDM	0.250	0.90
62	silicone pure	0.350	0.90
92	butyl hot melt	0.240	0.90
104	silica gel	0.130	0.90
151	insulation 0.035 W/mK	0.035	0.90
255	Small Cavities < 2 x 2 mm²	0.031	0.90
	TRANSMAT: Equivalent material (radiosity)		
	Cavity EN10077		

Boundary Conditions

Col.	Name	θ [°C]	h [W/m²K]
170	exterior	0.0	25.00
174	interior (normal) horizontal heat flow	20.0	7.70
182	indoors (reduced)	20.0	5.00
	BC_FREE: Single convective node (radiosity)		
177	highly ventilated cavity upwards heat flow		

Equivalent thermal transmittance: U_f

Equivalent thermal transmittance	U_f	=	3.123	W/m²K	= (Φ / (θ$_i$ - θ$_e$) - U$_1$ w$_1$ - U$_2$ w$_2$) / w$_f$
Thermal coupling coefficient	L_{2D}	=	1.1016	W/mK	= Φ / (θ$_i$ - θ$_e$)
	Φ	=	22.032	W/m	
	θ$_i$	=	20.00	°C	
	θ$_e$	=	0.00	°C	
	U$_1$	=	0.317	W/m²K	(top edge of bitmap)
	w$_1$	=	0.4016	m	(distance no. 2)
	U$_2$	=	1.233	W/m²K	(bottom edge of bitmap)
	w$_2$	=	0.4874	m	(distance no. 3)
	w$_f$	=	0.1196	m	(distance no. 1)

Produced by BISCO 13
www.physibel.be/en/products/bisco
physibel

BISCO Report

Project: **bisco vertical T2 rev04**
Author: **name**
Company: **company**
Date: **29/04/2025**

Materials

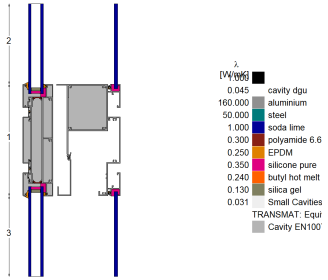

Temperatures

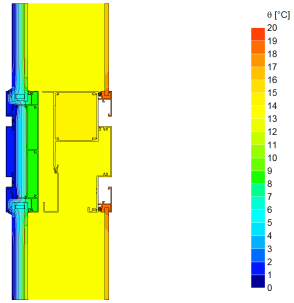

Heat flow

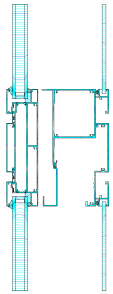

BISCO Report

Project: **bisco vertical T2 rev04**
Author: **name**
Company: **company**
Date: **29/04/2025**

Materials

Col.	Name	λ [W/mK]	ε [-]
0		1.000	0.90
3	cavity dgu	0.045	0.90
8	aluminium	160.000	0.90
13	steel	50.000	0.90
18	soda lime	1.000	0.90
44	polyamide 6.6 with 25 % glass fibre	0.300	0.90
60	EPDM	0.250	0.90
62	silicone pure	0.350	0.90
92	butyl hot melt	0.240	0.90
104	silica gel	0.130	0.90
255	Small Cavities < 2 x 2 mm²	0.031	0.90
	TRANSMAT: Equivalent material (radiosity)		
	Cavity EN10077		

Boundary Conditions

Col.	Name	θ [°C]	h [W/m²K]
170	exterior	0.0	25.00
174	interior (normal) horizontal heat flow	20.0	7.70
182	indoors (reduced)	20.0	5.00
	BC_FREE: Single convective node (radiosity)		
177	highly ventilated cavity upwards heat flow		

Equivalent thermal transmittance: U_f

Equivalent thermal transmittance	U_f	= 2.144	W/m²K	= (Φ / (θ$_i$ - θ$_e$) - U$_1$ w$_1$ - U$_2$ w$_2$) / w$_f$	
Thermal coupling coefficient	L_{2D}	= 0.9409	W/mK	= Φ / (θ$_i$ - θ$_e$)	
	Φ	= 18.818	W/m		
	θ$_i$	= 20.00	°C		
	θ$_e$	= 0.00	°C		
	U$_1$	= 1.232	W/m²K	(top edge of bitmap)	
	w$_1$	= 0.1730	m	(distance no. 2)	
	U$_2$	= 1.232	W/m²K	(bottom edge of bitmap)	
	w$_2$	= 0.1730	m	(distance no. 3)	
	w$_f$	= 0.2400	m	(distance no. 1)	

Produced by BISCO 13
www.physibel.be/en/products/bisco
physibel

BISCO Report

Project: **bisco vertical T1 rev03**
Author: **name**
Company: **company**
Date: **29/04/2025**

Materials

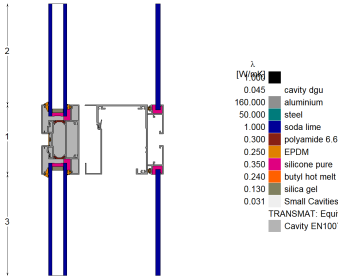

Temperatures

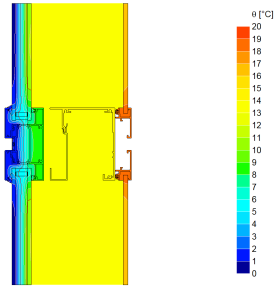

Heat flow

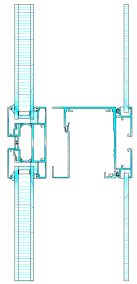

BISCO Report

Project: **bisco vertical T1 rev03**
Author: **name**
Company: **company**
Date: **29/04/2025**

Materials

Col.	Name	λ [W/mK]	ε [-]
0		1.000	0.90
3	cavity dgu	0.045	0.90
8	aluminium	160.000	0.90
13	steel	50.000	0.90
18	soda lime	1.000	0.90
44	polyamide 6.6 with 25 % glass fibre	0.300	0.90
60	EPDM	0.250	0.90
62	silicone pure	0.350	0.90
92	butyl hot melt	0.240	0.90
104	silica gel	0.130	0.90
255	Small Cavities < 2 x 2 mm²	0.031	0.90
	TRANSMAT: Equivalent material (radiosity)		
	Cavity EN10077		

Boundary Conditions

Col.	Name	θ [°C]	h [W/m²K]
170	exterior	0.0	25.00
174	interior (normal) horizontal heat flow	20.0	7.70
182	indoors (reduced)	20.0	5.00
	BC_FREE: Single convective node (radiosity)		
177	highly ventilated cavity upwards heat flow		

Equivalent thermal transmittance: U_f

Equivalent thermal transmittance	U_f	=	2.331	W/m²K	$= (\Phi / (\theta_i - \theta_e) - U_1 w_1 - U_2 w_2) / w_f$
Thermal coupling coefficient	L_{2D}	=	0.7059	W/mK	$= \Phi / (\theta_i - \theta_e)$
	Φ	=	14.118	W/m	
	θ_i	=	20.00	°C	
	θ_e	=	0.00	°C	
	U_1	=	1.232	W/m²K	(top edge of bitmap)
	w_1	=	0.1730	m	(distance no. 2)
	U_2	=	1.232	W/m²K	(bottom edge of bitmap)
	w_2	=	0.1730	m	(distance no. 3)
	w_f	=	0.1200	m	(distance no. 1)

Produced by BISCO 13
www.physibel.be/en/products/bisco
physibel

BISCO Report

Project: **bisco horizontal rev02 [2]**
Author: **name**
Company: **company**
Date: **27/04/2025**

Materials

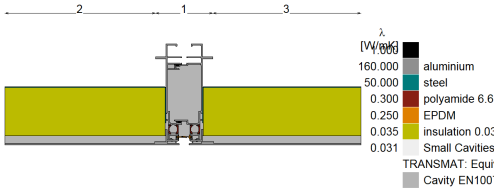

Temperatures

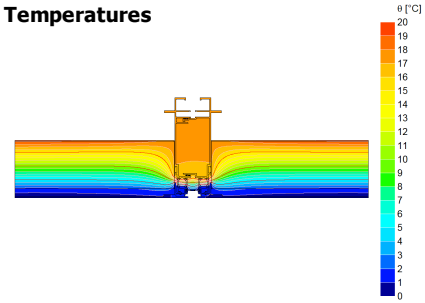

Heat flow

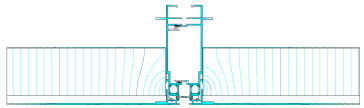

BISCO Report

Project: bisco horizontal rev02 [2]
Author: name
Company: company
Date: 27/04/2025

Materials

Col.	Name	λ [W/mK]	ε [-]
0		1.000	0.90
8	aluminium	160.000	0.90
13	steel	50.000	0.90
44	polyamide 6.6 with 25 % glass fibre	0.300	0.90
60	EPDM	0.250	0.90
151	insulation 0.035 W/mK	0.035	0.90
255	Small Cavities < 2 x 2 mm²	0.031	0.90
	TRANSMAT: Equivalent material (radiosity)		
	Cavity EN10077		

Boundary Conditions

Col.	Name	θ [°C]	h [W/m²K]
170	exterior	0.0	25.00
174	interior (normal) horizontal heat flow	20.0	7.70
182	indoors (reduced)	20.0	5.00

Equivalent thermal transmittance: U_f

Equivalent thermal transmittance	U_f	=	4.090	W/m²K	= (Φ / (θ_i - θ_e) - U_1 w_1 - U_2 w_2) / w_f
Thermal coupling coefficient	L_{2D}	=	0.6842	W/mK	= Φ / (θ_i - θ_e)
	Φ	=	13.684	W/m	
	θ_i	=	20.00	°C	
	θ_e	=	0.00	°C	
	U_1	=	0.311	W/m²K	(left edge of bitmap)
	w_1	=	0.3132	m	(distance no. 2)
	U_2	=	0.311	W/m²K	(right edge of bitmap)
	w_2	=	0.3083	m	(distance no. 3)
	w_f	=	0.1200	m	(distance no. 1)

Produced by BISCO 13
www.physibel.be/en/products/bisco
physibel

BISCO Report

Project: **Horizontal section-rev01**
Author: **name**
Company: **company**
Date: **02/04/2025**

Materials

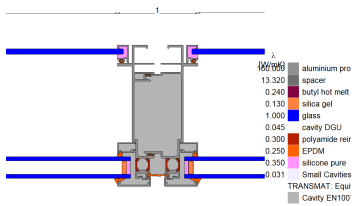

Temperatures

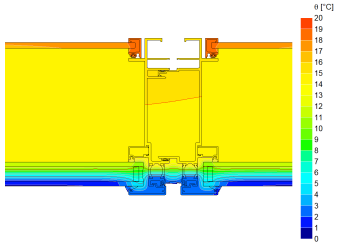

Heat flow

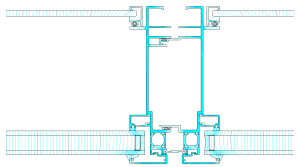

BISCO Report

Project: **Horizontal section-rev01**
Author: **name**
Company: **company**
Date: **02/04/2025**

Materials

Col.	Name	λ [W/mK]	ε [-]
4	aluminium profile	160.000	0.90
14	spacer	13.320	0.90
15	butyl hot melt	0.240	0.90
16	silica gel	0.130	0.90
18	glass	1.000	0.84
21	cavity DGU	0.045	0.90
33	polyamide reinforced	0.300	0.90
34	EPDM	0.250	0.90
35	silicone pure	0.350	0.90
255	Small Cavities < 2 x 2 mm²	0.031	0.90
	TRANSMAT: Equivalent material (radiosity)		
	Cavity EN10077		

Boundary Conditions

Col.	Name	θ [°C]	h [W/m²K]
48	exterior	0.0	25.00
49	interior (normal)	20.0	7.70
50	interior (reduced)	20.0	5.00

Equivalent thermal transmittance: U_f

Equivalent thermal transmittance Thermal coupling coefficient	U_f	=	W/m²K	= (Φ / (θ_i - θ_e) - U_1 w_1 - U_2 w_2) / w_f = Φ / (θ_i - θ_e)
	L_2	4.369	W/mK	
	Φ	1.7240	W/m	
	θ	34.480	°C	
	θ_i	20.00	°C	
	θ_e	0.00	°C	
	U_{w1}	1.200	W/m²K	(left edge of bitmap)
	U_{w2}	0.5000	W/m²K	(distance no. 2)
	w_2	1.200	m	(right edge of bitmap)
	w_f	0.5000	m	(distance no. 3)
		0.1200		(distance no. 1)

Produced by BISCO 13
www.physibel.be/en/products/bisco
physibel

BISCO Report

Project: **bisco vertical NEW rev02**
Author: **name**
Company: **company**
Date: **28/05/2025**

Materials

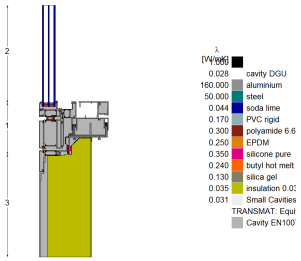

Temperatures

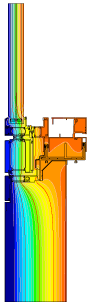

Heat flow

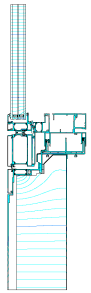

BISCO Report

Project: bisco vertical NEW rev02
Author: name
Company: company
Date: 28/05/2025

Materials

Col.	Name	λ [W/mK]	ε [-]
0		1.000	0.90
3	cavity DGU	0.028	0.90
8	aluminium	160.000	0.90
13	steel	50.000	0.90
18	soda lime	0.044	0.90
41	PVC rigid	0.170	0.90
44	polyamide 6.6 with 25 % glass fibre	0.300	0.90
60	EPDM	0.250	0.90
62	silicone pure	0.350	0.90
92	butyl hot melt	0.240	0.90
104	silica gel	0.130	0.90
151	insulation 0.035 W/mK	0.035	0.90
255	Small Cavities < 2 x 2 mm²	0.031	0.90
	TRANSMAT: Equivalent material (radiosity)		
	Cavity EN10077		

Boundary Conditions

Col.	Name	θ [°C]	h [W/m²K]
170	exterior	0.0	25.00
174	interior (normal) horizontal heat flow	20.0	7.70
182	indoors (reduced)	20.0	5.00

Equivalent thermal transmittance: U_f

Equivalent thermal transmittance	U_f	=	2.919	W/m²K	= (Φ / (θ_i - θ_e) - U_1 w_1 - U_2 w_2) / w_f
Thermal coupling coefficient	L_{2D}	=	0.8399	W/mK	= Φ / (θ_i - θ_e)
	Φ	=	16.799	W/m	
	θ_i	=	20.00	°C	
	θ_e	=	0.00	°C	
	U_1	=	0.600	W/m²K	(top edge of bitmap)
	w_1	=	0.3550	m	(distance no. 2)
	U_2	=	0.204	W/m²K	(bottom edge of bitmap)
	w_2	=	0.3752	m	(distance no. 3)
	w_f	=	0.1886	m	(distance no. 1)

Produced by BISCO 13
www.physibel.be/en/products/bisco
physibel

BISCO Report

Project: **bisco horizontal NEW rev01**
Author: **name**
Company: **company**
Date: **06/05/2025**

Materials

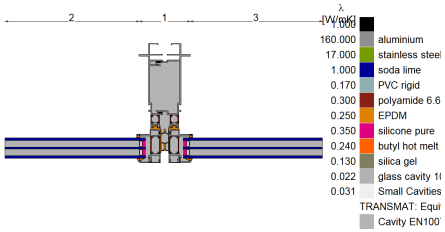

Temperatures

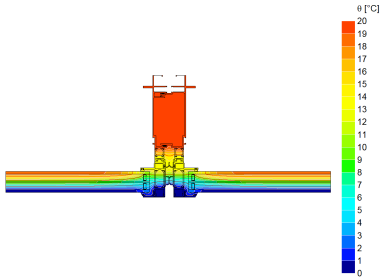

Heat flow

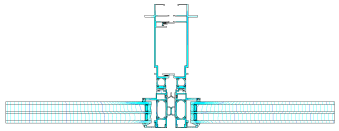

Produced by BISCO 13
www.physibel.be/en/products/bisco

BISCO Report

Project: **bisco horizontal NEW rev01**
Author: **name**
Company: **company**
Date: **06/05/2025**

Equivalent thermal transmittance: U_f

Equivalent thermal transmittance	U_f	=	3.581	W/m²K	= (Φ / (θ_i - θ_e) - U_1 w_1 - U_2 w_2) / w_f
Thermal coupling coefficient	L_{2D}	=	0.8028	W/mK	= Φ / (θ_i - θ_e)
	Φ	=	16.056	W/m	
	θ_i	=	20.00	°C	
	θ_e	=	0.00	°C	
	U_1	=	0.600	W/m²K	(left edge of bitmap)
	w_1	=	0.3134	m	(distance no. 2)
	U_2	=	0.600	W/m²K	(right edge of bitmap)
	w_2	=	0.3084	m	(distance no. 3)
	w_f	=	0.1199	m	(distance no. 1)

Materials

Col.	Name	λ [W/mK]	ε [-]
0		1.000	0.90
8	aluminium	160.000	0.90
11	stainless steel (austenitic/aust.ferritic)	17.000	0.30
18	soda lime	1.000	0.90
41	PVC rigid	0.170	0.90
44	polyamide 6.6 with 25 % glass fibre	0.300	0.90
60	EPDM	0.250	0.90
62	silicone pure	0.350	0.90
92	butyl hot melt	0.240	0.90
104	silica gel	0.130	0.90
194	glass cavity 10% air 90% argon	0.022	0.90
255	Small Cavities < 2 x 2 mm²	0.031	0.90
	TRANSMAT: Equivalent material (radiosity)		
	Cavity EN10077		

Boundary Conditions

Col.	Name	θ [°C]	h [W/m²K]
170	exterior	0.0	25.00
174	interior (normal) horizontal heat flow	20.0	7.70
182	indoors (reduced)	20.0	5.00

Produced by BISCO 13
www.physibel.be/en/products/bisco

BISCO Report

Project: **bisco horizontal NEW rev02 [2]**
Author: **name**
Company: **company**
Date: **27/04/2025**

Materials

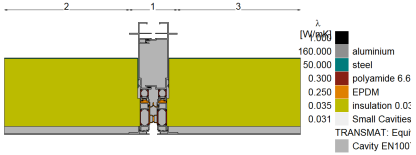

Temperatures

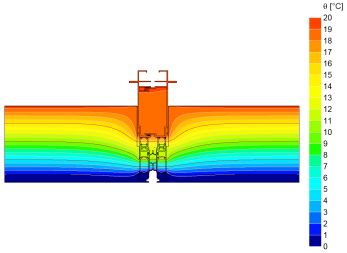

Heat flow

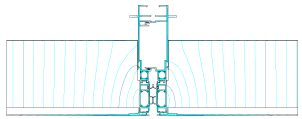

BISCO Report

Project: **bisco horizontal NEW rev02 [2]**
Author: **name**
Company: **company**
Date: **27/04/2025**

Materials

Col.	Name	λ [W/mK]	ε [-]
0		1.000	0.90
8	aluminium	160.000	0.90
13	steel	50.000	0.90
44	polyamide 6.6 with 25 % glass fibre	0.300	0.90
60	EPDM	0.250	0.90
151	insulation 0.035 W/mK	0.035	0.90
255	Small Cavities < 2 x 2 mm²	0.031	0.90
	TRANSMAT: Equivalent material (radiosity)		
	Cavity EN10077		

Boundary Conditions

Col.	Name	θ [°C]	h [W/m²K]
170	exterior	0.0	25.00
174	interior (normal) horizontal heat flow	20.0	7.70
182	indoors (reduced)	20.0	5.00

Equivalent thermal transmittance: U_f

Equivalent thermal transmittance	U_f	=	1.704	W/m²K	$= (\Phi / (\theta_i - \theta_e) - U_1 w_1 - U_2 w_2) / w_f$
Thermal coupling coefficient	L_{2D}	=	0.3236	W/mK	$= \Phi / (\theta_i - \theta_e)$
	Φ	=	6.472	W/m	
	θ_i	=	20.00	°C	
	θ_e	=	0.00	°C	
	U_1	=	0.192	W/m²K	(left edge of bitmap)
	w_1	=	0.3132	m	(distance no. 2)
	U_2	=	0.192	W/m²K	(right edge of bitmap)
	w_2	=	0.3084	m	(distance no. 3)
	w_f	=	0.1200	m	(distance no. 1)

Produced by BISCO 13
www.physibel.be/en/products/bisco
physibel

BISCO Report

Project: **bisco vertical NEW rev01**
Author: **name**
Company: **company**
Date: **06/05/2025**

Materials

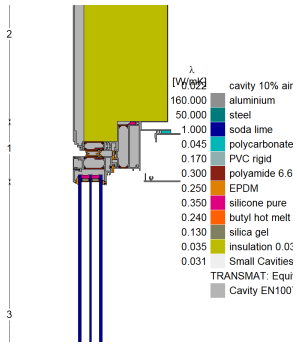

Temperatures

Heat flow

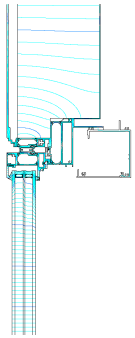

BISCO Report

Project: **bisco vertical NEW rev01**
Author: **name**
Company: **company**
Date: **06/05/2025**

Materials

Col.	Name	λ [W/mK]	ε [-]
2	cavity 10% air 90%argon	0.022	0.10
8	aluminium	160.000	0.90
13	steel	50.000	0.90
18	soda lime	1.000	0.90
21	polycarbonate	0.045	0.90
41	PVC rigid	0.170	0.90
44	polyamide 6.6 with 25 % glass fibre	0.300	0.90
60	EPDM	0.250	0.90
62	silicone pure	0.350	0.90
92	butyl hot melt	0.240	0.90
104	silica gel	0.130	0.90
151	insulation 0.035 W/mK	0.035	0.90
255	Small Cavities < 2 x 2 mm²	0.031	0.90
	TRANSMAT: Equivalent material (radiosity)		
	Cavity EN10077		

Boundary Conditions

Col.	Name	θ [°C]	h [W/m²K]
170	exterior	0.0	25.00
174	interior (normal) horizontal heat flow	20.0	7.70
182	indoors (reduced)	20.0	5.00

Equivalent thermal transmittance: U_f

Equivalent thermal transmittance	U_f	= 2.546	W/m²K	$= (\Phi / (\theta_i - \theta_e) - U_1 w_1 - U_2 w_2) / w_f$
Thermal coupling coefficient	L_{2D}	= 0.7019	W/mK	$= \Phi / (\theta_i - \theta_e)$
	Φ	= 14.037	W/m	
	θ_i	= 20.00	°C	
	θ_e	= 0.00	°C	
	U_1	= 0.195	W/m²K	(top edge of bitmap)
	w_1	= 0.3393	m	(distance no. 2)
	U_2	= 0.600	W/m²K	(bottom edge of bitmap)
	w_2	= 0.5501	m	(distance no. 3)
	w_f	= 0.1200	m	(distance no. 1)

Produced by BISCO 13
www.physibel.be/en/products/bisco
physibel